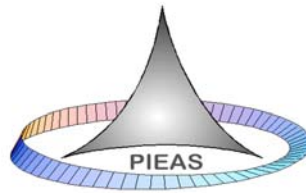


Department of Physics and Applied Mathematics

**Measurement of Seasonal and Spatial Variation
of Indoor Radon and Development of a Passive
Dosimeter for Thoron's Progeny**

By

Said Rahman



**Pakistan Institute of Engineering and Applied Sciences (PIEAS)
Nilore, Islamabad 45650, Pakistan
August 2008**

Department of Physics and Applied Mathematics

**Measurement of Seasonal and Spatial Variation
of Indoor Radon and Development of a Passive
Dosimeter for Thoron's Progeny**

By

Said Rahman

Submitted to the Department of Physics and
Applied Mathematics in partial fulfillment
of the requirements for the degree of

Doctor of Philosophy

at the

**Pakistan Institute of Engineering and Applied Sciences (PIEAS)
Nilore, Islamabad 45650, Pakistan
August 2008**

Declaration

I declare that all material in this thesis which is not my own work has been identified and that no material has previously been submitted and approved for the award of a degree by this or any other university.

Signature: _____

Author's Name: Said Rahman

It is certified that the work in this thesis is carried out and completed under my supervision.

Supervisor:

Dr. Matiullah,
Deputy Chief Scientist,
Department of Physics and Applied Mathematics,
PIEAS, Nilore, Islamabad*

* Present Position: Head NTSG, Physics Division, PINSTECH, Nilore, Islamabad.

Dedicated

To

My sweet family members:

My parents, sisters, brother Gul Rahman and his family, my wife and Children(Farida Rahman, Uzma Rahman, Maryam Bibi, Inam ullah Khan, Atta ullah Khan and Subhanullah Khan) and especially to my younger brother Khair-ur-Rahman

Acknowledgements

First of all I am thankful to Allah Who gave me the energy and health to complete this research work. There are a large number of people who have helped me in a number of ways to complete this PhD thesis. I am grateful to Chairman SUPARCO, who allowed me to pursue my higher studies. I am also grateful to Mr. Wazart Ali Khan ex-senior member SUAPRCO and Mr. Imran Iqbal, Member(SAR), who helped me in the initial stages of my studies. I am grateful to Dr. Badar Ghauri, Director SPAS and Mr. Rahmatullah Jilani, Mr. Mohammad Ashiq and Miss Rizla Zareen GMs(SPAS) for their help and encouragement during my studies. I am also grateful to my friends and colleagues Siraj Munir, Mr. Mati-ul-haq Managers (SPAS Division) and Mr. Muhammad Farooq and Zahir Ali Managers (RSA Division) for their support and encouragement during the entire period of my studies. Special thanks to the Higher Education Commission of Pakistan for their financial support through Indigenous PhD fellowship.

I am grateful to my supervisor Dr. Matiullah for his help and guidance during the entire period of my studies. I am also grateful to my respected teacher Professor S.A. Durrani for his encouragement and guidance during his stay in PIEAS. I am also grateful to Dr. Nasir Majid Mirza, Dr. Sikandar Majid Mirza, Dr. Masoor Ikram and Dr. Shaid Qamar for their guidance and help during my studies in PIEAS. I am grateful to Mr. Shakeel-ur-Rehman, Muhammad Basim, Attaullah and Mummamad Tariq Sadeeq of DPAM, PIEAS for their help in every matter and I miss their nice company very much. I am grateful to Mrs. Munazza Faheem my colleague and office mate during my Ph.D studies for her help in different matters.

I am also grateful to the staff of the SSNTD and Radiation Protection Dosimetry laboratories for their all time help and support during my studies. I am specially grateful to Mr. Mohammad Asif of SSNTD Laboratory for his hospitality and cooperative behavior. I am grateful to Dr. S.A. Mujahid, DCS Physics Division for his generous support to analyze different samples using HPGe detector as well as guidance in technical matters. Thanks are also due to the staff of the environmental radiation laboratory, PD PINSTECH for their support.

I am really grateful to my Professor, host and friend Professor Dr. Daniel, J. Steck of the St. John University, MN USA who helped me a lot in my research work during my stay in the USA. I am also grateful to him and his family for their hospitality during my stay. I am grateful to Dr. Dean Langely, Head Department of Physics St. John University MN, USA and his family members especially to the two young Chaps Marcus and Mathayas for their nice company to visit Duluth harbor.

I am also grateful to Asst. Professor Rahal Hamad, Department of computer science of the St. John University, MN USA for providing fulltime support in different matters during my stay in USA. I am grateful to Patty Washer resident warden of the EMMAUS Hall for help during my stay in the EMMAUS Hall.

I am grateful to the residents of the houses who allowed me to place the dosimeter in their homes for this research work. I am especially grateful to Taj Wali and Abdul Rehman of Bajuar Agency, Ziarat Khan, Munshi Khan, and Sahibzada of Mohmand Agency, Zia-ur-Rehman of Charsadda, Habib Ullah Khan, Chargul Rustum, Asad Khan, Haider Ali and Yahya Bacha of Rustum, Faseh Bacha of Mardan, Asad Qaiser, Amjad Ali and Mazhar Ali of Swabi for their support during my research work. I am also grateful to Mr. Shafqat for help in the grinding and crushing of different types of soil and other types of building materials samples.

Last but not the least I am grateful to my family members who supported and encouraged me a lot during my studies, their prayers and good wishes always accompanied me.

Said Rahman[†]

[†] [E-mail:saidrahman@yahoo.com](mailto:saidrahman@yahoo.com), said.rahman@gmail.com

Table of Contents

List of Publications.....	VI
List of Tables.....	VIII
List of Figures	XII
Chapter One.....	3
An Overview of Environmental Radioactivity	3
1.1. Introduction	3
1.2. Properties of Radon.....	3
1.3. Sources of Indoor Radon.....	5
1.4. Release Mechanism of Radon	6
1.5. Radiation Hazards	9
1.6. Equilibrium Factor	12
1.7. Radon Concentration Measurement Devices	14
1.7.1. Passive Techniques	15
1.7.1.1. <i>Charcoal Canister Technique</i>	15
1.7.1.2. <i>Solid State Nuclear Track Detectors (SSNTDs)</i>	16
1.7.1.3. <i>Electrets</i>	17
1.7.1.4. <i>Thermoluminescent Detectors (TLDs)</i>	18
1.7.2. Active Techniques.....	18
1.7.2.1. <i>Ionization Chamber</i>	18
1.7.2.2. <i>Scintillation Cell</i>	19
1.7.2.3. <i>Two Filter Method</i>	19
1.7.2.4. <i>Active Pylon Detectors /Continuous Monitoring</i>	20
1.7.2.5. <i>Surface Barrier Detector (SBD)</i>	21
1.7.2.6. <i>Monitoring of Radon and Thoron Daughters</i>	21
1.8. Sampling Methods of Radon Measurements.....	22
1.8.1. <i>Sampling Based on Radon Adsorption</i>	22
1.8.2. <i>Sampling Based on Radon Solubility or Absorption</i>	22
1.8.3. <i>Diffusion-based Samplers</i>	23
1.8.4. <i>Permeation-based Samplers</i>	23
1.9. Etched Track Detectors	23
1.10. CR-39 Polymeric Track Detectors.....	25

1.11.	Formation of the Latent Tracks	25
1.11.1.	<i>Thermal-Spike Model</i>	26
1.11.2.	<i>Ion-Explosion Spike Model</i>	26
1.11.3.	<i>Track Formation in Polymers</i>	27
1.12.	Chemical Etching	27
1.13.	Natural Radioactivity	31
	Chapter Two	34
	Experimental Procedures and Salient Features of the Selected Area for the Present Study	34
2.1.	Geology and Physical Features of the Area Surveyed	35
2.1.1.	<i>Geography</i>	37
2.1.2.	<i>Climatic Conditions</i>	37
2.2.	Building Characteristics	39
2.3.	Selection of the Houses for Indoor Radon Measurements	40
2.4.	Occupancy Factor	41
2.5.	Weighted Average Indoor Radon	41
2.6.	Seasonal Correction Factor	42
2.7.	Comparison of Yearly Average and Seasonally Measured Average Measurements	42
2.8.	CR-39 Detector and its Chemical Etching	42
2.9.	Radon Exhalation Rate	42
2.9.1.	<i>Setup for CR-39 Detector</i>	43
2.9.2.	<i>Calculation of the Exhalation Rate</i>	44
2.10.	Gamma Spectroscopy	45
2.10.1.	<i>Processing and Preparation of Samples</i>	46
2.10.2.	<i>Gamma Spectrometry</i>	46
2.11.	Electret Ion Chambers	47
2.12.	Measurement of Radon Progenies with Alpha Contamination Chambers	48
2.13.	Active Solid State Alpha Detector for Measuring the Surface Deposited Activity	49
2.14.	Ultrafine Particle Counter (UPC) P-track	49
2.15.	Active Alpha Detectors to Measure Surface Deposited Activity	50
2.16.	Measurement of Unattached Fraction using Ludlum scintillation cell	51

2.17.	Electrostatic Collection of Alpha-emitters (RAD7 Active Detector)	51
	Chapter Three	53
	Natural Radioactivity Measurements in Pakistan - An Overview	53
3.1.	Introduction	53
3.2.	Summary of the Studies Conducted in Pakistan	54
3.3.	Reported Indoor Radon Studies for Pakistan	57
3.4.	Summary of the Results	58
3.5.	Conclusions.....	63
	Chapter Four.....	65
	Measurement of Seasonal and Spatial Distribution of Indoor Radon Levels	65
4.1.	Introduction	65
4.2.	Materials and Methods	66
4.3.	Results	66
4.4.	Yearly Minimum-Maximum Indoor Radon Concentration	75
4.5.	Seasonal Correction Factor	78
4.6.	Seasonally Averaged and Yearly Averaged Indoor Radon	78
4.7.	Comparison of Indoor Radon Levels in Bedrooms and Drawing Rooms	80
4.8.	Dose Estimation	81
4.9.	Excess Lung Cancer Risk.....	82
4.10.	Discussion.....	86
4.11.	Conclusions.....	90
	Chapter Five	99
	Experimental Studies on Radon Exhalation Rate from the Soil, Sand and Brick Samples	99
5.1.	Introduction	99
5.2.	Calculation of the exhalation rate	101
5.3.	Results	103
5.4.	Discussion.....	107
5.5.	Conclusions.....	111
	Chapter Six.....	112
	Measurement of Natural Radioactivity in Soil and other Building Materials.	112
6.1.	Introduction	112
6.2.	Measurements	113

6.3.	Results	115
6.3.1.	<i>Specific activities and radium equivalent activity</i>	115
6.3.2.	<i>External and Internal Indices</i>	118
6.3.3.	<i>Calculations of Effective Dose</i>	120
6.4.	Discussion.....	121
6.5.	Conclusions.....	126
Chapter Seven		127
Electrets as a Radon Progenies Dosimeter		127
7.1.	Introduction	127
7.2.	Components of E-PERMS.....	128
7.3.	Principal of Measurement of Alpha Contamination.....	129
7.4.	Alpha Contamination Electret Measurement System as Radon Progeny Dosimeter.....	130
7.4.1.	<i>Experimental Approach</i>	130
7.4.2.	<i>Measurement of Radon using Electrets</i>	130
7.5.	Calculation of the Performance Factor for The Measurement of Radon Progeny	133
7.6.	Results and Discussion.....	137
7.6.1.	<i>Long-term Electrets</i>	137
7.6.2.	<i>Short-term high sensitivity electrets</i>	139
7.7.	Equilibrium and Unattached Fraction of Radon using E-RPISU.....	143
7.8.	Principle of Operation of E-RPISU	144
7.9.	Conclusions.....	146
Chapter Eight		147
Development of Passive Thoron Progeny Dosimeter		147
8.1.	Introduction	147
8.2.	Effect of Deposition of Thoron	148
8.3.	Measurement Techniques of Thoron and its Progenies.....	148
8.4.	Thoron Measurement	149
Thoron progenies Measurement.....		151
8.6.	Materials and Methods.....	152
8.6.1.	<i>Theory of Measurement of Radon Progeny Dosimeter using Solid State Nuclear Track Detector</i>	152

8.6.2.	<i>Determination of Efficiency of Different Plastics/Filter as Energy Absorber ..</i>	153
8.7.	Technical specifications and Construction Procedure of Surface Deposition Detectors	155
8.8.	Initial Testing of the New Surface Deposition Dosimeters	156
8.9.	Measurement of Particle Concentration.....	162
8.11.	Air borne Progeny Fraction Measurement	171
8.11.1.	<i>Measurement of unattached fraction using Ludlum scintillation detector.....</i>	171
8.11.2.	<i>Radon and Thoron Progeny Equilibrium and Unattached Fraction</i>	174
8.12.	Calibration Factor for the New Thoron Surface Deposition Dosimeters....	175
8.13.	Dose from Thoron Progeny	176
8.14.	Conclusions.....	180
Chapter Nine	181
Conclusions and Future Recommendations	181
9.1.	Conclusions.....	181
9.2.	Future Recommendations	190
References	191
APPENDICES	214

List of Publications

1. Daniel J. Steck, **Said Rahman** and Matiullah (2008). Electrets as a Radon Progenies Dosimeter-Feasibility Study. J. Radiol. Prot (under review)
2. **Said Rahman**, Daniel J. Steck and Matiullah (2008). Development of a CR-39 based passive thoron progeny dosimeter - Preliminary studies Radiat. Meas. (under review)
3. **Said Rahman**, Matiullah and B.M.Ghauri (2008).Comparison of seasonal and yearly average indoor radon levels using CR-39 detectors. Radiat. Meas (under review)
4. **Said Rahman**, Munazza Faheem, Matiullah (2008).Natural Radioactivity Measurements in Pakistan - An Overview. J. Radiol. Prot. **28**, 1–10.
5. Munazza Faheem, **Said Rahman**, Shafi-ur-Rahman and Matiullah (2008).Radon – an environmental hazard. Science International, 20(1), 59-61.
6. Munazza Faheem, **Said Rahman**, Matiullah (2008).A Review of Radon Measurement Studies in Pakistan. J. Radiol. Prot. 28 (2008) 283–292.
7. **Said Rahman**, Matiullah and Badar Ghauri (2008). Effect of moisture on the radon exhalation rate from soil, sand and brick samples collected From NWFP and FATA, Pakistan. Radiat. Protect. Dosim., 130(2),172-177.
8. **S. Rahman**, Matiullah, S. A. Mujahid and S. Hussain (2008). Assessment of radiological hazards due to the presence of natural radionuclides in samples of building materials collected from the northwestern areas of Pakistan. J. Radiol. Prot. Radiol. Prot. 28, 205–212.
9. Matiullah, A. Ahad, Munazza Faheem and **Said Rahman** (2008). Measurement of radioactivity in vegetation of the Bahawalpur division and Islamabad federal capital territory – Pakistan. Radiat. Meas. Radiation Measurements 43 (2008) S532–S536.
10. Muhammad Rafique, Shahida Jabeen, M. Ikram Shahzad, **S. Rahman**, Shujaht Bukhari and Matiullah (2008).Measurement of Indoor Radon concentration and Dose Estimation in the city of Muzaffarabad after Earthquake (Oct. 2005), during summer, Azad Kashmir, Pakistan. J. Radiol. Prot(under review).
11. **S.Rahman**, Matiullah, Z. Rahman, N. Mati and B.M. Ghauri (2007). Measurement of indoor radon levels in North West Frontier Province and federally administered tribal areas- Pakistan during summer. Radiat. Meas. 42 (2), 304-310.
12. **S. Rahman**, N. Mati, Matiullah and B. Ghauri (2007). Radon Exhalation Rate From the Soil, Sand and Brick Samples Collected from NWFP and FATA, PAKISTAN. Radiat. Protect. Dosim. 124(4), 392-399.
13. Daniel J. Steck, **Said Rahman** and David Harrison (2007). Passive Radon Progeny Dosimeters: Feasibility Studies. 17th National Radon Conference of AARST, Jacksonville, Florida, USA, September, 2007

14. **S. Rahman**, Matiullah, S. A. Mujahid and S. Hussain (2007).Assessment of the radiological hazards due to naturally occurring radionuclides in soil samples collected from the North Western areas of Pakistan. Radiat. Protect. Dosim., 2008 128(2),191-197.
15. **S. Rahman**, N. Mati, Matiullah and B.M. Ghauri (2007).Seasonal indoor radon concentration in the North West Frontier Province and federally administered tribal areas—Pakistan. Radiat. Meas. 42, 1715 – 1722.
16. **S. Rahman**, M. Faheem, S. Rehman, and Matiullah (2006).Radon awareness survey in Pakistan. Radiat. Protect. Dosim., 121 (3), 333–336.
17. S. Rehman, Matiullah, S. Rehman and **S. Rahman** (2006).Studying ^{222}Rn exhalation rate from Soil and Sand Samples using CR-39 detectors. Radiat. Meas., 41(6), 708-713.
18. S. A. Durrani and **Said Rahman** (2006).Radon as a possible indicator of impending earthquakes. Presented at: International Conference on 8 October 2005 Earthquake in Pakistan: It's Implications & Hazard Mitigation Islamabad, 18-19 January 2006.
19. **Said Rahman**, Shakeel-ur-Rehman, Munazza Faheem, Matiullah, Badar Ghauri and S. A Durrani (2006).A feasibility study of setting up radon measurement field stations for earthquake prediction in Pakistan. Paper presented at the 23rd International Conference on Nuclear Tracks in Solids, held in Beijing, China from 11-15 September, 2006.

List of Tables

- Table 1.1: Correlation coefficients between the radon concentration in the soil air and atmospheric pressure, soil and ambient temperature and atmospheric humidity.
- Table 1.2: Average annual effective dose per caput.
- Table 2.1: Long-term average climatic conditions of Mardan, Swabi as recorded in the Meteorological station Risalpur.
- Table 2.2: Long-term average climatic conditions of Mardan, Swabi as recorded in the meteorological station Peshawar.
- Table 2.3: Different types of materials used for the fabrication of surface deposition dosimeter.
- Table 4.1: Indoor radon levels in Bq m^{-3} in bed rooms and drawing rooms of all the houses which were surveyed in NWFP and FATA areas of Pakistan during the Summer season.
- Table 4.2: Weighted average indoor radon during the Summer season.
- Table 4.3: Indoor radon levels in Bq m^{-3} in bedrooms and drawing rooms of all the houses which were surveyed in NWFP and FATA areas of Pakistan during the Autumn season.
- Table 4.4: Weighted Average indoor radon during the Autumn season.
- Table 4.5: Indoor radon levels in Bq m^{-3} in bed rooms and drawing rooms of all the houses which were surveyed in NWFP and FATA areas of Pakistan in the Winter Season
- Table 4.6: Weighted average indoor radon during the Winter season.
- Table 4.7: Indoor radon levels in Bq m^{-3} in bed rooms and drawing rooms of all houses surveyed in NWFP and FATA areas of Pakistan in Spring season.
- Table 4.8: Weighted average indoor radon in the Spring season.
- Table 4.9: Minimum, maximum and average radon concentration levels in Bq m^{-3} during the four seasons and yearly averaged exposed detectors in the NWFP and FATA.
- Table 4.10: Average ratio of the indoor radon levels in bedroom to drawing room in the selected area.
- Table 4.11: Annual effective dose calculated using ICRP-65 and UNSCEAR-2000 conversion factor
- Table 4.12: Mean effective dose in mSv expected to be received by the inhabitants of the area using ICRP-65 and UNSCEAR, 2000 conversion factors.
- Table 4.13: Excess relative risk of lung cancer due to the indoor radon in the selected areas.
- Table 4.14: Yearly average indoor radon in the Bedrooms and Drawing Rooms of the selected area.
- Table 4.15: Weighted average Indoor radon levels in the NWFP and FATA, Pakistan.
- Table 5.1: Radon exhalation rate ($\text{mBq.m}^{-2}.\text{h}^{-1}$) from different soil samples having 0%, 15%, 30% and 45% moisture content (MC), collected from the district Swabi.
- Table 5.2: Radon exhalation rate ($\text{mBq.m}^{-2}.\text{h}^{-1}$) from different soil samples having 0%, 15%, 30% and 45% moisture content (MC), collected from the district Mardan.

- Table 5.3:Radon exhalation rate($\text{mBq}\cdot\text{m}^{-2}\cdot\text{h}^{-1}$) from different soil samples having 0%, 15%, 30% and 45% moisture content (MC), collected from the district Charsadda.
- Table 5.4:Radon exhalation rate($\text{mBq}\cdot\text{m}^{-2}\cdot\text{h}^{-1}$) from different soil samples having 0%, 15%, 30% and 45% moisture content (MC), collected from the Mohmand agency.
- Table 5.3:Radon exhalation rate($\text{mBq}\cdot\text{m}^{-2}\cdot\text{h}^{-1}$) from different soil samples having 0%, 15%, 30% and 45% moisture content (MC), collected from the district Charsadda.
- Table 5.4:Radon exhalation rate($\text{mBq}\cdot\text{m}^{-2}\cdot\text{h}^{-1}$) from different soil samples having 0%, 15%, 30% and 45% moisture content (MC), collected from the Mohmand agency.
- Table 5.5:Radon exhalation rate($\text{mBq}\cdot\text{m}^{-2}\cdot\text{h}^{-1}$) from different soil samples having 0%, 15%, 30% and 45% moisture content (MC), collected from the Bajuar agency.
- Table 5.6:Radon exhalation rate ($\text{mBq}\cdot\text{m}^{-2}\cdot\text{h}^{-1}$) from different soil samples having 0%, 15%, 30% and 45% moisture content (MC), collected from the different areas of NWFP and FATA.
- Table 5.7:Radon exhalation rate ($\text{mBq}\cdot\text{m}^{-2}\cdot\text{h}^{-1}$) from different soil samples having 0%, 15%, 30% and 45% moisture content (MC), collected from the selected area.
- Table 5.8:Statistical analysis of the present data regarding the radon exhalation rate as a function of moisture contents applying student T-test was applied to the data.
- Table 5.9:Published data concerning radon exhalation rate along with the present results.
- Table 6.1:Natural radioactivity, radium equivalent activity in $\text{Bq}\cdot\text{kg}^{-1}$, external and internal hazard indices and effective doses in the samples collected from the district Swabi.
- Table 6.2:Natural radioactivity, radium equivalent activity in $\text{Bq}\cdot\text{kg}^{-1}$, external and internal hazard indices and effective doses in the samples collected from the district Mardan.
- Table 6.3:Natural radioactivity, radium equivalent activity in $\text{Bq}\cdot\text{kg}^{-1}$ external and internal hazard indices and effective dose in the samples collected from the district Charsadda.
- Table 6.4:Natural radioactivity, radium equivalent activity in $\text{Bq}\cdot\text{kg}^{-1}$, external and internal hazard indices and effective doses in the samples collected from the Mohmand agency.
- Table 6.5:Natural radioactivity, radium equivalent activity in $\text{Bq}\cdot\text{kg}^{-1}$, external and internal hazard indices and effective doses in the samples collected from the Bajuar agency.
- Table.6.6: ^{226}Ra , ^{232}Th , ^{40}K and Ra_{eq} , external and internal hazard indices and effective dose measured in brick samples which were collected from the districts Swabi, Mardan and Charsadda.
- Table 6.7: ^{226}Ra , ^{232}Th , ^{40}K and Ra_{eq} , external and internal hazard indices and effective dose measured in the sand samples collected from Swabi, Mardan, Charsadda districts as well as Mohmand and Bajuar agencies.

Table 6.8:²²⁶Ra, ²³²Th, ⁴⁰K and Ra_{eq} , external and internal hazard indices and effective dose measured in the marble samples collected from the selected area.

Table 6.9:²²⁶Ra, ²³²Th, ⁴⁰K and Ra_{eq} , external and internal hazard indices and effective dose measured in the cement samples collected from the area under study.

Table 6.10:Comparison of the present values with some other data reported for other parts of Pakistan.

Table 6.11:Comparison of the present study with other data reported for different parts of the world (All the activities are shown in $Bq.kg^{-1}$).

Table 7.1:Radon concentration measurements made in the exposure room using standard electrets.

Table 7.2a:Voltage drop in volts of different long term electrets used as radon progeny monitors.

Table 7.2b:Normalized voltage drop (NVPD) in Volts/day of different long-term electrets used as radon progeny monitors.

Table 7.2c:Performance factor of different long-term electrets used as radon progeny monitors.

Table 7.3a:Voltage drop of different short-term electrets used as radon progeny monitors.

Table 7.3b:Normalized voltage drop of different short-term electrets used as radon progeny monitors.

Table 7.3c:Performance factor ($V/d. pCi.l^{-1}$) of different short-term electrets used as radon progeny monitors.

Table 7.4a:Voltage drop of different short-term electrets used as radon progeny monitors.

Table 7.4b:Normalized voltage drop of different short-term electrets used as radon progeny monitors.

Table 7.4c:Performance factors of different short term electrets used as radon progeny monitors

Table 7.5:Equilibrium factor and unattached fraction of radon decay products using ERIPSU

Table 8.1:Efficiency of different materials for the Detection of ²¹⁸Po ²¹⁴Po and ²¹²Po

Table 8.2:Surface deposited ²¹²Po activity in different chambers.

Table 8.3:Track density in different regions of the surface deposition detector in the small thoron Chamber Run-1

Table 8.4:Radon and thoron concentration in the small Chamber (Experiment Run-1)

Table 8.5:Track density in different regions of the surface deposition detector in the small thoron Chamber Run 2.

Table 8.6:Radon and thoron concentration in the small Chamber Run-2.

Table 8.7:Radon and thoron concentration in the Medium sized thoron chamber.

Table 8.8:Track density in different regions of the surface deposition detector in the Medium size thoron Chamber.

Table 8.9:Radon and thoron concentration in the exposure room during the exposure of the surface deposition detectors in the room (15 days).

Table 8.10:Track density in different regions of the surface deposition detector in the exposure room.

Table 8.11: Ultrafine particles concentration, Equilibrium factor, unattached fraction of Radon and thoron progenies.

Table 8.12: Indoor radon, thoron and their progenies concentration and the dose delivered by thoron progeny.

List of Figures

- Figure 1.1: Some parameters used to describe the geometry of the etched tracks.
- Figure 1.2: Construction for the calculation of etched-track parameters for a track of constant V_T , lying normally to the detector surface. The semi-cone-angle is denoted by δ .
- Figure 2.1: Map of the selected area. The shaded portion in the above map shows the selected area.
- Figure 2.2: Efficiency calibration curve of the HPGe detector using mixed radionuclides calibration source prepared in Marinelli geometry.
- Figure 4.1: Minimum and maximum radon concentration levels in each season in the listed areas of the NWFP and FATA.
- Figure 4.2: Mean seasonal indoor radon concentration in the listed areas of the NWFP and FATA, Pakistan.
- Figure 4.3: Yearly average radon concentration levels in NWFP and FATA.
- Figure 4.4: Yearly average minimum and maximum indoor radon concentration levels in Bq m^{-3} in bedrooms and drawing rooms of the area selected.
- Figure 4.5: Seasonal correction factor for the listed area of NWFP and FATA.
- Figure 4.6: Yearly and seasonally averaged yearly radon levels in the Swabi district.
- Figure 4.7: Yearly and seasonally averaged yearly radon levels in the Mardan district.
- Figure 4.8: Yearly and seasonally averaged yearly radon levels in the Charsadda district.
- Figure 4.9: Yearly and seasonally averaged yearly radon Levels in the Mohmand agency.
- Figure 4.10: Yearly and seasonally averaged yearly radon levels in the Bajuar agency.
- Figure 7.1: Electret ion chambers used for measurement of radon and thoron progeny deposited on the surface.
- Figure 8.1: Radon decay chain.
- Figure 8.2: Thoron decay chain.
- Figure 8.3: Normalized surface deposition rate of radon progenies under different aerosols conditions.
- Figure 8.4: Normalized surface deposition rate of thoron progenies under different aerosols conditions.
- Figure 8.5: Normalized airborne radon progenies for different aerosols conditions.
- Figure 8.6: Airborne thoron progenies in the exposure room under different aerosols conditions.

Abstract

Radon has long been recognized as one of the indoor air problems. There is a strong relation between radon and lung cancer. It is the second leading cause of the lung cancer after cigarette smoking. The present research work concerning the **Measurement of seasonal and spatial variation of indoor radon and development of a passive dosimeter for thoron's progeny** is divided into two parts. The first part deals with the field and laboratory measurements which were performed using the passive radon dosimeters and in the second part laboratory experiments were carried out to develop a new passive thoron progeny dosimeter.

Chapter 1 gives a brief introduction to radon, its health effects, measurement techniques and the instruments used for the measurement of indoor radon concentration. Different dose conversion relations and excess lung cancer reports have also been discussed in this chapter. Chapter 2 describes different types of equipments and materials used in the research work. Information about the geology, climatic conditions and building characteristics of the houses surveyed have also been given in this chapter. It also includes procedure of the samples preparation for the measurement of radioactivity and radon exhalation rate in the laboratory using active and passive detectors. In chapter 3 reviews reported studies conducted in Pakistan concerning the measurement of natural radioactivity and indoor. Chapter 4 discusses the results and discussion of the present work concerning radon measurement performed throughout the years in four cycles which has covered all the seasons. Seasonal correction factor, weighted average indoor radon levels excess lung cancer risk and the dose delivered to the inhabitants using the local occupancy factor have also been included in this chapter. Chapter 5 deals with the results and discussions about the radon exhalation from the soil, sand and brick samples which were collected from the selected area. Effect of moisture contents on the radon exhalation rate using a closed can technique has also been presented in the chapter. The effect of back diffusion on the radon exhalation has also been studied and included in this chapter. Measurement of the natural radioactivity in the soil and other building materials,

like sand, brick, marble and cement samples which were collected from the selected area has been dealt with in chapter 6.

Research work performed at the University of St., John University USA has been included in chapter 7 and 8. These chapters include experiments performed in the exposure room using the electret ion chambers. Radon concentration in the exposure room was measured using both short term and long term electrets. It also includes the results of the performance factor for the alpha contamination chambers using the electrets as radon progeny dosimeter. Experiments were performed using both short term high sensitivity and long term (low sensitivity) electrets. Development of a new passive thoron progeny dosimeter using the principle of the surface deposition has been discussed in chapter 8. This chapter includes an introduction about the different types of active and passive equipments used for the measurement of thoron. It also discusses the calibrations of different types of active detectors for the measurements of surface deposited activities on the glass surfaces. Finally chapter 9 concludes the present research work and includes future recommendations.

Chapter One

An Overview of Environmental Radioactivity

1.1. Introduction

Every person, animal and object present on our planet earth are subjected to radiation and may indeed contain it. We cannot see it, smell it or feel it, but it is with us all the times. Natural radioactivity on earth has been in existence ever since the planet was formed and there are about 60 radionuclides present in nature. About 82% of the environmental radiation is from natural sources, the largest of which is radon. Some areas of the world, called high background radiation areas (HBRAs), have anomalously high levels of background radiations. Extreme HBRAs are found in Guarapari (Brazil), southwest France, Ramsar (Iran), parts of China and the Kerala coast of India (Dissanayake, 2005).

Radon exposure is known to be the second leading cause of lung cancer after cigarette smoking. In the past several decades, there have been more epidemiologic investigations exploring the association between radon (and its progeny) and lung cancer than any other environmental carcinogen. Studies concerning occupationally radon-exposed miners and direct observation from the individuals exposed to radon in their homes provide a firm scientific foundation which proves that radon is a major environmental carcinogen (IARC, 1988; ICRP, 1987; Nero, 1988; NRC, 1991; NRC, 1999; UNSCEAR, 2000).

1.2. Properties of Radon

Radon was discovered by the German chemist Friedrich E. Dorn. Radon has nine (9) short lived isotopes, but the most important is radon-222 (^{222}Rn), radon-220 (Thoron ^{220}Rn) and radon-219 (Actinon, ^{219}Rn). For millennia, advances in human progress have been tied to our ability to protect ourselves from the harmful effects of the

environment—ranging from human waste to the organic and inorganic by-products of everyday living and noxious gases. With the passage of time, humans have learnt more about the environment. With regard to the ill effects on human health of gases and fumes inside mines have been known since antiquity. Thus, Lucretius (95-55 BC), the Roman Epicurean poet-philosopher, in Book VI (Meteorology and Geology) has written that what malignant breath is exhaled by gold mines! How it acts upon men's features and complexions!. Vapors given off by the earth and blown out into the open, into the unconfined spaces of the air" (Lucretius, 55 BC). Of more recent origin, according to Steinhäusler (1988), are the medical observations of the redoubtable Swiss physician, Paracelsus (1493-1541) and Agricola in the sixteenth century "when it was noted that the mining population in parts of Germany (Schneeberg) and Bohemia (St Joachimsthalin Czechoslovakia) were suffering from a widespread fatal lung disease known as 'male metallorum' [metal sickness] or 'Schneeberger Krankheit' [Schneeberg Illness]. It was not until the nineteenth century that lung cancer was identified as the primary cause of death for about 75% of all miners in the Schneeberg region".

For humans, the greatest importance among radon isotopes is attributed to ^{222}Rn because it is the longest lived of the three naturally produced isotopes (Durrani and Illic 1999). It is well-known that airborne short-lived radon and thoron progeny inhalation has a large contribution towards the radiation exposure of the public (NRC, 1999; ICRP, 1994; UNSCEAR, 2000). Radon is an inert element in the gaseous form, with atomic number of 86. It is colorless, odorless, tasteless and radioactive. It is non reactive towards chemical agents. It is the heaviest member of the rare gas group (~100 times heavier than hydrogen and ~7.5 times heavier than air). When cooled below its freezing point, radon exhibits brilliant phosphorescence that becomes yellow at lower temperatures and orange-red at the temperature of the liquid air (CRC, 2001). Being a noble gas, it has greater ability to migrate freely through soil, air, etc. (Matiullah et al, 1993). There are no sinks for radon and it is estimated that only negligible quantity escape to the stratosphere (Gingrich, 1983). As a result, the ultimate and sole fate of radon is transformation or degradation through radioactive decay. Radon is readily absorbed on charcoal, silica gel and similar substances. This property serves to separate it from other gases by collecting it on activated charcoal.

^{222}Rn has been used as a tracer for the origin and trajectory of convective atmospheric transport of air masses to test general circulation models. ^{222}Rn has also been used in more quantitative studies particularly to determine vertical matter diffusion coefficients. ^{222}Rn is assumed to be generated by the land mass of a continent and using models for its mixing and transport in the atmosphere, outdoor air concentrations are calculated at a certain distance of the continent and compared with measurements performed at some other points in sea (Neman et al., 2005; Lee et al., 2001).

1.3. Sources of Indoor Radon

Radon comes from uranium that has been in the ground since the time the earth was formed. The rate of radon seepage is variable, partly because the amounts of uranium in the soil vary considerably (BEIR VI, 1999). Radon flows from the soil into the outdoor air and also into the air in homes from the movement of gases in the soil beneath homes. Outside air typically contains very low levels of radon, but it builds up to higher concentrations indoors when it is unable to disperse. Generally sources of radon in dwellings are, radon exhaled from the building materials and the soil/rocks below the building and inflow of radon containing air (Aldenkamp et al., 1992). According to significance the indoor radon sources may be classified in the following order as soil beneath the building, building materials, outdoor air, portable water supplies and natural gas (UNSCEAR, 2000).

Characterization of the indoor sources of radon requires consideration of the rate at which radon is generated in the source materials and its modes of transport through various materials into the indoor environment. The property of the materials which is considered most significant for the material to be an indoor radon sources, is the radium (^{226}Ra) contents in that material. A slight differences in ^{226}Ra concentrations result in greatly varying ^{222}Rn concentrations. However, all the radon produced in the grain does not escape from the grain and its release depends on the porosity of the materials/ emanation coefficients and exhalation rate from the materials which are briefly discussed below.

1.4. Release Mechanism of Radon

The release mechanism of radon from the grain to the indoor environment is governed by emanation and exhalation. The release of radon from mineral grain to the pore space is called emanation. Emanation is described by emanation coefficient which is the ratio of the radon produced in the grain of the materials to the radon in the pore space of the material. Its value is different for different materials and it depends on the grain size of the materials. Smaller the grain size will cause more emanation and vice versa. Emanation is governed by the law of conservation of momentum. The value of the emanation coefficient is of the order of 0.2–0.3 (Durrani and Ilic, 1997) for common constituents of building material (e.g., sand). The emanation increases with increase in the water contents in materials as moisture absorbs the recoil energy partly and the probability for radon atom remaining within the pore space is enhanced. The residual nucleus ^{222}Rn recoils and is able to leave the rock grain provided it is close enough to the grain boundary and is free to migrate in the pore space of soil (Mujahid et al., 2005). The first possibility for escape is direct ejection of the radon atom by the recoil alpha emission. Conservation of momentum reveals that residual radon nucleus has energy of 86 keV which is sufficient to move the recoiling radon through 26 nm of SiO_2 (Fleisher, 1997; Durrani and Ilic, 1997).

Radon moves by diffusion and forced flow. Diffusion inevitably occurs even though its extent is limited. Hence diffusive migration sets a lower limit on the transport of radon. Forced flow depends on pressure gradients which may or may not be present in every situation. Diffusive flow in the materials is controlled by open, connected porosity. Higher porosity enable more extensive diffusive transport, but it is critical to consider only that fraction of the pore space that allows through motion. Near surface radon escapes into the atmosphere thereby lowering the natural concentration to near zero at the surface producing a near surface gradient whose profile is set by diffusion and mean life of radon concentration. If the radium concentration, porosity and emanation for a type of soil or the material are known then maximum radon concentration ‘C’ that can occur in the pore space can be calculated by the following equation

$$C = \frac{Aed(1-p)}{p} \quad (1)$$

Where 'A' is radium content, 'e' is emanation coefficient, 'd' is diffusion coefficient and 'p' is the porosity of the material. Smaller the particles in which the radon atom is formed, greater is the chance of the atom escaping from it. Emanation is greater in finer grained particles. For clay it is between 40 - 70%. One parameter of importance is the ability of the gas to leave the grains of the soil after it is produced. The fraction of radon atoms, generated in the soil grains and reaching the pore volume of the soil is known as the emanation coefficient. This coefficient depends basically on the soil grain size-distribution, on the porosity and on the water content (Baixeras 2001). Emanation and transport mechanisms depend to a large extent on soil moisture content. Thus, radon flux at the soil surface is strongly affected by the weather conditions (Ferry et al., 2001). A reduction in the bricks exhalation from 50% to 90% is obtained when inner sides of the walls are painted. Since most of the dwellings in the cities are painted using different types of paints, very little contribution seems to come out from the building material which is in agreement with indoor results (Segoviat et al., 1994). Table 1.1 show the correlation between the radon concentration in the soil air and atmospheric pressure, soil and ambient temperature and atmospheric humidity

It is a well known fact that radon emanation is affected by moisture. The models which explain radon emanation can be considered to come in three types. One is to predict the maximum possibility of radon emanation assuming uniform distribution of radium in a solid grain independent of the moisture. The other two are to explain moisture effect on radon emanation, but their aims are different from each other. The first of them aims to demonstrate a theory explaining microscopic phenomena of radon emanation employing observed macroscopic phenomena of radon emanation under moist condition. The second aims to predict the leveling-off value of radon emanation under moist conditions employing an observed data of radon emanation under dry conditions.

Sasaki et al., have reported that emanation coefficient is affected by the moisture content. They have proposed close-packed spherical grain model and studied quantitatively if it can well predict the leveling-off value of radon emanation coefficient (Sasaki et al., 2004). The other mechanism which affect radon concentration is exhalation. The release of radon from pore space into the air is called exhalation. A

measure of exhalation is given by the exhalation rate, which is defined as the number of radon atoms leaving the material per unit surface area per unit time. Radon exhalation rate is highly affected by the parameters like atmospheric pressure, temperature and wind force. According to the published data, 60.4% of the indoor radon comes from the ground and surrounding soil of the buildings (Sun et al., 2004). The most important factor, controlling exhalation of radon from soil is geological structure of the top layer of the ground. Another important factor is rocks underlying the soil to the depth of about 10 m because radon cannot migrate from deeper levels due to its relatively short half life. The measurement technique of radon exhalations from the construction materials using nuclear track detectors (NTDs) was reported by Abu-Jarad in 1980 which is called the “can technique” (Rehman et al., 2003).

For radon transport through a porous medium, information on its generation, the structure of the medium, the physical processes causing the transport driving forces and the interaction of radon with the medium partitioning between air and water phase and adsorption at the solid interface are required (Cozmuta and van der Graaf, 2001).

Table 1.1: Correlation coefficients between the radon concentration in the soil air and atmospheric pressure, soil and ambient temperature and atmospheric humidity.

S.No	Parameter	Correlation coefficient
1.	Soil temperature	0.752
2.	Ambient temperature	0.754
3.	Atmospheric pressure	-0.861
4.	Atmospheric humidity	-0.555

It is well documented that drops in atmospheric pressure may cause an increase in the radon transport into a house. This affect may, however, often be of relatively short duration and at most last only as long as the pressure is still dropping. Among the physical and geological factors characterizing the radon risk of a given type of the bedrock and subsoil are the radium concentration and permeability. Therefore, geological

classification is needed to be done on the basis of these parameters. If large variations in the exhalation rate occur during the growth time, the mean exhalation rate deduced from the gamma activity of the sample will outweigh the values of the exhalation rate occurring during the later part of the growth period (Stranden et al., 1985). The soil-gas radon concentration as well as the radon exhalation rate from the ground may vary often greatly over a small distance (Martin and Matěj, 2002).

1.5. Radiation Hazards

Radiation effects comprise of (1) deterministic effects that occur with certainty after doses high enough to cause major cell killing and (2) stochastic effects that are considered to occur more or less in proportion to the dose at all dose levels. The table 1.2 shows average dose received due to different radiation sources (Bølviken, 2001).

Table 1.2: Average annual effective dose per caput.

1.	Source	Dose (mSv.yr ⁻¹)
2.	Natural background	2.4
3.	Diagnostic Medicine	0.4 (0.02-1.2) ¹
4.	Atmospheric weapon testing	0.005
5.	Chernobyl accident	0.001
6.	Nuclear fuel cycle	0.0001
7.	Occupational Exposure	0.001 (1.3) ²

¹Global value (least developed countries-highly developed countries)

²Global value (worker average)

Out of 98% of the average radiation dose received by human beings is from natural sources, about 52% is due to the inhalation of radon, thoron and their progenies present in the dwellings (UNSCEAR, 1988). The International agency for Research on Cancer (IARC) has recognized radon as a class A carcinogen and as such it is considered to have no minimum acceptable dosage threshold (IARC, 1988).

In many epidemiological studies as well as in the case control studies of the radon risk, the excess number of cancers are related to the radon concentration (given in Bq m⁻³), and not to the radon progeny exposure. A justification for such an approach has

resorted to the assumption that there is self compensation between the radiation doses from the unattached and attached fractions (Nikezic and Yu, 2005). As mentioned in the BEIR VI report that there is good evidence that a single alpha particle can cause major genomic changes in a cell, including mutation and transformation which may cause lung cancer as most cancers are of monoclonal origin (James et al., 2004). From this it is concluded that no safe level of exposure can be determined. Quantitative risk estimates may be obtained from a recent large residential study, which are in general agreement with a linear extrapolation of risks observed in miners (Theakston, 2000).

The excess risk of lung cancer due to the radon is about 16% per 100 Bq.m⁻³ throughout a wide range of exposure levels, then radon in homes currently accounts for about 9% of the deaths from lung cancer and hence 2% of all cancer deaths in Europe (Darby et al., 2005).

In order to measure the effect of radon on lung cancer, eighteen case-control studies of residential radon and lung cancer have been published, including seven studies in North America, nine in Europe and two in China. Some of these studies reported a positive or weakly positive association between lung cancer risk and residential radon concentration, while others have reported results consistent with no association (Krewski et al., 2002).

Two approaches can be taken to quantify the relationship between the exposure to ambient radon and radon progeny and the resulting lung cancer incidence: the 'epidemiological approach', in which epidemiological data on lung cancer incidence are directly related to the cumulative exposures and the 'dosimetric approach', in which the lung cancer incidence is predicted on the basis of cellular doses in bronchial epithelium (Hofmann,1998). Epidemiological and dosimetric approaches for determining the dose and risk to the lungs from exposure to radon and its decay products differ by a factor of about 3 (Meinhold, 2004). Data regarding higher dose exposures in miner populations, when extrapolated to low dose levels, suggests a linear no-threshold (LNT) relationship of lung cancer and radon. Ecologic studies are performed to study the effect of a carcinogen in an area (Heath et al., 2005).

Dose from exposure to radon daughters is primarily related to the intake of Potential Alpha Energy Concentration (PAEC) and the conversion coefficient is influenced by aerosol size. James et al. have observed that in the aerosol conditions which are normally encountered, radon concentration is a better index of dose than the concentration of PAEC, which require measurement of the unattached fraction ‘f_p’ attached fraction ‘f_a’ and equilibrium factor ‘F’ to improve the assessment of dose.

The BEIR VI committee has chosen to use the lung-cancer information from studies of miners, who were more heavily exposed to radon, to estimate the risks posed by radon exposure in homes. A linear model for extrapolation of risk from miners to residential populations is a reasonable approach. At present, the “time since exposure” provides a reasonable basis for the risk assessment (BEIR VI; 1999). The BEIR IV committee used data from 4 cohort studies of the underground miners and reported lung-cancer risk associated with radon-progeny using a linear relative risk model: $RR = 1 + \beta\omega$, where $\beta\omega$ estimates the excess relative risk (ERR) (NRC, 1988), ω is exposure and β estimates the increment in ERR for unit change in exposure ‘ ω ’.

Combined analysis of 11 cohorts of over 60,000 underground miners conducted by Lubin et al. and updated by the U.S. National Research Council which provides a comprehensive assessment of the lung cancer risks associated with radon. The BEIR VI committee modeled the excess relative risk (ERR) as a linear function of past exposure to radon. This model allows the effect of exposure to vary flexibly with the length of time that has passed since the exposure, with the exposure rate, and with the attained age. The mathematical form of the model for ERR (NRC , 1999) is:

$$ERR = \beta (w_{5-14} + \theta_{15-24} w_{15-24} + \theta_{25+} w_{25+})\phi_{age}\gamma_z \quad (2)$$

The parameter β represents the slope of the exposure-risk relationship. Exposure in the last 5 years is excluded as it is not biologically relevant to the cancer risk—and exposures in 3 windows of past time, namely 5-14, 15-24, and 25 or more years previously. Those exposures are labeled w_{5-14} , w_{15-24} , and w_{25+} , respectively and each is allowed to have its own relative level of effect, θ_{5-14} (set equal to unity), θ_{15-24} , and θ_{25+} , respectively. The rate of exposure also affects risk through the parameter γ_z ; thus, the effect of a particular level of exposure increases with decreasing exposure rate, as

indexed either by the duration of exposure or the average concentration at which exposure was received. The ERR also declines with increasing age as described by the parameter ϕ_{age} (Lubin et al., 1995).

The BEIR VI suggested two alternative preferred models namely the “exposure-age-concentration model” and the “exposure-age-duration model”. Both of the alternative models calculate the fractional increase in lung cancer risk due to a specified exposure.

For the relatively low exposure rates or long time durations, the risk per unit (WLM) exposure is maximal and increases linearly with the radon exposure (US EPA, 2003). In the present research work “exposure-age-concentration model” has been used in order to calculate the excess lung cancer from the measured indoor radon concentration. Using the ICRP-65 (ICRP, 1993) and UNSCEAR 2000 (UNSCEAR, 2000) dose conversion factors the effective dose to the inhabitants of the selected area was also calculated.

Many uncertainties affected the extrapolation of the risk from miners to the general population, the main being: (i) the average radon concentration in mines was about 100 times higher than in dwellings (ii) the composition of the inhaled air in dwellings is quite different from that in mines (iii) the characteristics of the exposed groups differ widely, miners being strong-built adult males exclusively (Bochicchio, 2005).

1.6. Equilibrium Factor

The short-lived decay products of radon gas are assumed to achieve a state of radioactive equilibrium with their parent in open air, with an effective half-life of about 30 min. If one considers only radioactive disintegration, the state of equilibrium generally varies as a function of the mean age of the radon atoms. Atmospheric processes such as turbulent mixing or wet and dry deposition however results in a state of disequilibrium between the activity concentration of radon gas in air and its decay products associated with the aerosols. The state of equilibrium can then be described by the equilibrium factor, F , i.e. the ratio of the equilibrium equivalent concentration to the radon activity concentration:

$$F = \frac{EEC}{C_{Rn}} \quad (3)$$

There is a wide range of values reported for F from individual outdoor measurements, ranging from 0.1 to 1 (Winkler et al., 2001). Equilibrium factors between radon and its progeny and between thoron and its decay products depend on the ventilation rate inside the room (Misdag et al., 2001; Galmarini, 2006). Knowledge of the amount of the short-lived radon progenies in air is necessary to obtain: (1) equilibrium factor (F) and (2) the unattached fraction (f_p) of radon progeny. The fraction of indoor radon progeny attached to airborne particles is highly dependent on particle concentration (Martell, 1983). Risk from radon as a source of radiation should be evaluated and controlled like the risks from any other radiation sources and that the “as low as reasonably achievable” (ALARA) principle should prevail (Suess, 1995; Godoy et al., 2002). Dose from the radon progenies can be calculated using the dose conversion factor (DCF) which varies for attached and unattached fraction of radon progenies.

$$C_p = C_{pae} + C_{pu} \quad (4)$$

Where C_p is the potential alpha energy concentration, C_{pae} is the aerosol attached potential alpha energy concentration and C_{pu} is the potential energy concentration of the unattached fraction.

$$DCF = DCF_{ae} + DCF_u \quad (5)$$

Where DCF is the dose conversion factor for the radon progenies, DCF_{ae} is the conversion factor for the aerosol attached fraction and DCF_u is the conversion factor for the unattached fraction. The particle concentration varies between 10^3 particles. cm^{-3} and 10^6 particles. cm^{-3} depending upon the aerosols sources and human activities indoors and out doors. Unattached fraction can be approximated by the semi-empirical equation $f_p = 400/Z(cm^{-3})$, where Z is the aerosols concentration. Thus dose conversion factor values for the radon decay product aerosols and the unattached clusters vary between 4-10 mSv.WLM⁻¹ and 0.3-32 mSv.WLM⁻¹, respectively (Porstendörfer, 1999).

The lungs dose due to the unattached radon decay products is much greater than the dose due to the radon progeny attached to the aerosol particles (Yu et al., 2005). Unattached fraction can be measured directly or can be calculated from the concentration measurement aerosols. The f_p values vary from 0.005 and 0.2 and depend on the concentration number of the aerosols (Porstendörfer, 1996).

The dose conversion factor varies in indoor air as $9.1 + 64f_p$. Thus unattached fraction has a greater influence in the DCF. Depending on the aerosols conditions, the dose varies over 4.2-11.5 mSv WLM⁻¹ in homes and in work places it varies from 4.2-7.1 mSv WLM⁻¹. In the case of normal aerosol conditions, the DCF varies 8-11.5 mSv WLM⁻¹ (Porstendörfer, 2001). Freshly generated ²¹⁸Po ions are mostly positively charged (88%) and react rapidly with trace gases and vapors in air and become small particles called clusters or “unattached” decay products with a size spectrum between 0.5 and 3 nm diameters. Neutralisation of the unattached ²¹⁸Po ions can be described by three processes: Recombination with small air ions, electron scavenging by OH radicals formed by radiolysis of water vapour and charge transfer by molecules of lower ionization potential (Pagelkopf and Porstendörfer, 2003; Porstendörfer, 1994).

1.7. Radon Concentration Measurement Devices

The environmental radon concentration is a function of time and climatic conditions. To monitor radon, both active and passive techniques have been developed. Active methods are usually used for short-term measurements of radon. Passive methods are more suitable for the assessment of radon exposure over long time scales and can be used for large-scale surveys at a moderate cost (Ahn and Lee, 2005).

Measurement of ²²²Rn and ²²⁰Rn concentrations can provide information on the upper limit for the potential α -energy exposure due to the presence of their daughters in air. The concentration of ²²²Rn and ²²⁰Rn is generally easier to measure than the concentration of any associated individual daughters (Amgarou, 2003). Radon and its daughters are alpha emitters and its progenies ²¹²Pb, ²¹⁴Bi and ²¹⁰Pb and ²¹⁰Bi are β emitter and γ -rays accompany their β emission. Thus radon or its progenies can be measured by measuring one or other type of radiation emitted by them. Different techniques like nuclear emulsion, adsorption, solid scintillation, liquid scintillation,

gamma spectroscopy, beta monitoring, solid state alpha detectors, electrometer or electroscopes, ionization chambers, surface barrier detectors, Thermoluminescent phosphors and electrets can be used in its measurements. To estimate population exposure, radon concentration instead of radon progeny is generally measured. Solid-state nuclear track detectors (SSNTDs) are low-cost, small-sized devices for large-scale studies in which radon concentration in dwellings can very easily be measured (UNSCEAR, 2000). Further the absorbed dose to the lungs is approximately proportional to the radon concentration rather than to the radon decay product concentration (James, 1987).

In active sampling generally radon and its decay products are brought either into the vicinity of a detector or into a collector device by forced pumping while in passive sampling radon and its decay products are collected through their natural diffusion (or permeation) into the sampler, containing a detector. The terms active and passive are also used to designate radiation detectors which operate with and without power supply, respectively. Totally passive monitoring systems work well for the measurement of only radon gas. Passive measurements are also most suitable for large-scale survey of radon concentrations in the indoor air. The measurements of radon decay products can be carried out by totally active monitoring systems, i.e. by using active sampling and real-time alpha detection and spectrometry. In this regard, some of the most commonly used methods are discussed briefly here.

1.7.1. Passive Techniques

1.7.1.1. Charcoal Canister Technique

Activated charcoal has capacity for adsorbing and retaining radon. Therefore, conventional charcoal canisters can be used to measure radon. It works on the adsorption of radon on charcoal, which was first observed by Rutherford (1906). Charcoal canisters are a convenient screening technique that gives a measure of the average radon over the time period that the canisters are on the site (generally about 1 to 3 days). One advantage of this device is the simplicity of construction. In the configuration described by Cohen and Nason (Cohen and Nason, 1986) a 1.5-centimeter deep bed of charcoal is placed in a commercial metal "ointments can" which has a 3-inch diameter and 1-inch height and a

4 inch diameter hole is drilled in the top of the can which is covered with a fine-mesh screen. This allows radon to enter by diffusion, with little convection. A desiccant is added to remove the water vapor. Before the detector is sent to the measurement site, it is baked out and the hole is covered with tape in order to block the unwanted radon before it is placed in the site where measurement is sought. At the site, the detector is exposed to the ambient atmosphere for time up to one week, after which the tape is replaced. The detector is then returned to the laboratory and is counted with gamma-ray detection system.

1.7.1.2. Solid State Nuclear Track Detectors (SSNTDs)

A heavy charged particle leads to intensive ionization when it passes through insulating materials. Along the path of the particle, a zone called the latent track is created, which is enriched with free chemical radicals and other chemical species. If a piece of material containing the latent track is exposed to some chemically aggressive solution (such as aqueous NaOH or KOH solution), the chemical reaction would be more intensive in the latent track. Such a solution is called the etchant. Through etching, the latent track becomes visible as a particle “track” which may be seen under an optical microscope (Nikezic and Yu, 2006).

Among the attractive features of SSNTD detectors is the availability in different shapes and dimensions, the possibility to be placed practically at any point, the insensitivity to β and γ yields, the high dynamic range and the true time integrating capability. As they do not require power supply or maintenance during the exposure and the costs of the detectors as well as of the processing are rather low, they are suitable for large scale surveys (Sima, 2001).

The most commonly used SSNTD is CR-39, which is based on the polymer of alil diglycol carbonate diethylene glycol bis allyl carbonate (PDAC) having formula $(C_{12}H_{18}O_7)_n$. There are two different modes of its usage in radon measurements: (a) as open (bare) detector and (b) as detector in a diffusion chamber. In the case of bare detector, humidity and dust affect the detection of alpha particles and the detector sensitivity is dependent on the equilibrium factor between radon and its short-lived progeny.

The diffusion chamber is a cup covered with a filter paper on the top and is frequently equipped with a CR-39 detector that is usually placed on the bottom of the cup. Progeny atoms move randomly in the chamber volume and can deposit onto available inner surfaces before decay. The deposition changes the irradiation geometry of the detector, i.e., detector sensitivity is dependent on the fraction of radon progenies decaying in the air prior to the deposition. The behavior of radon progenies inside the chamber (as well as the aerosol properties and air velocity inside the chamber) is unknown and it is difficult to estimate the fraction of radon progenies decaying prior to the deposition. The deposition fraction depends on different environmental conditions (Nikezic and Yu, 2000).

Another type of passive track detector is LR-115 film (Kodak-Pathé, France) (Odqlqlü et al., 2001). The cellulose nitrate LR-115, having a thickness of about 12 µm, is a very useful material for the registration of alpha particles radon exhalation rates of building materials (Amrani et al., 1999). A major drawback of SSNTD is that they only integrate the received flux of particles. They do not provide time dependent response (Misdaq et al., 2001).

1.7.1.3. Electrets

Electret ion chambers are inexpensive, light-weight, passive charge-integrating devices for accurate measurement of different types of radiations. These detectors are more suitable for indoor radon measurements (Dua et al., 1999a,b). Electrets ion detectors which contain an electro-statically charged Teflon disk are widely used for long-term radon measurement. Ions generated by the decay of radon strike and reduce the surface voltage of the Teflon disk. By measuring the voltage reduction, the radon concentration can be calculated. The amount of voltage drop on the electret provides an accurate correlation to the number of ions collected and hence the concentration of the alpha-emitting isotope like radon (Kasper,1999). The longer they are left in place, the better sensitivity they are capable of providing. The EIC system is remarkably accurate and sensitive (Kitto, 2005). Electrets are also sensitive to gamma rays, therefore, correction for it is required when used for the measurement of radon.

1.7.1.4. Thermoluminescent Detectors (TLDs)

When an ionizing particle travels within a crystal it ejects some electrons from their normal position into the conduction band, leaving holes in the valance band. The electrons are then trapped into the defects of the crystal and stored there in a very stable position. If later on the crystal is heated the energy given to the electrons allow them to escape from their trap. Based upon this principle, several types of Thermoluminescent dosimeters have been developed. In this method if alpha particles hit TLD, subsequent heating of it will release an amount of light which is proportional to the total energy of the alpha particles. TLDs are sensitive to alpha, beta and gamma radiation, a procedure has to be adopted to determine the alpha contribution only. Two TLDs one of the TLDs is wrapped in a foil that will exclude all alpha particles, but the beta and gamma radiations are not excluded. After a certain time the TLDs are retrieved and analyzed by heating those to 300 °C in the appropriate read out equipment. The contribution from alpha radiation can be determined by subtracting the energy of first TLD (exposed to only beta and gamma radiation) from second TLD (exposed to alpha, beta and gamma radiation) and hence the radon activity is measured (Tommasino, 1998; Vaupotič and Kobal, 2003).

1.7.2. Active Techniques

1.7.2.1. Ionization Chamber

An ionization chamber is essentially a capacitor, usually of cylindrical shape, in which an electric field is established between two electrodes. If the radon containing air is admitted to the field, the radiation from the decay of the radon daughters atoms will ionize the air and a current will flow between the electrodes. Over a period of approximately 3-4 hours, the radon in the chamber grows into a state of transient equilibrium with its short-lived daughters. Current can be measured any time. For low level of environmental samples typical measurement time ranges from 30 to 60 min. It is possible to measure the concentration of 5 Bq.m⁻³ with an uncertainty of about 10-20 % (Friedmann, 1983).

1.7.2.2. Scintillation Cell

Scintillation produced by the alpha particles are detected by the use of scintillation cells developed by Lucas (Lucas 1957). The cell is coated on the inside with ZnS (Ag), except for a clear window of quartz, glass or plastic. The cells filled with air or other gases containing radon, are placed on top of and with the end window in direct contact with, a photomultiplier in a light-tight enclosure. Energy of alpha is converted into light pulses and the resulting electrical pulses from the photomultiplier are counted by a discriminator /scalar. The activity in the cell will grow over the first three hours before the state of transient equilibrium is established. The normal procedure is to wait 2-3 hours after the filling before the activity is counted. The efficiency of the cell is about 70-80 % . The volume of most scintillation cells is from one hundred to a few hundred cm³. The lower limit of detection is about 0.5 Bq.m⁻³.

Alpha-particle scintillation counting with liquid scintillator: In an alternative scintillation counting technique a liquid scintillator is used in place of the ZnS and the radon laden air is entered into the scintillator. In one application of this approach the radon-bearing air is passed through an organic solvent in which radon is highly soluble at low temperatures. The solvent with radon is then introduced into a vial containing a liquid scintillator. Liquid scintillation are also used for the measurement of radon exhalation LSC offers low detection limit of the exhalation coefficient as low as 0.1 mBqm⁻² s⁻¹ (Bahtijari et al., 2007; Nishikawa et al., 1988). Liquid scintillation technique is popular for radon analysis due to the high solubility of radon in organic solvents (Prichard et al., 1991).

1.7.2.3. Two Filter Method

This technique is used to measure both radon and its daughters concentrations. Air is passed through first filter so that radon daughters are removed and allow the air to pass through a long decay chamber so that the daughters grow again and are collected on the second filter. The filters are counted separately; radon concentration is determined from the second filter and its daughter concentration from the first filter. Air is drawn at a typical rate of 10 ℓ.min⁻¹ and usually for a period of five min. The front filter will remove all the daughters in the air sample and the second filter will collect those daughters being

produced by the decay of radon in the air while it passes through the cylinder. The alpha activity from the filter at the end of sampling is then a measure of the radon concentration in the sample air. For environmental monitoring purposes, large volume two-filter cylinder can have lower limit of detection of 0.7 Bq.m^{-3} .

1.7.2.4. Active Pylon Detectors /Continuous Monitoring

Radon concentration changes significantly and rapidly with time. Therefore grab sampling may not give an adequate value of the radon levels and thus require continuous monitoring of radon. It is the most useful method for studying the effect of atmospheric parameters like pressure, humidity, temperature and wind, etc. on radon concentration. Continuous measurements of radon concentration can be done by AB-5 Pylon monitor (Chalupnik and Wysocka, 2003). Electronic detectors can also be used for the measurement of radon/ thoron and their progenies. These devices give the results of individual daughters and the gas concentration. This is usually based on the gamma ray interaction with matter. Semiconductors like Si or Ge crystal are used for this purpose. This instrument has the property, if programmed, gives the time dependent concentration of radon and its daughters. However these instruments could not be used in field due to the requirement of the power. Some portable solid state devices are now available for this purpose. Method based on small accumulation chambers connected to a continuous Radon Gas Monitor RAD7, is equipped with a solid state alpha detector. The method allows the simultaneous measurements of radon and thoron using only the ^{218}Po peak for ^{222}Rn and ^{216}Po peak for ^{220}Rn . RAD7 can produce an energy spectra in the range of 0-10 MeV with a resolution of 0.05 MeV which differentiates α particles emitted from the progeny of ^{220}Rn and ^{222}Rn . Eight energy ranges, called windows A-H, are defined in the spectrum for data analysis. Window A collects α particles from ^{218}Po decay (6.00 MeV), which is used for the determination of ^{222}Rn .

Window B collects α particles from ^{216}Po decay (6.78 MeV), which is used for the determination of ^{220}Rn . Window C collects α particles from ^{214}Po decay (7.69 MeV) and may also be used for the determination of ^{222}Rn . Filters are installed on the top of the sampler of RAD7 to screen out the progenies of ^{220}Rn and ^{222}Rn , so that only the gas concentrations are measured. A desiccant drying tube containing anhydrous CaSO_4 is

installed to maintain a relative humidity of the incoming air below 10% during the measurements which is monitored by a humidity sensor. The sensitivity of the a particle detector is lowered significantly when the relative humidity is too high (Thomas et al., 2000).

1.7.2.5. Surface Barrier Detector (SBD)

Surface barrier detector is a semiconductor detector which is operated under reversed biased conditions. The alpha particles from radon decay enters the depletion region and creates electron hole pairs. Electron flow in one direction, holes in the other and total number of electrons collected can form an electronic pulse whose amplitude is proportional to the energy of the radiation. However, one disadvantage of the SBD is its sensitivity to light. The thin entrance windows are optically transparent and photons striking the detector surface can reach the active volume (Knoll, 2000).

1.7.2.6. Monitoring of Radon and Thoron Daughters

Dose delivered to the lungs is not due to radon, rather it is due to the short lived radon daughters, therefore it is necessary to measure the daughter's concentrations in different environments. The methods are based on the analysis of the activity from a filter (or detector) on which the daughters have been deposited. Three counts of this activity will determine both the individual daughters concentrations and the potential alpha energy concentration when certain relations are assumed between the daughter's concentrations. If the goal is to measure PAEC, one count exact method is used. For this purpose, there are two commonly used methods Kusnetz and the Rolle methods, differing only in the choice of sampling, waiting and counting times. The protocol is 5-40-2, 5-90-2. With Rolle method counting starts 1-6 minutes after sampling depending upon the length of the counting time. The alpha particles deposited on a filter are counted using scintillation counter.

Two Count Methods

The one count method is simple. By using two uncorrelated counts it is possible to improve one or both of these characteristics. The commonly used two counts methods are Hill Method, James and Strong (J-S) method, Shreve Method, 3R/WL method and Markov method.

Three counts methods

The three uncorrelated counts during and or after samplings are in principle used for individual progeny measurements. The **Tsivoglou method** and the **modified Tsivoglou method** are used.

Tsivoglou method: In the original Tsivoglou method the activity from a filter is measured at three time intervals (i.e. 5, 15, and 30 min after sampling). The amount of air sampled is about 50 l. Because count rates are used instead of integrated counts, even at high concentrations the reproducibility may only be good with in 20-30 %. This method is modified by Thomas and in the Modified Tsivoglou method integration at the three intervals are used instead of count rates which reduces uncertainty of the Tsivoglou method considerably. The most commonly used scheme is sampling for 5 min and counting form 2-5 min, from 6-20 min and 21 to 30 min after the end of sampling. By distinguishing between the 6 MeV α -particles from ^{218}Po and the 7.69 MeV from ^{214}Po α -particles concentration of radon daughters can be calculated. However, in this case the delay between the sampling and counting should be as small as possible due to the short half life of ^{218}Po (NEA/OECD, 1983).

1.8. Sampling Methods of Radon Measurements

Depending on the equipment used, the sampling techniques may be divided into the following categories.

1.8.1. Sampling Based on Radon Adsorption

By adsorption, an extremely thin layer of radon gas adheres to the surfaces of the solids. Important adsorbent materials for radon are silica gels and zeolite minerals. Passive radon measurements can be achieved by adsorbing radon on activated charcoal, which is analysed by gamma ray spectrometry at the end of the exposure. Passive detectors such as TLDs can also be used in combination with activated charcoal. The activated charcoal detectors have a response that is highly dependent on the temperature and humidity.

1.8.2. Sampling Based on Radon Solubility or Absorption

Radon is moderately soluble in water and its solubility depends on water temperature, the colder the water, greater is the solubility of radon. At normal environmental temperature,

radon concentrations are greatest, intermediate and least in the organic liquids, gas and the water phases, respectively.

1.8.3. Diffusion-based Samplers

Diffusion-type samplers are based on the natural diffusion of radon gas into the vicinity of a detector or a trapping medium (typically activated charcoal). Transport of radon gas through a porous membrane occurs predominantly by diffusion through the free space represented by the pore structure. Porous membranes always ensure that aerosol and radon daughters will not enter into the sensitive volume of the detector. It is used for the discrimination of radon and thoron. Diffusion-based transport across porous membranes is also subject to the deposition of particulate material in the membrane pores, which leads to a decrease of the diffusion efficiency.

1.8.4. Permeation-based Samplers

An efficient way to eliminate thoron and water vapour is to use permeation-based samplers. The cup-type container is closed by a nonporous membrane, in which the radon transport occurs by permeation. Permeation across a non-porous membrane is controlled by the solubility of the gas in the membrane material and by the diffusion of the dissolved molecules across the membrane under a concentration gradient. Using a suitable cup volume, thickness, area and the diffusion characteristics of the permeation membrane, it is possible to discriminate the thoron gas and to measure radon concentration. Polyethylene-based permeation samplers with activated charcoal or liquid scintillators have been successfully used for the measurement of radon gas in water (Dixon and Scivyer, 1999).

1.9. Etched Track Detectors

As this research work has been performed using SSNTDs, therefore it would be informative to briefly discuss track formation materials and basic principles of the formation of tracks in it. The study began in 1958 when Young observed etched tracks of fission fragments in LiF crystals. The number of these tracks showed a complete correspondence with the estimated number of fission fragments being recoiled into the crystal from the uranium foil. In 1959, Silk and Barnes observed hair latent tracks of fission fragments in mica using Transmission Electron Microscope (TEM). During early

1960s the team of Walker, Fleisher and Price pioneered the extensive development of this method. They extended the etching technique of Young to mica, glasses, plastics and mineral crystals (Fleischer et al., 1975; Durrani and Bull, 1987).

Due to the durability, the simplicity and the specific nature of the response of Solid State Nuclear Track Detectors (SSNTDs) led to their rapid application in a wide variety of applications in many branches of science and technology. These applications include studies in nuclear physics, radiography, cosmic rays, dosimetry, environmental science, geosciences, indoor radon measurement, earth sciences, mineral exploration, etc. (Fleischer et al., 1975).

The basic principle of track detectors is based on the fact that the passage of a heavily ionizing charged particle through a solid insulator creates microscopic trails of radial damage along its path. These latent tracks can be visualized by etching these trails. Particle tracks are formed in many insulating materials but not in conductors or semiconductors. The classification of track-storing and non-track-storing materials depends on electrical resistivity. Materials with values greater than $\sim 2000 \Omega\text{-cm}$ generally store tracks (Durrani and Bull, 1987). The condition for stable latent-track formation is sometimes expressed as a limiting value for the material resistivity. However, there is not a unique value of resistivity above which the track effect always appears. In this way, the material resistivity cannot serve as the unique criterion for track formation. Although the track effect is relatively well known and the technique is rather simple and straightforward, yet there is not a unique theory that explains track formation. However, the basic physical processes phase in which the initial particle delivers its energy to the atoms surrounding its path is very short in time; stopping of the particle occurs within a time of the order of picoseconds. A series of ionizations and excitations occurs and will create more and more free electrons and damaged molecules are created close to the particle track. Physiochemical phase, new chemical species are created by interactions of the damaged molecules. During etching, the interactions of these new chemical species with the etching solution are stronger than that with the undamaged detector material.

1.10. CR-39 Polymeric Track Detectors

CR-39 (Columbia Resin-39) is the trade name of the thermoset plastic which is a polymeric form of diethylene glycol bis, allyl carbonate (PDAC). Its simple formula is $(C_{12}H_{18}O_7)_n$. Its excellent nuclear track recording properties were first reported by Cartwright et al in 1978. CR-39 can detect protons of energy up to 10 MeV and has a wide range (several tens of MeV) for α -particles detection (Durrani and Bull, 1987). CR-39 is highly isotropic, homogenous, relatively stable to the environmental conditions (unlike, say, LR 115). Much-work has been done to study the properties of CR-39 (Al-Najjar and Durrani, 1984; Green et al., 1982) confirming that it is a desirable solid state nuclear track detector.

The track recording efficiency of CR-39 also depends on the processing conditions and can therefore be modified, to some extent, by the processing conditions adopted. This includes etchant type, strength, temperature, and etching time. Extensive work has also been done to optimize the etching conditions using NaOH and KOH (Durrani and Bull, 1987).

1.11. Formation of the Latent Tracks

The range of a 6 MeV alpha particle in CR-39 is only about 40 μm , which means that on the average ~ 3700 ion pairs are created per micrometer, or 3–4 ion pairs per nanometer. This primary ionizing process triggers a series of new chemical processes that results in the creation of free chemical radicals and other chemical species. Along the path of the alpha particle, a zone enriched with free chemical radicals and other chemical species is then created. This damaged zone is called a latent track. In conductive materials and in semiconductors, the process of recombination occurs and the latent tracks are not stable. A comprehensive survey on the materials that show the track effect is given by Fleischer et al (Fleischer et al., 1975).

As a result of the electronic and atomic collision-cascades, a cloud of interstitial atoms and vacancies are formed in the close vicinity of the ion trajectory. In inorganic solids the minimum energy of an atom to be removed from its original site and be displaced to another site (i.e. displacement energy) is of the order of 10–15 eV. On the

other hand the organic plastic detectors being made of long chain of molecules, the energy required to break the chain is considerably low i.e. 2–3 eV.

In order to explain track formation, several models/criteria have been proposed. These include, total energy loss model (dE/dx), primary ionization criterion, Restricted Energy Loss (REL), Secondary-Electron Energy Loss, Radius-Restricted Energy Loss (RREL) and lineal event-density (LED). Each criterion has its merits and demerits and is open to criticism. For further details the reader is referred to Durrani and Bull (Durrani and Bull, 1987). All the above models are used to explain the track formation in polymers while for crystals the following models are used.

1.11.1. Thermal-Spike Model

In this model it is assumed that energetic particle produce intense heating of the localized region in the lattice. The energy loss leads to electronic and atomic collisions. The atomic collision-cascade deposits its energy in the close vicinity of the ion trajectory. The thermal spike model simplifies the complex effects of the atomic collision-cascade by assuming a simple thermal distribution. According to the thermal spike model the deposited energy corresponds to an abrupt temperature rise in a small cylindrical volume around the ion trajectory at the time of passage $t = 0$. With the passage of the time i.e. for $t > 0$, thermal energy diffuses away from the ion trajectory. The thermal spike creates defects via thermal activation which are remaining as ‘frozen defects’ along the ion trajectory due to the rapid quenching of the temperature. In order for a material to register track the heat conductivity in the material should be low. Electron-phonon collisions are expected to be the predominant energy loss process in insulators and the excitation is communicated to the lattice more efficiently in such materials. This explains the inability of metals to show etchable tracks as the thermal spike becomes too broad and diffuses in the metal lattice, whereas in insulators a narrow intense spike is produced which leads to sufficient localized radiation damage capable of producing etchable tracks.

1.11.2. Ion-Explosion Spike Model

In ion explosion spike model a charged particle passing through the insulating material results in a high concentration of positive ions along its path due to the coulomb interaction. If the recombination time is long compared with the lattice vibration time

($\sim 10^{-13}$ s) mutual repulsion drives the ions into interstitial positions and leaving behind a vacancy-rich cylindrical core. For track formation, the electrostatic stress (i.e. the Coulomb repulsive forces within the ionized region) should be greater than the mechanical strength or lattice-bonding forces. The maximum permissible density of free electrons must be low. This condition restricts track formation to good insulators and excludes metals. The positive ion core contain a high concentration of holes. Tracks will not be formed in materials having high hole mobility. This model is currently the most widely accepted in the tracks field.

1.11.3. Track Formation in Polymers

In organic polymers, the passage of heavily charged particles results in scissions or a number of broken polymer. Chemically reactive sites are formed at the points of scission, which may be enlarged when an etchant such as NaOH enters the damaged region by dissolving the distorted and degraded portions. Both ions and excited molecules may acquire considerable vibrational energy and undergo bond rupture to form a complex array of stable molecules, free radicals and ionized molecules. The net effect on the plastic is the production of many broken molecular chains and production of a damaged region known as latent tracks.

The latent track is chemically transformed or removed by an etchant that leads to an observable etched track. The evolution of track shape during the etching process depends mainly on the ratio of track etch rate V_T and bulk etch rate V_B .

1.12. Chemical Etching

The process of enlarging the size of the latent tracks produced by heavily ionizing particles is called etching and the solution used for this purpose is called etchant. The size of track depends upon the concentration of etching solution, etching time and temperature.

In order to etch the detectors, an elastic spring (holding many detectors) is attached to a wire and immersed into the etching solution within a beaker. The top of the beaker is covered with a glass lid to avoid evaporation. The beaker is then placed in a temperature controlled water bath. At the end of the etching, the detectors are removed and washed under running tap water, to remove the etching residue from the etch pits.

After drying, the detectors are counted under an optical microscope. The etched track diameters are typically a few μm in size and grow larger in size after prolonged etching. During the chemical etching material is placed in a suitable etchant, the solution preferentially attacks the damaged core of the track and penetrates along its length with track etch velocity V_T while the surrounding undamaged material is attacked at a lower rate of bulk etch rate V_B , the bulk etch rate velocity. V_B is generally constant for given etching conditions, whereas V_T depends on the amount of damage present in the region of the core. Track development is governed by the ratio $V = V_T/V_B$ and track formation is not possible if $V \leq 1$. In other words, the condition $V > 1$ must be fulfilled for tracks to be formed.

The simplest case of track development refers to that when the incident particle enters a detector under normal incidence with respect to the detector surface. In this case the track formed is circular in shape and the parameters that are used to describe the geometry of etched tracks are shown in Figure 1.1. As may be seen in this Figure, R = full length of the latent track (unetched); L = length of track attacked by the etchant up to a given moment; L_e = observed length of the etched track; h = thickness of the surface removed by etching; d = diameter of the etch-pit opening.

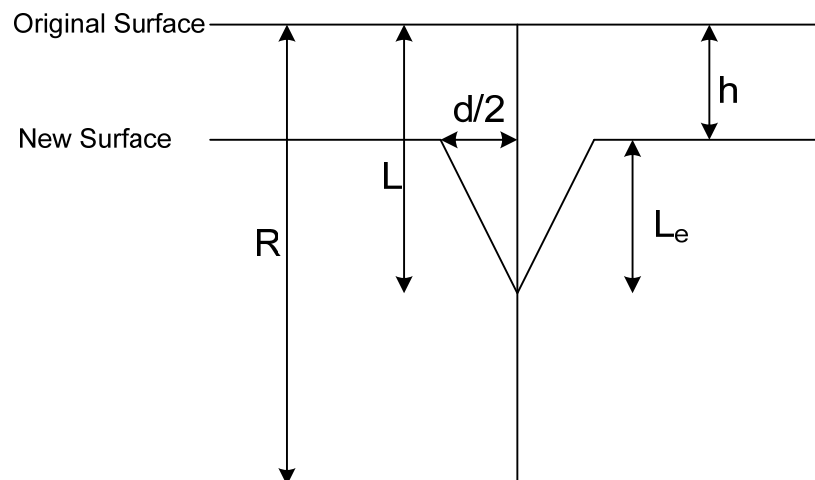


Figure 1.1: Some parameters used to describe the geometry of the etched tracks.

The linear rate of attack down the track is V_T is assumed to be very small compared with the final dimensions of the etched track, so that during etching time t , the etch pit will extend to a distance L from the point of origin, where $L = V_T t$. However, the surface is also being removed at a rate V_B , so that the length of the etch pit is

$$L_e = V_T t - V_B t \quad (6)$$

the formation of a cone with semi-cone angle δ given by

$$\sin \delta = \frac{V_T t}{L} = \frac{V_B t}{V_T t} = \frac{V_B}{V_T} \quad (7)$$

This angle $\delta = \sin^{-1} \left(\frac{V_B}{V_T} \right)$ is also known as the critical angle of etching (θ_c). In materials such as glasses where V_T is not very much greater than V_B , etched tracks with large cone angles are produced. In plastics and minerals in which $V_T \gg V_B$, long needle-like tracks of much smaller cone angle are usually produced.

The diameter of the track may be calculated by using the following relation (Durrani & Bull)

$$d = 2V_B t \sqrt{\frac{(V_T - V_B)}{(V_T + V_B)}} \quad (8)$$

The diameters of the surface openings of etched tracks increase with increasing V_T , reaching a maximum of $2V_B t$ when $V_T \gg V_B$.

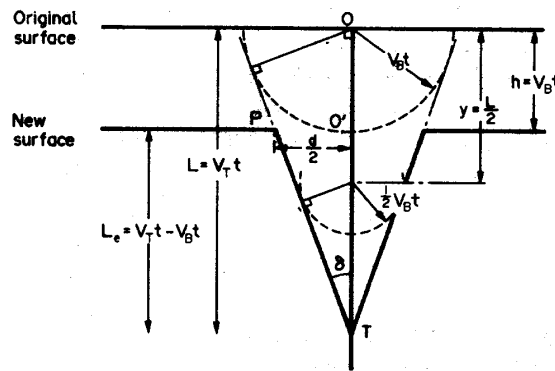


Figure 1.2: Construction for the calculation of etched-track parameters for a track of constant V_T , lying normally to the detector surface. The semi-cone-angle is denoted by δ .

In most realistic applications, the incident particles strike the detector with oblique incidence instead of normal incidence. But in case of radon and its progenies alphas or cosmic rays all incident angles are possible. It is, therefore, important to describe track growth for oblique incidence. This problem was considered in detail by Somogyi and Szalay (Somogyi and Szalay, 1973). The cross-section between a track in the conical phase and the post-etching surface is an ellipse and the corresponding track opening is elliptical. The ellipse is characterized by its major axis D and its minor axis d . These two parameters are important characteristics of a track opening for oblique incidence.

According to Somogyi and Szalay during the etching, the major axis of the track opening passes through three phases, while the minor axis develops through two phases. After some lengthy calculations, it can be shown that major axis diameter of elliptical track is given by (Durrani and Bull, 1987).

$$D = \frac{2V_B t \sqrt{V_T^2 - V_B^2}}{V_T \sin \theta + 1} \quad (9)$$

Where as the expression for minor axis d of the track opening, could be calculated using the following relation.

$$d = 2V_B t \sqrt{\frac{V \sin \theta - 1}{V \sin \theta + 1}} \quad (10)$$

In order to determine V_T , CR-39 is usually irradiated with ^{252}Cf fission fragments at normal incidence. Then, for $\theta = 90^\circ$, the relation for d can be simplified as

$$D = d = 2V_B t \sqrt{\frac{V - 1}{V + 1}} \quad (11)$$

Where $V = V_T/V_B$. As the track etch rate for fission fragments is very much higher than the bulk etch rate (so that $V \gg 1$), the above equation reduces to:

$$D = d \cong 2V_B t$$

$$V_B \cong \frac{D}{2t} \quad (12)$$

Thus a measurement of the diameter of the normally incident fission-fragment tracks at a known etching time yields a value for the bulk etch rate. For further details, the reader is referred to Durrani and Bull, 1987.

1.13. Natural Radioactivity

Natural sources of radiation are cosmic rays and naturally occurring radioactive substances existing in the earth itself and inside the human body. Natural sources that account for exposure to the environmental radiation include radon (59%), terrestrial gamma rays (19%), cosmic rays (12%), and water and food (10%). Terrestrial gamma radiation dose rates vary mainly with geology, building materials, housing type and age of the building (Billon et al., 2005). The annual global per caput effective dose due to the natural radiation sources is 2.4 mSv (UNSCEAR, 2000). Few regions in the world, which are known for high background radiation areas (HBRAs), are due to the local geological controls and geochemical effects and cause enhanced levels of terrestrial radiation (UNSCEAR, 1993, 2000). Very HBRAs are found at Guarapari, coastal region of Espirito Santo and the Morro Do Forro in Minas Gerais in Brazil (Bennett, 1997; Paschoa, 2000). Yangjiang, in China (Wei and Sugahara, 2000); southwest coast of India (Sunta, 1993); Ramsar and Mahallat in Iran (Sohrabi, 1998) in the United States and Canada (NCRP, 1987). The interactions of cosmic-ray particles in the atmosphere produce a number of radionuclides, including ^3H , ^7Be , ^{14}C and ^{22}Na . These nuclides are called cosmogenic nuclides.

Naturally occurring radionuclides of terrestrial origin (also called primordial radionuclides) are present in various degrees in all media in the environment, including the human body itself. Only those radionuclides with half-lives comparable to the age of the earth and their decay products, exist in significant quantities in different types of materials. Secondary radionuclides are radiogenic isotopes derived from the decay of primordial radionuclides. They have shorter half-lives than primordial radionuclides. Natural environmental radiation depends on geological and geographical conditions (Klement, 1982).

Irradiation of the human body from external sources is mainly due to the gamma radiations from radionuclides in the ^{238}U and ^{232}Th series and from ^{40}K . These

radionuclides are also present in the body and irradiate the various organs with alpha and beta particles, as well as gamma rays. Some other terrestrial radionuclides, including those of the ^{235}U series, ^{87}Rb , ^{138}La , ^{147}Sm and ^{176}Lu , exist in nature but at such low levels that their contributions to the dose to humans is negligible. Terrestrial radionuclides present at trace levels in all soils, however, the specific levels are related to the types of rock from which the soils originate. Higher radiation levels are associated with igneous rocks such as granite and lower levels with sedimentary rocks. The activity concentration of ^{40}K in soil is an order of magnitude higher than that of ^{238}U or ^{232}Th .

Building materials contribute to the gamma radiation, mainly ^{40}K , ^{226}Ra , ^{232}Th and their progenies. Radioactivity levels in various building materials such as soil, sand, etc. have been reported by many workers from different geological regions in the world (Beretka and Mathew, 1985; Zikovsky and Kennedy, 1992; Tahir et al., 2005). Natural radioactivity in soil depends on soil type, mineral make up and density. Igneous rocks of granitic composition are strongly enriched in Th and U (on an average $15\ \mu\text{g g}^{-1}$ of Th and $5\ \mu\text{g g}^{-1}$ of U), compared to the rocks of basaltic or ultramafic composition ($<1\ \mu\text{g g}^{-1}$ of U). There are exceptions, however, as some shales and phosphate rocks have relatively high content of those radionuclides (Tzortzis and Tsertos, 2004). These radionuclides are also part of food cycle and it is contained in variable amount in different types of consumable items. The level of uptake depends on the physical and chemical properties of the radionuclides and also on the environmental matrix of interest. In order to measure the concentration of these primordial radionuclides and the dose delivered by it, various types of instrument are used. These primordial nuclides are generally detected by the gammas emitted by these nuclides. The ambient gamma dose rate can be measured by using a NaI(Tl) Scintillometer (Amutha et al., 2005).

Instrumental neutron activation analysis (INAA) can be used for accurate elemental determination, as it is a powerful method for the direct analysis of solid food samples without dissolution thus eliminating the possibility of contamination. The technique also offers low detection limits for many inorganic elements (Waheed et al., 2004). For larger areas to be surveyed natural radionuclides aerial survey are also carried out. In such type of surveys gamma-ray spectrometer of energy range of 40 keV to 3000

keV with data control and storage and flight positioning instrumentation are used (Schwarz et al., 1992).

External exposure indoors depends mainly on construction materials (i.e. on concentrations of radionuclides present in these materials). Serious efforts should be made to understand relationships between exposure and construction materials, in order to find out the ways of assessment of this exposure and identify practical and user-friendly ways of evaluation from the point of view of radiation protection. For this reason the studies of exposure owing to the radionuclides in construction materials and their radiological evaluation are performed. Indoors dose rate depends on parameters like amount of construction material used and geometry of the premises. The most important parameter is concentration of radionuclides in the construction materials (Pilkyte et al., 2005). The availability of large intrinsic germanium detectors such as high purity germanium detector (HPGe) has opened new perspectives for fast, accurate and reliable environmental measurements. Both NaI(Tl) and HPGe detectors are most commonly used with the striking contrast of results obtained with these two types of detectors. Resolution with HPGe detectors is better by a factor of 30 or more than that obtained with NaI(Tl) conventional detectors. As a result of the improved resolution, many nuclear energy levels that could not even be seen with NaI(Tl) detectors are identified easily with HPGe detectors (EG&G, ORTEC).

Due to the large decrease of counting efficiency with the distance from detector surface, which limit the usefulness of tall beakers, it was suggested to count large environmental samples in reentrant beakers, which covers the detectors from all directions, called Marinelli beakers or also inverted well beakers (IEBB, 1997). Densities of environmental samples vary appreciably, typically from 0.5 g.cm^{-3} (dry organic material) to 1.5 g.cm^{-3} (soil). This is the reason why it is so important to be able to prepare a calibrated Marinelli standard in each laboratory (Lavi and Alfassi , 2005). The use of extended sources in γ -ray spectrometry improves the sensitivity of detection thus enabling the measurement of low-activity environmental samples

Chapter Two

Experimental Procedures and Salient Features of the Selected Area for the Present Study

Having briefly discussed radon, its health hazards and natural radioactivity in the previous chapter, this chapter deals with the geology, building characteristics, climate, populations and building materials of the selected area. Different types of active and passive equipments used for the measurement of indoor radon and sampling procedures have also been discussed.



Figure 2.1: Map of the selected area. The shaded portion in the above map shows the selected area.

2.1. Geology and Physical Features of the Area Surveyed

The major portion of the selected area (shaded portion in Figure 2.1) lies in Peshawar basin which is intermountain basin situated at the southern margin of the Himalayas and northwest of the Indus Plain. It came into existence during the plio-Pliocene time due to the uplifting of the Attock-Cherat Range. The lower Swat-Buner Schistose group and Swat granitic gneisses bound the Peshawar basin in northeast (Burbank and Tahirkhele 1985). These rocks are regarded to form the base of the stratigraphic sequence of the basin. The southern part of these rocks covers the Malakand Mountains and stretch eastward into the lower Swat-Buner area. The areas surveyed in this study comprised of low hills and alluvial plains in the Mardan, Swabi and Charsadda districts. The plains have mixed composition of eroded materials from the hills including clays, sand and pebbles (Riaz et al., 1998; Martin et al., 1962). The Bajuar agency consists of diorite rocks which indicates a continuation of metamorphic and igneous rocks consistent with the northern mountain chain. Soils in the Bajuar agency are considered to be generally fertile, varying from silt loam to loam containing a medium degree of organic matter (SIEE, 2005). Mohmand agency has diverse igneous lithologies which occur as alternating sheeted masses, intrusive, apparently concordant along the sequence of metasediments of Paleozoic age and metabasites. Sufaid Koh range forms part of the Cretaceous-tertiary Himalayan orogenic system. The rocks are of Triassic, Carboniferous and older–Paleozoic ages (Siraj et al., 2000).

The district Swabi may be divided into two parts, the northern hilly areas and the southern plain. The major parts of these hilly areas are in the northeast. There are also hills on the northwest called Naranji hills, the height of these hills are from 750 m to 1400 m. The plain areas of the district are intersected by a number of streams and many small riverine. The soil of the Swabi district has developed either from alluvium or loess plains. Texture of river alluvium ranges from sandy loam, sand and loam approaching clay. The soil of loess plains ranges from in texture from silt loam to silty clay loam or silty clay. The soil is irrigated for general cropping with canals supplemented by well-irrigation.

The district Swabi exhibits the following rock units Salkhala foundation, Manki formation, Sobra formation, Tanawal formation, Ambar formation, Misri banda Formation, Panjpir formation, Granites and Sills/Dykes. The Salkhala formation is the oldest unit of the area which comprises chlorite quartzite-mica schist, graphitic schist, marble and quartzite. The formation has been assigned pre-Cambrian age. The Manki formation is characterized by phyllites, slate sand subordinate gray waxes and limestone and quartzite lenses. It is assigned a pre-Cambrian age. Sobra formation consist of limestone with subordinate quartzite and sandstone, its age is pre-Cambrian. Tanawal formation is quite thick and is comprised predominately of quartzite, quartzose sandstone and subordinate argillite, its age is Precambrian. Ambar formation consists of dolomite limestone with interrelations of quartzite and phyllites. It is assigned a Cambrian age. Misri banda Quartzite mainly of quartzite with subordinate argillite and lenses of conglomerates. The age of the formation is early to middle Ordovician. Panjpir formation consists dominantly of argillite, phyllites and subordinate lenses of limestone and quartzite. The formation has been assigned silurian age. Granite and Doleritic Sills/Dykes: In some parts of the district are some granitic rocks and doleritic sills/dykes at places which have been given Permian to carboniferous age.

Mardan district may broadly be divided into two parts. Northeastern hilly area and southwestern plain. The entire northern side of the district is bounded by hills. Rivers flows from north to the south. Most of the streams drain into the Kabul River. Charsadda is a part of the plain called Peshawar valley. This valley presents the appearance of having been remote centuries ago, the bed of a vast lake whose banks are formed by the surrounding mountains and whose waters were fed by the rivers that are now channeling through outfits of the former sub-igneous bed. Hills encircle it on every side except one, where the Kabul River flows out to join the Indus River.

Most of the plains are composed of light and porous sandy soil to a depth of 1 to 6 m below this lies the sandy mixture of clay often combined with beds of nodular limestone followed by gravel and sand. The plain consists of fine alluvial deposits the composition and depth of which varies in different localities and at different distances from the surfaces.

2.1.1. Geography

The district Swabi (district census ,2000) lies between 33-55' and 34-25'N and 71-49' to 72 - 49' East longitudes. It is bounded by the district Buner in the north, in the east by Haripur district, on the south by district Attock, on the west by the Mardan and Nowshera Districts. The district Mardan (district census ,1999) lies from 34-05' N to 34-32' N and 71-48' to 72-25' E. It is bounded on the north by Buner district and Malakanad Protected area, on the east by the Swabi and Buner Districts, on the south by the Nowshera district and on the west by the Charsadda district and the Malakanad protected area. The total area of the district is 1632 km².

Charsadda (district Census Report No. 68) lies between 34-03 and 34-28N and 71-28 and 71-53 E longitudes. It is bounded by the Malakand district on the north, the Mardan district on the east, the Nowshera and Peshawar districts on the south and the Mohmand agency on the west. The Charsadda district lies in the central plain of the Peshawar valley. The Kabul River enters at a point near the south west of the district. It flows along the southern boundary of the district and crosses the district in the extreme south eastern corner. Mohmand agency lies 34° 30' N, 71° 20' E and was created in 1951. It covers an area of 2,296 km² and its population is estimated to be around 334,453. The Mohmand agency shares a border with the Bajuar agency to the north, the Dir district to its east, the district of Peshawar to its southeast and Afghanistan to the west. Bajuar agency, the smallest in size having an area of 1290 km² was created in 1973. Bajuar shares a border with Afghanistan's Kunar province to the north west; Pakistan's Dir district to its north east and the Mohmand agency to its west.

2.1.2. Climatic Conditions

The Swabi, Mardan and Charsadda districts have extreme climates. The summer season is extremely hot. A steep rise of temperature is observed from May to June. Even July, August and September record quite high temperatures. During May and June, dust storms are quite frequent at night. The temperature reaches to its maximum in the month of June. Due to the intensive cultivation and irrigation the tract is humid and the heat is oppressive. A rapid fall in temperature is recorded from October onwards. The coldest month is January. Towards the end of the cold weather there are occasional

thunderstorms and hail storms. The maximum rainfall is received in July and August during which the weather becomes hot and humid. The relative humidity is quite high through out the year. Maximum humidity is recorded in December. No meteorological station is operating in the Swabi and Mardan districts and the data recorded in the Risalpur is the station which can represent the Swabi and Mardan district.

In the Charsadda, Mohmand and Bajuar, the average winter rainfall is higher than that of the summer rainfall. Charsadda district, Mohmand and Bajuar Agencies are close to Peshawar. Therefore, the data recorded in Peshawar can represents the Charsadda and Mohmand agency well. Tables 2.1 & 2.2 show maximum and minimum average temperature, precipitation and humidity recorded at Peshawar. However, the climate of the Bajuar agency is cold and the summer season is relatively less hot while the winter season is very cold.

Table 2.1: Long-term average climatic conditions of Mardan, Swabi as recorded in the meteorological station Risalpur.

Month	Maximum Temperature	Minimum Temperature	Precipitation (mm)	Relative humidity (%)
January	18.3	4	26	58.6
February	19.5	6.3	42.7	57.5
March	23.7	11.2	78.4	58.4
April	30	16.4	48.9	51.7
May	35.9	21.3	27	37.3
June	40.4	25.7	27.7	36.2
July	37.7	26.6	42.3	55
August	35.7	25.7	67.7	64.6
September	35	22.7	17.9	58.7
October	31.2	16.1	9.7	54.9
November	25.6	9.6	12.3	60.1
December	20.1	4.9	23.3	63.7
Mean	29.4	15.9	35.3	60.1

Table 2.2: Long-term average climatic conditions of Mardan, Swabi as recorded in the meteorological station Peshawar.

Month	Maximum Temperature	Minimum Temperature	Precipitation (mm)	Relative humidity (%)
January	17.9	2	35.4	69.3
February	19.2	5.1	53.2	67.5
March	23.8	9.9	80.2	67.1
April	30.3	15.1	46.6	56.4
May	36.6	20	26.2	39.4
June	41.5	24.9	18.3	36.0
July	38.5	26.3	113.4	55.4
August	36.2	25.4	125.8	66.4
September	35.6	22.1	39.9	60.1
October	31.7	14.5	13.8	60.3
November	25.3	7.3	15.7	67.9
December	19.3	2.7	28.9	73.3
Mean	29.6	14.64	597.6	60.1

2.2. Building Characteristics

In the district Swabi 68% houses were constructed at least 10 years ago according to the 1998 census. About 69% housing units were constructed from the baked bricks and cemented blocks. Shaped stones were used in the construction of the outer walls in the urban and rural area in the district. About 65% roofs of the housing units were built of wood and bamboo whereas 23% were built from reinforced cement concrete or bricks (RCC/RBC). According to the latest census, urban proportion of the district Mardan is 20%. Housing units with 2 to 4 rooms is ~ 66%. About 67% housing units were constructed at least 10 years ago according to 1998 census. The district has 50% of the walls in the standard category of baked bricks/blocks and stone with cement bonding and 48% of the houses are made of unbaked bricks with mud bonding. The wooden category is 1%. The predominant construction materials of roofs of the housing units (~75) are built from baked bricks supported by the girder or wooden log/bamboo. While 16% of

the housing units have been bonded with RCC/RBC for roofs. About 7% houses have roofs which have been constructed from the cement/iron sheets. About 71 % of the housing units were constructed at least 10 years ago, according to the 1998 census record. Unbaked bricks/ earth bounded were the main construction material used in the construction of the outer walls of the buildings representing 69% followed by baked bricks, blocks and shaped stones, 28%. In the rural areas, main material used in the construction of walls are unbaked bricks, stones etc., whilst in the urban areas it was baked bricks, shaped stones etc, where this percentage is recorded as 50%. For the construction of roofs, about 85% of the housing units used wood and bamboo as construction materials in the roofs of their buildings. About 8% used reinforced cement concrete or bricks (RCC/RBC), 4% used cement/iron sheet while remaining ~3% have used other construction materials. Marked difference was observed in construction materials in urban and rural housing units though the wood/bamboo is still the main materials used in both the areas. There are ~ 79% housing units in urban areas and 87 % in rural areas that have used such materials.

2.3. Selection of the Houses for Indoor Radon Measurements

In the present study, houses surveyed in the Mardan, Swabi and Charsadda districts were built from baked bricks and cement. Each room contained one or two windows. These included both single and double storey houses. Each house contained at least two rooms. Dosimeters were installed in a bedroom and drawing room of each of the selected house. In the case of double storey houses, dosimeters were installed in bedroom and drawing room located at the ground floor. All the houses surveyed were detached and semi-detached houses. The roofs were made of cement and concrete. Houses surveyed in the Mohmand agency were large detached houses and made of mud and stones. All the houses surveyed were single storey containing relatively larger number of rooms (i.e. up to 10 rooms). There were usually one or no windows in the rooms. The houses surveyed in the Bajuar agency were single storey and were made of mud with poor ventilation system. Each house had at least four rooms. Most of the houses surveyed in the Mohmand agency had no electricity supply.

In each district/agency, forty representative houses were selected for indoor radon levels measurements. Dosimeters were installed at head height in bedroom and drawing room of each house at the ground floor. These dosimeters were exposed to radon for three months in each of the four seasons of the year. After exposure to radon, dosimeters were collected, etched and counted an optical microscope.

2.4. Occupancy Factor

Occupancy factor plays a major role in the dose calculation due to the indoor radon. Therefore, information about the indoor occupancy were collected and average occupancy factor for each district/ agency as well as overall average occupancy factor for the selected area was calculated, which was slightly lower than that reported by other workers (Killip, 2004). Information about the indoor occupancy was collected during the installation of the dosimeters. Information was obtained through direct interviews with the occupants of the houses where the dosimeters were installed. Occupancy factors for the Swabi, Mardan, Charsadda, Mohmand and Bajuar were found to be 0.49, 0.41, 0.48, 0.51 and 0.50, respectively with an average value of 0.48. Besides indoor occupancy, information about the usage of the bedrooms and drawing rooms were also obtained from the occupants. This data revealed that occupants spent ~ 60% of their indoor time in the bedroom and ~ 40% time in drawing room.

2.5. Weighted Average Indoor Radon

Weighted average indoor radon concentration was calculated using the occupancy values of the bedrooms and drawing rooms. Weighted average annual arithmetic mean for each house was calculated using the following formula.

Weighted average radon concentration = $(0.4 \times \text{drawing room} + 0.6 \times \text{bedroom})$ indoor radon concentration (however in the houses where only one detector was retrieved from the home was considered as a representative of that home and was included in the analysis of the data). An average radon level in the bedrooms and drawing rooms levels in each house was calculated. Using the mean annual radon levels in each house, annual effective dose was calculated using the ICRP-65 and UNSCEAR conversion factors (Jing, 2005; UNSCEAR, 2000).

2.6. Seasonal Correction Factor

The seasonal correction factor was calculated by dividing the arithmetic mean of each season (i.e. summer, autumn, winter, spring) by the annual arithmetic mean. The seasonally averaged data as well as yearly averaged data was calculated by adding the summer, autumn, winter, spring data and dividing it by 4, annually averaged data was also calculated. In Pakistan, summer season span over June, July and August, autumn season is from September to November, winter season begins in December and ends in February and spring season begins in March and ends in May (Shamshad, 1988). CR-39 based radon dosimeters were used in this study, which was carried out from June 1, 2005 to May 31, 2006.

2.7. Comparison of Yearly Average and Seasonally Measured Average Measurements

In order to measure effect of the long-term exposure of CR-39 detector with respect to the seasonal measurements, two detectors were installed in each drawing room (living room). One detector was replaced four times (i.e. in each season) during the year for seasonal measurement and the other one was exposed to the indoor radon for the whole year. The results were compared with each other. Using the annual weighted average values of indoor radon concentration and the BEIR-VI formula, excess relative lung cancer risk was calculated.

2.8. CR-39 Detector and its Chemical Etching

CR-39 based National Radiological Protection Board (NRPB), now called the Radiation Protection Division of the Health Protection agency, UK dosimeters were used in this study. CR-39 detectors were etched in 25% NaOH at 80 °C. After measuring track densities manually with an optical microscope, they were then related to the radon concentration level using calibration factor of 2.7 tracks.cm⁻².h⁻¹/kBq.m⁻³ (Miles, 2005).

2.9. Radon Exhalation Rate

In order to study the potential of different building materials as an indoor radon source, radon exhalation was measured in the samples of soil, sand and bricks which were collected from the selected area. Samples were collected in such a way that it were representative of the district/agency and were spatially disturbed over the district/agency.

2.9.1. Setup for CR-39 Detector

In order to study radon exhalation rate from the most commonly used building materials, samples were collected from the Swabi, Mardan and Charsadda districts of NWFP as well as from the Mohmand and Bajuar agencies of FATA, Pakistan. These included soil, sand and bricks sample. From each districts/agency, 10 soil representative samples were collected. In the case of sand, a total number of ten samples (i.e. 2 samples per district/agency) were collected from streams wherefrom people collect & transport sand and use it in the construction of their houses. Due to the inconvenience, bricks are not commonly used in agencies. Therefore, brick samples were collected only from the Swabi, Mardan and Charsadda districts (4 samples per district).

All the samples were crushed and dried in an oven at 110 °C. These samples (each weighing 200 g) were then put into the plastic containers of volume $5.4 \times 10^3 \text{ cm}^3$. The grain sizes of soil/brick and sand were 0.002 mm - 0.06 mm and 0.06 mm to 2 mm, respectively. The texture of the soil/brick samples was uniform and fine whereas the texture of the sand samples was coarse. No compaction was used during the placement of the samples in the containers (Just slight shaking was performed to level the surface of the samples). In order to sieve the crushed samples, 200 and 250 meshes were used.

After installing the CR-39 based NRPB radon dosimeters at a height of 25 cm from the surface of the samples, the containers were then hermetically sealed. Dosimeters were exposed to radon for 40 and some for 80 days. This resulted in exposure of the dosimeters to variable levels of radon concentration (i.e. starting from zero concentration level to equilibrium concentration level). In order to calculate the effective time of the radon exposure, following relation was used (Durrani and Iliç, 1997)

$$T_{effective} = t - \tau(1 - e^{-\lambda t}) \quad (1)$$

Where τ is the mean life of radon (5.5 days), t is the total exposure time (days) and λ is the ^{222}Rn decay constant.

After the exposure, CR-39 detectors were etched in 25% NaOH at 80 °C for 16 h and counted under an optical microscope. The track densities were related to the radon concentration level.

To study the effect of humidity, a series of experiments were performed by adding different moisture contents in these samples and then the containers were hermetically sealed. Dosimeters were exposed to radon for 60-80 days in phase one, two and three (using dried (0%), 15% and 30% moisture contents by weight) of the experiment and for 65 days in the fourth and final phase using 45% moisture content by weight.

2.9.2. Calculation of the Exhalation Rate

Measured radon concentration values were used to calculate the exhalation rate using the following equations (Rehman et al., 2006)

$$F_0 = \frac{C(t)[\omega A + \lambda V]}{A \left[1 - e^{-\left(\frac{\omega A}{V} + \lambda\right)t} \right]} \quad (2)$$

$$F = F_0 - \omega C \quad (3)$$

Where

A = Surface area of the sample (cm²), V = volume of the void space in a closed chamber,

t = ²²²Rn accumulation time in a closed chamber.

$\omega = \varepsilon \lambda Z_0$, known as back diffusion constant for given material.

Z₀ = Thickness of the sample in the sealed chamber.

C(t) = ²²²Rn concentration just on the surface of the sample which has to be exhaled from the surface of the sample to the void space of the chamber.

$$F_0 = R\rho_b\lambda EZ_0 \quad (4)$$

λ = ²²²Rn decay constant (h⁻¹)

ρ_b = Bulk density of the sample (kg.m⁻³)

E = (E_{air} + E_{water} + E_{solid}) Sum of fractional emanation coefficient of ²²²Rn in air, water and adsorbed phase.

R = Concentration of ²²⁶Ra (Bq.kg⁻¹)

All the quantities on the right hand side in Eq. (2) are known except $C(t)$ which was experimentally determined for CR-39 based NRPB radon dosimeter. Putting the value of $C(t)$ in Eq. (2), exhalation rate, F_0 was determined.

In a closed chamber which contains a sample, ²²²Rn concentration increases with the passage of time from zero to its maximum value. After reaching its maximum value, back diffusion of radon also take place which reduces the ²²²Rn concentration by a factor ω in the chamber. Therefore, exhalation rate F , corrected for back diffusion, was determined using Eq (3). Exhalation rate was also calculated using the following equation (Abu-Jarad et al., 1980)

$$E_x = \frac{CtV\lambda}{S[t-1/\lambda(1-e^{-\lambda t})]} \quad (5)$$

Where E_x is radon exhalation rate (mBq.m⁻²-h⁻¹), C is mean radon concentration as measured by CR-39 detector (Bq.m⁻³), V is volume of the can (m³), t is the exposure time, λ is the radon decay constant and S is the surface area from which radon is exhaled into the closed can.

2.10. Gamma Spectroscopy

Natural radioactivity was also measured in the soil, sand, brick, marble and cement samples collected from the selected area. For the gamma spectroscopy, a total of fifty soil samples (i.e., 10 samples from each district/agency) were collected from three districts and two tribal agencies from undisturbed sites to ensure that there was no influence of man-made structures and anthropogenic activities. Similarly, thirty-eight

samples of the building materials were also collected from the Swabi, Mardan and Charsadda districts as well as from the Mohmand and Bajuar agencies of the federally administered tribal areas (FATA) Pakistan. These included 10 samples of brick from the above-mentioned three districts and 2 samples of sand from each district/agency, 12 marble samples from all the districts/agencies and five branded cement samples from the selected area.

2.10.1. Processing and Preparation of Samples

Samples (each weighting 1.5 kg) were crushed, sieved and dried at 110°C for 24 hours. The samples were placed in Marinelli beakers and were hermitically sealed. These sealed beakers were then placed in undisturbed position for a period of two months in order to attain equilibrium between long-lived parents (^{226}Ra , ^{232}Th , ^{40}K) and their shorter-lived daughters. It may be noted here that if the containers are not hermitically sealed then this will result in some portion of the radon to exhale from the container and thus will underestimate the results. However, escape of radon during crushing will have no effect on the results because after crushing the container were kept for sufficiently long time to attain nearly secular equilibrium after sealing.

2.10.2. Gamma Spectrometry

The gamma spectrometer used for obtaining the spectra was a P-type HPGe detector. The resolution and relative efficiency of the detector for 1332 keV (^{60}Co) was 2.5 keV and 90%, respectively. Figure 2.2 shows the efficiency calibration curve of the HPGe detector using mixed radionuclides calibration source.

The detector and preamplifier were placed inside a low-background well-type lead shielding and cooled by liquid nitrogen from vertical dipstick cryostat. Energy and efficiency calibration of the detector were performed using standard point sources and mined nuclides gamma reference source (from AEA technology QSA GmH, Germany). Background signals were periodically recorded for the similar time periods and were subtracted from each result obtained.

Spectra were collected for about 12 hours in order to get sufficient counts at the desired peaks. ^{226}Ra concentration was determined by means of its progeny photo peaks of gamma-ray lines: ^{214}Pb (295.21 keV, 352 keV) and ^{214}Bi (609 keV, 1120.29 keV),

^{232}Th was determined through its progeny photo peaks of gamma-ray lines: ^{228}Ac (338.32 keV, 911.21 keV, 968.97 keV) whereas ^{40}K activity was measured directly through its gamma-ray energy peak of 1460.83 keV. The software Personnel Computer Analyzer (PCA-II) was used for the collection and analysis of the spectra.

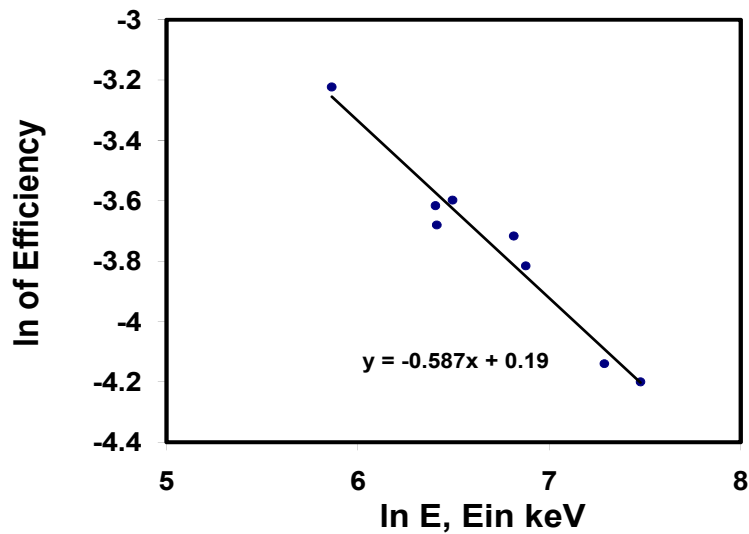


Figure 2.2: Efficiency calibration curve of the HPGe detector using mixed radionuclides calibration source prepared in Marinelli geometry

2.11. Electret Ion Chambers

In order to measure the indoor radon, equilibrium factor and unattached fraction of radon, electret ion chambers (EIC) and electret radon progeny integrating sampling unit (E-RPISU) was used, which are briefly described below.

Commercially available electret ion chambers, so called electret-passive environmental radon monitors (E-PERM), were used for the radon measurement. E-PERM system consists of three components (1) electrostatically charged Teflon called electrets (2) an ion chamber made of conductive plastics to which an electret can be loaded (3) a Voltage reader to read the surface potential of the electrets. In the present study, two types of electrets which were made of Teflon were used. Experiments were performed using both short term (high sensitivity) and long term (low sensitivity)

electrets. The electrets produces electric field and thus are capable of attracting opposite sign charge generated by the decay of radon/thoron and its daughter products within the chamber.

For the measurement of radon/thoron and its progenies different types of chambers were used. Nuclear radiation emitted by radon/thoron or other radioactive materials during decay generates ions in the volume of the conductive plastic and are collected on the charged electrets. There are different configuration of the chambers. The chamber that have a dome and on/off facility, called standard “S” chamber. In the present study the standard chamber having short term electrets (SST) combination was used. In order to read the potential of the electret the electronic instrument called surface potential electric voltage reader (SPER) was used. To measure the potential drop of the electret, before placing the electret in the chamber its initial value was recorded (I), after exposure the final voltage (F) of the electret was recorded, the exposure time in days “D” was also recorded. The calibration factor ‘CF’ for E-PERM was calculated using the standard procedures.

2.12. Measurement of Radon Progenies with Alpha Contamination Chambers

Electret ion chambers (EIC) with its aluminized Mylar window facing down is used to measure alpha radiation from the contaminated surfaces. Area monitored is 48.7 cm^2 and the response of electret ion chamber is used for all the alpha radiations emitted from different isotopes. The results are expressed in alpha counts per 100 cm^2 in 4π geometry.

In the present work EICs were used in the inverted form for the measurement of radon and thoron progenies deposited on the surfaces. In these experiments electret ion chamber with Mylar side was directed upward. Ionization produced by radon progenies were measured instead of alpha contamination on the surfaces. In order to measure the performance factor (PF) of this alpha contamination chamber, radon concentration was measured simultaneously using the standard chambers with short-term electrets. Experiments were performed using both short term (high sensitivity) and long term (low sensitivity) electrets.

As these chambers are also sensitive to gamma radiation, therefore, to correct the readings for the gamma background an additional electret with plastic cover which blocked the detection of alpha radiation was also used.

2.13. Active Solid State Alpha Detector for Measuring the Surface Deposited Activity

To measure the efficiency of different plastics/ filter materials and also to measure the surface deposited α activity active solid state surface barrier detector was used.

Computerized APTEC alpha-spectroscopic multi-channel analyzer was calibrated for the measurement of the radon and thoron progenies. The system worked by connecting semiconductor diode detector through a pre-amplifier and an amplifier and finally into a special MCA card built into the computer.

To calibrate the APTEC (Surface barrier detector) three standard sources, namely ^{230}Th , ^{241}Am 25mm diameter each and ^{230}Th of square shaped source were used. The efficiency of the detector was measured by using ^{241}Am and ^{230}Th which came out to be 0.26. Using the flat ^{230}Th source and having distance of 4 mm between the detector and the source, the efficiency of the detector was measured as 0.19. ^{214}Po source was placed under the APTEC silicon (Si) crystal alpha detector (Surface barrier detector) below the filtering (attenuating) materials (plastics) and the counts were collected for sufficient time in order to obtain peaks for the ^{214}Po and ^{212}Po .

In order to develop passive dosimeters, different types of plastic sheets were used and their efficiencies for radon and thoron progenies were calculated.

2.14. Ultrafine Particle Counter (UPC) P-track

Dose due to the radon/thoron progenies depends on radon/thoron concentration and the attachment of the progenies to the aerosols particles. Unattached fractions of radon and thoron progenies concentration depend on the particle size and number in the indoor environment. Ultrafine particles (particle 0.1 micrometers or smaller in diameter) contribute little to the total mass but exist in very high number concentrations, especially in the urban areas. Particles of this size can almost unrestrictedly enter into the lungs and result in a greater inflammatory potential

In the present study, ultrafine particles were measured on an hourly basis using the Condensation Particle Counting (CPC) P-track system. It uses the condensation particle counting technique. In order to measure the affect of different aerosol generating activities, the following cleaning and burning activities were performed in the indoor environment. HEPA filter, HEPA filter with ionizer, Candle burning, Cigarette smoking, Propane cooker, The Joe smoker system, etc.

Table 2.3: Different types of Materials used for the fabrication of surface deposition dosimeter.

S.No	Material	Gauge
1.	Mylar	8
2.	MM	16
3.	3M2708+M	58
4.	CI75	75
5.	CI92	92
6.	CI75+2708	125
7.	3M125	145
8.	FFMM	200±50
9.	FFM	200±51
10.	FFM-07	200±50
11.	3M114	200
12.	3M146-07	285
13.	3MM	250

2.15. Active Alpha Detectors to Measure Surface Deposited Activity

In order to measure surface deposited activity during the different indoor aerosols conditions, two different types of active solid state detectors were used which were APTEC and Science Applications International Corporation (SAIC) ® Alpha Analyzers of model AP-2 systems.

These handheld AP-2 systems having programmable windows which allowed ^{218}Po , ^{214}Po and ^{212}Po counting for up to one hour with out any interruption. Before its usage these detectors were calibrated using standard sources of ^{232}Th , ^{241}Am and ^{238}U . Using the

calibration information ^{218}Po , ^{214}Pb , and ^{214}Bi - ^{214}Po activities in case of radon and ^{212}Pb and ^{212}Bi - ^{212}Po in the case of thoron progenies activities on the surfaces of the glass sheets were calculated.

A spreadsheet was setup to accept the raw data as an input from the specified detectors, perform the necessary correction and then output the initial activities (equilibrium values) of ^{218}Po , ^{214}Pb , and ^{214}Bi - ^{214}Po . After experimental consideration, the protocol developed by Dumm (Dumm, 2005) was used. This protocol contains a practical set of counting intervals that minimized uncertainty. For instance, the long interval needed to be short enough to be convenient for making several measurements in a day and the SAIC AP-2 detectors could only count for an hour without being restarted. Thoron as the element of interest was determined from its progeny ^{212}Pb which has a half life of 10.6 h for which a protocol was developed to collect the count for one hour.

Air Borne Progeny Measurements

2.16. Measurement of Unattached Fraction using Ludlum scintillation cell

To correlate the airborne radon/thoron attached to the aerosols or unattached progenies activity to the surface deposited activity, both airborne activity and the surface deposited activity measurement were performed simultaneously. Airborne progenies were measured using the active scintillation cell system. Two different protocols were used to measure for radon and thoron progenies due to the difference in their half lives. For the measurement of radon progenies, Tsivoglou method was used which is based on the one minute counting interval for 50 min for the concentration of ^{218}Po , ^{214}Pb and ^{214}Bi – ^{214}Po after sampling of 5 min. For thoron progeny measurement the counting protocol developed by Khan, Busigin and Philips (KBP) was used (Khan and Philips, 1982; Khan et al., 1982). The time at which the surface deposition of thoron was measured a sample from the indoor air was also taken. 50% cutoff of the screen was measured using the relation provided by Knutson et al. Cooking or any other activity involving burning increases the ultrafine particles concentration.

2.17. Electrostatic Collection of Alpha-emitters (RAD7 Active Detector)

In order to measure ^{222}Rn and ^{220}Rn in the exposure room, active detector RAD7 was used which works on the principle of electrostatic collection of the α -emitters with

spectral analysis. The RAD7 system contains a solid-state ion-implanted planar silicon detector and a built-in pump with a flow rate of $1 \text{ l}\cdot\text{min}^{-1}$. The detector operates in external relative humidity ranging from 0% to 95% and internal humidities of 0% – 10% with a sensitivity of 4 Bq m^{-3} and an upper linear detection limit of 800 kBq m^{-3} . The detector was calibrated with an accuracy of $\pm 5\%$. The spectra are in 200 channels and the RAD7 groups these channels into eight windows of energy ranges. A, B, C, and D are the major windows and E, F, G, and H are the diagnostic windows. Window A covers the energy range from 5.40 to 6.40 MeV, showing the total counts from 6.00 MeV α particle from the 3-min ^{218}Po decay (daughter of ^{222}Rn). Window B covers the region 6.40 MeV – 7.40 MeV, showing the total counts of 6.78 MeV α -particles from the ^{216}Po (^{220}Rn daughter). Window C represents total counts of the 7.69 MeV α particles from ^{214}Po (the fourth nuclide in the ^{222}Rn decay chain), while the window D represents the total counts of the 8.78 MeV α particles from the decay of ^{212}Po (the fourth nuclide in the ^{220}Rn decay chain). In other words, windows A and B represent “new” ^{222}Rn and ^{220}Rn , while windows C and D represent “old” ^{222}Rn and ^{220}Rn , respectively. The RAD7 separates ^{222}Rn and ^{220}Rn signals by their progeny's unique α - particle energies with little cross-interference (Durrige, 2000). In the present work RAD7 data of radon and thoron was collected on hourly basis while collecting the surface deposited or airborne activity. Relative humidity(RH) in the instrument was maintained below 10% throughout the measurement. In the case it is raised above 10%, then desiccant should be replaced as it would be depleted. The RAD7 underestimate (reads low) if the internal RH rises above 10%. For thoron the sample tubing was kept short in order to reduce its decay in the tube due to its shorter half life.

Chapter Three

Natural Radioactivity Measurements in Pakistan - An Overview

3.1. Introduction

Over the last few decades, there has been an increased concern about the public exposure associated with the enhanced natural radiation environment. The study of the distribution of primordial radionuclides allows the understanding of the radiological implication of these elements due to the γ -ray exposure of the body and irradiation of lungs tissues from inhalation of radon and its daughters (Alam et al., 1999; Singh et al., 2005).

The presence of natural radioactivity in building materials results in the internal and external exposure to the occupants. In particular, it is important to assess the radiation hazards arising due to the use of soil, sand and other building materials in the construction of dwellings. Assessment of the gamma radiation dose from natural sources is of particular importance because it is the largest contributor to the external dose of the world population (UNSCEAR, 1988). The most commonly encountered primordial radionuclides are ^{238}U , ^{232}Th , their decay products and ^{40}K . The level of the natural radioactivity in soil, in the surrounding environment and the associated external exposure due to the gamma radiation depends primarily on the geological and geographical conditions of the region (UNSCEAR, 2000).

A normal male containing 140 g of K has about 4400 Bq due to ^{40}K . Since K is found in the intracellular fluids, about 98% of the K in the body is within cells. Thus at least 98 % of these disintegrations take place within the body cells and are potentially capable of altering the cell's DNA. The body content of K is under strict homeostatic control and is maintained at a relatively constant level of about 140g/70 kg. This natural ^{40}K delivers a dose 0.2 mSv/yr to the gonads and other soft tissues and 0.15 mSv/yr to bone. In soil and other rocks, its concentration has a vast variation. Average

concentrations of ^{40}K in continental crust and soil are 850 and 400 Bq.kg^{-1} , respectively where as in rocks it ranges from 70 - 1500 Bq.kg^{-1} (Rowland: <http://www.rerowland.com/K40.html>; Eisenbud and Gesell, 1997).

Due to the increasing social concern, a large number of research groups are engaged in the measurement of natural radioactivity on national levels worldwide (Tzortzis and Tsertos, 2004; Ahmed et al., 1997; Merdanoglu and Altinsoy, 1997; Tzortzis et al., 2003; Veiga et al., 2006; Xinwei, 2005). In this regard, considerable work concerning the measurements of natural radioactivity and indoor radon have also been carried out in Pakistan. In this regard, a brief review of the published data so far, is presented in this chapter

3.2. Summary of the Studies Conducted in Pakistan

Measurement of natural radioactivity in Pakistan gained momentum in early 90's and a number of articles were reported in the international research journals. In this regard, Tufail et al., 1994a&b; Tufail et al., 1992a&b; Tufail et al., 1993) have reported gamma activity in the samples of bricks which were collected from the Rawalpindi and Islamabad areas, ceramic products of Lahore and in cement samples collected from several factories of Pakistan. They have also measured activities in the dwellings of some selected areas of Pakistan. Ali et al. (1997) have reported gamma-ray activity and dose rate from brick samples collected from some areas of the North West Frontier Province (NWFP), Pakistan. Qazi and Jafri (1996) have reported measurement of radio-ecological survey on Miocene-Pliocene rocks of Qabool Khel area. Khan et al. (1998) have measured natural radioactivity due to ^{40}K , ^{226}Ra and ^{232}Th in the samples of phosphate rock, which were collected from various localities of the Hazara division of Pakistan as well as from the locally prepared products and imported fertilizer. Jamil et al. (1998) have reported measurements of radionuclides in coal samples collected from the Punjab and Balochistan provinces. Butt et al. (1998) have carried out environmental gamma radiation mapping of Pakistan. Zaidi et al. (1999) have reported radium equivalent activity in sand samples and building materials collected from the Rawalpindi/Islamabad. They have also measured uranium and thorium contents in the collected samples using

instrumental neutron activation analysis(INAA). Tufail *et al.* (2000) have reported natural radioactivity in marble samples.

Iqbal *et al.* (2000) have reported ^{226}Ra , ^{232}Th and ^{40}K activities in marble samples using NaI (TI) gamma-ray spectrometer with a matrix-inversion-based spectral stripping technique. Khan and Khan(2001) have monitored natural gamma-emitting radionuclides in Portland cement manufactured in the North West Frontier Province (NWFP) of Pakistan. Aslam *et al.* (2002) have determined natural radioactivity in various types of marbles available in the Rawalpindi/Islamabad using HPGe gamma-ray spectrometer. Khan *et al.* (2002) have measured activity concentrations of natural gamma-emitting radionuclides in baked brick samples, collected from six highly populated areas of the North-West Frontier Province (NWFP) of Pakistan. Ali *et al.* (2002) have measured natural radioactivity in the building materials samples collected from the quarries and outcrops of the rock units forming the Shewa-Shahbaz Garhi igneous complex, North-West Pakistan.

Khan *et al.* (2003) have reported the natural radioactivity in the aquatic media (i.e., river, stream and drinking water) from the samples of northwestern areas of Pakistan. Jabbar *et al.* (2003a) have measured natural and fallout radionuclide concentrations in the environment of Islamabad which according to them was within the permissible limits. Akhter *et al.* (2003a) have reported the nutritional status of dietary potassium and the radiological impact of its isotope ^{40}K for the Pakistani population. They have determined potassium concentration in dietary samples by atomic absorption spectrometry. Akhter *et al.* (2003b) have also determined radiation doses due to the ingestion of thorium activity by the general public. Matiullah *et al.* (2004) have reported gamma activity from primordial radionuclides measured in the soil of the Bahawalpur division using gamma spectrometry technique.

Akhtar *et al.* (2004a&b) have measured natural radioactivity in virgin and fertilized saline soils as well as in the barren soil of Lahore. Chaudhry *et al.* (2002) have reported specific activity of natural radionuclides in the agricultural soil of eastern salt range of Pakistan. Akram *et al.* (2004) have used fission-track technique for the estimation of uranium concentration in drinking water collected from the natural springs

of the Muzaffarabad and hilly areas of Reshian, Azad Kashmir. Akhtar *et al.* (2004) have measured amount of radioactivity in the fertile soil, in NIAB (Nuclear Institute for Agriculture and Biology) at Faisalabad, Pakistan. Zaidi *et al.* (2004) have measured natural radioactivity in the samples of sand, stone and building materials collected from Karachi using γ -ray spectrometry and instrumental neutron activation analysis (INAA).

Khan *et al.* (2005) have reported activity concentrations of naturally occurring radionuclides i.e., ^{226}Ra , ^{232}Th and ^{40}K in sand samples of the North Western areas of Pakistan using gamma-spectrometry. Tahir *et al.* (2005) have reported activity concentration in the soil samples collected from different districts of the Punjab province. Younis *et al.* (2005) have studied natural and fall-out radionuclides in samples of soil, vegetation and water collected from some regions of the North West Frontier Province (NWFP) of Pakistan. Akram *et al.* (2006) have reported measurement of gamma emitting radionuclides in shallow marine sediments off the Sindh coast using a gamma spectrometry technique. Tufail *et al.* (2006a) have measured gamma ray activity mass concentrations in phosphate rock and fertilizer samples collected from different fertilizer manufacturing factories and suppliers in Pakistan.

Natural radioactivity has been measured by Tufail *et al.* (2006b) in barren and cultivated soil of the Faisalabad area in the Punjab province of Pakistan. Akram *et al.* (2006) have reported concentration of natural and artificial radionuclides in the bottom sediments of the Karachi Harbour/Manora channel area. Rehman *et al.* (2006) have measured the radium and uranium contents in different ore samples. Akram *et al.* have measured natural radionuclide contents of ^{226}Ra , ^{228}Ra and ^{40}K in the inter-tidal sediments collected from selected locations off the 745 km long Balochistan Coast. Akhtar *et al.* (2007) have measured natural radioactivity in soil samples collected from the agricultural farms consisting of saline and normal soil which had been under fertilizer treatment for the past many years to investigate the effect of fertilizers in soil and wheat grown in those sites. Fatima *et al.* (2007a&b) have measured activity concentrations of the natural radionuclides in soil samples of the southern Punjab, Pakistan by gamma-ray spectrometry. In another study, they have reported natural radioactivity in different brands of drinking water in the cities of Islamabad and Rawalpindi using gamma

spectrometry technique. Akhter *et al.* (2007) have measured daily dietary intakes of three naturally occurring long-lived radionuclides for the adult population of Pakistan using neutron activation analysis, inductively coupled plasma mass spectrometry (ICP-MS) and atomic absorption spectrometry (AAS), respectively. Tufail *et al.* (2007) have measured activity concentrations of primordial radionuclides in bricks, which were fabricated from saline soil of the Lahore and Faisalabad in the Punjab province of Pakistan. Faheem *et al.* (2008). have reported measurement of ^{226}Ra , ^{232}Th and ^{40}K concentrations in samples of soil and building material collected from the Gujranwala, Gujrat, Hafizabad, Sialkot, Mandibahauddin and Narowal districts of the Punjab province.

3.3. Reported Indoor Radon Studies for Pakistan

A number of studies concerning indoor radon have been conducted in Pakistan. A brief review of these studies is given below. Najeeb *et al.*(2005) have used CN-85 SSNTD tubes to measure radon/thoron concentration in the Lahore and Kasur cities. Indoor radon concentrations were also measured by Akram *et al.* (2005) in some dwellings of the Skardu city, northern Pakistan. A series of studies have also been reported by Iqbal *et al.* (2007a,b,c) in dwellings of the Jhelum valley, Azad Jammu and Kashmir and in the Muzaffarabad city Rawalakot areas of the Azad Jammu and Kashmir.

Tufail *et al.* (1988,1992) have measured indoor radon in the bed rooms, kitchens and drawing rooms of the houses of Lahore, Islamabad and Rawalpindi cities. Tufail *et al.* (1993) have reported measurement of radon concentration, gamma ray activities in dwellings of the Dera Ismail Khan and have estimated the internal and external doses for the dwellers of the area.

Matiullah *et al.* (2003) have measured indoor radon concentration levels in seven major cities, namely, Fort Abbas, Minchin Abad, Hasilpur, Bahawalpur, Liaquatpur, Rahimyar Khan and Sadiq Abad of the Bahawalpur Division. Khan *et al.* (2005) have measured radon concentration in the new and old buildings of the Fatima Jinnah Women University (FJWU) campus, Rawalpindi, Pakistan. In all the above mentioned studies solid state nuclear track detectors have been used for the measurement of indoor radon concentration. For further details, the readers is referred to the review paper by Faheem *et al.* (2008).

3.4. Summary of the Results

In the preceding section, the natural radioactivity measurements studies reported by different groups in Pakistan. In this section their reported results would be discussed. Tufail *et al* have reported average activity values of 43.3 ± 6.0 , 52.2 ± 6.0 and 631.3 ± 82.7 Bq.kg⁻¹ for ²²⁶Ra, ²³²Th and ⁴⁰K, respectively. They have also estimated radium equivalent concentration value of 168.6 ± 17.8 Bq.kg⁻¹ in the bricks samples collected from the Rawalpindi and Islamabad region. Tufail *et al*. have reported activity due to ⁴⁰K which ranged from 144.10 ± 24.37 Bq.kg⁻¹ to 834.00 ± 31.69 Bq.kg⁻¹ with an average value of 403.46 ± 5.64 Bq.kg⁻¹. For ²²⁶Ra, they have reported specific activity values which ranged from 63.06 ± 3.48 Bq.kg⁻¹ to 123.90 ± 5.42 Bq.kg⁻¹ with an average value of 83.43 ± 0.90 Bq.kg⁻¹. In the case of ²³²Th, the specific activity values varied from 10.02 ± 4.88 Bq.kg⁻¹ to 124.50 ± 4.44 Bq.kg⁻¹ with an average value of 85.84 ± 0.88 Bq.kg⁻¹. They have also reported specific activity of natural radionuclides in the cement samples. According to them, specific activity for ⁴⁰K varied from 41.4 ± 34.4 Bq.kg⁻¹ and 308.7 ± 32.5 Bq.kg⁻¹. For ²²⁶Ra, the specific activity varied from 17.5 ± 3.3 Bq.kg⁻¹ and 60.3 ± 3.6 Bq.kg⁻¹. The range of activities for ²³²Th was between 15.6 ± 2.2 Bq.kg⁻¹ and 50.8 ± 3.9 Bq.kg⁻¹. In another article they have reported ²²⁶Ra, ²³²Th and ⁴⁰K activity values in the dwellings of Dera Ismail Khan which were 26.9, 26.0 and 759.1 Bq kg⁻¹, respectively. Qazi and Jafri have reported surface radioactivity, ranging from 150 ± 25 to 350 ± 25 counts.s⁻¹. They have also reported trace amounts of uranium contents in the plants and animals samples of the area surveyed.

Khan *et al*. have reported very high ²²⁶Ra content in phosphate rock and in local/imported fertilizers which varied from 307.7 Bq.kg⁻¹ to 617.5 Bq.kg⁻¹. Jamil *et al*. have reported maximum activity concentrations for ²²⁶Ra, ²³²Th and ⁴⁰K as 31.4 ± 3 , 32.7 ± 3.2 and 21.4 ± 5 Bq.kg⁻¹, respectively in the coal samples which were collected from the Punjab and Balochistan provinces. Butt *et al*. have reported total gamma activity for alluvium (shales and clays), sandstone, lime stone, shales as 810.75, 440.13, 113.97 and 947.79 Bq.kg⁻¹, respectively. For Ultrabasic rocks, basic rocks, granite and metamorphic, intermediate to acidic rocks and metamorphic schist and gneiss, they have reported total gamma activity as 10.30 Bq.kg⁻¹, 240.26 Bq.kg⁻¹, 1295.70 Bq.kg⁻¹, 511.06 Bq.kg⁻¹ and 966.29 Bq.kg⁻¹, respectively. Zaidi *et al*. have reported mean radium equivalent activities

for sand, cement and bricks as 62 Bq.kg^{-1} , 44 Bq.kg^{-1} and 101 Bq.kg^{-1} , respectively. They have also reported ^{232}Th concentration in the samples of bricks, sand and cement which ranged from $6.7 - 7.5(27-31 \text{ Bq.kg}^{-1})$, $3.6 - 5.2 (15-21 \text{ Bq.kg}^{-1})$ and $1.7 - 3.7(7-15 \text{ Bq.kg}^{-1}) \mu\text{g.g}^{-1}$, respectively. For ^{238}U , concentration values varied from $2.3 - 2.7 \mu\text{g.g}^{-1}$ ($29-34 \text{ Bq.kg}^{-1}$), $0.51 - 1.2 \mu\text{g.g}^{-1}$ ($6-15 \text{ Bq.kg}^{-1}$) and $1.2 - 1.7 \mu\text{g.g}^{-1}$ ($15-21 \text{ Bq.kg}^{-1}$) in the samples of bricks, sand and cement, respectively using INAA. In the marble samples, Tufail *et al.* have reported average specific activity values of 27 , 26 and 58 Bq.kg^{-1} for ^{226}Ra , ^{232}Th and ^{40}K , respectively. Iqbal *et al.* have reported activity concentrations values for the marble samples which ranged from $4 - 63 \text{ Bq.kg}^{-1}$, $9 - 40 \text{ Bq.kg}^{-1}$ and $7 - 105 \text{ Bq.kg}^{-1}$ for ^{226}Ra , ^{232}Th and ^{40}K , respectively.

Khan and Khan have reported range of combined specific activity due to the ^{40}K , ^{226}Ra and ^{232}Th as $187.8 \pm 63.5 \text{ Bq.kg}^{-1} - 573.2 \pm 73.1 \text{ Bq.kg}^{-1}$ for Portland cement; $54.5 \pm 16.1 \text{ Bq.kg}^{-1} - 183.9 \pm 31.4 \text{ Bq.kg}^{-1}$ for limestone; $87.1 \pm 30.7 \text{ Bq.kg}^{-1} - 297.1 \pm 64.4 \text{ Bq.kg}^{-1}$ for gypsum; $696.4 \pm 79.1 \text{ Bq.kg}^{-1} - 1043.9 \pm 85.0 \text{ Bq.kg}^{-1}$ for slate; and $490.9 \pm 54.5 \text{ Bq.kg}^{-1} - 570.2 \pm 59.8 \text{ Bq.kg}^{-1}$ for latrite. Aslam *et al.* have reported activity concentration of ^{40}K , ^{226}Ra and ^{232}Th from 6.15 Bq.kg^{-1} to $159.65 \text{ Bq.kg}^{-1}$, 1.45 Bq.kg^{-1} to 29.34 Bq.kg^{-1} and 1.16 Bq.kg^{-1} to 6.28 Bq.kg^{-1} , respectively. Khan *et al.* have reported average values of the activity concentrations due to ^{40}K , ^{226}Ra and ^{232}Th as $680.3 \pm 22.2 \text{ Bq.kg}^{-1} - 784.4 \pm 30.7 \text{ Bq.kg}^{-1}$, $36.9 \pm 3.5 \text{ Bq.kg}^{-1} - 51.9 \pm 3.3 \text{ Bq.kg}^{-1}$ and $52.5 \pm 3.6 \text{ Bq.kg}^{-1} - 67.6 \pm 3.1 \text{ Bq.kg}^{-1}$, respectively. Ali *et al.* have reported fairly high mean concentrations of $51 \pm 16 \text{ Bq.kg}^{-1}$ of ^{238}U , $70 \pm 20 \text{ Bq.kg}^{-1}$ of ^{232}Th and $1272 \pm 367 \text{ Bq.kg}^{-1}$ of ^{40}K in the samples which were collected from the quarries and outcrops of the rock units forming the Shewa-Shahbaz Garhi igneous complex, North-West Pakistan.

Khan *et al.*, have reported annual ingestion of radionuclides in the aquatic samples, using local consumption rates (average over the whole population) of 0.9 l d^{-1} , as 49.2 , 6.2 and 1.1 Bq. y^{-1} for ^{40}K , ^{226}Ra and ^{232}Th , respectively. Akhter *et al.* have reported average dietary potassium concentration as $4.54 \pm 0.89 \text{ mg/g}$ ($134 \pm 26 \text{ Bq.kg}^{-1}$) which led to potassium dietary intake of $2.69 \pm 0.54 \text{ g/day}$. For this intake, daily ^{40}K activity of 79.94 Bq was reported. They have also reported thorium concentration, determined using instrumental neutron activation analysis. Their reported values which

varied from 1.6 ng g^{-1} ($0.0027 \text{ Bq.kg}^{-1}$) to 12 ng g^{-1} (0.054 Bq.kg^{-1}) and the median daily thorium intake was $2.7 \text{ } \mu\text{g.d}^{-1}$. Matiullah *et al.* have reported the measured mean activity of ^{226}Ra , ^{232}Th and ^{40}K as $32.9 \pm 0.9 \text{ Bq.kg}^{-1}$, $53.6 \pm 1.4 \text{ Bq.kg}^{-1}$, and $647.4 \pm 14.1 \text{ Bq.kg}^{-1}$, respectively. The mean radium equivalent activity Ra_{eq} , for the selected area was reported as $158.5 \pm 4.1 \text{ Bq.kg}^{-1}$

Akhtar *et al.* have reported activity concentrations for the naturally occurring radionuclides, namely ^{40}K , ^{238}U , and ^{232}Th in the virgin and fertilized saline soil samples. ^{40}K , for virgin and cultivated saline soil was $500 - 610.2 \text{ Bq.kg}^{-1}$ and $560.2 \text{ Bq.kg}^{-1} - 635.6 \text{ Bq.kg}^{-1}$, respectively; ^{238}U , $26.3 \text{ Bq.kg}^{-1} - 31.6 \text{ Bq.kg}^{-1}$ and $30.3 - 38.7 \text{ Bq.kg}^{-1}$, and ^{232}Th , $50.6 - 55.3 \text{ Bq.kg}^{-1}$ and $50.6 \text{ Bq.kg}^{-1} - 64.0 \text{ Bq.kg}^{-1}$, respectively. They have also reported the activity of natural radionuclides to be ^{40}K , $524.84 \text{ Bq.kg}^{-1} - 601.62 \text{ Bq.kg}^{-1}$, ^{226}Ra , $24.73 \text{ Bq.kg}^{-1} - 28.17 \text{ Bq.kg}^{-1}$ and ^{232}Th , $45.46 \text{ Bq.kg}^{-1} - 52.61 \text{ Bq.kg}^{-1}$ in the barren soil of Lahore.

Chaudhry *et al.* have reported average specific activities of ^{40}K , ^{226}Ra and ^{232}Th in the soil samples as 666 Bq.kg^{-1} , 51 Bq.kg^{-1} and 59 Bq.kg^{-1} , respectively. Akram *et al.* have reported uranium concentration in water samples, collected from the Muzaffarabad and Reshian area, which ranged from $0.03 \pm 0.01 \text{ } \mu\text{g.l}^{-1}$ ($0.0004 \pm 0.0001 \text{ Bq.kg}^{-1}$) to $6.67 \pm 0.14 \text{ } \mu\text{g.l}^{-1}$ with an average value of $1.36 \pm 0.05 \text{ } \mu\text{g.l}^{-1}$ ($0.0170 \pm 0.0006 \text{ Bq.kg}^{-1}$). Akhtar *et al.* have also reported activity concentration of the concerned radionuclides for the NIAB soil as: ^{40}K , $614.4 - 670.7 \text{ Bq.kg}^{-1}$; ^{226}Ra , $28.6 - 32.6 \text{ Bq.kg}^{-1}$; and ^{232}Th , $51.6 \text{ Bq.kg}^{-1} - 60.3 \text{ Bq.kg}^{-1}$. Zaidi *et al.* have reported that specific activities in samples of sand, stone and building materials, collected from Karachi, had radium equivalent activity less than 370 Bq.kg^{-1} . Khan *et al.* have reported activity concentrations of ^{226}Ra , ^{232}Th and ^{40}K in sand samples, collected, from NWFP as $36.9 - 51.9 \text{ Bq.kg}^{-1}$, $52.5 - 67.6 \text{ Bq.kg}^{-1}$ and $680 - 784 \text{ Bq.kg}^{-1}$, respectively. Tahir *et al.* have reported mean activity concentrations of ^{232}Th , ^{226}Ra and ^{40}K as $41 \pm 8 \text{ Bq.kg}^{-1}$, $35 \pm 7 \text{ Bq.kg}^{-1}$ and $615 \pm 143 \text{ Bq.kg}^{-1}$ in soil samples which were collected from different districts of the Punjab. They have measured mean values of radium equivalent index (Ra_{eq}) as $141 \pm 27 \text{ Bq.kg}^{-1}$.

Younis *et al.* have reported average specific activities of ^{40}K , ^{226}Ra and ^{232}Th in the soil samples as $307 \pm 101 \text{ Bq.kg}^{-1}$, $10.2 \pm 3 \text{ Bq.kg}^{-1}$ and $2 \pm 6 \text{ Bq.kg}^{-1}$, respectively. They observed that vegetation samples had smaller values of specific activities and even the analysis of water samples showed values less than lower limit of detection (LLD) for the above-mentioned radionuclides. Akram *et al.* have reported activity concentration in various sediment samples off the Sindh coast, Arabian sea which varied from $15.93 \pm 5.22 \text{ Bq.kg}^{-1}$ to $30.53 \pm 4.70 \text{ Bq.kg}^{-1}$ for ^{226}Ra , 11.72 ± 1.22 to $33.94 \pm 1.86 \text{ Bq.kg}^{-1}$ for ^{228}Ra and $295.22 \pm 32.83 \text{ Bq.kg}^{-1}$ to $748.47 \pm 28.75 \text{ Bq.kg}^{-1}$ for ^{40}K , respectively.

Tufail *et al.* have reported activity mass concentrations of ^{238}U (^{226}Ra) in samples of phosphate rocks which were collected from the Jordan and Pakistan as 428 ± 11 and $799 \pm 10 \text{ Bq.kg}^{-1}$, respectively. In triple-superphosphate fertilizer, they reported activity mass concentrations of ^{238}U as $701 \pm 21 \text{ Bq.kg}^{-1}$. They have also reported activity concentration of natural radionuclides in barren and cultivated soils. For ^{40}K , the values were $499 \text{ Bq.kg}^{-1} - 604 \text{ Bq.kg}^{-1}$ and $563 \text{ Bq.kg}^{-1} - 629 \text{ Bq.kg}^{-1}$, respectively; for ^{226}Ra , $24-29$ and $27-33 \text{ Bq.kg}^{-1}$, and for ^{232}Th , $49-54 \text{ Bq.kg}^{-1}$ and $46-62 \text{ Bq.kg}^{-1}$. Akram *et al.* have measured activity concentration in samples which were collected from the bottom sediments of Karachi Harbour/Manora channel area. They have reported ^{226}Ra , ^{228}Ra , and ^{40}K activities in sea sediment samples from their studied area which varied from $18.5 \pm 4.3 \text{ Bq.kg}^{-1}$ to $29.1 \pm 3.8 \text{ Bq.kg}^{-1}$ for ^{226}Ra , $11.7 \pm 1.2 \text{ Bq.kg}^{-1}$ to $27.7 \pm 4.2 \text{ Bq.kg}^{-1}$ for ^{228}Ra and $332.2 \pm 9.3 \text{ Bq.kg}^{-1}$ to $729.2 \pm 36.7 \text{ Bq.kg}^{-1}$ for ^{40}K . For Layari river, the activity values varied from 14.9 ± 2.6 to $29.7 \pm 2.9 \text{ Bq.kg}^{-1}$, $8.6 \pm 0.9 \text{ Bq.kg}^{-1}$ to $31.6 \pm 1.3 \text{ Bq.kg}^{-1}$ and 197.3 ± 11.6 to $643.7 \pm 25.9 \text{ Bq.kg}^{-1}$, respectively for ^{226}Ra , ^{228}Ra and ^{40}K . Rehman *et al.* have calculated ^{238}U contents that ranged from 13 to 37 ppm in the ore samples. Akram *et al.*, have measured natural radioactivity in various sediment samples which ranged from $14.4 \pm 2.5 \text{ Bq.kg}^{-1}$ to $36.6 \pm 3.8 \text{ Bq.kg}^{-1}$ for ^{226}Ra , $9.8 \pm 1.2 \text{ Bq.kg}^{-1}$ to $35.2 \pm 2.0 \text{ Bq.kg}^{-1}$ for ^{228}Ra and $144.6 \pm 9.4 \text{ Bq.kg}^{-1}$ to $610.5 \pm 23.9 \text{ Bq.kg}^{-1}$ for ^{40}K . Radioactivity values measured by Akhtar *et al.* in soil samples of the agricultural farms which were from $550-644 \text{ Bq.kg}^{-1}$, $20-35 \text{ Bq.kg}^{-1}$ and $42-58 \text{ Bq.kg}^{-1}$ for ^{40}K , ^{226}Ra and ^{232}Th , respectively.

Fatima *et al.* have reported mean radium equivalent activity (Ra_{eq}) as 96.7 ± 5.2 Bq.kg⁻¹ in the soil samples of the southern Punjab. In another study, they have reported mean concentrations of ²²⁶Ra, ²³²Th and ⁴⁰K in bottled drinking water as 11.3 ± 2.3 Bq.kg⁻¹, 5.2 ± 0.4 Bq.kg⁻¹ and 140.9 ± 30.6 mBq.ℓ⁻¹, respectively. Akhter *et al.*, have reported daily intakes of ²³²Th, ²³⁸U and ⁴⁰K which ranged from 4 mBq to 29 mBq, 17 mBq to 82 mBq and 51 Bq to 128 Bq, respectively. Geometric means of these intakes due to these radionuclides were 10 mBq d⁻¹, 33 mBq d⁻¹ and 78.5 Bq.d⁻¹, respectively. Tufail *et al.* have reported activity mass concentrations of ⁴⁰K, ²²⁶Ra and ²³²Th measured in the brick samples as 567.7 ± 38.3 (493–631 Bq.kg⁻¹), 28.4 ± 3.8 (23–35 Bq.kg⁻¹), and 56.0 ± 4.6 (46–65) Bq.kg⁻¹, respectively.

Faheem *et al.* have reported average ²²⁶Ra, ²³²Th and ⁴⁰K concentrations in samples of soil and building material which were collected from six districts of the Punjab province ranging from 20 ± 9 Bq.kg⁻¹ to 43 ± 17 Bq.kg⁻¹, 29 ± 8 Bq.kg⁻¹ to 53 ± 9 Bq.kg⁻¹ and 98 ± 38 Bq.kg⁻¹ to 621 ± 189 Bq.kg⁻¹, respectively. Whereas average radium equivalent activities were found to range from 69 ± 25 Bq.kg⁻¹ to 165 ± 32 Bq.kg⁻¹.

In the work reported so far for Pakistan, emphasis has been made on the health hazards associated with the natural radioactivity present in soil and other building materials. Besides measurement of natural radioactivity in soil and building materials, limited data is also available for Pakistan concerning the use of natural radioactivity in exploration of uranium and other related minerals deposits in different types of rocks and soil. Few articles regarding measurements of natural radioactivity in air have also been reported. Most of the studies related to the natural radioactivity have been conducted using high purity germanium detector (HPGe). In several reported studies, relatively low resolution NaI (TI) detector has also been used using spectrum stripping technique. Fission track dating technique has also been used to measure naturally occurring uranium in rocks and water samples. Some reported research papers are based on the use of INAA technique for the measurement of gamma ray activity of radionuclides present in different food and vegetable samples.

The lowest reported values for ^{226}Ra , ^{232}Th and ^{40}K were as 1.45 Bq.kg^{-1} , 1.16 and 7 Bq.kg^{-1} , whilst the highest were 799 Bq.kg^{-1} , 124 Bq.kg^{-1} and 1272 Bq.kg^{-1} , respectively. Relatively low activity concentrations of natural radionuclides have been reported for marble samples whereas higher values have been reported for phosphate rocks samples. Reported range of uranium concentration in water samples is from $0.03 \pm 0.01 \mu\text{g.l}^{-1}$ ($0.0004 \pm 0.0001 \text{ Bq.kg}^{-1}$) to $6.67 \pm 0.14 \mu\text{g.l}^{-1}$ with an average value of $1.36 \pm 0.05 \mu\text{g.l}^{-1}$ ($0.0170 \pm 0.0006 \text{ Bq.kg}^{-1}$). The reported values for natural radioactivity show a wide variation in the activity concentration of the concerned radionuclides in different types of rocks, soil, sand and bricks. Uptake of radionuclides due to the use of different types of diets and bottled mineral water used in Pakistan has also been reported and its radiological effects have been assessed. Radioactivity measurements have also been reported for the land used for cultivation of different types of crops. According to the reported data, natural radioactivity present in the building materials is relatively low. However, the area for which the data is reported represents a very small portion of the cultivated land of Pakistan and therefore further research work in this regard will be of much interest. In view of the above discussion, a comprehensive study was planned for the present research work and was conducted in some selected parts of the NWFP, Pakistan. Spatial and seasonal variations of indoor radon, radon exhalation rate and natural radioactivity from soil and other different building materials were studied which are presented in this thesis.

3.5. Conclusions

To conclude, reported data concerning measurement of natural radioactivity in the soil, sand, brick, marble and other building materials for Pakistan and a brief review of indoor radon data have been presented in this chapter. Reported radioactivity values show a wide variation of activity contents in different types of soil and other building materials. Most of the reported studies are based on using high purity germanium detectors (HPGe) whereas in some studies, NaI (Tl) detector using spectrum stripping technique and INAA have also been used. High contents of natural radioactivity have been reported for phosphate rocks. Therefore, great care is needed to be taken using these rocks for different purposes. Fission track dating technique has also been used for the measurement of uranium contents in different types of rocks. All the reported values of the natural

radioactivity and indoor radon concentration are within the permissible limits and do not pose any serious threat to the general public.

After reviewing the studies conducted in Pakistan concerning measurement of Natural radioactivity and indoor radon, the next chapter deals with the analysis of the work done in this research work regarding the measurement of Indoor radon and its spatial and temporal variations in some selected parts of the NWFP, Pakistan.

Chapter Four

Measurement of Seasonal and Spatial Distribution of Indoor Radon Levels

4.1. Introduction

Indoor radon levels are known to vary from house to house which in turn depends on radon source, building characteristics, natural daily cycle, other longer temporal and spatial cycles, related to occupancy, geological and meteorological factors, dwelling characteristics and habits of the occupants (Arvela, 1995; Majborn, 1992; Groves-Kirkby et al., 2006). In countries with relatively higher contributions from building materials, the winter to summer ratios should be lower (Arvela, 1995).

According to the measurements, in the very same room the yearly average of radon concentration may also change by 25–50% from year to year (Papp et al., 2001). Radon concentration varies throughout the year with the greatest concentrations occurring during the winter months in homes but outdoor concentrations are greatest during the summer months (Grainger et al., 2005; Bochicchio, 2004). For radon concentration temporal variations, a 12-month total period of measurement is generally considered the best estimate of the average value. In order to determine annual average from the indoor radon levels, measured for a less than a year, seasonal correction factor has to be applied (Grainger et al., 2000; Baysson et al., 2003; Karpinńska et al., 2005; Bochicchio, 2005).

Longer measurements give more accurate estimates of the annual average concentrations than short measurements; the magnitude of the improvement caused by using longer measurements is not well established as the long-term exposure may reduce the efficiency of the detector for the registration of tracks.

In view of the above introduction a systematic studies were conducted aiming at the following objectives (1) To measure indoor radon levels, its seasonal and spatial variations in some selected areas of the North West Frontier Province (NWFP) and Federally Administered Tribal Areas (FATA), Pakistan. (2) To set a baseline data for these areas which would be of great help for radiological database of Pakistan. (3) To calculate the seasonal correction factor. As the area under study has four distinct seasons, variation in the indoor radon levels was expected. (4) A study was also conducted to compare yearly average of the seasonal measurements with that of the yearly exposed CR-39 detectors in order to study the affect of the long-term exposure on CR-39 detectors.

4.2. Materials and Methods

In order to measure the above-mentioned quantities a series of field experiments were designed in the selected area of NWFP and FATA. Details of the installation of the dosimeters and selection of the houses is given in chapter 2.

For the analysis of the seasonally averaged, yearly averaged and the yearly exposed CR-39, only those homes were accepted wherefrom both seasonal and yearly exposed radon dosimeters were recovered. It may be noted here that from 28, 30, 25 houses of Charsadda, Swabi and Mardan and 27, 29 houses in Mohmand and Bajuar agency, all the seasonally dosimeters exposed in all the seasons and yearly exposed radon dosimeters were recovered, respectively.

CR-39 detectors were then etched in 25% NaOH at 80 °C and track densities were then related to the radon concentration levels using calibration factor of $2.7 \text{ tracks.cm}^{-2}.\text{h}^{-1}/\text{kBq.m}^{-3}$. Using the mean annual radon levels in each house, annual effective dose was calculated using the ICRP-65 and UNSCEAR conversion factors (Jing, 2005; UNSCEAR, 2000). Using the annual weighted average values of indoor radon concentration and the BEIR VI formula, excess relative risk of lung cancer were calculated.

4.3. Results

As mentioned above, ^{222}Rn concentration levels were determined using the calibration factor of $2.7 \text{ tracks cm}^{-2} \text{ h}^{-1}/\text{kBq m}^{-3}$. Having determined the ^{222}Rn concentrations, statistical analysis of the data was performed. Geometric mean, arithmetic mean and

Table 4.1: Indoor radon levels in Bq m⁻³ in bed rooms and drawing rooms of all the houses which were surveyed in NWFP and FATA areas of Pakistan during the Summer season.

H. No	Mohmand		Bajuar		Swabi		Mardan		Charsadda	
	Bed Room	Drawing Room	Bed Room	Drawing Room	Bed Room	Drawing Room	Bed Room	Drawing Room	Bed Room	Drawing Room
1	53±5	L	170±4	86±4	52±4	46±5	21±8	29±5	95±5	34±4
2	50±5	43±5	80±4	45±5	65±4	55±5	78±5	32±5	68±5	32±6
3	58±4	38±5	72±4	85±4	56±4	48±5	57±4	31±5	L	43±4
4	50±5	72±3	127±4	44±5	51±4	50±5	267±4	74±4	80±5	52±5
5	45±5	L	43±5	76±4	L	55±5	68±4	39±5	323±5	72±5
6	246±4	107±4	58±5	35±5	35±6	31±5	45±5	38±5	56±5	55±5
7	39±5	54±6	57±4	56±4	38±5	47±5	66±5	36±5	96±5	85±5
8	34±5	L	147±4	111±5	28±5	55±5	186±5	103±5	154±5	55±5
9	48±5	23±5	116±4	112±5	102±4	99±5	55±5	39±5	91±4	45±5
10	25±6	47±7	L	L	36±5	48±5	40±5	L	54±5	281±5
11	60±5	L	90±4	90±4	88±4	45±5	51±5	45±7	96±5	56±5
12	52±5	62±4	50±5	48±5	53±4	54±4	42±5	48±4	L	L
13	105±4	59±5	43±5	44±5	36±5	44±5	31±5	51±4	74±5	47±4
14	67±4	79±4	46±4	52±4	36±5	50±4	58±5	45±5	52±5	48±5
15	60±4	39±5	131±4	36±5	L	63±4	28±6	28±5	57±5	L
16	41±5	55±4	49±5	L	171±3	99±5	49±6	65±5	59±5	65±5
17	189±5	124±5	71±4	87±4	24±5	44±5	46±5	34±5	45±6	95±5
18	36±6	78±4	42±5	43±5	24±6	77±4	80±5	31±5	92±4	147±5
19	122±4	77±4	91±4	58±5	L	55±4	23±7	L	51±5	69±5
20	L	76±4	96±4	84±4	54±4	31±5	60±5	57±5	63±5	69±5
21	61±5	37±5	89±4	48±5	88±4	42±5	59±5	18±6	95±4	81±5
22	73±4	42±5	57±4	55±4	34±5	72±4	49±5	76±4	76±5	47±5
23	106±4	115±4	97±4	72±4	33±5	50±5	26±6	L	115±5	45±5
24	37±5	50±4	63±4	90±4	24±6	49±5	50±5	81±4	97±5	47±5
25	58±55	54±7	L	79±4	32±5	34±5	29±5	25±5	L	28±5
26	L	82±5	L	62±4	25±6	45±5	32±5	30±5	32±5	35±5
27	42±5	L	97±4	48±5	74±5	44±5	46±5	33±5	96±5	69±6
28	L	45±5	176±4	38±5	36±5	51±5	57±7	58±5	53±5	38±6
29	33±5	63±4	137±4	123±4	L	47±5	L	62±4	110±5	L
30	29±6	51±4	35±5	31±6	41±5	40±5	L	L	L	L
31	L	65±55	43±5	46±6	33±5	L	41±7	46±5	75±5	48±5
32	L	L	70±4	125±4	50±4	48±5	L	56±3	91±5	63±5
33	71±4	78±5	61±5	87±4	25±6	L	L	48±6	64±5	113±4
34	50±5	54±5	51±5	29±5	L	72±5	115±4	66±4	61±5	50±5
35	40±5	68±5	100±4	106±4	L	106±5	53±4	33±5	92±5	64±5
36	71±4	L	37±5	75±4	89±4	42±5	35±5	30±5	85±5	78±4
37	63±5	45±5	32±5	41±5	112±4	120±5	42±5	29±5	89±5	59±4
38	L	36±4	50±5	45±5	42±5	62±4	33±5	50±5	L	L
39	78±4	58±4	L	43±5	13±6	44±5	38±6	30±5	65±5	39±5
40	33±5	54±4	54±4	40±5	71±4	71±5	29±5	53±5	83±5	65±5

standard deviation were calculated for each season. Radon concentration levels observed in each house during the summer season are shown in table 4.1.

As may be seen in table 4.1, in summer season indoor radon concentration levels varied from 25 ± 6 to 246 ± 4 Bq m⁻³ and 23 ± 5 to 124 ± 5 Bq m⁻³ in the bed rooms and drawing rooms of the Mohmand agency, respectively. In the Bajuar agency, radon concentration level varied from 32 ± 5 to 176 ± 4 Bq m⁻³ and 29 ± 5 to 125 ± 4 Bq m⁻³ in bedrooms and drawing rooms, respectively. In the Swabi district, variation in the radon concentration level ranged from 13.4 ± 6 to 171 ± 3 Bq m⁻³ and 31 ± 5 to 120 ± 5 Bq m⁻³ in bedrooms and drawing rooms, respectively. In the Mardan district, radon concentration level varied from 21 ± 8 to 267 ± 4 Bq m⁻³ and 18 ± 6 to 103 ± 5 Bq m⁻³ in bedrooms and drawing rooms, respectively. In the Charsadda district, this variation ranged from 32 ± 5 Bq m⁻³ to 323 ± 5 and 28 ± 6 to 281 ± 6 Bq m⁻³, respectively. According to the weighted average indoor radon in the Mohmand agency varied from 34 ± 6 to 191 ± 4 Bq m⁻³ while in the Bajuar agency, it varied from 33 ± 5 to 137 ± 5 Bq m⁻³. As may be seen in table 4. 2, variation of indoor radon in Mardan and Swabi districts is from 24 ± 7 Bq m⁻³ to 189 ± 4 Bq m⁻³ and 24 ± 6 to 142 ± 4 Bq m⁻³, respectively. Maximum variation of radon occurred in Charsadda, which ranged from 33 ± 6 to 222 ± 5 Bq m⁻³. All the houses selected in the Mohmand and Bajuar agencies were detached houses whereas more than 50% houses in the Charsadda, Mardan and Swabi districts were detached houses. The remaining houses were semi-detached. No significant difference was observed in the radon levels measured in detached and semi-detached houses.

As may be seen in table 4.3, in autumn season indoor radon concentration level varied from 36 ± 6 to 131 ± 4 Bq m⁻³ and 39 ± 6 to 147 ± 5 Bq m⁻³ in the bed rooms and drawing rooms of the Mohmand agency, respectively. In the Bajuar agency, radon concentration level varied from 45 ± 4 to 191 ± 4 Bq m⁻³ and 47 ± 6 to 221 ± 4 Bq m⁻³ in bedrooms and drawing rooms, respectively. In the Swabi district, variation in the radon concentration level ranged from 52 ± 5 to 155 ± 4 and 43 ± 6 to 188 ± 4 Bq m⁻³ in bedrooms and drawing rooms, respectively. In the Mardan district, radon concentration level varied from 50 ± 5 to 126 ± 6 Bq m⁻³ and 57 ± 6 to 126 ± 5 Bq m⁻³ in bedrooms and drawing rooms, respectively. In the Charsadda district, this variation ranged from 50 ± 5 Bq m⁻³ to 318 ± 5 and 42 ± 5 to 132 ± 5 Bq m⁻³, respectively.

Weighted average indoor radon in the Mohmand agency varied from 46 ± 6 to $124 \pm 4 \text{ Bq m}^{-3}$ while in the Bajuar agency it varied from 47 ± 4 to $173 \pm 4 \text{ Bq m}^{-3}$. As may be seen in table 4.4, variation in the indoor radon in the Mardan and the Swabi districts is from 60 ± 5 to $105 \pm 4 \text{ Bqm}^{-3}$ and 53 ± 6 to $122 \pm 4 \text{ Bq m}^{-3}$, respectively. Maximum variation in the indoor radon occurred in the Charsadda district, which ranged from 58 ± 4 to $234 \pm 5 \text{ Bq m}^{-3}$.

As may be seen in table 4.5, in winter season indoor radon concentration levels varied from 51 ± 6 to $238 \pm 5 \text{ Bq m}^{-3}$ and 50 ± 7 to $117 \pm 4 \text{ Bq m}^{-3}$ in the bed rooms and drawing rooms of the Mohmand agency, respectively. In the Bajuar agency, radon concentration level varied from 41 ± 7 to $176 \pm 5 \text{ Bq m}^{-3}$ and 40 ± 6 to $213 \pm 4 \text{ Bq m}^{-3}$ in bedrooms and drawing rooms, respectively. In the Swabi district, variation in the radon concentration level ranged from 33 ± 7 to 203 ± 4 and 33 ± 7 to $138 \pm 4 \text{ Bq m}^{-3}$ in bedrooms and drawing rooms, respectively. In the Mardan district, radon concentration level varied from 37 ± 5 to $248 \pm 4 \text{ Bq m}^{-3}$ and 44 ± 6 to $146 \pm 6 \text{ Bq m}^{-3}$ in bedrooms and drawing rooms, respectively. In the Charsadda district, this variation ranged from $55 \pm 7 \text{ Bq m}^{-3}$ to 319 ± 5 and 48 ± 7 to $146 \pm 6 \text{ Bq m}^{-3}$, respectively.

As may be seen in table 4.6, in the Mohmand agency weighted average indoor radon in the winter season varied from 25 ± 6 to $189 \pm 5 \text{ Bq m}^{-3}$ while in the Bajuar agency, it varied from 44 ± 6 to $187 \pm 5 \text{ Bq m}^{-3}$. Table 4.6 the variation of indoor radon in Mardan and Swabi Districts are from 48 ± 5 to $177 \pm 4 \text{ Bqm}^{-3}$ and 40 ± 7 to $148 \pm 4 \text{ Bq m}^{-3}$ respectively. Maximum variation of radon occurred in Charsadda, which ranged from 53 ± 7 to $226 \pm 6 \text{ Bq m}^{-3}$.

As may be seen in table 4.7, in Spring season indoor radon concentration levels varied from 30 ± 6 to $131 \pm 5 \text{ Bq m}^{-3}$ and 22 ± 7 to $129 \pm 5 \text{ Bq m}^{-3}$ in the bed rooms and drawing rooms of Mohmand agency, respectively. In the Bajuar agency, radon concentration level varied from 29 ± 6 to $349 \pm 5 \text{ Bq m}^{-3}$ and 27 ± 7 to $229 \pm 5 \text{ Bq m}^{-3}$ in bedrooms and drawing rooms, respectively. In Swabi district, variation in the radon concentration level ranged from 32 ± 6 to 156 ± 5 and 26 ± 6 to $79 \pm 5 \text{ Bq m}^{-3}$ in bedrooms and drawing rooms, respectively.

Table 4.2: Weighted average indoor radon during the Summer season.

Detector No	Mohmand	Charsadda	Bajuar	Swabi	Mardan
1.	53±5	70±4	137±4	50±5	24±7
2.	47±5	53±5	66±5	61±4	60±5
3.	50±4	43±4(D)	77±4	53±4	47±5
4.	60±4	69±5	94±4	51±4	189±4
5.	45±5	222±5	56±5	55±5(D)	56±4
6.	191±4	56±5	49±5	33±5	42±5
7.	45±5	91±5	56±4	41±5	54±4
8.	34±6(B [‡])	115±5	133±4	39±5	153±4
9.	38±5	72±5	114±4	100±4	49±5
10.	34±6	145±5	L	41±5	40±5(B)
11.	60±5(B)	80±5	90±4	71±4	48±5
12.	56±5	L	49±5	53±4	45±4
13.	84±4	63±4	43±5	39±5	39±5
14.	72±4	50±5	48±4	41±5	53±5
15.	52±4	57±5(B)	93±4	63±4(D)	28±5
16.	47±5	61±5	49±5(B)	142±4	55±6
17.	163±5	65±5	77±4	32±5	41±5
18.	53±5	114±5	43±5	45±5	60±5
19.	104±4	58±5	77±4	55±4(D)	23±7(B)
20.	767±4(B)	65±5	91±4	45±4	59±5
21.	52±5	90±4	73±4	69±4	43±5
22.	61±4	64±5	56±4	49±4	60±5
23.	110±4	87±5	87±4	39±5	26±6(B)
24.	43±4	77±5	74±4	34±5	63±5
25.	56±6	28±6(D)	79±4	33±5	28±5
26.	82±5(D)	33±5	62±4	33±5	31±5
27.	42±5(B)	85±5	78±4	62±5	41±5
28.	45±5(D)	47±5	121±4	42±5	57±6
29.	45±5	110±5(B)	132±4	47±5(D)	62±4(D)
30.	39±5	L	33±5	40±5	L
31.	65±4(D)	64±5	44±5	33±5(B)	43±6
32.	L	80±5	92±4	49±5	56±3(D)
33.	74±4	84±5	71±5	25±6	48±6(D)
34.	51±5	57±5	42±5	72±5(D)	95±4
35.	52±4	81±5	103±4	106±5(D)	45±5
36.	71±4(B)	82±5	52±5	70±5	33±5
37.	55±5	77±4	35±5	115±4	37±5
38.	36±4(D)	L	48±5	50±4	40±5
39.	70±4	55±5	43±5(D)	26±6	35±5
40.	41±5	75±5	48±5	71±4	39±5

[‡] B= Bedroom data only and D= Drawing room Data only and L= detector is lost.

Table 4. 3: Indoor radon levels in Bq m⁻³ in bedrooms and drawing rooms of all the houses which were surveyed in NWFP and FATA areas of Pakistan during the Autumn season.

H No	Mohmand		Bajuar		Swabi		Mardan		Charsadda	
	Bed Room	Drawing Room	Bed Room	Drawing Room	Bed Room	Drawing Room	Bed Room	Drawing Room	Bed Room	Drawing Room
1	62±5	63±5	86±4	82±4	68±6	56±6	60±5	76±7	63±5	61±5
2	50±6	56±5	102±4	58±5	80±5	59±5	61±5	73±6	73±5	81±5
3	74±4	69±5	71±5	61±6	89±5	108±4	90±4	L	77±5	59±5
4	60±6	77±5	99±4	89±4	100±5	73±5	126±6	58±6	86±5	68±5
5	56±6	68±5	96±4	68±4	104±5	68±5	54±5	71±5	79±5	73±5
6	77±5	70±5	83±5	90±4	66±4	105±4	75±4	126±5	58±5	89±5
7	54±6	52±5	111±4	91±4	86±5	63±5	63±5	68±5	83±6	132±5
8	L	L	97±5	165±4	66±5	62±5	67±5	84±4	82±5	45±5
9	57±5	48±6	74±4	142±4	155±4	72±5	85±5	66±5	63±5	L
10	68±4	60±5	141±4	221±4	L	L	121±4	80±4	90±6	76±5
11	63±5	L	L	63±5	73±5	65±5	56±6	71±5	78±6	64±5
12	79±5	77±5	67±5	71±6	81±4	80±5	74±5	69±6	L	L
13	68±4	52±5	L	L	99±4	58±5	68±5	64±5	178±6	54±6
14	64±5	51±6	51±5	60±4	73±5	70±5	69±5	64±5	68±5	93±4
15	64±5	59±5	94±4	78±4	56±6	62±5	62±6	82±6	76±6	64±5
16	69±5	89±5	67±6	47±6	85±5	85±5	75±5	61±5	85±5	64±6
17	L	53±5	171±4	76±3	74±5	188±4	76±5	L	78±5	L
18	36±6	62±5	137±5	95±4	82±5	89±5	73±4	77±5	81±5	104±5
19	85±5	91±4	78±4	167±4	100±5	85±5	74±6	75±5	50±5	L
20	L	63±5	L	L	72±5	81±4	103±5	96±5	72±5	88±4
21	96±5	147±4	45±4	50±5	109±4	L	65±4	81±5	115±6	100±5
22	86±5	84±5	85±4	66±4	75±5	72±5	83±5	62±6	59±5	83±5
23	131±4	71±5	60±4	92±4	79±5	66±5	65±5	84±4	318±5	107±5
24	78±5	70±5	60±4	76±3	75±6	55±5	73±5	72±5	68±4	42±5
25	47±6	61±5	191±4	78±4	64±5	67±4	67±5	L	68±5	72±5
26	120±4	131±4	174±4	106±4	66±6	64±4	71±4	71±5	71±5	44±5
27	121±4	71±5	61±5	73±5	52±5	56±5	75±5	68±6	78±5	80±5
28	88±4	75±5	84±4	67±6	L	112±5	68±5	67±6	81±5	77±5
29	71±5	95±5	91±5	75±5	105±5	55±5	79±6	80±5	99±5	85±5
30	86±5	93±5	74±5	79±5	80±5	90±4	100±5	74±5	63±6	57±5
31	80±5	61±5	51±5	55±5	86±5	80±5	74±5	62±5	89±5	68±5
32	L	L	119±4	103±4	62±5	45±5	59±6	69±5	72±5	75±5
33	104±5	L	97±5	60±4	76±4	53±6	73±5	65±5	67±5	71±4
34	124±5	74±5	47±4	63±5	63±6	64±5	68±6	72±5	71±5	77±5
35	72±6	83±4	51±5	73±4	L	140±5	73±5	78±5	L	102±5
36	64±5	84±5	57±5	69±4	82±5	43±6	78±5	76±5	135±5	71±6
37	55±6	62±5	80±4	92±4	151±4	59±6	70±6	60±5	85±5	113±5
38	96±4	39±6	78±5	53±5	94±5	62±5	76±5	57±6	L	74±5
39	75±4	64±6	90±4	97±4	82±5	96±4	50±5	74±5	64±5	49±5
40	86±5	87±5	82±4	97±5	55±6	50±5	68±6	66±6	82±6	76±5

Table 4.4: Weighted average indoor radon during the Autumn season.

H. No.	Mohmand	Charsadda	Bajuar	Swabi	Mardan
1.	62±5	62±5	84±4	95±5	66±6
2.	52±6	76±5	84±4	53±5	66±5
3.	72±4	70±5	67±5	34±6	90±4(B)
4.	67±6	79±5	95±4	59±6	99±6
5.	61±6	77±5	85±4	40±6	61±5
6.	74±5	70±5	86±5	53±5	95±4
7.	53±6	103±6	103±4	36±6(B)	65±5
8.	L	67±5	124±5	40±5	74±5
9.	53±5	63±5(B)	101±4	97±5	77±5
10.	65±4	84±6	173±4	124±6	105±4
11.	63±5(B)	72±6	63±5(D)	47±6	62±6
12.	78±5	L	69±5	83±5	72±5
13.	62±4	128±6	L	37±6	66±5
14.	59±5	78±5(B)	55±5	40±4	67±5
15.	62±5	71±6	88±4	48±6	70±6
16.	77±5	77±5	59±6	46±6	69±5
17.	53±5	78±5	133±4	41±6	76±5(B)
18.	46±6	90±5	120±5	111±5	75±4
19.	87±5	50±5(B)	114±4	40±6	74±6
20.	63±5	78±5	L	35±6(D)	100±5
21.	116±4	109±6	47±4	44±7	71±4
22.	85±5	83±5	77±4	51±5	75±5
23.	107±4	234±5	73±4	26±6(D)	73±5
24.	75±5	58±4	66±4	47±6	73±5
25.	53±5	70±5	146±4	47±5	67±5(B)
26.	124±4	60±5	147±4	52±5	71±4
27.	101±4	79±5	66±5	L	72±5
28.	83±4	79±5	77±4	46±6	68±5
29.	81±5	93±5	85±5	33±5(B)	79±6
30.	89±5	61±6	76±5	55±6	90±5
31.	72±5	81±5	53±5	48±5	69±5
32.	L	73±5	113±4	71±5	63±6
33.	104±5(B)	69±5	82±5	51±6	70±5
34.	104±5	73±5	53±4	51±6	70±6
35.	76±5	102±5(D)	60±5	44±6	75±5
36.	72±5	109±5	62±5	38±6	77±5
37.	58±6	113±5	85±4	85±4	66±6
38.	73±5	74±5(D)	68±5	39±6(B)	68±5
39.	71±5	58±5	93±4	74±5(D)	60±5
40.	86±5	80±6	88±4	59±6	67±6

Table 4.5: Indoor radon levels in Bq m⁻³ in bed rooms and drawing rooms of all the houses which were surveyed in NWFP and FATA areas of Pakistan in the Winter season.

H No	Mohmand		Bajuar		Swabi		Mardan		Charsadda	
	Bed Room	Drawing Room	Bed Room	Drawing Room	Bed Room	Drawing Room	Bed Room	Drawing Room	Bed Room	Drawing Room
1	136±5	91±5	117±5	129±5	147±4	72±5	49±6	55±5	96±5	71±7
2	74±5	54±6	41±7	56±5	66±5	44±6	67±5	75±5	75±6	69±7
3	141±5	78±5	L	73±5	58±6	67±5	67±5	59±5	76±7	67±6
4	L	99±5	112±5	158±5	60±5	54±6	169±4	L	58±7	56±6
5	141±5	57±5	123±5	62±5	51±7	86±5	83±5	80±4	78±7	85±5
6	60±6	109±5	L	77±5	74±5	98±5	122±4	146±6	66±6	65±6
7	60±5	58±6	98±5	73±5	49±7	71±5	51±6	62±6	77±6	90±6
8	L	80±5	L	126±5	143±5	91±5	198±4	65±5	62±6	62±6
9	69±6	84±5	45±5	140±5	103±5	69±5	65±5	55±5	58±6	52±7
10	L	62±6	120±5	83±5	100±5	88±5	161±5	76±5	71±7	110±5
11	72±6	L	169±5	213±4	76±5	79±5	43±6	108±5	72±6	48±7
12	91±5	63±6	91±5	58±6	55±6	40±6	L	68±4	L	L
13	114±5	56±6	43±6	46±6	95±5	76±5	83±5	63±5	55±7	51±6
14	53±6	70±6	107±4	94±5	51±6	58±6	59±5	45±6	71±6	L
15	68±6	60±6	69±5	101±4	45±6	50±6	64±5	77±4	73±6	63±6
16	69±5	58±6	176±5	53±6	L	61±7	67±5	L	65±7	91±5
17	107±5	62±6	42±7	69±5	63±5	66±5	66±5	55±6	69±6	75±5
18	98±5	70±5	139±5	89±5	112±5	70±5	55±5	63±6	101±5	81±5
19	58±5	105±6	53±6	40±6	147±4	L	L	L	77±6	70±6
20	65±6	99±5	49±6	101±5	60±6	72±6	104±5	94±5	88±5	76±6
21	102±5	54±6	L	L	L	68±6	101±5	71±5	70±7	146±6
22	72±5	L	73±4	80±5	203±4	65±5	56±5	122±5	L	66±6
23	93±4	60±6	103±5	70±5	L	45±6	111±5	L	319±5	87±7
24	52±6	64±6	49±5	44±5	92±5	95±5	L	57±6	70±6	85±5
25	52±6	52±6	154±5	76±5	104±5	69±5	114±5	123±5	91±5	73±6
26	L	83±5	126±5	82±5	33±7	51±6	61±6	52±6	89±5	L
27	83±6	64±5	L	76±5	35±7	47±6	65±6	59±6	74±5	L
28	52±6	58±6	94±5	119±4	L	70±5	68±6	57±5	L	64±6
29	51±6	56±6	150±5	98±5	66±6	L	66±5	63±6	77±7	103±5
30	69±5	77±5	56±5	53±5	73±5	71±5	248±4	70±5	85±6	82±6
31	82±5	107±5	115±5	137±5	49±6	61±5	59±6	69±5	134±5	67±6
32	L	L	L	L	78±5	33±7	55±6	50±6	81±6	111±4
33	58±6	53±6	103±4	104±5	118±4	64±6	58±6	44±6	102±6	108±5
34	82±5	117±4	144±5	53±6	82±6	72±6	63±5	67±6	89±5	87±5
35	76±6	78±5	61±6	125±4	39±7	138±4	37±5	65±5	80±5	66±6
36	70±6	81±6	49±6	L	65±5	L	57±6	47±6	93±5	78±6
37	55±6	66±6		89±5	119±4	77±5	58±5	51±7	103±5	96±5
38	54±6	50±7	151±5	112±4	49±6	70±5	62±5	46±6	81±5	51±6
39	69±5	62±5	101±4	71±5	77±5	71±6	72±5	54±6	86±6	75±6
40	238±5	116±5	173±5	102±5	113±4	47±7	139±5	69±5	79±6	72±7

Table 4.6: Weighted average indoor radon during the Winter season.

House No.	Mohmand Winter	Charsadda Winter	Bajuar Winter	Swabi Winter	Mardan Winter
1.	118±5	86±6	122±5	117±4	51±6
2.	66±5	73±6	47±6	57±5	70±5
3.	116±5	72±7	73±5(D)	62±6	64±5
4.	99±5(D)	57±7	130±5	58±5	169±4(B)
5.	107±3	81±6	99±5	65±6	82±5
6.	80±6	66±6	71±5	84±5	132±5
7.	59±5	82±6	88±5	58±6	55±6
8.	80±5(D)	62±6	126±5(D)	122±5	145±4
9.	75±6	56±6	83±5	89±5	61±5
10.	25±6	87±6	105±5	95±5	127±5
11.	72±6(B)	62±6	187±5	77±5	69±6
12.	80±5	L	78±5	49±6	68±4(D)
13.	91±5	53±7	44±6	87±5	75±5
14.	60±6	71±6(B)	102±4	54±6	53±5
15.	65±6	69±6	82±5	47±6	69±5
16.	65±5	75±6	127±5	61±7(D)	67±5
17.	89±5	71±7	53±6	64±5	66±5
18.	87±5	93±5	119±5	95±5	58±5
19.	77±5	74±6	48±6	147±4(B)	L
20.	79±6	83±5	70±6	65±6	100±5
21.	83±5	100±7	L	68±6(D)	89±5
22.	72±5(B)	66±6(D)	76±4	148±4	82±5
23.	80±5	226±6	90±5	45±6(D)	111±5
24.	57±6	76±6	47±5	93±5	57±6
25.	52±6	84±5	123±5	90±5	114±5
26.	83±5(D)	89±5(B)	108±5	40±7	57±6(D)
27.	75±6	74±5(B)	76±5(D)	40±7	63±6
28.	54±6	64±6(D)	104±5	70±5(D)	64±6
29.	53±6	87±6	129±5	66±6	65±5
30.	72±5	84±6	55±5	72±5	177±4
31.	92±5	107±5	124±5	54±6	63±6
32.	L	93±5	L	60±5	53±6
33.	56±6	104±6	103±4	96±5	52±6
34.	96±5	88±5	108±5	78±6	65±5
35.	77±6	74±5	87±5	79±6	48±5
36.	74±6	87±5	49±5(B)	65±5(B)	53±6
37.	59±6	100±5	89±5	102±4	55±6
38.	52±6	69±5	135±5	57±6	56±5
39.	66±5	82±6	89±5(D)	75±5	65±5
40.	189±5	76±6	145±5	87±5	111±5

In the Mardan district, radon concentration level varied from 24 ± 6 to 135 ± 5 Bq m⁻³ and 25 ± 7 to 180 ± 5 Bq m⁻³ in bedrooms and drawing rooms, respectively.

In Charsadda district this variation ranged from 45 ± 7 Bq m⁻³ to 236 ± 4 Bq m⁻³ and 36 ± 7 to 182 ± 5 Bq m⁻³, respectively. According to the weighted average indoor radon in spring season (table 4.8) in Mohmand agency varied from 33 ± 6 to 105 ± 5 Bq m⁻³ while in Bajuar agency it varied from 39 ± 6 to 236 ± 5 Bq m⁻³. As may be seen from table 4.8 the variation of indoor radon in the Mardan and Swabi districts were from 24 ± 6 to 109 ± 5 Bq m⁻³ and 34 ± 6 to 124 ± 6 Bq m⁻³, respectively. Maximum variation of radon occurred in Charsadda, which ranged from 44 ± 6 to 214 ± 4 Bq m⁻³.

4.4. Yearly Minimum-Maximum Indoor Radon Concentration

Minimum and maximum indoor radon concentration levels observed in each district/agency for each season are shown in figure 4.1, as may be seen in this figure radon concentration levels in district Mardan vary from 21 ± 8 to 267 ± 4 Bq m⁻³ in bedrooms and from 18 ± 6 to 180 ± 5 Bq m⁻³ in drawing rooms respectively. In the district Swabi, the variation in the indoor radon concentration level ranged from 13 ± 6 to 203 ± 4 Bq m⁻³ in bedrooms and from 26 ± 6 to 188 ± 4 Bq m⁻³ in drawing rooms. In the district Charsadda indoor radon variations ranged from 32 ± 5 Bq m⁻³ to 323 ± 5 Bq m⁻³ in bedrooms and from 28 ± 6 to 318 ± 5 Bq m⁻³ in drawing rooms, respectively.

In the Mohmand agency, indoor radon concentration levels varied from 25 ± 6 to 246 ± 4 Bq m⁻³ and from 22 ± 7 to 129 ± 5 Bq m⁻³ in the bedrooms and drawing rooms, respectively. In the Bajuar agency, radon concentration level was found to vary from 29 ± 6 to 349 ± 5 Bq m⁻³ and 27 ± 7 to 229 ± 5 Bq m⁻³ in bedrooms and drawing room, respectively. Seasonal arithmetic and geometric mean and their respective standard deviations are shown in Figure 4.2.

District wise yearly average indoor radon levels are shown in Figure 4.3 whereas Figure 4.4 shows minimum and maximum values of the yearly average for each district. As may be seen in Figure 4.3, minimum yearly average for bedrooms is 69 ± 31 Bq m⁻³ and for drawing rooms the mean values is 63 ± 20 Bq m⁻³. Minimum yearly average value of 38 ± 7 Bq m⁻³ was found in a bedroom of the Swabi district (see, Figure 4.4).

Table 4.7: Indoor radon levels in Bq m⁻³ in bed rooms and drawing rooms of all houses surveyed in NWFP and FATA areas of Pakistan in Spring season.

H. No	Mohmand		Bajuar		Swabi		Mardan		Charsadda	
	Bed Room	Drawing Room	Bed Room	Drawing Room	Bed Room	Drawing Room	Bed Room	Drawing Room	Bed Room	Drawing Room
1	74±5	40±6	83±5	61±5	118±5	61±5	51±5	46±5	52±6	54±6
2	33±6	94±5	119±5	53±5	57±5	46±6	44±6	51±5	L	48±6
3	100±5	42±6	72±5	79±5	34±6	34±7	52±5	61±5	50±6	45±6
4	32±6	129±5	34±6	86±5	60±6	58±5	L	L	50±6	53±6
5	91±5	52±5	46±6	47±6	42±6	37±6	32±6	51±5	52±6	65±6
6	48±6	22±7	90±5	96±5	52±5	55±6	51±5	61±5	51±6	49±6
7	120±5	L	46±6	35±7	36±6	L	64±5	32±6	53±6	54±6
8	52±5	43±5	86±4	122±5	42±5	38±6	L	L	L	36±7
9	71±5	29±6	49±5	103±5	109±5	78±5	59±5	55±6	46±6	57±6
10	40±6	33±6	138±4	86±5	154±6	79±5	97±5	114±4	80±5	80±5
11	63±5	L	73±5	79±6	51±6	42±6	56±5	50±6	L	55±6
12	57±5	39±6	50±5	L	101±5	57±6	L	96±5	L	L
13	68±5	63±5	57±5	54±6	33±6	44±5	25±7	24±6	66±5	58±6
14	L	99±5	L	92±5	41±6	38±6	64±5	51±6	59±5	59±6
15	117±5	86±5	50±6	45±6	52±6	42±6	58±5	135±5	50±6	59±6
16	78±5	99±5	101±5	49±5	41±6	53±5	58±5	48±5	52±6	60±6
17	L	L	65±5	48±6	41±6	42±6	33±6	35±6	71±5	41±6
18	52±5	36±6	96±5	L	156±5	44±6	180±5	24±7	65±6	61±6
19	86±5	100±5	69±6	68±5	36±6	46±6	73±5	L	61±6	68±6
20	65±5	72±5	148±5	135±5	L	35±6	56±5	55±5	L	55±6
21	74±5	77±5	54±5	61±5	38±9	54±5	56±5	57±5	236±4	182±5
22	62±6	105±5	29±6	55±5	51±5	50±6	L	L	59±6	53±6
23	131±5	L	349±5	67±5	L	26±6	26±6	85±5	74±5	59±6
24	74±5	39±5	97±5	56±5	42±6	54±5	48±5	42±6	50±6	60±5
25	59±5	44±5	L	56±5	55±5	35±6	L	122±5	55±6	82±5
26	59±5	54±5	75±5	69±4	46±5	60±5	L	34±6	50±6	57±6
27	123±5	41±5	87±5	54±6	L	L	60±5	60±5	52±6	49±6
28	30±6	44±5	68±6	51±5	49±6	42±6	29±6	37±6	70±5	48±6
29	45±6	L	49±6	229±5	33±5	L	48±5	50±6	50±6	58±6
30	39±6	92±4	38±6	65±5	48±6	66±5	41±5	100±5	56±5	61±6
31	35±6	30±6	L	L	53±5	40±5	46±6	58±5	46±6	42±6
32	L	61±5	96±4	40±6	98±4	31±6	81±5	44±6	51±6	48±6
33	68±5	L	65±6	47±6	44±6	62±5	L	32±6	45±7	53±6
34	61±5	100±5	L	50±6	40±6	68±5	48±5	82±5	164±5	55±6
35	74±5	102±5	51±5	59±5	36±6	55±7	44±6	41±6	52±6	81±5
36	60±5	47±6	46±5	59±5	32±6	47±6	46±6	30±6	52±6	57±6
37	59±6	32±6	55±5	27±7	102±4	59±5	129±5	95±5	74±5	85±5
38	64±5	38±6	52±6	46±6	39±6	L	35±6	L	46±6	49±6
39	L	79±5	48±5	49±5	L	74±5	26±7	54±5	54±6	63±5
40	96±5	42±6	68±6	70±5	46±6	79±5	55±5	54±6	113±4	51±6

Table 4.8: Weighted average indoor radon in the Spring season.

H.No	Mohmand	Charsadda	Bajuar	Swabi	Mardan
1.	60±5	53±6	74±5	63±6	48±5
2.	57±6	48±6(D)	93±5	72±5	48±5
3.	77±5	48±6	75±5	97±5	57±5
4.	71±6	51±6	55±6	89±5	L
5.	75±5	57±6	46±6	90±5	43±5
6.	38±6	50±6	92±5	82±4	57±5
7.	120±5(D)	53±6	42±6	77±5	45±6
8.	48±5	36±7(D)	100±4	64±5	L
9.	54±5	50±6	71±5	122±4	57±6
10.	37±6	80±5	117±4	L	107±4
11.	38±5	55±6(D)	75±5	70±5	52±6
12.	50±5	L	50±5(B)	81±4	96±5(B)
13.	66±5	63±5	56±5	83±4	24±6
14.	99±5(D)	59±5	92±5(D)	72±5	56±6
15.	105±5	54±6	48±6	58±6	104±5
16.	86±5	55±6	80±5	85±5	48±5
17.	L	59±5	58±5	120±5	35±6
18.	46±5	63±6	96±5(B)	85±5	86±6
19.	92±5	64±6	69±6	94±5	73±5(D)
20.	68±5	55±6	143±5	76±5	55±5
21.	75±5	214±4	57±5	109±4(B)	57±5
22.	79±6	57±6	39±6	74±5	L
23.	131±5(B)	68±5	236±5	74±5	61±5
24.	60±5	54±6	81±5	67±6	44±5
25.	53±5	66±6	56±5(D)	65±5	122±5(B)
26.	57±5	53±6	73±5	65±5	34±6
27.	90±5	51±6	74±5	54±5	60±5
28.	36±6	61±5	61±6	112±5(D)	34±6
29.	45±6(B)	53±6	121±6	85±5	49±6
30.	60±5	58±5	49±6	84±5	76±5
31.	33±6	44±6	L	84±5	53±5
32.	L	50±6	74±5	55±5	59±6
33.	56±5	48±	58±6	67±5	32±6(B)
34.	77±5	120±5	50±6(D)	63±6	68±5
35.	85±5	64±6	54±5	140±5(D)	42±6
36.	55±5	54±6	51±5	66±5	36±6
37.	60±6	78±5	44±6	114±5	109±5
38.	51±5	47±6	50±6	81±5	35±6(D)
39.	79±5(D)	58±6	48±5	88±5	43±6
40.	74±5	88±5	69±6	53±6	54±6

In drawing rooms, a minimum value of $39 \pm 5 \text{ Bq m}^{-3}$ was observed in the district Swabi as well as in the Mohmand agency. Maximum value of $207 \pm 5 \text{ Bq m}^{-3}$ was found in a bedroom of the Charsadda district. According to the weighted yearly average, a minimum value of $47 \pm 5 \text{ Bq m}^{-3}$ was found in the Mohmand agency and a maximum value of $154 \pm 5 \text{ Bq m}^{-3}$ was observed in the district Charsadda. Minimum and maximum weighted yearly average indoor radon came out to be 66 ± 27 and $83 \pm 39 \text{ Bq m}^{-3}$ respectively. Overall arithmetic mean of the area surveyed in the present study was found to be $72 \pm 32 \text{ Bq m}^{-3}$.

4.5. Seasonal Correction Factor

The seasonal correction factor was calculated by dividing the arithmetic mean, calculated for each cycle (i.e. summer, autumn, winter and spring seasons), by the annual arithmetic mean. The results obtained are shown in Figure 4.5. For bedrooms, the seasonal correction factor was found to be 1.15 ± 0.47 , 0.87 ± 0.55 , 0.92 ± 0.37 and 1.14 ± 0.56 for spring, winter, autumn and summer seasons, respectively. For drawing rooms, the seasonal correction factor was found to be 1.14 ± 0.39 , 0.91 ± 0.35 , 0.89 ± 0.34 and 1.17 ± 0.39 for spring, winter, autumn and summer seasons, respectively. Overall seasonal weighted correction factor came out to be 1.15 ± 0.43 , 0.89 ± 0.47 , 0.91 ± 0.35 , 1.15 ± 0.49 for spring, winter, autumn and summer seasons, respectively. The results show that there is a slight difference in the seasonal correction factor of the bedrooms and drawing rooms. Individual data values observed in different seasons show wide variations as compared to the average seasonal correction factor.

4.6. Seasonally Averaged and Yearly Averaged Indoor Radon

In order to know the affect on efficiency of these detectors, comparison of the seasonally measured average indoor radon concentration and the yearly exposed CR-39 detector was made. Whilst taking seasonal measurements, one detector was placed in the drawing rooms for one year. In this section, the data of only those detectors have been taken into account for which both the detectors in drawing rooms in all the four seasons and the yearly exposed detectors were recovered. Minimum, maximum and average indoor radon concentration levels observed in each district/agency for each season as well for the

yearly exposed CR-39 detectors are shown in table 4.9 whereas the individual values are shown in Figures 4.6 – 4.10.

Table 4.9: Minimum, maximum and average radon concentration levels in Bq m^{-3} during the four seasons and yearly averaged exposed detectors in the NWFP and FATA.

Location		Summer	Autumn	Winter	Spring	Seasonal Average	Yearly Average
Swabi	Min	26±6	33±5	45±5	31±5	39±5	23±5
	Max	79±5	138±4	188±4	120±5	110±5	92±6
	Average	50±14	68±20	79±30	58±22	64±13	50±15
Mardan	Min	18±6	60±5	45±6	25±7	46±7	27±5
	Max	81±4	126±5	146±6	180±5	90±5	92±6
	Average	43±15	74±13	68±22	58±32	61±11	49±15
Charsadda	Min	36±7	48±6	42±5	32±5	50±5	37±6
	Max	182±5	146±6	132±5	280±5	137±5	100±6
	Average	61±26	80±21	77±21	69±48	72±21	58±16
Mohmand	Min	22±7	50±7	39±6	23±6	39±6	32±5
	Max	129±5	117±4	147±4	107±4	94±5	156±4
	Average	64±30	76±21	73±23	57±18	68±15	61±31
Bajuar	Min	31±6	53±5	40±5	27±5	53±5	20±5
	Max	123±4	167±5	213±4	229±4	131±5	112±5
	Average	67±27	85±29	94±37	69±37	79±21	71±26

As may be seen in table 4.9, radon concentration levels vary from 39 ± 5 to $110 \pm 5 \text{ Bq m}^{-3}$, with an average of $64 \pm 13 \text{ Bq m}^{-3}$ and from 23 ± 5 to $92 \pm 6 \text{ Bq m}^{-3}$ having an average of $50 \pm 5 \text{ Bq m}^{-3}$ in the drawing rooms of the district Swabi using seasonally and yearly exposed CR-39 detectors, respectively.

In the district Mardan, radon concentration varied from 46 ± 7 to 90 ± 5 in the case of seasonally measured yearly values with an average $61 \pm 11 \text{ Bq m}^{-3}$ and from 27 ± 5 to $92 \pm 6 \text{ Bq m}^{-3}$ in the case where CR-39 were exposed for the year with an average of $49 \pm 15 \text{ Bq m}^{-3}$. In the district Charsadda, variation in the indoor radon level range from 50 ± 5 to 137 ± 5 with an average of 72 ± 21 in the seasonally exposed CR-39 and from

37 ± 6 to 100 ± 6 Bq m⁻³ having an average of 58 ± 16 Bq m⁻³ in the yearly exposed CR-39 detectors, respectively.

In the Mohmand agency, variation in the indoor radon was found to range from 39 ± 6 - 94 ± 5 Bq m⁻³ with an average of 68 ± 15 , and in the range of 32 ± 5 to 156 ± 4 with an average of 61 ± 31 Bq m⁻³ in the case of seasonally exposed and yearly exposed detectors, respectively. In the Bajuar agency, variations in the indoor radon ranged from 53 ± 5 Bq.m⁻³ to 131 ± 5 Bq m⁻³ in the case of seasonally exposed CR-39 detector with an average of 79 ± 21 Bq m⁻³ whilst it varied from 20 ± 5 to 112 ± 5 Bq m⁻³ having an average of 71 ± 26 Bq m⁻³ for the yearly exposed detectors.

4.7. Comparison of Indoor Radon Levels in Bedrooms and Drawing Rooms

It would be informative to compare the indoor radon concentration levels observed in bedroom and drawing room of the same house. As mentioned earlier, all the dosimeters were installed on ground floor, and the houses surveyed were mainly detached type. Ratio of the radon level in the bedroom to that of radon level in the drawing room was determined. Results obtained are shown in table 4.10 In the Mohmand agency and Swabi district, no significant difference was observed in the radon levels in the bedrooms and drawing rooms in the summer season. In the Mardan districts, Bajuar agency and Charsadda districts, this ratio was found to be 1.4, 1.4 and 1.5, respectively. Radon levels were found to be relatively higher in bedrooms as compared to that in drawing rooms. This may be due to the ventilation system, because drawing rooms have usually better ventilation than that of bedrooms in houses of the areas studied. In summer season, largest fluctuation in the bedroom/drawing room ratio was found in the Charsadda district. The bedroom to drawing room ratio varied from 0.2 to 4.5.

In Autumn season, radon average levels in bedrooms and drawing rooms of the Mardan district and Mohmand agency were almost similar. The ratio varied from 0.6 - 2.2 and 0.4-1.7, respectively. In the Swabi it varied from 0.4 - 2.6 with an average of 1.2 whilst in the Charsadda district it varied from 0.6 - 3.3 with an average of 1.2. In the Bajuar agency, it varied from 0.5 - 2.5 with an average of 1.1. In the winter season only in the Mohmand agency this ratio was equal whilst in all the areas average radon in bedroom was 20% higher as compared to that in the drawing rooms.

Minimum ratio of 0.3 was observed in the Bajuar and Swabi and Maximum value of 3.7 was noted in the Charsadda district. In spring season, the average radon concentration in bedrooms was higher than that of the drawing rooms.

Table 4.10: Average ratio of the indoor radon levels in bedroom to drawing room in the selected area.

Location	Quantity	Summer	Autumn	Winter	Spring	Average
Mardan	Minimum	0.5	0.6	0.4	0.1	0.8
	Maximum	3.6	2.2	3.5	3.3	2.9
	Average	1.4	1.0	1.2	1.2	1.2
Mohmand	Minimum	0.4	0.4	0.4	0.3	0.6
	Maximum	2.2	1.7	1.8	4.0	2.3
	Average	1.1	1.0	1.0	1.1	1.0
Swabi	Minimum	0.3	0.4	0.3	0.6	0.5
	Maximum	2.1	2.6	3.1	3.6	2.0
	Average	1.0	1.2	1.2	1.2	1.2
Bajuar	Minimum	0.5	0.5	0.3	0.2	0.6
	Maximum	4.6	2.5	3.3	5.2	2.3
	Average	1.4	1.1	1.2	1.3	1.3
Charsadda	Minimum	0.2	0.6	0.5	0.6	0.8
	Maximum	4.5	3.3	3.7	3.0	2.6
	Average	1.5	1.2	1.2	1.1	1.2

A minimum ratio of 0.1 was observed in the district Mardan whilst maximum ratio of 5.2 was observed in the Bajuar agency. In general, this ratio shows that radon concentration in bedrooms is higher than that in the drawing rooms, respectively.

4.8. Dose Estimation

In order to estimate the annual mean effective dose H (mSv) expected to be received by the general public due to the radon and its progeny, ICRP 65 and UNSCEAR 2000 recommended conversion factors and the annual weighted average indoor radon levels were used. Initially, ICRP recommended occupancy factor of 0.8 was used to calculate the dose. The ICRP factor is higher than that of the average occupancy factor of the selected area (i.e., 0.48). Therefore, using the actual occupancy factor, the dose received

by the public will be ~ 40% lower than that if ICRP recommended conversion factor is used. The results obtained using actual occupancy factor are shown in table 4.11, which shows the mean values of the effective dose received due to the weighted average indoor radon levels. Using ICRP-65 conversion factor, minimum and maximum values of 0.34 ± 0.05 and 1.41 ± 0.05 mSv were obtained in Bajuar agency. UNSCEAR recommended factor yielded minimum and maximum values of 1.20 ± 0.17 and 4.97 ± 0.17 mSv, respectively. In the Swabi ICRP recommended factor yielded minimum and maximum values of 0.50 ± 0.06 and 1.10 ± 0.05 and where as UNSCEAR 2000 factor gave minimum and maximum values of 1.78 ± 0.21 and 3.89 ± 0.17 mSv, respectively.

In the Mohmand agency annual effective dose varied form 0.52 ± 0.06 to 1.33 ± 0.06 mSv and 1.82 ± 0.21 to 4.69 ± 0.19 mSv for ICRP and UNSCEAR conversion factors, respectively. In the district Mardan, annual effective dose showed variation from 0.33 ± 0.04 to 0.97 ± 0.04 using ICRP conversion factor whilst using UNSCEAR factor it varied from 1.47 ± 0.16 to 4.28 ± 0.16 mSv, respectively. In the Charsadda district variation in the dose was form 0.56 ± 0.06 to 1.59 ± 0.05 mSv and from 1.98 ± 0.20 to 5.59 ± 0.19 mSv in the cases of ICRP and UNSCEAR conversion factors, respectively.

Mean annual effective doses (see, table 4.12) were 0.70 ± 0.28 , 0.46 ± 0.20 , 0.79 ± 0.38 , and 0.78 ± 0.32 and 0.85 ± 0.40 mSv for the Swabi, Mardan and Charsadda districts and Mohmand and Bajuar agency, respectively. The UNSCEAR 2000 conversion factor resulted in mean annual effective doses of 2.48 ± 1 , $2.03 \pm .89$, 2.79 ± 1.33 , 2.76 ± 1.12 , 3.10 ± 1.46 mSv in the Swabi, Mardan, Charsadda districts and Mohmand and Bajuar agencies, respectively.

4.9. Excess Lung Cancer Risk

In order to calculate the excess lung cancer risk, BEIR VI conversion factors were used (NRC, 1988; Lubin et al., 1994). U.S. National Research Council, BEIR VI committee modeled the excess relative risk (ERR) as a linear function of the past exposure to radon. This model allows the effect of exposure to vary flexibly with the length of time that has passed since the exposure, with the exposure rate, and with the attained age. The mathematical form of the model for ERR (NRC, 1999) is:

$$ERR = \beta (w_{5-14} + \theta_{15-24} w_{15-24} + \theta_{25+} w_{25+}) \rho_{age} \gamma_z \quad (2)$$

The parameter β represents the slope of the exposure-risk relationship. Exposure in the last 5 years is excluded as it is not biologically relevant to the cancer risk—and exposures in 3 windows of past time, namely 5-14, 15-24, and 25 or more years previously is taken into account. Those exposures are labeled w_{5-14} , w_{15-24} , and w_{25+} , respectively and each is allowed to have its own relative level of effect, θ_{5-14} (set equal to unity), θ_{15-24} , and θ_{25+} , respectively. The rate of exposure also affects risk through the parameter γ_z ; thus, the effect of a particular level of exposure increases with decreasing exposure rate, as indexed either by the duration of exposure or the average concentration at which exposure was received (Lubin et al., 1995).

Two alternative preferred models namely the “exposure-age-concentration model” and the “exposure-age-duration model” have been proposed by BEIR VI. In the present work excess lung cancer risk is calculated using the weighted average radon concentration and the “exposure-age-concentration model”. Occupancy factor is the main parameter which affects the risk.

Therefore, local occupancy factor was used to calculate the risk. In order to make the comparison US EPA occupancy factor was also used. For calculation of excess lung cancer risk two age groups (i.e., 55 and 35 yr) were selected. An assumption was made that radon concentration over the years is same as measured in this study. The results are shown in table 4.13. Excess relative risk (ERR) variation in the Swabi district was form 0.31 ± 0.04 to 0.69 ± 0.03 for 35 yr age and for 55 yr inhabitants its values were 0.25 ± 0.03 to 0.55 ± 0.03 , respectively. If US EPA conversion factor is used then these values comes out to be 0.36 ± 0.03 to 0.78 ± 0.03 and 0.29 ± 0.03 to 0.63 ± 0.03 for 35 and 55 yr age, respectively.

In the Mardan district, ERR varied from 0.26 ± 0.03 to 0.76 ± 0.03 for 35 yr of age and from 0.21 ± 0.03 to 0.61 ± 0.03 for 55 yr of age inhabitants, respectively. The US EPA conversion values yielded excess lung cancer from 0.36 ± 0.03 to 1.04 ± 0.03 and 0.29 ± 0.03 to 0.83 ± 0.03 for 35 and 55 yr age, respectively.

Table 4.11: Annual effective dose calculated using ICRP-65 and UNSCEAR-2000 conversion factor.

Bajuar		Swabi		Mohmand		Mardan		Charsadda	
ICRP-65	UNSCEAR	ICRP-65	UNSCEAR	ICRP-65	UNSCEAR	ICRP-65	UNSCEAR	ICRP-65	UNSCEAR
1.11±0.05	3.91±0.17	0.86±0.05	3.03±0.19	0.82±0.06	2.90±0.20	0.33±0.04	1.47±0.16	0.70±0.05	2.47±0.19
0.77±0.05	2.72±0.19	0.65±0.05	2.28±0.19	0.61±0.06	2.17±0.21	0.43±0.04	1.88±0.16	0.68±0.06	2.41±0.20
0.77±0.05	2.73±0.18	0.65±0.06	2.28±0.20	0.87±0.05	3.06±0.19	0.42±0.03	1.86±0.15	0.64±0.06	2.26±0.21
0.99±0.05	3.51±0.18	0.68±0.05	2.39±0.19	0.73±0.06	2.57±0.20	0.97±0.04	4.28±0.16	0.66±0.06	2.33±0.20
0.76±0.05	2.68±0.18	0.68±0.06	2.39±0.21	0.81±0.06	2.86±0.20	0.42±0.04	1.87±0.16	1.13±0.06	3.97±0.20
0.81±0.05	2.85±0.18	0.67±0.05	2.35±0.18	1.05±0.06	3.71±0.20	0.57±0.04	2.51±0.16	0.62±0.06	2.20±0.20
0.77±0.05	2.71±0.18	0.59±0.06	2.07±0.20	0.69±0.06	2.44±0.21	0.38±0.04	1.69±0.17	0.85±0.06	3.00±0.20
1.26±0.05	4.44±0.17	0.70±0.06	2.48±0.19	0.56±0.06	1.96±0.20	0.87±0.04	3.82±0.16	0.82±0.06	2.89±0.20
0.98±0.05	3.46±0.17	1.08±0.05	3.81±0.17	0.61±0.06	2.14±0.21	0.43±0.04	1.88±0.16	0.61±0.06	2.15±0.21
1.40±0.05	4.94±0.17	0.92±0.05	3.24±0.19	0.52±0.06	1.82±0.21	0.69±0.04	3.05±0.17	1.02±0.06	3.60±0.20
1.18±0.05	4.16±0.18	0.70±0.05	2.48±0.19	0.71±0.06	2.51±0.20	0.40±0.04	1.79±0.16	0.74±0.06	2.60±0.21
0.66±0.05	2.33±0.19	0.70±0.05	2.49±0.19	0.73±0.06	2.57±0.20	0.47±0.04	2.07±0.16	L	L
0.51±0.05	1.79±0.20	0.65±0.05	2.30±0.18	0.84±0.05	2.96±0.18	0.36±0.04	1.58±0.15	0.79±0.06	2.80±0.20
0.75±0.05	2.65±0.17	0.55±0.06	1.93±0.20	0.74±0.06	2.59±0.20	0.40±0.04	1.77±0.16	0.66±0.05	2.33±0.19
0.82±0.05	2.91±0.18	0.55±0.06	1.96±0.21	0.78±0.06	2.75±0.20	0.47±0.04	2.09±0.16	0.65±0.06	2.30±0.21
0.84±0.05	2.96±0.20	0.95±0.05	3.34±0.19	0.76±0.06	2.67±0.19	0.42±0.03	1.86±0.15	0.69±0.06	2.44±0.20
0.85±0.05	3.01±0.18	0.68±0.05	2.40±0.19	1.33±0.06	4.69±0.19	0.35±0.04	1.53±0.15	0.70±0.06	2.46±0.20
0.98±0.05	3.47±0.19	0.89±0.05	3.14±0.19	0.64±0.06	2.25±0.20	0.49±0.04	2.16±0.16	0.93±0.05	3.28±0.19
0.82±0.05	2.88±0.19	0.86±0.05	3.04±0.19	0.99±0.05	3.50±0.19	0.41±0.03	1.81±0.15	0.65±0.06	2.31±0.20
1.08±0.05	3.80±0.19	0.63±0.05	2.21±0.19	0.77±0.06	2.72±0.20	0.55±0.04	2.42±0.16	0.76±0.05	2.67±0.18
0.62±0.05	2.20±0.17	0.73±0.06	2.57±0.21	0.90±0.06	3.17±0.20	0.45±0.04	2.00±0.16	1.32±0.05	4.67±0.19
0.66±0.05	2.33±0.17	0.85±0.05	3.00±0.18	0.82±0.05	2.91±0.19	0.51±0.04	2.23±0.15	0.66±0.05	2.32±0.19
1.29±0.05	4.55±0.17	0.55±0.05	1.95±0.19	1.12±0.05	3.97±0.18	0.45±0.03	2.01±0.14	1.59±0.05	5.59±0.19
0.71±0.05	2.51±0.16	0.64±0.06	2.25±0.20	0.65±0.06	2.28±0.20	0.41±0.04	1.82±0.16	0.68±0.05	2.41±0.18
1.41±0.05	4.97±0.17	0.62±0.06	2.20±0.19	0.59±0.06	2.08±0.22	0.56±0.04	2.45±0.17	0.70±0.06	2.48±0.20
0.34±0.05	1.20±0.17	0.50±0.06	1.78±0.21	0.98±0.05	3.45±0.18	0.35±0.03	1.54±0.16	0.56±0.06	1.98±0.20
0.79±0.05	2.78±0.18	0.55±0.06	1.94±0.20	0.87±0.05	3.07±0.19	0.41±0.03	1.81±0.15	0.74±0.05	2.60±0.19
0.97±0.05	3.41±0.18	0.56±0.06	1.98±0.20	0.62±0.06	2.19±0.20	0.39±0.04	1.72±0.16	0.65±0.05	2.31±0.19
1.24±0.05	4.37±0.18	0.65±0.06	2.29±0.19	0.65±0.06	2.28±0.21	0.45±0.04	1.98±0.17	0.86±0.06	3.02±0.20
0.57±0.05	2.00±0.20	0.67±0.05	2.35±0.19	0.71±0.06	2.52±0.20	0.80±0.04	3.52±0.16	0.70±0.06	2.45±0.21
0.78±0.05	2.76±0.18	0.61±0.06	2.14±0.20	0.73±0.06	2.56±0.21	0.40±0.04	1.76±0.16	0.76±0.05	2.70±0.19
0.99±0.05	3.48±0.19	0.62±0.05	2.20±0.18	L	L	0.40±0.03	1.76±0.15	0.76±0.05	2.69±0.19
0.84±0.05	2.95±0.18	0.67±0.06	2.37±0.20	0.75±0.06	2.63±0.20	0.37±0.04	1.65±0.16	0.79±0.06	2.77±0.19
0.72±0.05	2.55±0.19	0.68±0.06	2.41±0.21	0.90±0.06	3.19±0.19	0.52±0.03	2.30±0.15	0.87±0.05	3.08±0.18
0.81±0.05	2.84±0.18	0.70±0.06	2.48±0.22	0.80±0.06	2.81±0.20	0.37±0.04	1.62±0.16	0.78±0.05	2.77±0.19
0.59±0.05	2.08±0.18	0.61±0.06	2.16±0.20	0.75±0.06	2.65±0.21	0.35±0.04	1.54±0.16	0.86±0.05	3.03±0.19
0.62±0.05	2.18±0.18	1.10±0.05	3.89±0.17	0.64±0.06	2.26±0.21	0.47±0.04	2.05±0.17	0.91±0.05	3.20±0.18
0.80±0.05	2.82±0.19	0.63±0.05	2.22±0.19	0.64±0.06	2.28±0.21	0.37±0.04	1.64±0.16	0.63±0.06	2.23±0.20
0.78±0.05	2.77±0.17	0.67±0.06	2.36±0.20	0.78±0.06	2.75±0.18	0.35±0.03	1.56±0.14	0.65±0.06	2.29±0.19
0.93±0.05	3.28±0.18	0.71±0.06	2.52±0.19	1.08±0.06	3.80±0.20	0.47±0.04	2.09±0.16	0.82±0.06	2.90±0.20

Table 4.12: Mean effective dose in mSv expected to be received by the inhabitants of the area using ICRP-65 and UNSCEAR, 2000 conversion factors.

S.No	Conversion Factor	Bed Room AM±SD	Drawing Room AM±SD	Bed Room GMG±GSD	Drawing Room GM±GSD	Overall Weighting AM±SD	Overall Weighted AM±SD
Charsadda	ICRP-65	0.83±.44	0.72±.28	0.78±0.01	0.68±.01	0.79±.38	0.74±.01
	UNSCEAR	2.95±1.56	2.55±.98	2.74±.05	2.41±.05	2.79±1.33	2.61±.05
Mardan	ICRP-65	0.48±.24	0.43±.15	0.44±.01	0.41±.01	0.46±.20	0.42±.01
	UNSCEAR	2.13±1.05	1.88±.65	1.94±.04	1.79±.04	2.03±.89	1.85±.04
Swabi	ICRP-65	0.73±.33	0.66±.21	0.67±.02	0.63±.01	0.70±.28	0.65±.02
	UNSCEAR	2.57±1.17	2.34±.76	2.36±.06	2.24±.05	2.48±1	2.29±.05
Mohmand	ICRP-65	0.81±.36	0.74±.26	0.75±.02	0.70±.01	0.78±.32	0.72±.02
	UNSCEAR	2.85±1.27	2.62±.90	2.64±.06	2.47±.05	2.76±1.12	2.54±.05
Bajuar	ICRP-65	0.92±.44	0.80±.35	0.80±.02	0.74±.01	0.85±.40	0.77±.02
	UNSCEAR	3.23±1.60	2.90±1.26	2.92±.06	2.69±.05	3.10±1.46	2.79±.06
Over all	ICRP-65	0.78±.38	0.70±.26	0.71±.01	0.66±.01	0.74±.33	0.69±.01
	UNSCEAR	2.75±1.34	2.46±.90	2.50±.05	2.32±.05	2.61±1.16	2.43±.05

In the Charsadda district the ERR values varied from 0.35 ± 0.03 to 0.99 ± 0.03 and 0.28 ± 0.03 to 0.79 ± 0.03 for 35 and 55 yr of age, respectively. However, for the EPA occupancy factor, these values varied from 0.41 ± 0.03 to 1.16 ± 0.03 and 0.33 ± 0.03 to 0.92 ± 0.03 for 35 and 55 yr of ages, respectively.

In the Mohmand agency, this variation was from 0.32 ± 0.04 to 0.83 ± 0.03 and from 0.26 ± 0.03 to 0.66 ± 0.03 for 35 and 55 yr ages respectively. For US EPA factor these values were 0.35 ± 0.04 - 0.91 ± 0.03 and 0.28 ± 0.03 to 0.73 ± 0.03 for 35 and 55 yr ages respectively. In the Bajuar agency, the excess lung cancer risk varied from 0.21 ± 0.03 to 0.89 ± 0.03 and 0.17 ± 0.02 to 0.71 ± 0.03 for the area using the local occupancy factor whilst it varied from 0.24 ± 0.03 to 1.0 ± 0.03 and from 0.19 ± 0.03 to 0.80 ± 0.03 for the 35 and 55 yr age groups using US EPA occupancy factor, respectively. In general, using the US EPA occupancy factor the BEIR VI gave 14% (Swabi), 10% (Mohmand), 37% (Mardan) 17% (Charsadda) and 12% (Bajuar) higher excess lung cancer risk as compared to the use of local occupancy factor for each district /agency with an average of 18%.

4.10. Discussion

Indoor radon concentration annual arithmetic mean of the present study ($72 \pm 32 \text{ Bq m}^{-3}$) lies within the published values of the for different countries (see, UNSCEAR, 2000 and references quoted there in). Comparing the present data with the neighboring country India, the present values are higher than the values reported for Ammachal Pradesh (45 Bq m^{-3}), Asam (42 Bq m^{-3}), Mizoram (38 Bq m^{-3}) whilst it is lower than that reported for Megahalaya (68 Bq.m^{-3}) (Dwivedia et al., 2005). For Pakistan, higher value of the arithmetic mean of 111.34 Bq m^{-3} has been reported for Skardu City, which is much higher than the mean value of the present study (Akram et al.,2005). Lower value of 31 Bq m^{-3} is reported for the Bahawalpur Division (Matiullah et al., 2003). Variation in the indoor radon concentration level in the houses surveyed may mainly be due to the local geological formations on which the houses have been built as well as ventilation system of the surveyed houses. Keeping socio-economic conditions of the area surveyed, nothing can be done about the first factor. Therefore, to minimize the indoor radon level, better ventilation systems are needed to be incorporated in these houses. This study revealed that Charsadda district and Bajuar agency has relatively higher indoor radon levels.

Different countries/agencies have recommended different maximum permissible limits for the indoor radon concentration levels in domestic properties. If we compare our results with ICRP recommended maximum constraint limit of 600 Bq m^{-3} (ICRP-65), EPA action level of 4 pCi.l^{-1} (148 Bq m^{-3}) or NRPB, UK limit of 200 Bq m^{-3} (NRPB, 1990) it is clear that all yearly arithmetic mean values of all the districts/agencies are below the recommended limits of ICRP, NRPB, UK or US EPA limits.

Only in seven bedrooms of the houses, yearly average indoor radon greater than that of the US EPA limits whilst all the values of the indoor radon concentration in drawing rooms are within the limits. According to the weighted average indoor radon concentration data, only in one house exceeded the EPA limit, no value is higher than NRPB and ICRP limits.

Individual readings in different houses exceeded the US EPA or NRPB limits i.e. 3, 2, 4 and 2 drawing rooms in spring, winter, autumn and summer respectively exceeded the EPA limit whilst one drawing room in each season exceeded the NRPB limit.

Table 4.13: Excess relative risk of lung cancer due to the indoor radon in the selected areas.

Bajuar		Swabi		Mohmand		Mardan		Charsadda	
Age 35	Age 55	Age 35	Age 55	Age 35	Age 55	Age 35	Age 55	Age 35	Age 55
0.70±0.03	0.56±0.02	0.53±0.03	0.43±0.03	0.51±0.04	0.41±0.03	0.26±0.03	0.21±0.02	0.44±0.03	0.35±0.03
0.49±0.03	0.39±0.03	0.40±0.03	0.32±0.03	0.38±0.04	0.30±0.03	0.34±0.03	0.27±0.02	0.43±0.04	0.34±0.03
0.49±0.03	0.39±0.03	0.40±0.03	0.32±0.03	0.54±0.03	0.43±0.03	0.33±0.03	0.26±0.02	0.40±0.04	0.32±0.03
0.63±0.03	0.50±0.03	0.42±0.03	0.34±0.03	0.45±0.04	0.36±0.03	0.76±0.03	0.61±0.02	0.41±0.04	0.33±0.03
0.48±0.03	0.38±0.03	0.42±0.04	0.34±0.03	0.50±0.04	0.40±0.03	0.33±0.03	0.27±0.02	0.71±0.04	0.56±0.03
0.51±0.03	0.41±0.03	0.41±0.03	0.33±0.03	0.65±0.04	0.52±0.03	0.45±0.03	0.36±0.02	0.39±0.04	0.31±0.03
0.49±0.03	0.39±0.03	0.37±0.04	0.29±0.03	0.43±0.04	0.34±0.03	0.30±0.03	0.24±0.02	0.53±0.04	0.42±0.03
0.80±0.03	0.64±0.03	0.44±0.03	0.35±0.03	0.35±0.03	0.28±0.03	0.68±0.03	0.54±0.02	0.51±0.04	0.41±0.03
0.62±0.03	0.50±0.02	0.67±0.03	0.54±0.02	0.38±0.04	0.30±0.03	0.34±0.03	0.27±0.02	0.38±0.04	0.30±0.03
0.89±0.03	0.71±0.02	0.57±0.03	0.46±0.03	0.32±0.04	0.26±0.03	0.55±0.03	0.44±0.02	0.64±0.03	0.51±0.03
0.75±0.03	0.60±0.03	0.44±0.03	0.35±0.03	0.44±0.03	0.35±0.03	0.32±0.03	0.25±0.02	0.46±0.04	0.37±0.03
0.42±0.03	0.33±0.03	0.44±0.03	0.35±0.03	0.45±0.03	0.36±0.03	0.37±0.03	0.30±0.02	L	L
0.32±0.04	0.26±0.03	0.41±0.03	0.32±0.03	0.52±0.03	0.42±0.03	0.28±0.03	0.23±0.02	0.50±0.04	0.40±0.03
0.47±0.03	0.38±0.02	0.34±0.04	0.27±0.03	0.46±0.04	0.37±0.03	0.32±0.03	0.25±0.02	0.41±0.03	0.33±0.03
0.52±0.03	0.42±0.03	0.34±0.04	0.28±0.03	0.49±0.03	0.39±0.03	0.37±0.03	0.30±0.02	0.41±0.04	0.33±0.03
0.53±0.04	0.42±0.03	0.59±0.03	0.47±0.03	0.47±0.03	0.38±0.03	0.33±0.03	0.27±0.02	0.43±0.04	0.35±0.03
0.54±0.03	0.43±0.03	0.42±0.03	0.34±0.03	0.83±0.03	0.66±0.03	0.27±0.03	0.22±0.02	0.44±0.03	0.35±0.03
0.62±0.03	0.50±0.03	0.55±0.03	0.44±0.03	0.40±0.04	0.32±0.03	0.39±0.03	0.31±0.02	0.58±0.03	0.46±0.03
0.52±0.03	0.41±0.03	0.54±0.03	0.43±0.03	0.62±0.03	0.49±0.03	0.32±0.03	0.26±0.02	0.41±0.04	0.33±0.03
0.68±0.03	0.54±0.03	0.39±0.03	0.31±0.03	0.48±0.04	0.38±0.03	0.43±0.03	0.35±0.02	0.47±0.03	0.38±0.03
0.40±0.03	0.32±0.02	0.45±0.04	0.36±0.03	0.56±0.03	0.45±0.03	0.36±0.03	0.29±0.02	0.83±0.03	0.66±0.03
0.42±0.03	0.33±0.02	0.53±0.03	0.42±0.03	0.51±0.03	0.41±0.03	0.40±0.03	0.32±0.02	0.41±0.03	0.33±0.03
0.82±0.03	0.65±0.02	0.34±0.03	0.27±0.03	0.70±0.03	0.56±0.03	0.36±0.03	0.29±0.02	0.99±0.03	0.79±0.03
0.45±0.03	0.36±0.02	0.40±0.04	0.32±0.03	0.40±0.03	0.32±0.03	0.32±0.03	0.26±0.02	0.43±0.03	0.34±0.03
0.89±0.03	0.71±0.02	0.39±0.03	0.31±0.03	0.37±0.04	0.29±0.03	0.44±0.03	0.35±0.02	0.44±0.03	0.35±0.03
0.21±0.03	0.17±0.02	0.31±0.04	0.25±0.03	0.61±0.03	0.49±0.03	0.28±0.03	0.22±0.02	0.35±0.03	0.28±0.03
0.50±0.03	0.40±0.03	0.34±0.04	0.27±0.03	0.54±0.03	0.43±0.03	0.32±0.03	0.26±0.02	0.46±0.03	0.37±0.03
0.61±0.03	0.49±0.03	0.35±0.04	0.28±0.03	0.39±0.04	0.31±0.03	0.31±0.03	0.24±0.02	0.41±0.03	0.33±0.03
0.78±0.03	0.63±0.03	0.40±0.03	0.32±0.03	0.40±0.04	0.32±0.03	0.35±0.03	0.28±0.02	0.54±0.04	0.43±0.03
0.36±0.04	0.29±0.03	0.41±0.03	0.33±0.03	0.44±0.03	0.35±0.03	0.63±0.03	0.50±0.02	0.44±0.04	0.35±0.03
0.49±0.03	0.39±0.03	0.38±0.04	0.30±0.03	0.45±0.04	0.36±0.03	0.31±0.03	0.25±0.02	0.48±0.03	0.38±0.03
0.62±0.03	0.50±0.02	0.39±0.03	0.31±0.03	L	L	0.32±0.03	0.25±0.02	0.48±0.03	0.38±0.03
0.53±0.03	0.42±0.03	0.42±0.03	0.33±0.03	0.46±0.04	0.37±0.03	0.30±0.03	0.24±0.02	0.49±0.03	0.39±0.03
0.46±0.03	0.36±0.03	0.43±0.04	0.34±0.03	0.56±0.03	0.45±0.03	0.41±0.03	0.33±0.02	0.55±0.03	0.44±0.03
0.51±0.03	0.41±0.03	0.44±0.04	0.35±0.03	0.50±0.03	0.40±0.03	0.29±0.03	0.23±0.02	0.49±0.03	0.39±0.03
0.37±0.03	0.30±0.03	0.38±0.04	0.30±0.03	0.47±0.04	0.37±0.03	0.27±0.03	0.22±0.02	0.54±0.03	0.43±0.03
0.39±0.03	0.31±0.03	0.69±0.03	0.55±0.02	0.40±0.04	0.32±0.03	0.37±0.03	0.29±0.02	0.57±0.03	0.45±0.03
0.51±0.03	0.40±0.03	0.39±0.03	0.31±0.03	0.40±0.04	0.32±0.03	0.29±0.03	0.23±0.02	0.40±0.04	0.32±0.03
0.50±0.03	0.40±0.02	0.42±0.03	0.33±0.03	0.48±0.03	0.39±0.03	0.28±0.03	0.22±0.02	0.41±0.03	0.32±0.03
0.59±0.03	0.47±0.03	0.44±0.03	0.35±0.03	0.67±0.03	0.54±0.03	0.37±0.03	0.30±0.02	0.52±0.03	0.41±0.03

Indoor radon in 4, 16, 4 and 9 bedrooms in different houses exceeded EPA limit in the spring, winter, autumn and summer season respectively. One drawing room data in each season exceeded the NRPB limit. Weighted average results in lesser fluctuation in the indoor radon concentration and no value exceeded the ICRP or NRPB limit and only few values are higher than US EPA limits. There is no available data indicating the seasonal variation of radon levels in this locality, therefore, the values obtained may provide a basis for the future studies. Other workers or groups have noted that the indoor radon levels are inversely related to the outside temperature, which was also found to be true in the present study. In a study carried out in UK, Pinel et al.1995, has reported seasonal correction factor which has similar trend as reported in this work.

Analysis of the annual averages of the data show that weighted average indoor radon has relatively lesser fluctuations as compared to the individual values. Radon levels showed wide variations measured in different seasons of the year. Highest and lowest indoor radon levels were observed in winter and summer seasons, respectively. From the observed indoor radon levels, seasonal correction factor was calculated and compared with the correction factors reported for other countries of the world. For example, Grainger et al., 2000, have reported seasonal correction factors of 1.17 and 0.85 for summer and winter in the Isle of Man, UK. Their results are in agreement with the seasonal factor derived in the present study. For France, Baysson et al., 2003 have reported seasonal correction factors of 0.93, 0.99, 1.075 and 0.99 for winter, spring, summer and autumn, respectively. The data of Baysson et al., 2003 show different trend compared with the present results. The results of Pinel et al. 1995 and UKCCS, 2000 agree well in winter with the values of the current study. The data reported by Matiullah et al., 2003 and Mishra et al., 2004 also show similar trend as that of the present data.

Highest seasonal correction factors of 1.33 ± 0.3 and 1.32 ± 0.47 were found for drawing rooms and bedrooms in the Mardan and Swabi districts in the summer season, respectively which is ~18% higher than the overall seasonal correction factor. Seasonal correction factor is higher in spring and summer seasons and lower in winter and autumn seasons. Although there are different average values of the indoor radon and seasonal correction factor for bedroom and drawing rooms yet this difference is not statistically

significant. Weighted average values of the present study revealed that Bajuar agency has relatively higher indoor radon levels as compared to the other districts/agency.

Comparison of the results of the yearly and seasonally exposed detector indicate that in the district Swabi, out of 30 values, in twenty-five drawing rooms the yearly averaged value was lower than the seasonally obtained average values. The individual values in each drawing room show fluctuations. Nevertheless, yearly exposed detectors gave value which were 23% lower than the seasonally measured values. In the district Mardan, 19 out of 25 in drawing rooms seasonally measured average radon was higher as compared to the yearly averaged indoor radon levels. The seasonally averaged value is ~19% higher than the yearly measured indoor radon levels in Mardan.

In the district Charsadda, out of 29 drawing rooms only two yearly exposed CR-39 detectors yielded indoor radon levels higher than the seasonally measured values. In general, the yearly average values were ~25% lower than the seasonally measured average values. In the Mohmand agency in 18 out of 27 drawing rooms, seasonally measured values were higher than the yearly measured values. In this agency, yearly values were on the average ~10% lower than the seasonally measured values. In the Bajuar agency, a similar trend was observed.

The reason of relatively lower yearly indoor radon levels may partially be due to the fact that a layer of dust may be settled on the surface of the CR-39 there by reducing the track registration efficiency of CR-39 because some of the alpha particles may lose its energy in the dead layer of the dust above the CR-39 detectors which in turn results in lower indoor radon levels. It has been shown (Homer and Miles, 1986) that heat and humidity in the presence of oxygen in the air can affect the sensitivity of the etched-track detector during their use to measure radon. The magnitude of the effect depends on the detector materials, the etching conditions and counting techniques. In one study (Wrixon et al., 1988), it has been reported that when tracks in CR-39 were counted using a semi-automatic system, the sensitivity of the etched track detector was reduced by 18% during the exposure of 6 months, resulting in an average sensitivity, which was lower 9% lower than that of the initially measured sensitivity. Corrections of such an effect must be taken into account in calculating the of radon concentrations.

As mentioned earlier, different countries/agencies have recommended different maximum permissible limits for indoor radon concentration level. For example, ICRP recommends a maximum constraint limit of 600 Bq m^{-3} (ICRP-65), EPA action level is 4 pCi.l^{-1} (148 Bq m^{-3}) and Health Protection agency, UK follow a limit of 200 Bq m^{-3} (NRPB, 1987 and 1990) for indoor radon level (domestic properties). It is worth mentioning here that Pakistan Nuclear Regulatory Authority (PNRA) is responsible for defining radiation exposure limits for occupational radiation workers and general population. Generally, ICRP recommended limits are adopted by the PNRA in Pakistan. However, so far, no limits have been defined for indoor radon concentration levels by the PNRA. Like other countries of the world, PNRA has also to define indoor radon exposure limits at some stage. In this regard, environmental conditions and economic conditions, etc. of Pakistan have to be taken into consideration. It is suggested that the value recommended by the ICRP may be adopted in this regard. However, for this purpose, extensive indoor radon monitoring is necessary to map the country to generate baseline data.

4.11. Conclusions

To conclude, indoor radon levels have been measured in some districts of the NWFP which included Swabi, Mardan and Charsadda as well the Mohmand and Bajaur Agencies of FATA. From the measured indoor radon levels, annual effective doses were calculated. All of the houses surveyed had indoor radon levels within permissible level when ICRP recommended limit of 600 Bq m^{-3} was used. Few houses had higher radon levels if NRPB (Health Protection agency) UK and US (environmental protection agency) EPA limits of 200 and 148 Bq m^{-3} were used. There is a higher fluctuation during the summer (by a factor of 5 in one case) in the indoor radon levels on the same floor in different rooms of the same house. However it may be mentioned here that Pakistan has variable geologies and climatic conditions. It is, therefore, suggested that an extensive study of the indoor radon levels through out the country may be initiated. Seasonal correction factor has been calculated and compared with the correction factors reported for other countries of the world. Maximum indoor radon concentration levels have been observed in the winter whereas minimum concentration levels were found in the summer season. The indoor radon levels have been found to depend on the season of

the year and therefore seasonal correction factor has to be applied in calculating the annual mean radon concentration from the measured data. The dose has to be calculated using local occupancy factor. Seasonally measured average values are higher as compared to the yearly exposed CR-39 detectors. Long term exposure of CR-39 reduces its results in reduced track registration efficiency due to the formation of a layer of non radioactive dust over the surface of the detectors. Seasonally measured values are ~13% higher than the yearly measured values.

After the detailed analysis of indoor radon and its spatial and temporal variations in the next chapter experiments about the radon exhalation rate has been discussed.

Table 4.14: Yearly average indoor radon in the bedrooms and drawing rooms of the selected area.

H. No	Mohmand		Bajuar		Mardan		Swabi		Charsadda	
	Bed Room	Drawing Room	Bed Room	Drawing Room	Bed Room	Drawing Room	Bed Room	Drawing Room	Bed Room	Drawing Room
1.	81±5	65±5	114±4	90±4	44±5	53±6	96±5	59±5	76±5	55±6
2.	52±5	62±5	86±5	53±5	64±5	56±6	67±5	51±5	72±5	57±6
3.	93±4	57±5	72±5	75±5	69±5	47±5	59±5	64±5	68±6	54±5
4.	47±6	94±5	93±5	94±5	187±5	66±5	68±5	59±5	68±6	57±5
5.	83±5	59±5	77±5	63±5	64±4	55±5	66±6	61±5	133±6	74±5
6.	108±5	77±5	77±5	75±5	76±5	90±5	57±5	72±5	58±5	64±5
7.	68±5	55±6	78±5	64±5	53±4	57±5	52±5	60±5	77±6	90±5
8.	43±5	62±5	110±4	131±5	150±5	84±5	70±5	62±5	99±5	50±6
9.	61±5	46±6	71±4	124±5	65±5	55±5	117±4	79±5	64±5	51±6
10.	44±5	50±6	133±4	130±5	109±6	84±6	97±5	72±5	74±6	137±5
11.	65±5	L	111±5	111±5	50±5	70±5	72±5	58±5	82±6	56±6
12.	70±5	60±5	64±5	59±6	71±5	62±4	72±5	58±5	L	L
13.	89±4	58±5	48±5	48±6	52±5	51±5	66±5	55±5	93±6	52±6
14.	61±5	75±5	68±4	75±5	59±5	55±5	50±5	54±5	62±5	67±5
15.	77±5	61±5	86±5	65±5	72±5	61±5	51±6	54±5	64±6	62±6
16.	64±5	75±5	98±5	50±6	60±5	61±5	99±5	75±6	65±6	70±5
17.	148±5	80±5	87±5	70±5	56±5	41±6	51±5	85±5	66±5	70±5
18.	56±5	61±5	104±5	76±5	58±6	88±5	93±5	70±5	85±5	98±5
19.	88±5	93±5	73±5	83±5	48±5	74±5	94±5	62±5	60±6	69±5
20.	65±6	77±5	98±5	107±5	81±5	76±5	62±5	55±5	74±5	72±6
21.	83±5	79±5	63±4	53±5	70±5	57±5	78±6	55±5	129±5	127±5
22.	73±5	77±5	61±5	64±4	63±5	87±5	91±5	65±5	65±5	62±5
23.	115±4	82±5	152±5	75±5	72±5	55±5	56±5	47±5	207±5	75±6
24.	60±5	56±5	67±5	67±4	55±5	65±5	58±6	63±5	71±5	59±5
25.	54±5	53±6	173±5	72±4	83±5	74±5	64±5	51±5	71±5	64±6
26.	90±5	88±5	L	80±4	50±5	51±5	43±6	55±5	61±5	45±6
27.	92±5	59±5	82±5	63±5	61±6	55±5	54±6	49±5	75±5	66±5
28.	57±5	56±5	106±5	69±5	58±6	53±6	43±6	69±5	68±5	57±6
29.	50±6	71±5	107±5	131±5	65±5	63±5	68±5	51±5	84±6	82±5
30.	56±5	78±5	51±5	57±5	149±6	62±5	60±5	67±5	68±6	67±6
31.	66±5	66±5	70±5	79±5	58±6	56±5	55±5	60±6	86±5	56±5
32.	L	L	95±4	89±5	53±6	64±5	72±5	39±5	74±5	74±5
33.	75±5	56±6	81±5	74±5	54±5	52±6	66±5	60±6	70±6	86±5
34.	79±5	86±5	81±5	49±5	82±5	63±5	62±6	69±5	96±5	67±5
35.	65±5	83±5	66±5	91±4	51±6	55±5	38±7	110±5	75±5	78±5
36.	66±5	71±6	47±5	68±4	50±5	50±6	67±5	44±6	91±5	71±6
37.	58±6	58±5	56±5	62±5	66±5	67±6	121±4	79±5	88±5	88±5
38.	71±5	39±6	83±5	64±5	57±5	47±6	56±5	65±5	64±6	58±6
39.	74±4	66±5	80±4	65±5	53±6	46±6	57±5	71±5	67±5	56±5
40.	113±5	75±5	94±5	77±5	73±5	61±5	71±5	62±5	89±5	66±6

Table 4.15: Weighted average indoor radon levels in the NWFP and FATA, Pakistan.

H. No	Mohmand	Swabi	Mardan	Charsadda	Bajuar
1.	75±5	81±5	48±5	68±5	104±4
2.	56±5	61±5	61±5	66±5	73±5
3.	79±5	61±5	60±5	62±6	73±5
4.	66±5	64±5	139±5	64±6	94±5
5.	74±5	64±6	61±5	109±5	71±5
6.	95±5	63±5	81±5	60±5	76±5
7.	63±5	55±5	55±5	82±6	72±5
8.	50±5	66±5	124±5	79±6	118±4
9.	55±5	102±5	61±5	59±6	92±4
10.	47±5	87±5	99±5	99±5	132±4
11.	65±5	66±5	58±5	72±6	111±5
12.	66±5	67±5	67±5	L	62±5
13.	76±5	62±5	51±5	77±6	48±5
14.	67±5	52±5	57±5	64±5	71±4
15.	71±5	52±6	68±5	63±6	78±5
16.	69±5	89±5	60±5	67±6	79±5
17.	121±5	64±5	50±5	68±5	80±5
18.	58±5	84±5	70±6	90±5	92±5
19.	90±5	81±5	59±5	63±6	77±5
20.	70±5	59±5	79±5	73±5	101±5
21.	81±5	69±6	65±5	128±5	59±4
22.	75±5	80±5	72±5	64±5	62±5
23.	102±5	52±5	65±5	154±5	121±5
24.	59±5	60±5	59±5	66±5	67±4
25.	53±6	59±5	79±5	68±5	132±4
26.	89±5	48±6	50±5	54±5	32±4
27.	79±5	52±5	59±6	71±5	74±5
28.	56±5	53±5	56±6	63±5	91±5
29.	59±5	61±5	64±5	83±6	117±5
30.	65±5	63±5	114±6	67±6	53±5
31.	66±5	57±5	57±6	74±5	73±5
32.	L	59±5	57±5	74±5	93±4
33.	68±6	63±5	54±5	76±5	79±5
34.	82±5	65±6	74±5	85±5	68±5
35.	72±5	66±6	53±5	76±5	76±5
36.	68±5	58±5	50±5	83±5	55±5
37.	58±6	104±4	67±5	88±5	58±5
38.	59±5	60±5	53±5	61±6	75±5
39.	71±5	63±5	50±6	63±5	74±5
40.	98±5	67±5	68±5	80±5	87±5

Figure 4.1: Minimum and maximum radon concentration levels in each season in the listed areas of the NWFP and FATA.

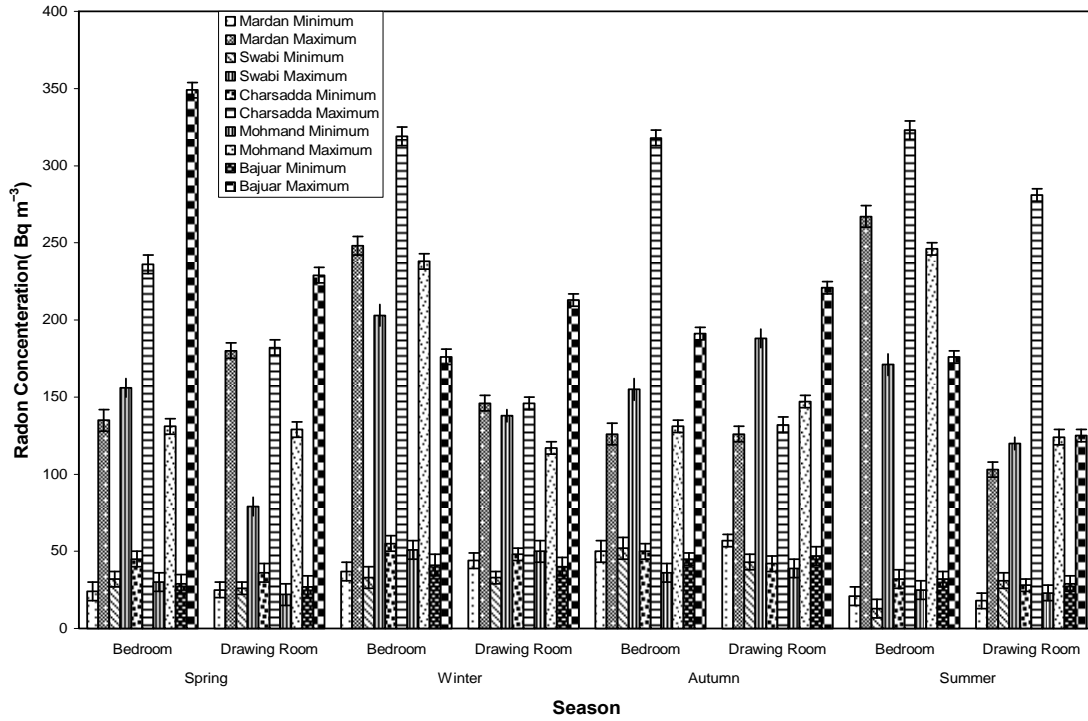


Figure 4.2: Mean seasonal indoor radon concentration in the listed areas of the NWFP and FATA, Pakistan.

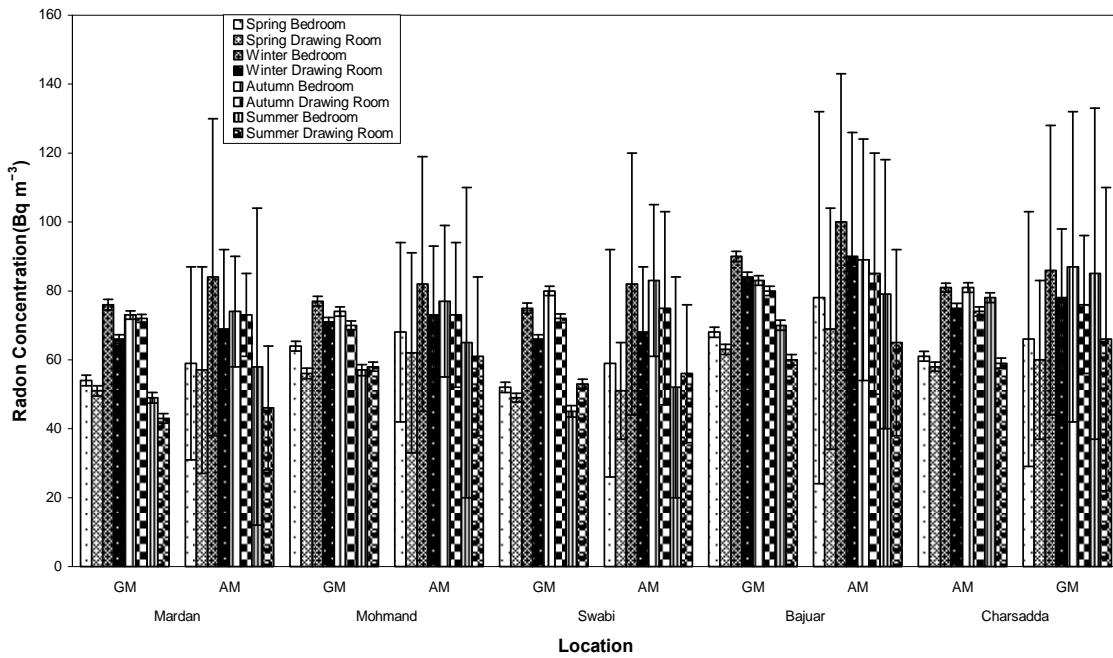


Figure 4.3: Yearly average radon concentration levels in NWFP and FATA.

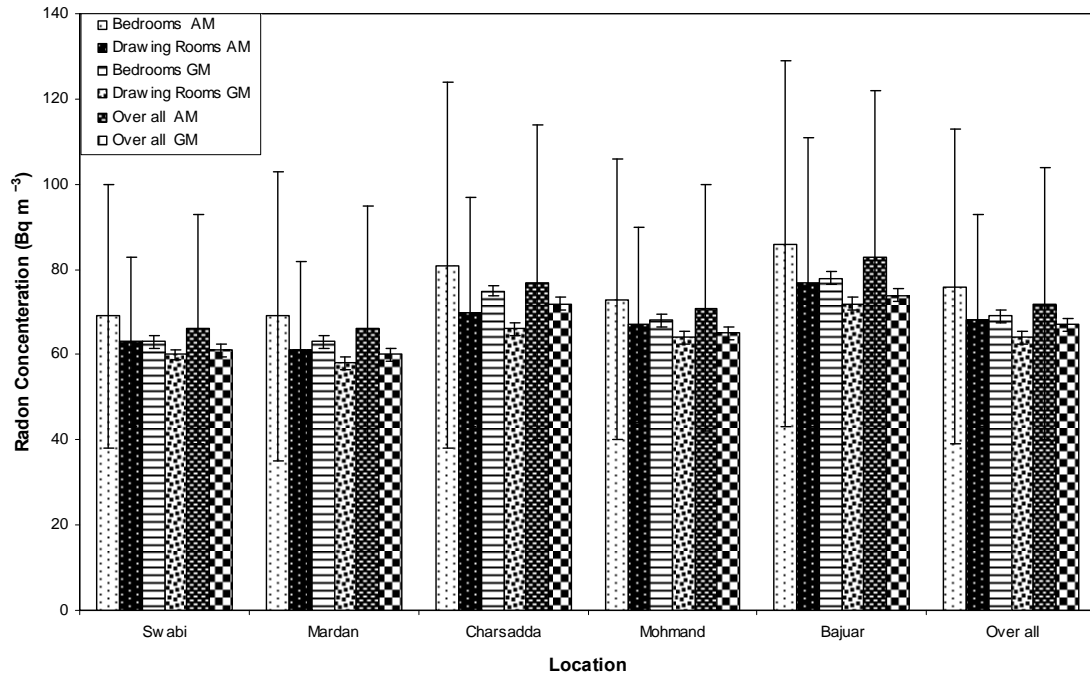


Figure 4.4: Yearly average minimum and maximum indoor radon concentration levels in Bq m^{-3} in bedrooms and drawing rooms of the area selected.

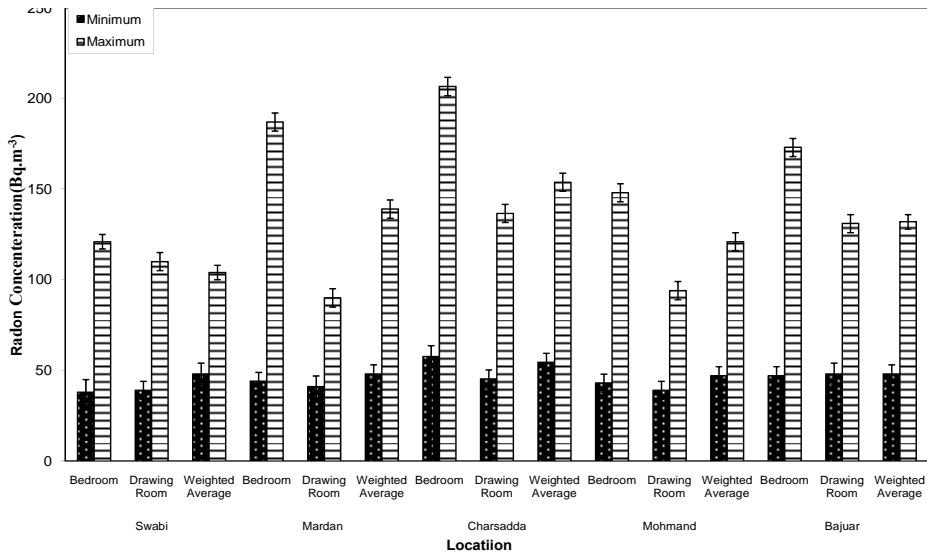


Figure 4.5: Seasonal correction factor for the listed areas of NWFP and FATA.

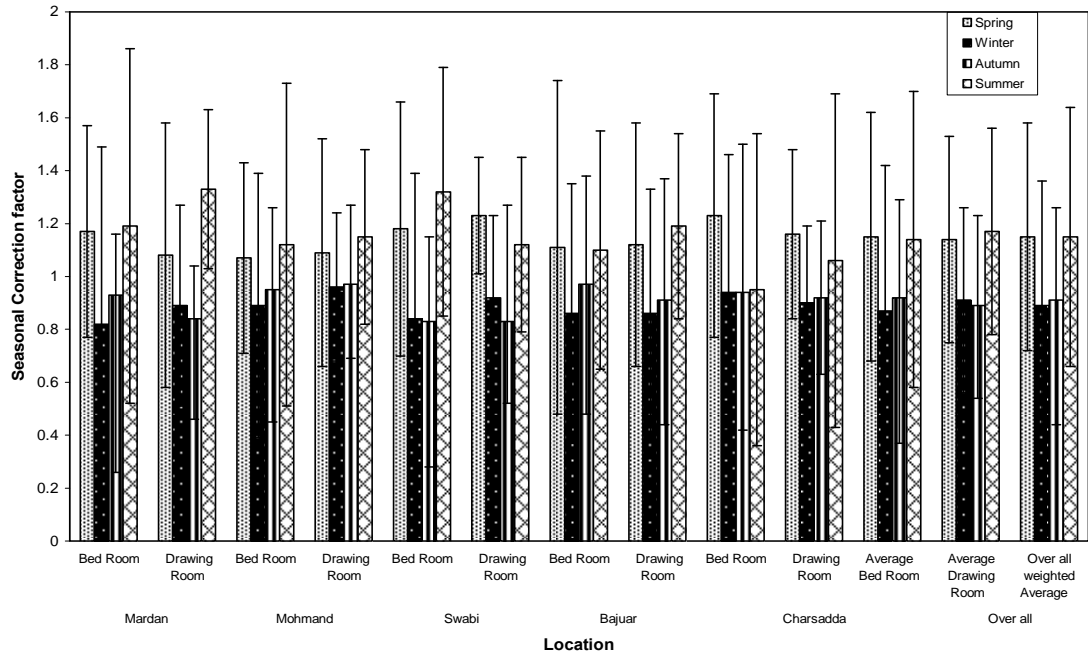


Figure 4.6: Yearly and seasonally averaged yearly radon levels in Swabi district.

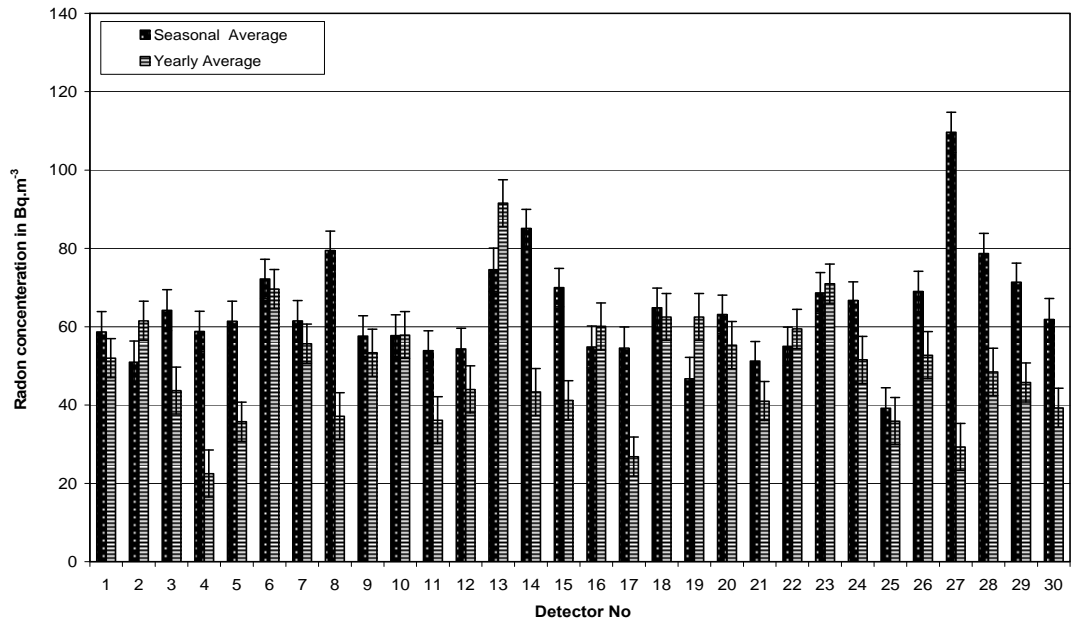


Figure 4.7: Yearly and seasonally averaged yearly radon levels in Mardan district.

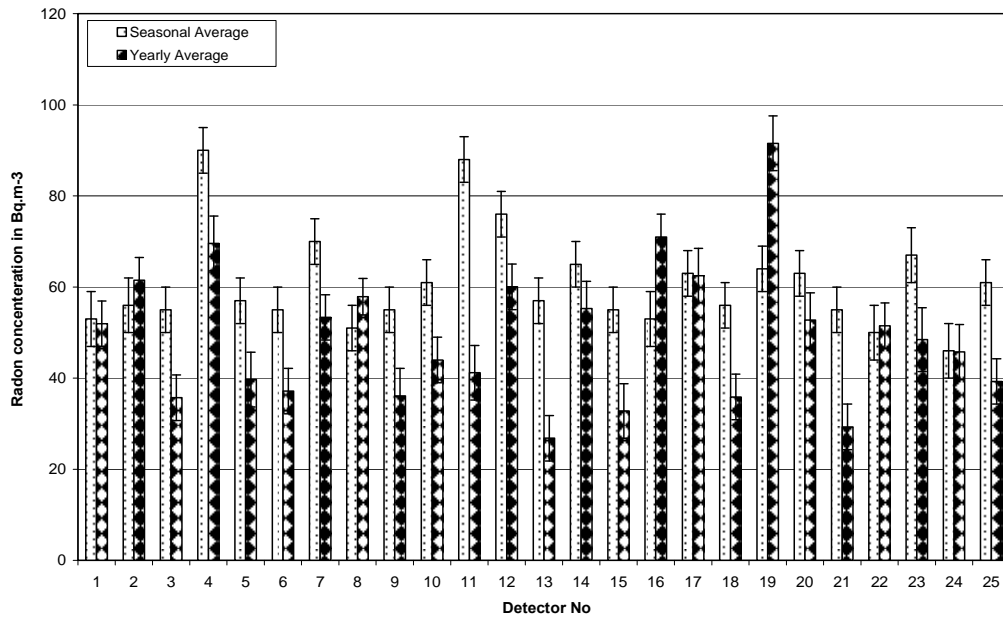


Figure 4.8: Yearly and seasonally yearly averaged radon levels in Charsadda district.

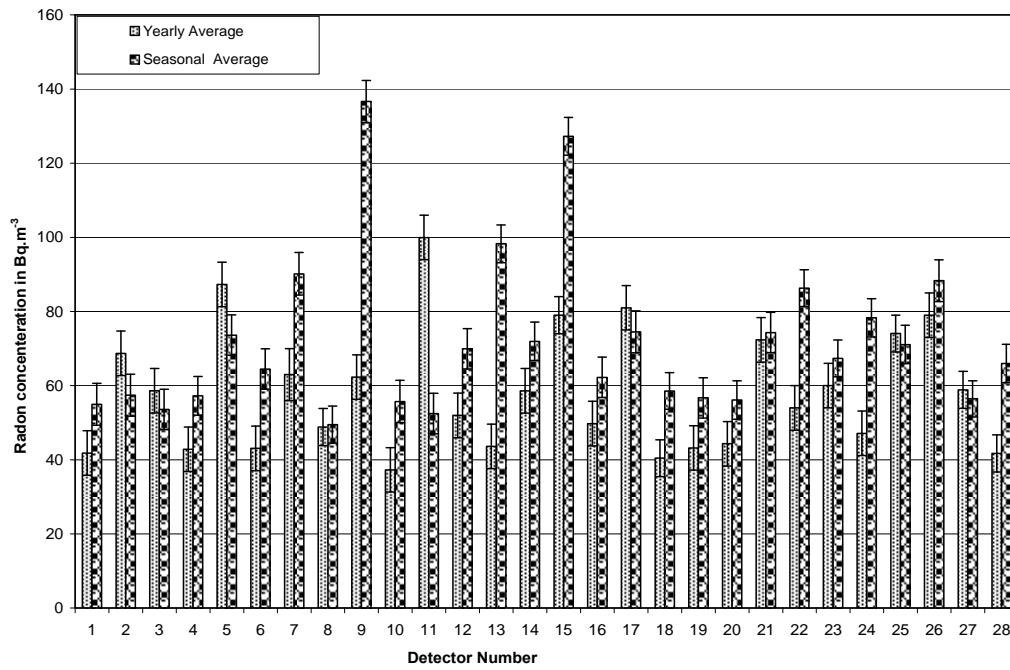


Figure 4.9: Yearly and seasonally averaged yearly radon levels in Mohmand agency.

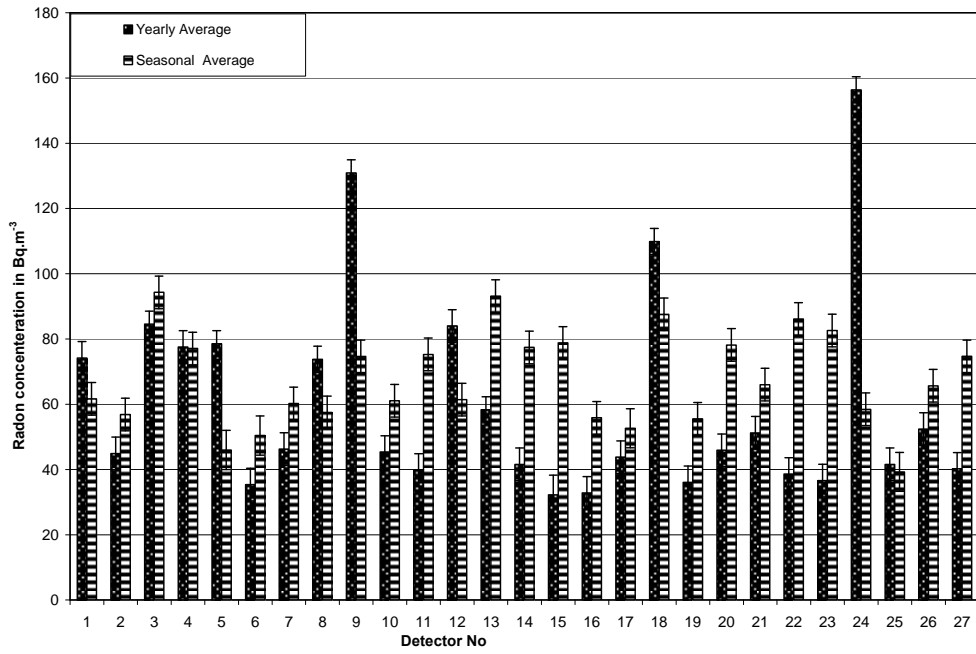
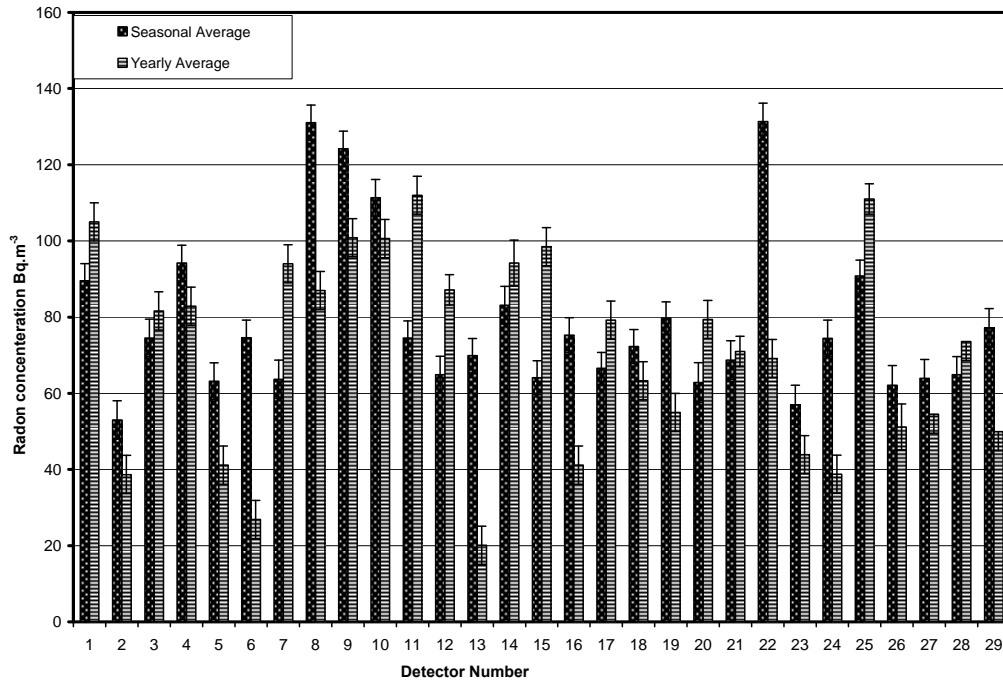


Figure 4.10: Yearly and seasonally averaged yearly radon levels in Bajuar agency.



Chapter Five

Experimental Studies on Radon Exhalation Rate from the Soil, Sand and Brick Samples

5.1. Introduction

In order to characterize building materials as an indoor radon source, knowledge of the radon exhalation rate from these materials is very important (BEIR-VI, 1999; Sharma and Virk, 2001). Radon produced in soil and other building materials is transported to the indoor air through diffusion and convective flow (Jang et al., 2005). During this process, a small fraction of the generated radon is able to escape to the atmosphere. A measure of exhalation is given by the exhalation rate, which is the number of radon atoms leaving the material per unit surface area per unit time. The parameters like atmospheric pressure, temperature and wind force greatly influence the radon exhalation rate. Rainfall or snow cover may lead to the temporal sealing of the soil surface, whereby ^{222}Rn is accumulated beneath the sealing and the exhalation rate is reduced. According to the published data, 60.4% of the indoor radon comes from the ground and surrounding soil of the buildings (Sun et al., 2004).

Building materials as indoor radon source has received a greater attention in some countries of the world (e.g., The Netherlands, China and Italy), where rocks enriched in radon isotopes precursors are used as building materials either as stony materials or in loose form to prepare cements (Tuccimei et al., 2006). In the Netherlands, radon from building materials constitutes 70% of the average radon concentration (Cozmuta et al., 2003). Low humidity conditions are known to dramatically reduce the radon exhalation rate from concrete (Roelofs and Scholten, 1994). In a latitudinal study carried out in Hong Kong, the radon exhalation rate was found to decrease with the age due to the gradual dehydration of the concrete (Yu et al., 1996).

Within building materials, the dominant transport mechanism of radon is molecular diffusion, which is driven by a gradient of concentration. The radon flux exhaled from this kind of materials varies from one medium to another, depending on the different physical parameters. The two main parameters of building materials are porosity and water content (Fournier et al., 2005; UNSCEAR, 2000). Cementitious materials such as concrete, brick, and ceramic tiles have the highest ^{222}Rn exhalation rates as compared to the fabricated materials (e.g. card boards) (Roelofs and Scholten, 1994; Jang et al., 2005). Radon exhalation from the soil surface in the US, determined using passive diffusion measurement technique has been reported to be in the range of 5.0 to 6.7 $\text{mBq m}^{-2} \text{s}^{-1}$ with an average value of $5.8 \pm 0.6 \text{ mBq m}^{-2} \text{s}^{-1}$ (Brounstein and Johnson, 2005).

It is highly desirable to study the radon exhalation form soil and other building materials used in the area chosen for the present study. Consequently radon exhalation rate from different samples of building materials, collected from NWFP and FATA, Pakistan, was selected using CR-39 based NRPB radon dosimeters. The effect of moisture contents on the radon exhalation rate from these materials was also studied.

Table 5.1: Radon exhalation rate ($\text{mBq.m}^{-2}.\text{h}^{-1}$) from different soil samples having 0%, 15%, 30% and 45% moisture content (MC), collected from the district Swabi.

Location	(MC 0 %)		(MC 15 %)		(MC 30 %)		(MC 45%)	
	I	II	I	II	I	II	I	II
Swabi	270±11	288±13	381±9	412±15	322±9	348±15	296±9	317±15
Bachai	285±11	304±12	363±9	392±15	371±9	401±14	294±12	315±12
Zaida	300±8	321±9	361±9	390±15	470±13	508±9	280±9	300±9
Gadoon Sw	246±9	263±10	216±8	234±9	259±8	259±15	406±15	265±12
Swabi City	155±11	166±12	313±9	338±15	290±15	313±11	277±11	297±15
Mangal Chai	203±10	217±10	364±15	392±15	372±15	401±11	476±9	515±9
R.Q Khan	141±10	151±11	364±15	393±11	579±15	625±11	253±11	271±12
Dagi	157±11	167±12	340±9	367±9	337±15	364±15	236±15	253±11
Yar Hussain	237±10	254±10	308±9	332±15	631±9	681±15	285±12	305±13
Lahore	288±9	308±8	327±15	353±11	335±15	362±12	324±9	347±15
AM±S.D	228±60	244±64	334±48	360±52	397±124	426±136	313±74	318±73
GM±GSD	220±1.16	241±1.17	330±1.09	356±1.09	381±1.16	408±1.17	306±1.11	312±1.11

For this study, samples were collected from the Swabi, Mardan and Charsadda districts of NWFP as well as from the Mohmand and Bajuar Agencies of FATA, Pakistan. From each district/agency, 10 soil representative samples were collected. In the case of sand, a total number of ten samples (i.e. 2 samples per district/agency) were collected from different streams of the selected area wherefrom people collect sand and transport it for the use in construction of their houses.

Table 5.2: Radon exhalation rate ($\text{mBq.m}^{-2}.\text{h}^{-1}$) from different soil samples having 0%, 15%, 30% and 45% moisture content (MC), collected from the district Mardan.

Location	(MC 0 %)		(MC 15 %)		(MC 30 %)		(MC 45 %)	
	I	II	I	II	I	II	I	II
Rustum	227±14	261±12	279±15	302±11	398±10	430±11	264±11	283±11
Fazal Abad	266±13	306±12	304±15	328±15	428±9	462±10	350±15	375±11
Taja	248±14	286±12	405±9	545±15	424±8	457±9	419±9	449±9
Taja(NW)	274±10	293±8	311±9	359±15	490±10	529±11	303±9	324±15
Tahat Bhai	294±11	314±8	333±15	324±11	371±10	401±11	303±9	324±15
Pat Baba	305±13	326±12	300±9	359±15	379±9	409±10	350±15	375±11
Chargul	206±10	220±8	333±9	337±15	302±9	326±10	303±9	325±9
Nawan Killi	309±9	331±12	312±9	359±15	294±10	317±11	264±11	283±11
Toro	199±10	212±9	333±9	383±15	391±11	422±12	303±9	325±9
Rustum	270±10	288±8	355±9	336±15	324±10	350±11	342±9	366±15
Average	260±39	284±41	327±35	363±68	380±61	410±66	320±47	343±50
GM	257±1.08	281±1.08	325±1.05	359±1.09	376±1.09	406±1.09	317±1.07	340±1.07

5.2. Calculation of the exhalation rate

In order to calculate effective time of the radon exposure, following relation was used (Durrani and Iliç, 1997):

$$T_{\text{effective}} = t - \tau(1 - e^{-\lambda t}) \quad (1)$$

Where τ is the mean life of radon (5.5 days), t is the total exposure time (days) and λ is the ^{222}Rn decay constant

Measured radon concentration values were used to calculate the exhalation rate using the following equations (Rehman et al., 2006).

$$F_0 = \frac{C(t)[\omega A + \lambda V]}{A \left[1 - e^{-\left(\frac{\omega A}{V} + \lambda\right)t} \right]} \quad (2)$$

$$F = F_0 - \omega C \quad (3)$$

Where

A = Surface area of the sample (cm²), V = volume of the void space in a closed chamber, t = ²²²Rn accumulation time in a closed chamber.

$\omega = \varepsilon \lambda Z_0$, known as back diffusion constant for given material.

Z_0 = Thickness of the sample in the sealed chamber.

$C(t)$ = ²²²Rn concentration just on the surface of the sample which has to be exhaled from the surface of the sample to the void space of the chamber.

$$F_0 = R \rho_b \lambda E Z_0 \quad (4)$$

λ = ²²²Rn decay constant (h⁻¹).

ρ_b = Bulk density of the sample (kg.m⁻³).

E = Sum of fractional emanation coefficient of ²²²Rn in air, water and adsorbed phase. ($E_{\text{air}} + E_{\text{water}} + E_{\text{solid}}$).

R = Concentration of ²²⁶Ra (Bq.kg⁻¹)

All the quantities on the right hand side in Eq. (2) are known except $C(t)$ which was experimentally determined for CR-39 based NRPB radon dosimeter. Putting the value of $C(t)$ in Eq. (2), exhalation rate, F_0 was determined.

In a closed chamber, which contains a sample, ²²²Rn concentration increases with the passage of time from zero to its maximum value. After reaching its maximum value, back diffusion of radon also take place, which reduces the ²²²Rn concentration by a

factor ω in the chamber. Therefore exhalation rate F , corrected for back diffusion, was determined using Eq (3). Exhalation rate was also calculated using the following equation (Abu-Jarad et al., 1980)

$$E_x = \frac{CtV\lambda}{S[t-1/\lambda(1-e^{-\lambda t})]} \quad (5)$$

Where E_x is radon exhalation rate ($\text{mBq.m}^{-2}.\text{h}^{-1}$), C is mean radon concentration as measured by CR-39 detector (Bq.m^{-3}), V is volume of the can (m^3), t is the exposure time, λ is the radon decay constant and S is the surface area from which radon is exhaled into the closed can. For further details, the reader is referred to ref. 25. The results these obtained using these two different relations are shown in table as (I and II for relation 3 and 5), respectively.

5.3. Results

As mentioned earlier, CR-39 detectors exposed in closed chambers to radon were etched in 25% NaOH at 80 °C for 16 h and counted under an optical microscope.

Table 5.3: Radon exhalation rate ($\text{mBq.m}^{-2}.\text{h}^{-1}$) from different soil samples having 0%, 15%, 30% and 45% moisture content (MC), collected from the district Charsadda.

Location	(MC 0 %)		(MC 15 %)		(MC 30 %)		(MC 45 %)	
	I	II	I	II	I	II	I	II
Charsadda bazaar	371±9	428±10	403±9	435±10	344±9	372±10	233±12	250±13
Umerzai	219±9	241±12	411±9	443±9	382±10	413±11	243±10	260±11
Halimzai	113±11	130±10	268±10	289±10	342±10	369±11	275±10	295±11
Kharaqy	233±11	268±14	265±8	445±10	336±10	362±12	336±10	359±11
Tangai	296±9	341±13	412±9	626±9	377±11	407±11	290±11	311±11
Sherpao	375±8	432±12	580±9	385±9	434±9	469±10	329±10	353±11
Shara	332±9	382±11	357±9	425±9	369±10	399±11	252±10	270±10
Pahlawan Qila	415±9	478±10	341±9	368±10	600±9	648±10	386±9	414±10
Mata	363±8	418±10	356±9	384±10	249±11	269±12	298±9	319±9
Garangi	324±11	373±9	319±10	311±10	338±10	365±10	294±12	318±12
Average	304±93	349±107	371±91	411±93	377±91	407±99	294±47	315±50
GM	287±1.22	329±1.22	362±1.12	402±1.12	368±1.12	398±1.12	143±1.08	290±1.08

From the measured track densities, ^{222}Rn concentration levels were calculated in closed plastic containers using the calibration factor of $2.7 \text{ tracks.cm}^{-2}.\text{h}^{-1}/\text{kBq.m}^{-3}$. Having determined the ^{222}Rn concentrations, exhalation rate from each sample was then

calculated using equation (3) and (5). Radon exhalation obtained at 0%, 15%, 30% and 45% moisture contents from these soil samples are shown in tables 5.1-5.5. As may be seen in these tables, variation in the radon exhalation rate ranged from 141 ± 10 (Rashaka Qaisar Khan) to 300 ± 8 $\text{mBq.m}^{-2}.\text{h}^{-1}$ (Lahore, district Swabi) with an average of 228 ± 60 $\text{mBq.m}^{-2}.\text{h}^{-1}$ in the soil samples collected from different locations of the district Swabi. In the district Mardan, variation in the radon exhalation rate was from 199 ± 10 (Toro) to 309 ± 9 $\text{mBq.m}^{-2}.\text{h}^{-1}$ (Nawan Killi, Rustum) with an average value of 260 ± 39 $\text{mBq.m}^{-2}.\text{h}^{-1}$. In district Charsadda, variation in the radon exhalation rate from soil samples was found to be from 113 ± 11 (Halimzai) to 415 ± 9 $\text{mBq.m}^{-2}.\text{h}^{-1}$ (Palwan Qila area) with an average value of 303 ± 93 $\text{mBq.m}^{-2}.\text{h}^{-1}$.

The exhalation rate from soil samples collected from the Mohmand agency varied from 146 ± 11 (Safi) to 316 ± 9 $\text{mBq.m}^{-2}.\text{h}^{-1}$ (Alingar) with an average value of 251 ± 44 $\text{mBq.m}^{-2}.\text{h}^{-1}$. In the Bajuar agency, the radon exhalation rate varied from 174 ± 9 $\text{mBq.m}^{-2}.\text{h}^{-1}$ (Loisum) to 311 ± 8 $\text{mBq.m}^{-2}.\text{h}^{-1}$ (Tangai area) with an average value of 252 ± 47 $\text{mBq.m}^{-2}.\text{h}^{-1}$.

Table 5.4: Radon exhalation rate($\text{mBq.m}^{-2}.\text{h}^{-1}$) from different soil samples having 0%, 15%, 30% and 45% moisture content (MC), collected from the Mohmand agency.

Location	(MC 0 %)	(MC 0 %)	(MC 15%)	(MC 15 %)	(MC 30 %)	(MC 30%)	(MC 45%)	(MC 45%)
	I	II	I	II	I	II	I	II
ZarGara	267±11	308±13	420±9	454±10	384±9	414±10	315±9	337±10
Jabar Mula	258±11	298±13	268±10	289±11	385±10	415±11	257±11	275±12
Qala Kawar	247±12	284±14	237±11	255±12	269±15	291±16	285±12	305±13
Mohammad Gat	255±12	294±14	401±9	433±10	399±15	431±16	328±9	352±10
Usman Jan Qala	250±13	288±15	330±10	357±10	389±12	420±11	345±12	369±13
Alingar	251±16	290±18	313±10	337±11	386±12	416±13	315±10	337±11
Qala Mohmand	290±11	310±11	340±10	367±10	316±12	341±13	313±10	335±11
Alingar Karkano	316±9	338±9	429±9	463±10	618±10	667±11	353±10	378±11
Nawagi Dag	228±9	243±10	342±9	370±9	341±11	368±12	367±10	394±11
Safi (Shewa)	146±11	157±11	299±9	323±9	295±10	319±11	225±10	242±11
Average	251±44	281±50	338±64	365±69	378±96	408±103	310±44	332±47
GM	247±1.11	276±1.12	332±1.10	359±1.10	369±1.12	398±1.12	307±1.08	329±1.08

Table 5.6 shows radon exhalation rate from different brands of the dried brick samples which were collected from the districts of Swabi, Mardan and Charsadda. The exhalation rate from dried brick samples was found to vary from 245 ± 12 to 364 ± 11 $\text{mBq.m}^{-2}.\text{h}^{-1}$

with an average value of $294 \pm 29 \text{ mBq.m}^{-2}.\text{h}^{-1}$. Table 5.7 shows radon exhalation rate from sand samples which were collected from the listed areas. As may be seen in table 5.6, variation in radon exhalation rate in the dried samples ranges from $205 \pm 16 \text{ mBq.m}^{-2}.\text{h}^{-1}$ (Mohmand agency) to $291 \pm 13 \text{ mBq.m}^{-2}.\text{h}^{-1}$ (Tangai, district Charsadda) with an average value of $248 \pm 25 \text{ mBq.m}^{-2}.\text{h}^{-1}$.

Using different levels of moisture contents radon exhalation showed a wide variation. As may be seen in tables 5.1-5.5 for soil, an average radon exhalation rate of $334 \pm 48 \text{ mBq.m}^{-2}.\text{h}^{-1}$ was found in the samples which were collected from the district Swabi at 15% moisture contents, level whilst at 30 % and 45% moisture content, average values came out to be 397 ± 124 and $313 \pm 74 \text{ mBq.m}^{-2}.\text{h}^{-1}$, respectively. For the district Mardan, average exhalation rate was 327 ± 35 , 380 ± 61 and $320 \pm 47 \text{ mBq.m}^{-2}.\text{h}^{-1}$ for 15%, 30% and 45% moisture content level, respectively.

Table 5.5. Radon exhalation rate($\text{mBq.m}^{-2}.\text{h}^{-1}$) from different soil samples having 0%, 15%, 30% and 45% moisture content (MC), collected from the Bajuar agency.

Location	(MC 0%)		(MC 15%)		(MC 30%)		(MC 45%)	
	I	II	I	II	I	II	I	II
Mashkanro	251±9	269±9	348±9	440±15	283±11	306±12	296±15	317±15
Loisum	174±9	186±9	333±9	360±9	362±9	390±15	299±15	321±15
Loi Juhar	243±9	260±10	385±9	484±15	477±9	515±15	426±15	456±11
Mamond	295±9	315±9	448±11	517±15	354±9	382±15	359±8	385±9
Zorbandar	269±8	288±9	479±9	369±12	372±15	402±15	342±9	366±15
Tangai	311±8	332±9	342±9	407±15	401±15	460±15	287±15	308±11
Khar	199±9	212±9	377±9	394±9	461±9	497±15	286±11	306±12
Asghar	206±8	220±9	365±9	433±15	393±12	425±13	403±9	432±9
Rashakai	305±9	326±9	401±15	480±15	420±9	453±9	303±15	324±15
Tangkhata	270±9	288±9	445±9	376±11	426±15	588±11	395±15	423±11
Average	252±47	270±50	392±50	426±54	395±56	442±80	340±53	364±57
GM	248±1.11	265±1.11	390±1.07	423±1.07	391±1.08	435±1.15	336±1.08	360±1.08

In the district Charsadda the average value for 15%, 30% and 45% moisture content was 371 ± 91 , 377 ± 91 and $294 \pm 47 \text{ mBq.m}^{-2}.\text{h}^{-1}$, respectively. In the Mohmand agency, the radon exhalation values were 338 ± 64 , 378 ± 96 and $310 \pm 44 \text{ mBq.m}^{-2}.\text{h}^{-1}$ for 15%, 30% and 45% moisture content levels, respectively whereas in the Bajuar agency, radon

exhalation rate was $392 \pm 50 \text{ mBq.m}^{-2}.\text{h}^{-1}$, 395 ± 56 and $340 \pm 53 \text{ mBq.m}^{-2}.\text{h}^{-1}$ for 15%, 30% and 45% moisture content levels, respectively. For bricks samples (see table 5.6), variation in the average exhalation rate ranged from 344 ± 60 to $362 \pm 36 \text{ mBq.m}^{-2}.\text{h}^{-1}$ for 15%, 30% moisture content levels. For 45% moisture content, its value was $310 \pm 45 \text{ mBq.m}^{-2}.\text{h}^{-1}$.

Table 5.6: Radon exhalation rate ($\text{mBq.m}^{-2}.\text{h}^{-1}$) from different brick samples having 0%, 15%, 30% and 45% moisture content (MC), collected from the different areas of NWFP and FATA.

Location	(MC 0 %)		(MC 15%)		(MC 30 %)		(MC 45%)	
	I	II	I	II	I	II	I	II
Star	364±11	389±12	411±8	451±9	379±15	415±11	285±9	315±9
Mumtaz	245±12	262±13	261±8	287±9	383±9	420±15	321±15	349±11
NR	309±11	331±11	421±8	462±9	276±12	302±13	295±9	321±15
PK	277±11	296±12	369±8	405±9	391±8	428±9	249±15	270±15
SS	296±12	316±13	308±8	337±9	341±8	374±9	333±8	363±15
PS	295±11	315±12	330±9	361±15	360±9	394±15	354±8	384±11
NS	276±11	295±12	287±9	315±9	357±9	392±9	292±15	317±11
KK	312±10	334±11	376±8	411±9	412±8	451±9	295±9	321±15
GD	269±12	288±13	271±9	298±15	371±9	407±15	249±15	270±15
PR	298±12	319±13	375±8	411±9	398±8	436±9	413±8	449±9
TB	284±11	304±12	292±8	319±9	353±9	387±9	302±8	328±9
SD	298±11	319±12	426±7	466±9	326±8	357±9	331±8	360±9
Average	294±29	314±31	344±60	377±65	362±36	397±40	310±45	337±49
GM	293±1.06	313±1.06	339±1.15	372±1.15	360±1.06	395±1.06	307±1.08	334±1.08

For sand samples (see table 5.7), average radon exhalation rate was in the range of 365 ± 22 , 393 ± 31 and $294 \pm 53 \text{ mBq.m}^{-2}.\text{h}^{-1}$ for 15%, 30% and 45% moisture contents, respectively. In order to know that whether change in exhalation rate is significant with respect to the change in moisture contents, results obtained concerning the change in the radon exhalation rate as a function of moisture content was tested applying Student T-Test (values below 0.05 are significant). The results of the paired T-test are given in table 5.8. According to this table, taking dried samples as a baseline data, the change in the exhalation rate is significant for the moisture content of 15%, 30% and 45% at 95% confidence level. Between 15% and 30% moisture content, the change in exhalation rate is significant for soil and sand samples. Similar trend was

observed for soil samples between 15% and 45% as may be seen in table 5.8. For 30%-45% moisture content, exhalation rate is significant in soil, sand and brick samples at 95% confidence level.

5.4. Discussion

For inter-comparison, exhalation rate was calculated using two different relations. The results obtained are shown in tables 5.1-5.7. As may be seen in these tables, the relation given by Rehman et al. yields relatively lower exhalation rate (~ 6-13 % less) as compared to that given by Abu-Jarad et al. (1980). This may be due to the inclusion of the back diffusion factor by Rehman et al. In the case of dried soil, higher average radon exhalation rate of $304 \pm 93 \text{ mBq.m}^{-2}.\text{h}^{-1}$ was found in the samples collected from the district Charsadda whereas lower value of average radon exhalation rate of $228 \pm 60 \text{ mBq.m}^{-2}.\text{h}^{-1}$ was observed in the district Swabi. In the case of dried sand samples, maximum radon exhalation rate of $291 \pm 13 \text{ mBq.m}^{-2}.\text{h}^{-1}$ was found in the samples collected from the district Charsadda.

As may be seen in table 5.5, higher average radon exhalation rate was observed at 15% moisture content from the sample collected from the Bajuar agency with an average of $392 \pm 50 \text{ mBq.m}^{-2}.\text{h}^{-1}$. Minimum value of $327 \pm 35 \text{ mBq.m}^{-2}.\text{h}^{-1}$ was found in the Mardan district. At 30% moisture content, average minimum was $377 \pm 91 \text{ mBq.m}^{-2}.\text{h}^{-1}$ for the Charsadda whilst a maximum value of $397 \pm 124 \text{ mBq.m}^{-2}.\text{h}^{-1}$ was observed from the soil samples collected from the district Swabi.

For 45% moisture content the lower average value of $294 \pm 47 \text{ mBq.m}^{-2}.\text{h}^{-1}$ was observed in samples collected from the district Charsadda whilst higher value of $340 \pm 53 \text{ mBq.m}^{-2}.\text{h}^{-1}$ was observed in samples, which were collected from the Bajuar agency respectively. Extensive data is available about the radon exhalation rate in the open literature.

Table 5.9 shows present data along with some already published data of the listed workers (Al-Jarallah et al., 2005; Oufni, 2003; Levin et al., 2002; Kumar et al., 2003; Hafez et al., 2001; Sroor et al., 2001; Amrani and Cherouati, 2001; Singh et al., 2005; Maged and Ashraf, 2005; El-Bahi, 2004; Yahong et al., 2002).

Table 5. 7: Radon exhalation rate ($\text{mBq}\cdot\text{m}^{-2}\cdot\text{h}^{-1}$) from different sand samples having 0%, 15%, 30% and 45% moisture content (MC), collected from the selected area.

Location	(MC 0 %)		(MC 15%)		(MC 30 %)		(MC 45%)	
	I	II	I	II	I	II	I	II
Gandab Khwar	291±13	331±11	384±15	421±13	358±9	393±15	230±11	250±11
Sheikh Baba	276±12	314±12	367±12	402±12	415±8	449±9	329±9	358±15
Maniri	244±13	277±12	392±11	429±13	419±9	459±9	255±15	277±11
Lahore	260±14	295±12	373±15	409±12	439±8	481±9	295±12	321±13
Rustum Khwar	265±12	301±11	342±15	375±11	381±9	417±15	274±12	298±13
Toro Nalai	242±15	275±13	333±12	364±11	374±9	381±9	268±11	291±12
Zorbandar	232±18	263±1	397±11	435±13	435±15	476±11	421±11	458±12
Sheih Khwar	233±15	265±13	368±15	404±12	398±8	436±9	311±15	338±11
Yaqurban	235±14	267±13	339±11	371±11	374±8	415±9	301±15	328±11
Tangai	205±16	232±14	360±9	394±12	347±9	382±15	260±15	282±11
Average	248±25	282±29	365±22	400±27	393±31	428±37	294±53	320±58
GM	247±1.05	281±1.05	365±1.03	400±1.03	392±1.04	427±1.05	290±1.09	316±1.09

Our results are seen to be within the reported values. A large variation in the exhalation rate of the reported values of is seen in table 5.9. For instance, Shweikani and Hushari (2005) have reported the exhalation rate ranging from $72000 - 32400000 \text{ mBq}\cdot\text{m}^{-2}\cdot\text{h}^{-1}$ ($20 \pm 5 - 9000 \pm 1000 \text{ mBq}\cdot\text{m}^{-2}\cdot\text{s}^{-1}$) whereas Dijk and Jong (2001) values range from 0.02 to $15.8 \text{ mBq}\cdot\text{m}^{-2}\cdot\text{h}^{-1}$. The world average radon exhalation rate (UNSCEAR, 2000) is $57600 \text{ mBq}\cdot\text{m}^{-2}\cdot\text{h}^{-1}$ ($0.016 \text{ Bq}\cdot\text{m}^{-2}\cdot\text{s}^{-1}$) which is also higher than the values observed in the present study. The radon exhalation rate is seen to increase (as compared to the dried samples) with moisture content up to 30%. At higher value of 45% moisture content, a decreasing trend is observed.

Both the formulae show the same trend of increase in exhalation rate with moisture content and yield results, which are in good agreement with each other. This increase in radon exhalation with moisture content may be explained as follow. As moisture content increases from 0% to 30% level, emanation from the grain increases which in turn results in an increase in the exhalation rate.

Table 5.8: Statistical analysis of the present data regarding the radon exhalation rate as a function of moisture contents applying student T-test was applied to the data.

MC	Swabi	Mardan	Charsadda	Mohmand	Bajuar	Soil(All Samples)	Sand	Brick
0-15%	0.00179	0.00459	0.05294	0.00228	1.30E-05	3.77E-12	8.33E-07	0.00219
0-30%	0.00474	0.00108	0.05356	0.00126	2.07E-04	8.25E-12	7.46E-07	4.83E-04
0-45%	0.01286	0.0106	0.72212	0.00754	0.00407	4.76E-06	0.048	0.32223
15-30%	0.13091	0.07831	0.87313	0.28154	0.91076	0.01618	0.01011	0.42907
15-45%	0.51814	0.55611	0.04227	0.27321	0.01703	0.0011	0.00174	0.12312
30-45%	0.13955	0.05729	0.00588	0.05625	0.02118	5.56E-06	3.70E-05	0.009

All values below 0.05 are significant

The recoiling radon nuclei from the alpha decay of radium atoms are more likely to stop in pore spaces if it contains water in the pore space. It may be noted here that radon does not "recoil" through the pore spaces; it goes through the porous material because it is an inert gas. Without water (i.e. 0% moisture content), the recoiling nuclei may travel through the less dense, air-filled pore space and become embedded in another grain. Once in the pore space, the atom is free to migrate out of the soil and thus radon exhalation increases with an increase in the moisture content.

However, when the pore space is completely filled with fluid, it causes a decrease in the radon exhalation rate because all fluid-filled (water) pore spaces inhibit the migration of emanated radon from the grain to the soil surface of the material and thus the exhalation decreases.

As moisture content was increased from 0% to 15%, 30% and 45%, on the average 34%, 46% and 13% increase was observed in the radon exhalation rate. Radon exhalation from samples increased up to 30% moisture content.

At 45% moisture content, a decreasing trend was observed. Radon exhalation rate at 45% moisture content is still higher than the exhalation rate from the dried samples.

Table 5.9: Published data concerning radon exhalation rate along with the present results.

Investigators	Range of Values in $\text{mBq.m}^{-2}.\text{h}^{-1}$
Al-Jarallah et al.	120-131000 ($.12 - 13.1 \text{ Bq.m}^{-2}.\text{h}^{-1}$)
Shweikani and Hushari	72000 - 32400000 ($20 \pm 5 - 9000 \pm 1000$ $\text{m Bq. m}^{-2}.\text{s}^{-1}$)
Oufni	3 -145 ($0.003 - 0.145 \text{ Bq.m}^{-2}.\text{h}^{-1}$)
Levin et al.	Soil type A 3300 ($3.3 \pm 0.9 \text{ Bq.m}^{-2}.\text{h}^{-1}$)
	B 7900 ($7.9 \pm 2.1 \text{ Bq.m}^{-2}.\text{h}^{-1}$)
	C 3600 ($3.6 \pm 1.3 \text{ Bq.m}^{-2}.\text{h}^{-1}$)
Kumar et al.	260-1500 ($0.26 - 1.5 \text{ Bq.m}^{-2}.\text{h}^{-1}$)
Hafez et al.	464 ($12.9 \times 10^{-5} \text{ Bq.m}^{-2}.\text{s}^{-1}$)
Sroor et al.	14117.08-59436.25($338.81 - 1426.47 \text{ Bq.m}^{-2}.\text{d}^{-1}$)
Amrani and Cherouati	45-153($0.003 - 0.145 \text{ Bq.m}^{-2}.\text{h}^{-1}$)
Singh et al.	246.63 -1100.00
Maged & Ashraf	11–223
El-Bahi	2549-7557 ($61.19 - 181.39 \text{ Bq.m}^{-2}.\text{d}^{-1}$)
Yahong et al.	10^{-3} - 10^{-4}
Van Dijk	0.02-15.8
World average radon exhalation rate	57600 ($0.016 \text{ Bq.m}^{-2}.\text{s}^{-1}$)
Present Study	Soil (261)
	Sand (265)
	Brick (292)

It was observed that from 0% to 15% moisture content, increase in exhalation rate was higher as compared with the increase of radon exhalation from 15-30% and 30-45% moisture contents. During the removal of the detectors from the sealed containers at higher moisture content, a layer of water content was found on the surface of the detector especially at 30 and 45% moisture content, which might have slightly affected the track registration efficiency of the CR-39 detector. However, it was very difficult to quantify this effect. In order to measure the radon exhalation rate, samples were first crushed and

then sieved. This phenomenon might also have some effect on the exhalation rate from these samples as compared to the undisturbed rocks/materials. As main factor of radon exhalation is the radium content in the materials and thus qualitatively it shows the behavior of the undisturbed rocks/materials.

The present data is reasonably in good agreement with the published data for Hong Kong (Yu et al., 1996). Fournier et al. (2005) have reported that radon exhalation sharply increases with water until the volumetric water content becomes higher than 30% for low porosity materials which is also in agreement with the present data. According to the paired T-test (see, table 5.8), change in the exhalation rate as a function of the moisture content is significant at 95% confidence level.

Cozmuta et al. (2003) have reported dependence of the radon-release rate on the moisture content for concrete under well controlled conditions. They have observed that the radon-release rate increases almost linearly up to moisture contents of 50% to 60% which are not in line with the present value (i.e. higher than the present values). The building materials selected have lower radon exhalation rate and are thus safe for use as construction materials.

5.5. Conclusions

To conclude, radon exhalation rate has been determined in soil, sand and brick samples collected from several districts of the NWFP, namely, Charsadda, Mardan and Swabi as well as Mohmand and Bajuar agencies, FATA, Pakistan. This study revealed that all the materials exhale radon with lower rate as compared to world average radon exhalation rate and would pose no serious threat if used in the construction of buildings. Effect of moisture content on the radon exhalation rate show that radon exhalation rate increases with an increase in the moisture content up to a certain level and then decreases with further increase in the moisture content. Radon exhalation rate measured using two different formulas are reasonably in good agreement. According to the paired T-test, change in the exhalation rate as a function of the moisture content is significant at 95% confidence level at 15%, 30% and 45% moisture contents.

Chapter Six

Measurement of Natural Radioactivity in Soil and other Building Materials

6.1. Introduction

Radioactivity is a part of our physical environment. The presence of natural radioactivity in soil and other building materials results in internal and external exposure to the occupants (Ahmad et al., 1997). Terrestrial radioactivity and the associated external exposure due to the gamma radiation depend primarily on the geological and geographical conditions and appear at different levels in the soils of each region (UNSCEAR 2000). The largest contribution to the radiation field is of natural origin: it is due to the cosmic rays, the natural radionuclides in soil and other building materials, radioactivity of the ground and the radioactive decay products of radon in the air. Naturally occurring building materials reflects the geological variations of their sites of origin, so their radiometric characterization provides a useful technique of acquiring better understanding of the local environment (Trevisi et al., 2005). Artificial radioactivity emitted from nuclear power plants, industrial plants and research facilities has smaller contribution to the overall radiation. These emissions are very small in normal operation, although large amounts of radioactivity can be released to the environment through accidents.

In view of the above discussion, it is highly desirable to determine natural radioactivity levels in the samples of soil and other building materials (e.g. brick, sand, marble and cement etc). In this regards, samples were collected from the Swabi, Mardan and the Charsadda districts of the North West Frontier Province (NWFP) Mohmand and Bajuar agencies of the federally administered tribal areas (FATA) Pakistan and analyzed in order to find its radiological significance. The prime objective of carrying out these

studies was to generate a baseline data for the selected area and then to set the standards and guidelines in the light of the international recommendations.

6.2. Measurements

In order to measure the natural radioactivity, P-type coaxial HPGe detector was used. Resolution and relative efficiency of the detector for 1332 keV from ^{60}Co was 2.5 keV and 90 %, respectively. The details of the detector, its cooling system and calibration have been discussed in chapter 2.

For the gamma spectroscopy, a total of fifty (i.e. 10 samples from each district/agency) soil samples were collected from the Swabi, Mardan and Charsadda districts as well as from the Mohmand and Bajuar Agencies of the federally administered tribal areas (FATA), Pakistan.

The specific activities (A) for ^{226}Ra , ^{232}Th and ^{40}K were calculated using the following relation.

$$A = \frac{C}{t \times P_r \times \eta} \quad (1)$$

Where 'C' represents the net counts, t is the data collection time, P_r is the emission probability and η is the efficiency of the detector for the corresponding peak.

Radium equivalent activity (Ra_{eq}) was calculated using the following relation (OECD, 1979).

$$R a_{eq} = A_{Ra} + 1.43 A_{Th} + 0.077 A_K \quad (2)$$

Where A_{Ra} , A_{Th} , A_K are the activity concentrations of thorium, uranium and potassium respectively. Absorbed dose was calculated (D_{air}) at ground level using the following equation (UNSCEAR, 2000).

$$D_{air} = 0.462A_{Ra} + 0.604A_{Th} + 0.417A_K \quad \text{nGy h}^{-1} \quad (3)$$

The absorbed dose was converted into the annual effective dose using the conversion where the value of Q is 0.7 Sv.Gy^{-1} for environmental exposure to the gamma rays of moderate energy and T is time of one year, i.e., 8760 hours.

Table 6.1: Natural radioactivity, radium equivalent activity in Bq.kg^{-1} , external and internal hazard indices and effective doses in the samples collected from the district Swabi.

Location	^{226}Ra (Bq.kg^{-1})	^{332}Th (Bq.kg^{-1})	^{40}K (Bq.kg^{-1})	Ra_{eq} (Bq.kg^{-1})	H_{ex}	H_{in}	Annual effective dose (mSv)
Swabi	54±3	56±3	710±55	190±12	0.51±0.03	0.66±0.04	0.54±0.04
Lahore(Anbar)	21±1	42±3	454±36	117±8	0.32±0.02	0.37±0.02	0.33±0.02
Zaida(Dodher)	24±2	40±2	349±28	108±7	0.29±0.02	0.36±0.02	0.31±0.02
Zaida	34±2	61±3	714±55	176±11	0.48±0.03	0.57±0.04	0.51±0.03
Rashaka	23±1	46±3	514±40	128±8	0.35±0.02	0.41±0.02	0.37±0.02
Rashaka(Q.K)	34±2	48±3	450±35	137±9	0.37±0.02	0.46±0.03	0.39±0.03
Yar Hussain	28±2	41±2	509±40	126±8	0.34±0.02	0.42±0.03	0.36±0.02
Dagi	23±1	38±2	360±28	104±7	0.28±0.02	0.34±0.02	0.30±0.02
Gadoon	16±1	34±2	320±26	65±4	0.18±0.01	0.22±0.01	0.25±0.01
Mangal Chai	42±3	42±2	495±39	140±9	0.38±0.02	0.49±0.03	0.40±0.03
Minimum m	16±1	34±2	320±26	65±4	0.18±0.01	0.22±0.01	0.25±0.01
Maximum	54±3	61±3	714±55	190±12	0.51±0.03	0.66±0.04	0.54±0.04
AM±SD	30±11	45±8	488±137	129±36	0.35±0.10	0.43±0.12	0.38±0.09
GM±GSD	28.15±1.2	44±1.09	471±1.15	124±1.16	0.34±1.16	0.41±1.17	0.37±1.13

$$E_{\text{air}}(\text{mSv}) = TQD_{\text{air}} \times 10^{-6} \quad (4)$$

In order to limit the radiation dose to permissible dose equivalent limit of 1 mSv.yr^{-1} , a number of models are available in the literature (ICRP, 1990). Using the following relations external and internal hazard indices were calculated (Beretka and Matthew, 1985).

$$H_{ex} = \frac{A_{Ra}}{370} + \frac{A_{Th}}{259} + \frac{A_K}{4810} \quad (5)$$

$$H_{in} = \frac{A_{Ra}}{185} + \frac{A_{Th}}{259} + \frac{A_K}{4810} \quad (6)$$

Table 6.2: Natural radioactivity, radium equivalent activity in Bq.kg⁻¹, external and internal hazard indices and effective doses in the samples collected from the district Mardan.

Location	²²⁶ Ra (Bq.kg ⁻¹)	³³² Th (Bq.kg ⁻¹)	⁴⁰ K (Bq.kg ⁻¹)	Ra _{eq} (Bq.kg ⁻¹)	H _{ex}	H _{in}	Annual effective dose (mSv)
Takht Bhai	35±2	48±3	489±39	142±9	0.38±.03	0.48±.03	0.40±.03
Kalamabad	53±3	86±5	1018±79	255±17	0.69±.04	0.83±.05	0.73±.05
H Khan Bagh	34±2	48±3	485±39	140±9	0.38±.03	0.47±.03	0.40±.03
Rustum	33±2	51±3	424±33	138±9	0.37±.02	0.46±.03	0.39±.03
Khairabad	30±2	44±3	463±36	130±9	0.35±.02	0.43±.03	0.37±.02
Nawan Killi	38±2	57±3	638±50	169±11	0.46±.03	0.56±.04	0.48±.03
Pat Baba	26±2	36±2	417±32	109±7	0.29±.02	0.36±.02	0.31±.02
Fazal Abad	29±2	33±2	487±38	114±8	0.31±.02	0.39±.03	0.33±.02
Toro	17±1	17±1	633±50	89±6	0.24±.02	0.29±.02	0.27±.02
Chargul	23±2	36±2	262±22	95±6	0.26±.02	0.32±.02	0.27±.02
Minimum	17±1	17±1	262±22	89±6	0.24±.02	0.29±.02	0.27±.02
Maximum	53±3	86±5	1018±79	255±17	0.69±.04	0.83±.05	0.73±.05
AM±SD	32±10	46±18	532±202	138±48	0.37±.13	0.46±.44	0.40±0.14
GM±GSD	31±1.17	42±1.24	502±1.9	132±1.17	0.36±1.17	0.44±1.16	0.38±1.16

Where A_{Ra} , A_{Th} , A_K are the activity concentrations of thorium, uranium and potassium, respectively. The error in the activity was calculated from the combined uncertainty in the efficiency of the detector, uncertainty in the net count rate, attenuation of the gamma rays by the sample. In the case of using two gamma rays peaks for the calculations of the activity, uncertainty in the yield was also included.

6.3. Results

6.3.1. Specific activities and radium equivalent activity

Tables 6.1–6.8 show measured specific activities of ²²⁶Ra, ²³²Th, ⁴⁰K radium equivalent activity, external and internal hazard indices and effective doses. Their arithmetic means

(AM) and geometric means (GM) are also shown in these tables. As may be seen in table 6.1 ^{226}Ra activity is found to vary from 16 ± 1 to $54 \pm 3 \text{ Bq.kg}^{-1}$, ^{232}Th activity from 61 ± 3 to $45 \pm 8 \text{ Bq.kg}^{-1}$ and ^{40}K activity from 488 ± 137 to $714 \pm 55 \text{ Bq.kg}^{-1}$ in the district Swabi. Average radium equivalent activity for the district Swabi was $129 \pm 36 \text{ Bq.kg}^{-1}$. In the district Mardan, ^{226}Ra activity was found to vary from 17 ± 1 to $53 \pm 3 \text{ Bq.kg}^{-1}$, whilst the average radium equivalent activity value was $138 \pm 48 \text{ Bq.kg}^{-1}$.

Table 6.3: Natural radioactivity, radium equivalent activity in Bq.kg^{-1} external and internal hazard indices and effective dose in the samples collected from the district Charsadda.

Location	^{226}Ra (Bq.kg^{-1})	^{232}Th (Bq.kg^{-1})	^{40}K (Bq.kg^{-1})	Ra_{eq} (Bq.kg^{-1})	H_{ex}	H_{in}	Annual effective dose (mSv)
Shara	27±2	42±2	502±39	126±8	0.34±.02	0.41±.03	0.36±.02
Pakban	20±1	27±2	339±27	85±6	0.23±.02	0.29±.02	0.25±.02
Pahlawan	29±2	84±5	575±45	194±12	0.52±.03	0.60±.04	0.54±.04
Zoorkandai	21±1	33±2	728±57	125±9	0.34±.02	0.40±.03	0.37±.03
Garangi	22±1	34±2	248±21	90±6	0.24±.02	0.30±.02	0.25±.02
Kharaqy	37±2	39±2	477±38	129±9	0.35±.02	0.45±.03	0.37±.02
Halimzai	17±1	17±1	648±51	91±6	0.25±.02	0.29±.02	0.28±.02
Sherpao	45±3	67±4	652±51	191±12	0.52±.03	0.64±.04	0.54±.04
Matta	39±2	54±3	586±46	161±11	0.44±.03	0.54±.04	0.46±.03
Umarzai	34±2	47±3	472±38	137±9	0.37±.02	0.4±.036	0.39±.03
Minimum	17±1	17±1	248±21	85±6	0.23±.02	0.29±.02	0.25±.02
Maximum	45±3	84±5	728±57	194±12	0.52±.03	0.64±.04	0.54±.04
AM±SD	29±9	44±20	523±147	133±39	0.36±.11	0.43±.13	0.38±.11
GM±GSD	28±1.18	41±1.26	500±1.18	128±1.16	0.35±1.16	0.42±1.16	0.37±1.17

^{232}Th activity varied from 17 ± 1 to $86 \pm 5 \text{ Bq.kg}^{-1}$ whilst ^{40}K varied from 262 ± 22 to $1018 \pm 79 \text{ Bq.kg}^{-1}$ in this district. In the district Charsadda ^{226}Ra activity varied from 17 ± 1 to $45 \pm 3 \text{ Bq.kg}^{-1}$, ^{232}Th varied from 17 ± 1 to $84 \pm 5 \text{ Bq.kg}^{-1}$ having an average value of $44 \pm 20 \text{ Bq.kg}^{-1}$ whilst ^{40}K varied from 248 ± 21 to $728 \pm 57 \text{ Bq.kg}^{-1}$ with an average value of $523 \pm 147 \text{ Bq.kg}^{-1}$. In the Mohmand agency ^{226}Ra activity varied from 8 ± 1 to $30 \pm 2 \text{ Bq.kg}^{-1}$, ^{232}Th from 7 ± 1 to $34 \pm 2 \text{ Bq.kg}^{-1}$ and ^{40}K varied from 153 ± 13 to $795 \pm$

62 Bq.kg⁻¹. Average radium equivalent activity for this agency was found to be 78 ± 30 Bq.kg⁻¹.

In the Bajuar agency, ²²⁶Ra activity varied from 8 ± 1 to 34 ± 3 Bq.kg⁻¹, ²³²Th from 9 ± 1 to 64 ± 4 Bq.kg⁻¹ and ⁴⁰K varied from 220 ± 19 to 836 ± 65 Bq.kg⁻¹. Average radium equivalent activity for this agency was found to be 116 ± 42 Bq.kg⁻¹.

Table 6.4: Natural radioactivity, radium equivalent activity in Bq.kg⁻¹, external and internal hazard indices and effective doses in the samples collected from the Mohmand agency.

Location	²²⁶ Ra (Bq.kg ⁻¹)	³³² Th (Bq.kg ⁻¹)	⁴⁰ K (Bq.kg ⁻¹)	Ra _{eq} (Bq.kg ⁻¹)	H _{ex}	H _{in}	Annual effective dose (mSv)
Safi	16±1	16±1	795±62	101±7	0.27±.02	0.32±.02	0.31±.02
Qalalalai	23±1	34±2	475±37	109±7	0.29±.02	0.36±.02	0.31±.02
Narogha	8±1	7±1	160±14	31±2	0.08±.01	0.10±.01	0.09±.01
Sheikh Baba	9±1	11±1	248±20	44±3	0.12±.01	0.14±.01	0.13±.01
Alingar	27±2	34±2	153±13	88±6	0.2±.024	0.31±.01	0.24±.02
Lakaro	30±2	34±2	458±36	114±8	0.31±.02	0.39±.03	0.33±.01
S.Khan koor	24±1	34±2	369±29	100±6	0.27±.02	0.33±.02	0.29±.02
Karkanai	11±1	16±1	199±16	49±3	0.13±.01	0.16±.01	0.14±.01
Qandari	8±1	13±1	325±11	52±3	0.14±.01	0.16±.01	0.15±.01
Ghalanai	19±1	28±1	386±11	89±3	0.24±.01	0.29±.01	0.15±.01
Minimum	8±1	7±1	153±13	31±2	0.08±.01	0.10±.01	0.09±.01
Maximum	30±2	34±2	795±62	114±8	0.31±.02	0.39±.03	0.33±.01
AM±SD	18±8	23±12	357±193	78±30	0.21±.08	0.26±.10	0.23±0.09
GM±GSD	16±1.30	20±1.34	315±1.24	71.3±1.26	0.19±1.25	0.23±1.27	0.21±1.26

As may be seen in table 6.6, ²²⁶Ra activity varied from 9 ± 1 to 50 ± 3 Bq.kg⁻¹, ²³²Th activity varied from 6 ± 1 to 68 ± 4 Bq.kg⁻¹ and ⁴⁰K activity varied from 77 ± 8 to 672 ± 52 Bq.kg⁻¹ in the brick samples which were collected from the selected area. Average radium equivalent activity for the brick samples is 129 ± 54 Bq.kg⁻¹.

In the sand samples (see table 6.7), ²²⁶Ra activity varied from 2 ± 1 to 31 ± 2 Bq.kg⁻¹ with an average value of 19 ± 9 Bq.kg⁻¹, ²³²Th activity varied from 6 ± 1 to 51 ± 3 Bq.kg⁻¹ having an average value of 30 ± 15 Bq.kg⁻¹ whilst ⁴⁰K activity varied from 424 ± 33 to 1745 ± 135 Bq.kg⁻¹ with an average value of 769 ± 461 Bq.kg⁻¹. Variation in the

radium equivalent activity ranged from 43 ± 3 to 234 ± 16 Bq.kg⁻¹ with an average value of 121 ± 57 Bq.kg⁻¹. In the marble samples (see table 6.8), ²²⁶Ra activity varied from 1 ± 1 to 62 ± 4 Bq.kg⁻¹, ²³²Th activity varied from 1 ± 1 to 66 ± 4 Bq.kg⁻¹ and ⁴⁰K activity varied from 25 ± 2 to 890 ± 69 Bq.kg⁻¹ whereas In marble samples radium equivalent activity varied from 24 ± 2 to 198 ± 13 with an average value of 67 ± 60 Bq.kg⁻¹.

Table 6.5: Natural radioactivity, radium equivalent activity in Bq.kg⁻¹, external and internal hazard indices and effective doses in the samples collected from the Bajuar agency.

Location	²²⁶ Ra (Bq.kg ⁻¹)	³³² Th (Bq.kg ⁻¹)	⁴⁰ K (Bq.kg ⁻¹)	Ra _{eq} (Bq.kg ⁻¹)	H _{ex}	H _{in}	Annual effective dose (mSv)
Delai	28±2	40±2	503±39	124±8	0.34±0.02	0.41±0.03	0.36±0.02
Mashkanro	9±1	18±1	220±19	51±4	0.14±0.01	0.16±0.01	0.15±0.01
Sabagai	8±1	15±1	836±65	94±7	0.25±0.02	0.28±0.02	0.29±0.02
Loisum	23±2	37±2	410±33	108±7	0.29±0.02	0.35±0.02	0.31±0.02
Luyjuhar	28±2	39±2	502±39	122±8	0.33±0.02	0.40±0.03	0.35±0.02
Tarakai	9±1	9±1	518±41	61±4	0.17±0.01	0.19±0.01	0.19±0.01
Tangai	25±2	35±2	386±30	105±7	0.28±0.02	0.35±0.02	0.30±0.02
Khar	25±1	49±	553±43	138±9	0.37±0.02	0.44±0.03	0.40±0.02
Zorbandar	33±2	59±3	687±53	170±11	0.46±0.03	0.55±0.04	0.49±0.03
Mamond	44±3	64±4	625±49	183±12	0.50±0.03	0.61±0.04	0.52±0.03
Minimum	8±1	9±1	220±19	51±4	0.14±0.01	0.16±0.01	0.15±0.01
Maximum	44±3	64±4	836±65	183±12	0.50±0.03	0.61±0.04	0.52±0.03
AM±SD	23±12	37±18	524±170	116±42	0.31±0.11	0.38±0.14	0.33±0.12
GM±GSD	20±1.36	31±1.38	496±1.20	108±1.23	0.29±1.23	0.35±1.24	0.31±1.22

In cement samples (table 6.9), ²²⁶Ra activity showed variation from 19 ± 1 to 34 ± 2 Bq.kg⁻¹, with an average value of 24 ± 6 Bq.kg⁻¹, ²³²Th activity varied from 13 ± 1 to 23 ± 1 Bq.kg⁻¹ with an average value of 18 ± 4 Bq.kg⁻¹ and ⁴⁰K activity varied from 215 ± 17 Bq.kg⁻¹ to 282 ± 22 Bq.kg⁻¹ with an average of 244 ± 29 Bq.kg⁻¹. Radium equivalent activity varied from 58 ± 4 to 80 ± 5 Bq.kg⁻¹ with an average value of 68 ± 9 Bq.kg⁻¹.

6.3.2. External and Internal Indices

External hazard indices from the soil samples collected from the district Swabi varied from 0.18 ± 0.01 to 0.51 ± 0.03 and internal indices varied from 0.22 ± 0.01 to 0.66 ± 0.04 with average values of 0.35 ± 0.10 and 0.43 ± 0.12 , respectively. In the district Mardan, variation in the external indices was from 0.24 ± 0.02 to 0.69 ± 0.04 with an

average value of 0.37 ± 0.13 , whilst internal hazard indices varied from 0.29 ± 0.02 to 0.83 ± 0.05 with an average value of 0.46 ± 0.44 . In the district Charsadda, the external hazard indices varied from 0.23 ± 0.02 to 0.52 ± 0.03 with an average value of 0.36 ± 0.11 whilst internal hazard indices showed variation in the range of 0.29 ± 0.02 to 0.64 ± 0.04 with an average of 0.43 ± 0.13 .

Table.6.6: ^{226}Ra , ^{232}Th , ^{40}K and Ra_{eq} , external and internal hazard indices and effective dose measured in brick samples which were collected from the districts Swabi, Mardan and Charsadda.

Location	^{226}Ra (Bq.kg ⁻¹)	^{232}Th (Bq.kg ⁻¹)	^{40}K (Bq.kg ⁻¹)	Ra_{eq} (Bq.kg ⁻¹)	H_{ex}	H_{in}	Annual effective dose (mSv)
MD	46±3	68±4	667±52	195±13	0.53±0.03	0.65±0.04	0.56±0.04
NR	45±3	56±3	620±48	173±11	0.47±0.03	0.59±0.04	0.49±0.03
SS	14±1	16±1	672±52	88±6	0.24±0.02	0.27±0.02	0.27±0.02
SB	9±1	6±1	360±28	45±3	0.12±0.01	0.14±0.01	0.14±0.01
PS	14±1	15±1	77±8	41±3	0.11±0.01	0.15±0.01	0.12±0.01
Mumtaz	36±2	42±2	641±50	146±10	0.39±0.03	0.49±0.03	0.42±0.03
GD	31±2	47±3	510±40	138±9	0.37±0.02	0.46±0.03	0.39±0.03
Star	25±2	57±3	550±43	149±10	0.40±0.03	0.47±0.03	0.42±0.03
PK	34±2	42±2	554±43	136±9	0.37±0.02	0.46±0.03	0.39±0.03
TB	50±3	58±3	583±46	178±11	0.48±0.03	0.62±0.04	0.51±0.03
Minimum	9±1	6±1	77±8	41±3	0.11±0.01	0.15±0.01	0.12±0.01
Maximum	50±3	68±4	672±52	195±13	0.53±0.03	0.65±0.04	0.56±0.04
AM±SD	30±15	41±21	523±182	129±54	0.35±0.15	0.43±0.18	0.37±0.15
GM±GSD	27±1.3	33±1.5	463±1.4	115±1.33	0.31±1.33	0.38±1.33	0.33±1.31

In the Mohmand agency, the external hazard indices varied from 0.08 ± 0.01 to 0.31 ± 0.02 with an average value of 0.21 ± 0.08 whilst internal hazard indices showed variation which ranged from range of 0.10 ± 0.01 to 0.39 ± 0.03 with an average value of 0.26 ± 0.1 . In the Bajuar agency, the external hazard indices varied from 0.14 ± 0.01 to 0.50 ± 0.03 with an average value of 0.31 ± 0.11 and internal hazard indices varied from 0.16 ± 0.01 to 0.61 ± 0.04 with an average of 0.38 ± 0.14 .

Variation in the external hazard indices in brick samples (see table 6.6) ranged from 0.11 ± 0.01 to 0.53 ± 0.03 with an average value of 0.35 ± 0.15 whilst internal indices varied from 0.15 ± 0.01 to 0.65 ± 0.04 with an average of 0.43 ± 0.18 . In the sand sample (see table 6.7), variation in the external indices was from 0.12 ± 0.01 to 0.63 ± 0.04 with an average value of 0.33 ± 0.15 and internal hazard indices varied from 0.12 ± 0.01 to 0.70 ± 0.05 with an average value of 0.38 ± 0.17 . In marble samples (see table 6.8), variation in the external indices was from 0.07 ± 0.01 to 0.57 ± 0.04 with an average value of 0.18 ± 0.16 and internal hazard indices varied from 0.08 ± 0.01 to 0.65 ± 0.04 with an average value of 0.23 ± 0.20 , respectively.

In the cement samples (table 6.9), external hazard indices varied from 0.16 ± 0.01 to 0.22 ± 0.01 with an average value of 0.19 ± 0.03 whilst internal hazard indices showed variation in the range of 0.21 ± 0.01 to 0.31 ± 0.02 with an average value of 0.25 ± 0.04 .

6.3.3. *Calculations of Effective Dose*

Annual effective dose from the soil and other building materials were calculated from the air absorbed doses using equation 4.

As may be seen in tables 6.1-6.5, in the district Swabi, annual effective dose varied from 0.25 ± 0.01 to 0.54 ± 0.04 mSv yr⁻¹. In the Mardan district, the variation was from 0.27 ± 0.02 to 0.73 ± 0.05 mSv yr⁻¹ (see tables 6.1-6.5). In the Charsadda district variation in the effective dose was from 0.25 ± 0.02 to 0.54 ± 0.04 mSv yr⁻¹. The effective dose equivalent in the Mohmand agency varied from 0.15 ± 0.01 to 0.52 ± 0.03 mSv yr⁻¹, and in the Bajuar agency the variation observed was in the range of 0.09 ± 0.01 to 0.33 ± 0.01 mSv yr⁻¹ with an average value of 0.23 ± 0.09 mSv yr⁻¹. As may be seen in tables 6.6 – 6.9, effective dose in the brick samples (see table 6.6), varied from 0.12 ± 0.01 to 0.56 ± 0.04 mSv yr⁻¹ with average value of 0.37 ± 0.15 mSv yr⁻¹. In the sand samples (see table 6.7), variation was from 0.14 ± 0.01 to 0.71 ± 0.05 mSv yr⁻¹ with an average value of 0.33 ± 0.15 mSv yr⁻¹.

In the marble samples (see table 6.8), variation in the effective dose was from 0.07 ± 0.01 to 0.57 ± 0.04 mSv yr⁻¹ with an average value of 0.20 ± 0.17 mSv. The

effective dose from the cement samples (see table 6.9) varied from 0.17 ± 0.01 to 0.23 ± 0.02 mSv yr⁻¹, with an average value of 0.20 ± 0.03 mSv yr⁻¹.

Table 6.7: ²²⁶Ra, ²³²Th, ⁴⁰K and Ra_{eq}, external and internal hazard indices and effective dose measured in the sand samples collected from Swabi, Mardan, Charsadda districts as well as Mohmand and Bajuar agencies.

Location	²²⁶ Ra (Bq.kg ⁻¹)	²³² Th (Bq.kg ⁻¹)	⁴⁰ K (Bq.kg ⁻¹)	Ra _{eq} (Bq.kg ⁻¹)	H _{ex}	H _{in}	Annual effective dose (mSv)
Gandab Kwar	26±2	51±3	1745±135	234±16	0.63±0.04	0.70±0.05	0.71±0.05
Sheikh Baba	22±1	43±3	1476±115	198±14	0.53±0.04	0.60±0.04	0.60±0.04
Toro Nalai	2±1	6±1	424±33	43±3	0.12±0.01	0.12±0.01	0.14±0.01
S.Killi Kwar	8±1	15±1	836±65	94±7	0.25±0.02	0.28±0.02	0.29±0.02
Yaqurban	19±1	24±1	483±38	90±6	0.24±0.02	0.30±0.02	0.27±0.02
Lahore	21±1	34±2	532±41	110±7	0.30±0.02	0.36±0.02	0.32±0.02
Maniri	31±2	47±3	510±40	138±9	0.37±0.02	0.46±0.03	0.39±0.03
Tangai Kwar	15±1	24±1	603±47	96±7	0.26±0.02	0.30±0.02	0.29±0.02
Rustum Kwar	21±1	16±1	548±43	86±6	0.23±0.02	0.29±0.02	0.26±0.02
Zorbandar	27±2	40±2	537±43	125±8	0.34±0.02	0.41±0.03	0.36±0.02
Minimum	2±1	6±1	424±33	43±3	0.12±0.01	0.12±0.01	0.14±0.01
Maximum	31±2	51±3	1745±135	234±16	0.63±0.04	0.70±0.05	0.71±0.05
AM±SD	19±9	30±15	769±461	121±57	0.33±0.15	0.38±0.17	0.33±0.15
GM±GSD	16±1.5	26±1.4	680±1.3	0.30±1.27	0.35±1.28	0.35±1.28	110±1.27

6.4. Discussion

The concentration of radionuclides under study in the soil samples collected from different localities varied from area to area. For example, a minimum value of 8 ± 1 Bq.kg⁻¹ for ²²⁶Ra was observed in samples from Naroga (Mohmand agency) and Sabagai (Bajuar agency) and maximum specific activity of 53 ± 3 Bq.kg⁻¹ in Kalambad (district Mardan) and 54 ± 3 Bq.kg⁻¹ was found in the Swabi city. ²³²Th activity was found to be 7 ± 1 Bq.kg⁻¹ (Narogha), 9 ± 1 Bq.kg⁻¹ (Tarakai) in the Mohmand and Bajuar agencies, respectively to 84 ± 5 Bq.kg⁻¹, 86 ± 5 Bq.kg⁻¹ in the Pahlawan in the district Charsadda and Kalambad (Mardan), respectively. A minimum specific activity for ⁴⁰K was 153 ± 13 Bq.kg⁻¹ in the Alingar area of the Mohmand agency and a maximum value of 1018 ± 79 Bq.kg⁻¹ was observed in the Kalambad, district Mardan. Radium equivalent activity

showed variation from $31 \pm 2 \text{ Bq.kg}^{-1}$ (Narogha) to $194 \pm 12 \text{ Bq.kg}^{-1}$ in Pahlawan area of the district Charsadda and $255 \pm 17 \text{ Bq.kg}^{-1}$ Kalamabad. If the measured radioactivity is compared with the geology of the area, it shows that alluvial soils have higher concentration of radioactive elements as compared to that of metabasites metamorphic and igneous rocks.

In general, average maximum specific activities for ^{226}Ra , ^{232}Th and ^{40}K were observed in the district Mardan and minimum in the Mohmand agency. The areas of Narogha, Sheik Baba, Qandari of Mohmand agency and Maskano, Sabagai, Tarakai in Bajuar agency have little vegetation cover. The observed ^{226}Ra and ^{232}Th specific activities in the samples collected from Maskano, Sabagai, Tarakai, Narogha, Sheik Baba and Qandari were very low and thus are safe to use as building materials.

Table 6.10 shows the results of the current study along with other data reported for different parts of Pakistan. It may be seen in this table that average activities calculated in the present study lies within the reported values; however the measured values for ^{40}K , in the present study are slightly higher than the world population weighted average value (420 Bq. kg^{-1}) as reported in the UNSCEAR 2000.

For ^{226}Ra , overall average minimum and maximum activities of $18 \pm 19 \text{ Bq.kg}^{-1}$ and $30 \pm 15 \text{ Bq.kg}^{-1}$ were observed in marble and sand samples, respectively. In general, minimum average activities for ^{232}Th were 18 ± 4 and $18 \pm 21 \text{ Bq.kg}^{-1}$ in cement and marble samples, respectively whereas maximum activity of $41 \pm 21 \text{ Bq.kg}^{-1}$ was observed in the sand samples collected from the selected area.

As the specific activities, radium equivalent activity and internal and external hazard indices of the soil samples reported in this study are within the acceptable limit. Therefore the use of these soils in the construction of dwellings is considered to be safe for the inhabitants especially the soil of Mohmand agency which has relatively low values of specific activities as compared to the other districts/agency.

Similarly, measured specific activities of ^{226}Ra , ^{232}Th and ^{40}K varied from sample to sample in the brick, sand, marble and cement samples. For example, both for ^{226}Ra and ^{232}Th , minimum value of $1 \pm 1 \text{ Bq.kg}^{-1}$ was observed in the marble samples

(Greenish). maximum value of 62 ± 4 (Dagi Mb) and (Pink M) 66 ± 4 Bq.kg⁻¹ was also observed in marble samples.

Table 6.8: ²²⁶Ra, ²³²Th, ⁴⁰K and Ra_{eq}, external and internal hazard indices and effective dose measured in the marble samples collected from the selected area.

Brand	²²⁶ Ra (Bq.kg ⁻¹)	²³² Th (Bq.kg ⁻¹)	⁴⁰ K (Bq.kg ⁻¹)	Ra _{eq} (Bq.kg ⁻¹)	H _{ex}	H _{in}	Annual effective dose (mSv)
Yellow	28±2	34±2	535±42	119±8	0.32±0.02	0.40±0.03	0.34±0.02
Pink M	41±3	66±4	819±64	198±13	0.54±0.03	0.65±0.04	0.57±0.04
Dagi Mb	62±4	2±1	25±2	66±4	0.18±0.01	0.34±0.02	0.19±0.01
Black M	34±2	54±3	665±52	161±11	0.44±0.03	0.53±0.03	0.46±0.03
Dark Green	10±1	8±1	93±8	29±2	0.08±0.01	0.11±0.01	0.08±0.01
White Swabi	7±1	7±1	115±9	27±2	0.07±0.01	0.09±0.01	0.08±0.01
Off-White	5±1	8±1	99±8	24±2	0.07±0.01	0.08±0.01	0.07±0.01
Reddish	6±1	7±1	98±8	24±2	0.06±0.01	0.08±0.01	0.07±0.01
Greenish	1±1	1±1	890±69	71±6	0.19±0.01	0.20±0.02	0.24±0.02
Dark Brown	8±1	15±1	56±5	34±2	0.09±0.01	0.11±0.01	0.09±0.01
Br. Mardan	6±1	8±1	103±8	25±2	0.07±0.01	0.08±0.01	0.07±0.01
Light Brown	11±1	8±1	94±8	30±2	0.08±0.01	0.11±0.01	0.09±0.01
Minimum	1±1	1±1	25±2	24±2	0.07±0.01	0.08±0.01	0.07±0.01
Maximum	62±4	66±4	890±69	198±13	0.54±0.03	0.65±0.04	0.57±0.04
AM±SD	18±19	18±21	299±328	67±60	0.18±0.16	0.23±0.20	0.20±0.17
GM±GSD	10±1.9	10±2	164±1.9	49±1.52	0.13±1.52	0.17±1.52	0.14±1.52

For ⁴⁰K, minimum value of 25 ± 2 Bq.kg⁻¹ and a maximum of 1745 ± 135 Bq.kg⁻¹ (Gandab Kawar) were observed in marble and sand samples, respectively.

For ⁴⁰K, average minimum value of 244 ± 29 Bq.kg⁻¹ was observed in brick samples whilst average maximum value of 769 ± 461 Bq.kg⁻¹ was observed in the cement samples. Average minimum radium equivalent value of 67 ± 60 Bq.kg⁻¹ was observed in the marble samples and maximum average value of 129 ± 54 Bq.kg⁻¹ was observed in sand samples. In table 6.11, present data of the sand, marble and cement samples have been compared with some other published data. As may be seen in table 6.11, ²²⁶Ra value of the present selected samples is slightly lower than those reported by the other groups.

Table 6.9: ^{226}Ra , ^{232}Th , ^{40}K and Ra_{eq} , external and internal hazard indices and effective dose measured in the cement samples collected from the area under study.

Brand	^{226}Ra (Bq.kg^{-1})	^{232}Th (Bq.kg^{-1})	^{40}K (Bq.kg^{-1})	Ra_{eq} (Bq.kg^{-1})	H_{ex}	H_{in}	Annual effective dose (mSv)
Chairman	21±1	23±1	264±21	74±5	0.20±0.01	0.26±0.02	0.21±0.01
Askari	34±2	17±1	282±22	80±5	0.22±0.01	0.31±0.02	0.23±0.02
Fuji	19±1	16±1	215±17	58±4	0.16±0.01	0.21±0.01	0.17±0.01
Cherat	25±2	13±1	219±17	60±4	0.16±0.01	0.23±0.01	0.17±0.01
Lucky	20±1	21±1	240±19	69±5	0.19±0.01	0.24±0.02	0.20±0.01
Minimum	19±1	13±1	215±17	58±4	0.16±0.01	0.21±0.01	0.17±0.01
Maximum	34±2	23±1	282±22	80±5	0.22±0.01	0.31±0.02	0.23±0.02
AM±SD	24±6	18±4	244±29	68±9	0.19±0.03	0.25±0.04	0.20±0.03
GM±GSD	23±1.1	18±1.1	243±1	68±105	0.18±.105	0.25±1.05	0.19±1.05

However, specific activity of ^{232}Th in some samples is higher and in some samples lower than those of the reported values. In spite of this trend, present average value of ^{232}Th is still lower than the world population weighted average values. Specific activity of ^{40}K is on the higher side as compared to the other reported studies especially the values obtained from the sand samples in the present study; however it is still in the range of the reported values. Average activities calculated in the present study lies within the reported values and are also lower than the world population weighted average value as reported in the UNSCEAR 2000.

Specific activities, radium equivalent activity and internal and external hazard indices for all the selected samples are within the acceptable limits. Therefore, use of these materials in construction of dwellings may be considered safe for the inhabitants from a radiological point of view.

In general, soil has more mean activity concentrations of ^{226}Ra , ^{232}Th and ^{40}K as compared to the brick, sand, marble and cement samples which were collected from the selected area whilst marble has the least concentration of the naturally occurring radionuclides. The results are comparable with those reported for some other parts of Pakistan.

Table 6.10: Comparison of the present values with some other data reported for other parts of Pakistan.

Location	^{226}Ra (Bq.kg ⁻¹)	^{332}Th (Bq.kg ⁻¹)	^{40}K (Bq.kg ⁻¹)	Reference
Faisalabad Barren soil	24–29	49–54	499–604	Tufail et al., 2006.
Faisalabad cultivated soil	27–33	46–62	563–629	Tufail et al., 2006.
Bahawalpur	32.9±0.9	53.6±1.4	647.4±14.1	Matiullah et al., 2004.
Punjab	41 ±8	35 ±7	615 ±143	Tahir(2005).
Nowshera	44	56	668	Khan, (2001).
Peshawar	42	56	562	Khan(1995).
Islamabad	38	59	690	Tufail(1991).
Lahore	18	28	570	Akhtar (2005).
NWFP and FATA	26±9	39±20	485±450	The present study

Table 6.11: Comparison of the present study with other data reported for different parts of the world (All the activities are shown in Bq.kg⁻¹).

Location	^{226}Ra (Bq.kg ⁻¹)	^{332}Th (Bq.kg ⁻¹)	^{40}K (Bq.kg ⁻¹)	Reference
Sri Lanka, Brick	35	72	585	Hewamanna et al.,2005
Pakistan, Marble	27	26	58	Tufail et al., 2000
China, Cement	64.7	48.7	161.3	Xinwei, 2005
Pakistan, Sand	36.9-51.9	52.5-67.6	680-784	Khan et al., 2005
Egypt, Cement	33± 17	14± 2.4	45± 26	Mahmud, 2007
Iran, Cement	33	30	700	Fathivand et al., 2007
World Range	17–60	11–64	140–850	UNSCEAR, 2000
World Population weighted Average	32	45	420	
Brick	30±15	41±21	523±182	The present study
Sand	19±9	30±15	769±461	The present study
Marble	18±19	18±21	299±328	The present study

6.5. Conclusions

Mean activity concentrations of ^{226}Ra , ^{232}Th and ^{40}K in soil sand, brick, marble and cement samples from the three districts and two Tribal Agencies were measured. The results are comparable with the values reported for the specific activities in some other parts of the country and also with worldwide findings. Radium equivalent activity external and internal hazard indices are well below the acceptable hazard limit of 370 Bq kg^{-1} (OECD, 1979; Beretka and Mathew, 1985) and 1, respectively. Therefore, the use of these soils as building materials in the construction of dwellings may be considered to be safe for the inhabitants. For soil higher average ^{226}Ra contents were found in the Mardan district and lower values have been measured for the Mohmand agency. Over all higher average ^{226}Ra was measured in the soil as compared to other studied building materials. In other studied building materials, bricks samples have more ^{226}Ra as compared to the other materials. Least ^{226}Ra was observed in the marble samples. In soil samples relatively higher average ^{232}Th activity was measured for the Mardan, Swabi and Charsadda districts as compared to the Mohmand and Bajuar agencies. Low ^{232}Th contents were measured in the marble and cement samples studied while sand has intermediate values between marble, cement and soil samples. Higher ^{40}K was measured in the soil of the Mardan district while low values are reported for the soil samples form Mohmand agency. Highest average ^{40}K was measured in the sand samples collected form the studies area. Relatively higher radium equivalent was measured in the Mardan district, and Lower in the Mohmand agency.

Chapter Seven

Electrets as a Radon Progenies Dosimeter

7.1. Introduction

A number of active and passive devices are currently being used for the measurement of ionizing radiations. Most of the passive devices, although relatively cheaper, are suitable only for a long-term measurements. Reading of such passive detectors is time consuming and its sensitivity, in some cases, is relatively low (respond to specific band of energy), its reading requires a time delay due to processing requirements (etchings) and thus the results are not instantly available. Unlike other passive devices electret ion chamber (EIC) provides rapid results. EICs are used for accurate measurement of different types of radiation including indoor radon measurements (Dua et al., 1999 & 2002). According to US EPA estimates, 30% to 40%, of radon researchers in USA utilize the electret ionization chambers (Colle' et al., 1995). In EICs, ionization current is integrated over a period of time by noting the drop in the surface voltage on electret that is placed inside an ion chamber. An electret is a sample of dielectric material (commonly Teflon) that carries a quasi-permanent electric charge.

As the amount of voltage drop on the electret provides an accurate correlation to the number of ions collected and hence to the total energy lost by the alpha-emitting isotope (Kasper, 1999). The EIC system is accurate and sensitive. The EIC system provides consistent, repeatable results that are, on average, within 5% accuracy. Aluminized Mylar window is used in case of measurement of alpha contamination on surfaces, to reduce the effect of dust (Dua, 1999; Sun et al., 2006).

The electret chambers may be reused again and again. The electrets are replaced after making 10 to 20 measurements until its voltage drops below 200V and it is then

recharged. EIC measurement performance is comparable to the scintillation technology.

The surface potential of electrets remains stable even under extreme conditions of relative humidity (Kotrappa et al., 1988; Mahat et al., 2001). In a study conducted in UK, at radon concentration of 500 Bq m^{-3} , the resulting perturbation was 3% over a 7-day deployment; at the typical value of 80 Bq m^{-3} it approached to 22% (Denman et al., 2001).

Electrets are sensitive to gamma rays and on the presence of a high gamma background an error ranging up to about 20% may be introduced (Usman et al., 1999; Kim et al., 2003; Righi, and Bruzzi, 2006; Espinosa et al., 2005; Pilkte and Butus et al., 2005; Paulus et al., 2003; Martinez et al., 1998; Samer et al., 2007; Clouvas et al., 2006; Gervino et al., 2007; Fricke et al., 1999).

This chapter deals with the use of EIC in measuring the radon concentration, determining the equilibrium factor and unattached fraction. Before discussing the experimental details it would be informative to briefly discuss main components of the electrets and its calibration.

7.2. Components of E-PERMS

Electret-passive environmental radon monitor (E-PERM) system consist of three components (1) electrostatically charged Teflon called electrets (2) an ion chamber made of conductive plastics to which an electret can be loaded (3) a voltage reader to read the surface potential of the electrets.

7.2.1. Electrets: Electrets are made of Teflon which is electrically charged by a special process so that it retains the charge permanently. Electrets are of two types (a) positive (b) negative. The surface charge of the electret is neutralized by collection of ions from the surroundings and the surface voltage of the electrets decrease proportionally when these ions are collected on the electret surface.

7.2.2. The electret ion chamber: Nuclear radiation emitted by radon or other radioactive materials during decay generates ions in air. When this occurs in the fixed volume of the conductive plastic chamber, the ions are collected on the charged electrets which work as a mean of measuring radiations. Such instrument is called electret ion chamber.

7.2.3. The Electret Reader: To read the potential of the electret the electronic instrument called surface potential electret voltage reader (SPER) is used. This reader is able to read the potential drop of a minimum of one volt (1V). To measure the integrated drop of potential drop of the electret, before placing the electret in the chamber its initial voltage (I) is recorded, after exposure the final voltage (F) of the electret and the exposure time in days is recorded. The calibration factor (CF) for E-PERM is calculated which is linearly related to the electret voltage drop over a range of 150V to 750V to the average voltage during the exposure.



Figure 7.1: Electret ion chambers used for measurement of radon and thoron progeny deposited on the surface.

7.3. Principal of Measurement of Alpha Contamination

The surface EIC with its aluminized Mylar window is used to measure alpha radiation from the contaminated surfaces or alpha emitters deposited on its surface. Area monitored is 48.7 cm² and the response of electric ion chamber is for all the alpha radiations from different isotopes. The results are expressed in alpha counts per 100 cm² in 4π geometry.

The calibration factor for measurement of alpha contamination with ST electrets is given by the following relation.

$CF = 0.0006416 + 2.4303 \times 10^{-7} \times (I+F)/2$ and the alpha contamination levels in unit of alpha disintegration per minute per 100 cm² is calculated by

$$A = \alpha(\text{dpm per } 100 \text{ cm}^2) = \frac{(I-F) \times 2.053}{CF \times T}$$

However when LT electrets are used the results may be multiplied by 11.5, if a window is used the result is multiplied by 1.794 (Part-II Section .4.Alpha Rev#0 ,1994). Electrets are sensitive to gamma radiation, to correct the electret readings for background gamma radiation; the background (BG) factor is introduced. BG depends on the chamber as well as on the place of measurement.

7.4. Alpha Contamination Electret Measurement System as Radon Progeny Dosimeter

7.4.1. Experimental Approach

As stated above, special electret ion chambers (EICs) can be used for the measurement of surface alpha contamination (see Figure 7.1). However in the present study these alpha contamination chambers have been used in a novel approach to measure its performance for the measurement of airborne radon progeny concentration through surface deposited radon progeny. In these experiments surface electret ion chambers have been used in such a way that Mylar side was directed upward and ionization produced by deposited radon progenies have been measured instead of alpha contamination. In order to measure the performance factor (PF) of this alpha contamination chamber radon concentration was measured side by side using the standard chambers with short term electrets to determine the radon concentration. Experiments were performed using both short term (high sensitivity) and long term (low sensitivity) electrets.

To correct the readings for the gamma background and radon gas, an electret with plastic cover (see Figure 7.1) which blocks the detection of alpha was used for the subtraction of the effect gamma radiation on these chambers. During the measurement aerosols conditions of the room was changed (i.e. from normal aerosol conditions with no turbulence or aerosols generating activity) to the use of different types of aerosols generating activities like propane cooking, candle burning, cigarette smoking and fan and using different High Efficiency Particle Air (HEPA) filters and unattached fraction and equilibrium factor was measured.

7.4.2. Measurement of Radon using Electrets

Commercially available E-PERMs were used to measure the indoor radon concentration during the experiments using alpha contamination chambers to measure the plate out

radon progeny concentration in the exposure room. As E-PERMs are sensitive to gamma rays therefore corrections were applied (Kotrappa and Stieff, 1992; 1993). In order to measure the radon using electrets two steps are involved. First the calibration factor (CF) was determined using the following formula

$$CF = \frac{\text{Volts}}{\frac{\text{pCi}}{l} \times \text{day}} = A + B \times \frac{(I + F)}{2}$$

Where A and B are constant for a particular E-PERM configuration and “I” and “F” are the initial and final voltages of the electrets exposed in the chamber. Radon concentration was then calculated by using the following relation

$$\text{RnC} \left(\frac{\text{pCi}}{l} \right) = \frac{(I-F)}{CF \times D} - BG$$

Where RnC is the radon concentration in units of pCi.ℓ⁻¹ or in Bqm⁻³ (1 pCi.L⁻¹ =37.5 Bqm⁻³), “I” and “F” are the initial and final voltage readings of the exposed electret. In the present work standard chamber “S” having volume of 200ml was used. Different configurations are used for making measurements i.e. when short term electret (ST) used in S-chamber, the e-perm is called “SST” e-perm. When a long term (LT) is loaded into “S” chamber the electret is called “SLT” E-PERM. In the present study “SST” configuration was used. The background values for S chamber are 0.087 R/h.

SST electrets were exposed to indoor radon concentration in the exposure room and its initial and final voltages were noted along with the exposure duration. Blue labeled (Short-term) electret in Standards chamber (SST) calibration factor was found using the following calibration factor (see table 7.1).

$$CF = 1.69776 + 0.0057420 \times \frac{(I + F)}{2}$$

These calibration factors are used in the 200-750V range (Kotrappa, 1990). Electrets have the following components of error.

1. The system imperfection error, which include uncertainty in chamber volume, electret thicknesses and other component parameters. It is 5 % (Kotrappa et al., 1990).
2. Error component 2: the error of the electret reading. There can be an uncertainty of as much as 1 volt in both initial and final readings; the error in the difference of the two readings is 1.4 volts. the percentage = $100 \times 1.4 / (I-F)$
3. Error component 3: error due to gamma background. the maximum error is about 0.1 to 0.2 pCi.l⁻¹
4. Total error is $E_t = \sqrt{E_1^2 + E_2^2 + E_3^2}$

Using standard radon chambers results obtained are shown in table 7.1. As can be seen from table 7.1 radon concentration as measured by using the short term high sensitivity electrets are stable and the variation between the different readings of the same exposure(run) is low. The exposure of four short term electrets on March 20, have radon concentration of 43 ± 6 pCi.l⁻¹, 44 ± 6 pCi.l⁻¹, 44 ± 5 pCi.l⁻¹ and 44 ± 5 pCi.l⁻¹ with standard deviation of ~ zero. Similar reading was obtained on March 30 and the two detectors showed the same value of 22 ± 4 pCi.l⁻¹ with no standard deviation.

The maximum variation among the reading of different electrets used in the same run was recorded in a run in which three electrets were exposed in which the two reading were 34 ± 8 , 34 ± 8 pCi.l⁻¹ and the third one had value of 158 ± 8 pCi.l⁻¹. This high difference thought to be the accidental drop due to the touching of the surface of the electret by hand or some other conducting materials, which have caused this high difference in the voltage drop.

In majority of the cases more than one electrets were exposed to the indoor radon and the reading were in a very good agreement For example, the exposure of five electrets on March 11 for 0.33 days gave results of 36 ± 6 , 32 ± 7 , 34 ± 7 , 33 ± 7 and 34 ± 6 pCi.l⁻¹ with an average of 34 ± 7 pCi.l⁻¹ and having standard deviation of only two. On March 12, exposure of five electrets for 0.71 days gave results of 58 ± 3 , 60 ± 3 , 57 ± 3 , 57 ± 3 and 70 ± 4 with an average of 60 ± 6 pCi.l⁻¹ and a standard deviation of this run is only 5. In total of 36 runs of experiments in which two or more than two electrets were exposed in the exposure room the standard deviation between different readings was less

than 10. In only three reading the standard deviation among the reading was higher than 10, which may be due to the accidental touching of the surface of the electrets which causes unwanted discharge of the surface. Measuring radon concentrations above 150 Bq m⁻³ (i.e., 4 pCi.ℓ⁻¹) the relative difference is normally less than 20% using electrets. The difference is mostly less than 10% for radon concentrations above (5.3 pCi ℓ⁻¹) 200 Bq m⁻³. If accurate results (variation 20%) are required for measurements made in time period of less than 6 months at low radon concentrations (below 200 Bqm⁻³), L-chambers with short-term electrets (LST combination) should be used (Vargas and Ortega, 2001). E-PERMs show better performance at a very high radon concentration (Gervino et al., 2004). The E-PERM provides to be very good for measuring the indoor radon concentration.

7.5. Calculation of the Performance Factor for The Measurement of Radon Progeny

Alpha contamination chambers were exposed to radon progeny and radon measurements were carried out using both standard radon chambers and active detector for a suitable time (see table 7.1). The performance factor was calculated and inter-compared for different environmental conditions using the long-term electret for the measurement of radon progenies. Short-term electret with thick plastic top cover was used for the measurement of background. The readings from long-term electrets were multiplied by 12.5 (due to low sensitivity of the long term electrets) and then the calculations were performed (Manual of E-PERMS Part-II - II.4.Alpha Rev#0,1994).

For the measurement of normalized Voltage drop of the long-term electrets, the following relation was used.

$$NVPD = \frac{((12.5 \times F_{LT} - F_{ST}) - (12.5 \times I_{LT} - I_{ST}))}{T(\text{Days})}$$

Normalized Voltage drop (NVPD), F_{LT} = Final reading of long-term electret, F_{ST} Final reading of short-term electret, I_{LT} = Initial reading of long-term electret, I_{ST} Initial reading T = Exposure time (in days).

Table 7.1: Radon concentration measurements made in the exposure room using standard electrets.

ID	Initial Volts (VI)	Final Volts (VF)	Calib.Facotr	Exposure (Days)	Rn(pCi.l ⁻¹)	Rn(Bq.m ⁻³)	Av Rn
ST 9979	347	324	1.89	0.33	36±6	1335	34±7
SQ 8344	431	410	1.94	0.33	32±7	1184	
SQ8431	360	338	1.9	0.33	34±7	1270	
SQ8293	315	294	1.87	0.33	33±7	1228	
SK 3783	494	471	1.98	0.33	34±6	1276	
ST 9979	324	246	1.86	0.71	58±3	2184	60±3
SQ 8344	410	328	1.91	0.71	60±3	2239	
SQ8431	338	261	1.87	0.71	57±3	2146	
SQ8293	294	218	1.84	0.71	57±3	2147	
SK 3783	471	374	1.94	0.71	70±4	2612	
ST 9979	246	225	1.83	0.35	32±7	1203	34±7
SQ 8344	328	306	1.88	0.35	33±7	1230	
SQ8431	261	237	1.84	0.35	37±6	1374	
SQ8293	218	197	1.82	0.35	32±7	1214	
SK 3783	374	350	1.91	0.35	35±6	1326	
SK 3783	350	293	1.88	0.63	47±3	1771	47±3
ST 9979	217	193	1.82	0.35	36±6	1366	
SQ 8344	303	278	1.86	0.35	37±6	1386	
SQ8431	231	206	1.82	0.35	38±6	1418	
SQ8293	182	159	1.8	0.35	35±6	1322	
SK 3783	293	268	1.86	0.35	37±6	1390	37±6
Su0079	366	339	1.9	0.35	39±6	1471	
SQ 8344	278	206	1.84	0.65	60±4	2242	
SQ8431	206	140	1.8	0.65	56±4	2098	
SQ8293	159	96	1.77	0.65	54±4	2032	
SK 3783	268	186	1.83	0.65	69±4	2570	60±4
Su0079	339	262	1.87	0.65	63±4	2356	
ST 9979	187	161	1.8	0.35	40±6	1497	
SQ 8344	206	180	1.81	0.35	40±6	1488	
SQ8431	140	116	1.77	0.35	37±6	1401	
SQ8293	96	73	1.75	0.35	36±6	1361	42±6
SK 3783	186	154	1.8	0.35	49±5	1853	
Su0079	262	231	1.84	0.35	47±5	1751	
SQ8424	461	386	1.94	0.63	61±4	2284	
SU0025	452	374	1.94	0.98	40±3	1502	
SU0081	267	198	1.83	0.98	37±3	1401	43±3
SU0007	184	114	1.78	0.98	39±3	1461	
SK3783	156	86	1.77	0.98	39±3	1475	
SQ8424	386	364	1.91	0.31	36±7	1346	
SU0081	198	177	1.81	0.31	36±7	1362	
SU0007	114	95	1.76	0.31	34±8	1263	32±8
SK3783	86	71	1.74	0.31	27±9	999	

(Table 7.1: continued)

SQ8424	364	302	1.89	0.68	48±3	1784	46±3
SU0025	369	302	1.89	0.68	51±3	1929	
SU0081	177	121	1.78	0.68	45±3	1705	
SU0007	95	39	1.74	0.68	47±3	1752	
SK3783	71	25	1.73	0.68	38±4	1443	
SQ8424	302	277	1.86	0.34	38±6	1429	30±8
SU0081	121	99	1.76	0.34	35±7	1329	
SU0007	39	24	1.72	0.34	25±9	920	
SK3783	25	11	1.71	0.34	23±10	860	
SQ8424	277	224	1.84	0.68	42±3	1560	40±3
SU0025	297	241	1.85	0.68	44±3	1641	
SU0081	99	54	1.74	0.68	37±3	1397	
SK9979	161	113	1.78	0.68	39±3	1463	
SQ8424	224	198	1.82	0.32	44±6	1662	41±6
SU0025	241	215	1.83	0.32	44±6	1653	
SU0081	54	35	1.72	0.32	34±8	1275	
SK9979	113	90	1.76	0.32	41±6	1520	
ST9995	355	333	1.9	0.71	15±6	581	16±6
SQ0098	382	357	1.91	0.31	41±6	1554	44±6
SQ 8366	346	320	1.89	0.31	44±6	1636	
SQ276	435	408	1.94	0.31	44±6	1655	
ST9995	333	306	1.88	0.31	46±6	1708	
SQ0098	357	280	1.88	0.65	62±4	2343	60±4
SQ 8366	320	246	1.86	0.65	61±4	2276	
SQ276	408	334	1.91	0.65	59±4	2215	
ST9995	306	238	1.85	0.65	56±3	2096	
SQ0098	280	247	1.85	0.33	53±5	1995	52±5
SQ 8366	246	216	1.83	0.33	49±5	1829	
SQ276	334	300	1.88	0.33	54±5	2022	
ST9995	238	207	1.83	0.33	51±5	1897	
SQ0098	247	188	1.82	0.66	48±3	1796	44±3
SQ 8366	216	157	1.81	0.66	48±3	1814	
SQ276	300	240	1.85	0.66	48±3	1797	
ST9995	207	167	1.81	0.66	33±4	1219	
SQ0098	188	162	1.8	0.33	43±6	1627	44±6
SQ276	240	213	1.83	0.33	44±6	1663	
ST9807	420	392	1.93	0.33	44±5	1632	
SU0101	381	353	1.91	0.33	44±5	1652	
SQ276	213	126	1.8	0.69	69±4	2591	72±4
ST9807	392	297	1.9	0.69	71±4	2680	
SU0101	353	254	1.87	0.69	75±4	2830	
ST9807	297	260	1.86	0.31	63±5	2367	64±5
SU0101	254	215	1.83	0.31	68±5	2531	
SU0022	306	270	1.86	0.31	61±5	2295	

(Table 7.1: continued)

ST9807	260	174	1.82	0.67	70±4	2620	71±4
SU0101	215	126	1.8	0.67	73±4	2754	
SU0022	270	183	1.83	0.67	70±4	2643	
ST9807	174	152	1.79	0.32	37±7	1392	36±7
ST9916	303	282	1.87	0.32	34±7	1273	
SU0022	183	161	1.8	0.32	37±7	1388	
ST9807	152	86	1.77	0.68	54±3	2015	61±4
ST9916	282	206	1.84	0.68	60±4	2233	
SU0022	161	74	1.77	0.68	71±4	2668	
ST9807	86	66	1.74	0.32	35±7	1329	39±7
ST9916	206	181	1.81	0.32	43±6	1606	
SU0022	74	53	1.73	0.32	37±7	1403	
ST9807	66	25	1.72	0.69	34±4	1257	36±4
ST9916	181	128	1.79	0.69	42±3	1576	
SU0022	53	13	1.72	0.69	33±4	1231	
ST9807	127	108	1.77	0.31	34±8	1266	75±8
ST9916	128	109	1.77	0.31	34±8	1266	
SU0022	161	74	1.77	0.31	158±8	5919	
ST9807	108	57	1.75	0.68	42±3	1571	41±3
ST9916	109	60	1.75	0.68	40±3	1507	
SJ5697	290	287	1.86	0.3	4±47	166	4±47
SJ5697	287	265	1.86	0.67	17±6	633	17±6
SJ5697	265	261	1.85	0.33	6±35	211	6±35
SJ5697	243	228	1.83	0.99	7±9	275	7±9
SJ5697	228	187	1.82	1	22±4	812	22±4
SJ5697	228	187	1.82	1	22±4	812	22±4
SJ5697	159	100	1.85	1.02	30±3	1140	32±3
SBH346	561	492	2	1.02	33±3	1233	
SB897	522	454	1.98	1.02	33±3	1229	
SBH346	492	416	1.96	1.21	31±2	1167	32±2
SB897	454	377	1.94	1.21	32±2	1197	
SBH346	416	370	1.92	0.79	29±3	1096	28±3
SB897	377	334	1.9	0.79	28±4	1034	

For the measurement of normalized voltage drop for short-term electret the following relation was used.

$$\text{NVPD} = \frac{((F_{\text{ST}} - F_{\text{BG}}) - (I_{\text{ST}} - I_{\text{BG}}))}{T(\text{Days})}$$

F_{BG} , I_{BG} are the final and initial reading of the background.

Performance factor (PF) was calculated using the following relation

$$\text{PF} = \frac{\text{NVPD}}{C_{\text{Rn}}}$$

C_{Rn} is radon concentration.

7.6. Results and Discussion

As may be seen in table 7.1 radon concentrations during the experiment was in the ranged from $30 \text{ pCi}\cdot\ell^{-1}$ to $60 \text{ pCi}\cdot\ell^{-1}$ ($1125\text{-}2250 \text{ Bq}\cdot\text{m}^{-3}$) with an over all average was $44 \text{ pCi}\cdot\ell^{-1}$. The duration of each experiment was 0.3 - 1 day. The results of NVPD and PF are shown in tables 7.2a –7.2c.

7.6.1. Long-term Electrets

The performance factor was also compared with the equilibrium factor and unattached fraction of the radon progenies. The results showed that long term electret can be used in the inverted form for the measurement of radon progenies as the voltage drop per $\text{pCi}\cdot\ell^{-1}$ of radon is such that in the case of long-term electret (less sensitive) duration of exposure may be kept relatively longer, in order to get a suitable voltage drop.

Three sets of long-term electrets were used in these experiments. As may be seen in table 7.2c, the performance factor calculated for the three long-term electrets varied from -1.1 to $11.0 \text{ V/d}\cdot\text{pCi}\cdot\ell^{-1}$ (Volt per day per Pico Curie per liter) with an average of $2.20 \pm 5.6 \text{ V/d}\cdot\text{pCi}\cdot\ell^{-1}$ for the electret labeled LL12059 (excluding the three failures) and from 0.49 to 13.64 with an average of $2.90 \pm 2.7 \text{ V/d}\cdot\text{pCi}\cdot\ell^{-1}$ (having one failure) for the LL2187 and for the electret labeled LL2257 the variation was from 0.52 to 12.51 $\text{V/d}\cdot\text{pCi}\cdot\ell^{-1}$ with an average of $2.60 \pm 2.2 \text{ V/d}\cdot\text{pCi}\cdot\ell^{-1}$ while the average of all the three electrets for each run had variation from 0.5 to $12.51 \text{ V/d}\cdot\text{pCi}\cdot\ell^{-1}$ with an over all average of $2.68 \pm 2.1 \text{ V/d}\cdot\text{pCi}\cdot\ell^{-1}$.

As may be seen in table 7.2c, there were only four times out of 108 readings that performance factor of the alpha contamination measurement detector was negative i.e

long-term electrets failed to work as a radon progeny monitor. The average of these electrets were in good agreement, showing that long term electret showed more fluctuations in the short term reading while for long term average there was relatively less fluctuations.

After analyzing the data for these electrets it may be concluded that in a higher radon progeny environment, the use of long-term electret as a radon progeny detector would be suitable while for low radon concentrations performance factor for short duration may be difficult carry out. However, if the sensitivity of voltage reader is enhanced from lower limit of one volt in the current voltage readers, to some lower values say millivolt (mV), then long-term electret can also be used in the low radon environments.

Table 7.2a: Voltage drop of different long term electrets used as radon progeny monitors (Volts).

Device	IV1	FV1	FV2	FV3	FV4	FV5	FV6	FV7	FV8	FV9
SCM 668	390	380	339	323	298	287	253	240	207	194
LL12059	507	501	493	492	486	482	475	470	459	457
LL2187	488	486	473	471	466	463	454	450	440	438
LL2257	437	433	424	421	412	410	403	400	388	387
Device	FV10	FV11	FV12	FV13	FV14	FV15	FV16	FV17	IV18	FV18
SCM 668	172	160	137	127	98	84	56	44	364	335
LL12059	450	448	439	435	427	427	414	414	414	407
LL2187	433	428	422	418	408	404	393	389	389	381
LL2257	376	372	369	365	355	353	340	339	339	330
Device	FV19	FV20	FV21	FV22	FV23	FV24	IV25	FV25	FV26	FV27
SCM 668	320	275	259	215	205	172	294	280	250	235
LL12059	402	389	385	375	373	361	361	358	348	342
LL2187	376	366	360	349	345	335	335	332	326	322
LL2257	325	310	306	297	296	285	285	281	275	270
Device	FV28	FV29	FV30	FV31	IV32	FV32	FV33	FV34	FV35	FV36
SCM 668	203	197	186	181	482	473	433	396	354	330
LL12059	332	331	328	327	326	322	315	304	295	291
LL2187	316	314	311	310	308	306	297	288	281	275
LL2257	263	262	258	257	256	253	244	235	226	222

Other possibility may be to use these low sensitivity electrets for a relatively longer duration measurements. Over all performance of these low sensitivity detectors

originally used for the measurement of alpha contamination, may also be used as radon progeny dosimeters and would thus work as alternative radon progeny monitor

7.6.2. Short-term high sensitivity electrets

The results of the short-term high sensitivity electrets are shown in table 7.3a – 7.3c. Table 7.3a shows the data of the voltage drop of the short term electret for different runs of the experiments

Table 7.2b: Normalized voltage drop (NVPD) in Volts/day of different long-term electrets used as radon progeny monitors.

Electret	NVPD1	NVPD2	NVPD3	NVPD4	NVPD5	NVPD6	NVPD7	NVPD8	NVPD9
LL12059	197	83	-10	78	108	84	138	161	39
LL2187	45	171	26	59	74	123	103	142	39
LL2257	121	101	63	137	39	84	68	180	-2
Electret	NVPD10	NVPD11	NVPD12	NVPD13	NVPD14	NVPD15	NVPD16	NVPD17	NVPD18
LL12059	98	38	134	125	170	-47	201	-36	86
LL2187	60	149	78	125	206	120	163	115	104
LL2257	172	112	22	125	206	37	201	2	123
Electret	NVPD19	NVPD20	NVPD21	NVPD22	NVPD23	NVPD24	NVPD25	NVPD26	NVPD27
LL12059	144	175	106	119	45	172	73	138	188
LL2187	144	119	184	138	121	135	73	65	109
LL2257	144	213	106	101	8	154	113	65	148
Electret	NVPD28	NVPD29	NVPD30	NVPD31	NVPD32	NVPD33	NVPD34	NVPD35	NVPD36
LL12059	135	21	39	24	41	48	93	104	33
LL2187	63	60	39	24	16	73	70	67	64
LL2257	81	21	57	24	29	73	70	104	33

Table 7.3b shows the normalized voltage drop during different runs of the experiment whereas table 7.3c shows the performance factor of the electret calculated for different runs during the experiment.

In order to measure the effect of orientation of the electret on its performance factor, the electrets were exposed in two orientation i.e., horizontal and vertical positions.

As can be seen in table 7.3c the performance factor of the detector placed in the horizontal orientation varied from 0.51 to 3.53 V/d.pCi.ℓ⁻¹ for electret labelled A whilst for electret labeled B it varied from 0.45 to 3.37 V/d.pCi.ℓ⁻¹ with an average varied from 0.48-3.45 V/d.pCi.ℓ⁻¹. For the electrets exposed in the vertical position the values varied

from 0.51 to 4.8 V/d.pCi.ℓ⁻¹ for electret C whilst for the other electret it varied from 0.74 to 3.81 V/d.pCi.ℓ⁻¹. The average value of the performance factor in the vertical position varied from 0.62 to 4.31 V/d.pCi.ℓ⁻¹. As may be seen in table 7.3c the performance factor of the electrets exposed in horizontal position is relatively higher as compared to those exposed in vertical positions. However this deviation in performance factor is not significant.

Table 7.2c: Performance factor in V/d.pCi.ℓ⁻¹ of different long-term electrets used as radon progeny monitors.

Electret	PF 1	PF 2	PF 3	PF 4	PF 5	PF 6	PF 7	PF 8	PF 9
LL12059	5.9	1.4	-0.3	1.7	2.9	1.4	3.3	3.7	1.2
LL2187	1.4	2.8	0.8	1.2	2.0	2.0	2.5	3.4	1.2
LL2257	3.6	1.7	1.9	2.9	1.0	1.4	1.6	4.3	-0.1
Average	3.6	2.0	0.8	1.9	2.0	1.6	2.5	3.8	0.8
%	63%	39%	139%	45%	47%	23%	34%	12%	92%
	PF 10	PF 11	PF 12	PF 13	PF 14	PF 15	PF 16	PF 17	PF 18
LL12059	2.1	1.3	3.3	3.1	11.0	-1.1	3.4	-0.7	1.9
LL2187	1.3	4.9	1.9	3.1	13.3	2.7	2.7	2.2	2.4
LL2257	3.8	3.7	0.5	3.1	13.3	0.8	3.4	0.0	2.8
Average	2.4	3.3	1.9	3.1	12.5	0.8	3.2	0.5	2.4
%	52%	56%	72%	0%	10%	227%	11%	295%	18%
	PF 19	PF 20	PF 21	PF 22	PF 23	PF 24	PF 25	PF 26	PF 27
LL12059	3.3	2.4	1.7	1.7	1.3	2.8	1.9	3.8	2.5
LL2187	3.3	1.7	2.9	1.9	3.4	2.2	1.9	1.8	1.5
LL2257	3.3	3.0	1.7	1.4	0.2	2.5	2.9	1.8	2.0
Average	3.3	2.3	2.1	1.7	1.6	2.5	2.2	2.5	2.0
%	0%	28%	34%	15%	100%	12%	26%	47%	26%
	PF 28	PF 29	PF 30	PF 31	PF 32	PF 33	PF 34	PF 35	PF 36
LL12059	3.3	4.7	2.3	4.2	1.3	2.2	2.9	3.3	1.1
LL2187	1.5	13.6	2.3	4.2	0.5	3.3	2.2	2.1	2.2
LL2257	2.0	4.7	3.4	4.2	0.9	3.3	2.2	3.3	1.1
Average	2.3	7.7	2.7	4.2	0.9	3.0	2.4	2.9	1.5
%	41%	68%	24%	0%	44%	22%	17%	23%	42%

Thus it may be concluded that orientation has insignificant effect on the performance of the electrets if used as a surface deposition activity monitor. Standard deviation for each run is shown in the table 7.3c. A maximum value of 34% and a

minimum value of 17% were recorded for the eight runs. These short-term electrets were found most suitable for the measurement of both high and low levels of radon progeny concentration. However, when high radon concentrations are present, short term measurement must be performed, otherwise the voltage drop may be too high .to the measurement will be inaccurate if the electret voltage is less than 150 V.

Table 7.3a: Voltage drop of different short-term electrets used as radon progeny monitors.

Device	IV	FV1	IV2	FV2	IV3	FV3	IV4	FV4	IV5	FV5	IV6	FV6	IV7	FV7	IV8	FV8
HorzA	368	258	517	348	460	422	412	392	392	361	352	173	568	541	537	449
ABlk	231	192	507	460	348	329	321	309	309	287	288	228	575	557	555	531
HorzB	480	319	446	328	477	437	503	483	483	449	337	135	569	545	541	455
BBlk	492	446	319	274	274	252	422	410	410	384	343	277	311	296	291	266
VertC	512	382	382	206	522	487	468	446	446	415	361	195	452	421	418	309
CBlk	294	256	256	214	471	451	440	428	428	406	336	273	572	559	554	532
VertD	506	345	488	353	500	458	444	427	427	392	391	189	458	423	420	328
BDBLK	594	549	549	500	353	332	324	311	311	289	327	264	325	307	303	280

Table 7.3b: Normalized voltage drop of different short-term electrets used as radon progeny monitors.

	NVPD1	NVPD2	NVPD3	NVPD4	NVPD5	NVPD6	NVPD7	NVPD8
HorzA	72.0	123.9	57.0	31.1	24.0	117.0	28.2	165.8
HorzB	116.6	74.1	54.0	31.1	21.3	133.7	28.2	158.0
VertC	93.3	136.1	45.0	38.9	24.0	101.2	56.3	225.3
VertD	117.6	87.3	63.0	15.6	34.7	136.6	53.2	178.7

An other series of measurements were also performed using short term electrets. The results obtained are shown in table 7.4a - 7.4c, below.

Table 7.3c: Performance factor (V/d. pCi.ℓ⁻¹) of different short-term electrets used as radon progeny monitors.

	PF1	PF2	PF3	PF4	PF5	PF6	PF7	PF8
HorzA	1.95	3.06	1.45	0.87	0.51	2.09	0.62	3.53
HorzB	3.15	1.83	1.37	0.87	0.45	2.39	0.62	3.37
VertC	2.52	3.36	1.14	1.09	0.51	1.81	1.24	4.80
VertD	3.18	2.16	1.60	0.43	0.74	2.44	1.17	3.81
Average	2.70	2.60	1.39	0.82	0.55	2.18	0.91	3.88
Average H	2.55	2.44	1.41	0.87	0.48	2.24	0.62	3.45
Average V	2.85	2.76	1.37	0.76	0.62	2.13	1.20	4.31
Std.Div.	22%	28%	14%	34%	23%	13%	37%	17%

Table 7.4a: Voltage drop of different short-term electrets used as radon progeny monitors.

Device	IV	FV1	FV2	FV3	FV4	FV5	FV6	FV7	FV8	FV9	IV10	FV10	FV11
SCQ497	719	710	707	680	654	571	481	389	337	276	494	468	451
SCQ559	719	717	715	706	695	657	622	581	556	517	507	495	489
SCQ553	698	697	695	675	649	563	473	380	328	269	260	237	220
SCQ499	713	712	712	700	690	649	612	567	541	499	289	278	272
SCQ480	721	720	716	694	671	597	516	430	382	325	295	270	249
SCQ576	682	681	679	672	659	624	592	552	524	473	227	218	210
SCQ542	725	723	721	701	677	597	510	406	351	293	323	300	283
SCQ508	720	720	718	708	697	658	621	578	553	511	254	244	236

Table 7.4b: Normalized voltage drop of different short-term electrets used as radon progeny monitors.

I.D	NVPD 1	NVPD 2	NVPD 3	NVPD 4	NVPD 5	NVPD 6	NVPD 7	NVPD 8	NVPD 9	NVPD 10	NVPD1 1
SCQ497	27.3	1.3	20.0	14.4	63.5	54.2	43.5	34.1	19.9	7.0	9.4
SCQ553	0.0	2.5	8.9	15.4	63.5	52.3	40.9	32.8	15.4	6.0	9.4
SCQ480	0.0	2.5	16.7	9.6	55.1	48.3	39.2	25.3	5.4	8.0	11.1
SCQ542	7.8	0.0	11.1	12.5	57.9	49.3	52.0	37.9	14.5	6.5	7.7
Average	8.8	1.6	14.2	13.0	60.0	51.0	43.9	32.5	13.8	6.9	9.4

Table 7.4c: Performance factors in $V/d.pCi.\ell^{-1}$ of different short term electrets used as radon progeny monitors.

I.D	PF1	PF2	PF3	PF4	PF5	PF6	PF7	PF8	PF9	PF10	PF11
SCQ497	2.73	0.13	2.00	1.44	1.25	1.53	1.21	1.05	0.57	1.44	2.19
SCQ553	0.00	0.25	0.89	1.54	1.25	1.47	1.14	1.01	0.44	1.24	2.19
SCQ480	0.00	0.25	1.67	0.96	1.08	1.36	1.09	0.78	0.17	1.65	2.59
SCQ542	0.78	0.00	1.11	1.25	1.13	1.39	1.44	1.17	0.41	1.34	1.79
Average	0.9	0.2	1.4	1.3	1.2	1.4	1.2	1.00	0.47	1.42	2.19
Std.Div.	147%	77%	36%	20%	7%	5%	13%	16%	18%	12%	15%

The results of another experiment using short term electrets high sensitivity are shown in table 7.4a – 7.4c. As may be seen in table 7.4c, the performance factor varied from 0.13 to 2.73 $V/d.pCi.\ell^{-1}$ for electret labeled SCQ497. The performance factor varied in the

range 0- 2.19 V/d.pCi.ℓ⁻¹ and 0- 2.59 V/d.pCi.ℓ⁻¹ for electrets labeled SCQ553 and SCQ542, whilst for electret SCQ542 it varied from 0 to 1.79 V/d.pCi.ℓ⁻¹. The average values varied from 0.2 to 2.19. The standard deviation varied from 0.05- 1.47 in different runs. These results show a good agreement among different runs and thus the alpha contamination detectors using short-term electrets can be used as radon progeny dosimeter. It also shows that the use of duplicate deposition detector is better from statistical point of view for reducing uncertainty in the readings and a better average value can be obtained.

7.7. Equilibrium and Unattached Fraction of Radon using E-RPISU

Equilibrium factor and unattached fraction of the radon progenies are the two important parameters required for the dose calculation. Radon entry and radon decay product distribution can vary with ambient weather and also with wind, temperature and aerosols conditions in the indoor environment. An increased percentage of unattached decay products leads to or results in a higher risk as compared to the aerosol-attached fraction (Porstendörfer, 2001). Because the amount of radon decay products in the breathing space depends on aerosols particles and turbulence. US EPA relates radon levels to the radon decay product levels by assuming that 40% of the radon decay products produced remain in the air for inhalation. However, this factor can vary between 0.1-0.9. Therefore, the simultaneous measurement of both radon and its progeny is desirable for producing an accurate estimate of radon progeny dose rate.

In order to measure unattached fraction and equilibrium factor of radon using E-PERMs an instrument called the Electret-Radon Progeny Integrating Sampling Unit (E-RPISU) was used (Kotrappa et al., 1989). This instrument can measure radon and its decay products simultaneously. The E-RPISU is composed of an air sampling pump, a flow meter and electret ion chambers, one for radon and two for radon progenies. The E-RPISU measures radon progeny with sampling heads (A and B), two flow-meters (A and B), flow-meter tamper resistant cap, ion chambers A and B), Box with pump and power supplies, time totalizer (no reset), power cord (110 V AC) and tubing.

7.8. Principle of Operation of E-RPISU

An air-sampling pump (0.3 to 0.6 liters per minute) is used to collect the radon progeny for a known sampling time on a 3.5 cm² filter sampler mounted on the side of an electret ion chamber. The flow rate of the pump is adjustable. Recommended flow rate is 0.3 to 0.6 liter per minute and the time is from 1 to 7 days. The filter paper and/or mesh is mounted in such a way that the collected progenies emit their radiation within the chamber. The alpha radiations emitted by the progenies are collected on the filter, which ionizes air in the electret ion chamber. The ions are continuously collected by the electret, providing integrated alpha activity collected on the filter paper. The initial and final readings of the electret, the flow rates and the duration of sampling recorded by the time totalizer are used in software to calculate the progenies concentration in terms of working level (WL) units (Progeny Group Limited).

Once the progeny concentration and radon concentration are known, equilibrium ratios can be calculated using the standard procedures. In order to measure the unattached fraction of radon decay products, air is sampled through a wire mesh in housing B. A down line filter in system B allows for a balanced airflow through both systems. Using these values, radon progeny concentration on both the filter and mesh were calculated using the same procedure. The ratio of the result with mesh to that of filter gives the unattached fraction.

From the measured data of radon and progenies equilibrium factor and unattached fraction were calculated. Radon concentration in pCi (1 pCi = 37.5 Bq.m⁻³) was calculated. Equilibrium factor $F = (PAEC)/C_{Rn}$ was calculated (Kotrappa et al., 1990). The results obtained using different aerosols conditions are shown in the table 7.5. As these measurements were performed under different environmental conditions, therefore, unattached fraction and equilibrium factor showed a wide range of variation. Maximum equilibrium factor of 87% and a minimum unattached fraction of 3% were measured under the smoky environment in the exposure room. One cigarette per hour was used in the Smoking 'Joe smoker' system for producing smoke in the indoor air of the exposure room.

Table 7.5: Equilibrium factor and unattached fraction of radon decay products using ERIPSU

Conditions	Start	Stop	Days	ERIPSU F	ERIPSU f
Calm no particles	3/27/2007 11:25	3/28/2007 9:00	0.90	3%	55%
Calm no particles	3/28/2007 10:00	3/29/2007 11:00	1.04	4.2%	51%
Calm no particles	3/29/2007 16:00	3/30/2007 9:00	0.71	2.9%	86%
No particles	3/30/2007 10:40	3/31/2007 11:00	1.01	11%	78%
Air freshener	3/31/2007 11:30	4/1/2007 15:40	1.17	17%	64%
Candle (low)	4/1/2007 16:00	4/2/2007 11:00	0.79	20%	55%
Candle (two)+Bathmist	4/2/2007 11:30	4/3/2007 14:00	1.10	21%	10%
DJS UL West	4/22/2007 12:00	4/24/2007 12:00	2.00	10%	44%
DJS LL main	4/24/2007 12:00	4/25/2007 16:00	1.17	6%	91%
Xroom HEPA	7/16/2007 10:20	7/17/2007 10:00	0.99	5%	35%
HEPA+ion	7/17/2007 13:22	7/18/2007 13:00	0.98	4%	32%
Cooking	7/19/2007 8:00	7/19/2007 16:00	0.33	74%	7%
Smoking	7/23/2007 10:00	7/23/2007 16:10	0.26	87%	3%
Smoking	7/24/2007 7:00	7/24/2007 16:00	0.38	61%	3%
None/None	8/16/2007 8:00	8/17/2007 8:25	1.02	13%	33%
Candle	8/17/2007 9:48	8/17/2007 17:28	0.32	83%	6%
Propane	8/23/2007 8:00	8/23/2007 18:40	0.44	56%	9%

Measurement performed under the calm conditions showed reduced equilibrium factor and higher unattached fraction. In this case, equilibrium factor varied from 3% to 13% and the unattached fraction varied from 33% to 86%. When Air freshener was used the equilibrium factor was measured as 17% and the unattached fraction was 64%, for low level of candle burning, equilibrium and unattached fraction were 20% and 55%, respectively.

Using Candle (two) + Bathmist the values for equilibrium ratio and unattached fraction were 21% and 10% respectively. When measurements were performed in an actual, occupied home environment (DJS House Colleegeville MN a standard US home) the values obtained for equilibrium and unattached fractions were in the range of 6% - 10% and 44% - 91%, respectively.

When aerosol sinks were used, the equilibrium ratio and unattached fraction also changed because both of them depend on the particle concentrations. For HEPA filter, the values were 5% and 35% and for HEPA filter + ionizer, they were 4% and 32% respectively. During cooking of meal, these values were 74% and 7%. For normal conditions these values were 13% and 33%, respectively. For candle burning, conditions equilibrium ratio and unattached fraction values were 83% and 6% respectively. When propane was burnt during the measurement equilibrium ratio and unattached fraction values were 56% and 9% respectively.

7.9. Conclusions

A series of measurements were performed to study the feasibility of using the electret ion chamber for the measurement of deposited radon progenies. The results showed that electret ion chambers can be used for this purpose. Both short-term and long term electret were studied. It was observed that for high levels of radon concentration, or for long term measurement low sensitivity (L type) electret is suitable whilst for short term measurement, or low levels of radon progeny concentration measurement, high sensitivity short term electrets can be used. Radon concentration measured using electrets showed very stable behavior and radon concentration derived from different electrets of the same exposure gave nearly the same results. The results of the long-term (low sensitivity) electrets showed more fluctuations than those of short-term (high sensitivity) electrets for short-term measurements. However, their long term average had less fluctuation. Use of the E-RIPUSU for the measurement of equilibrium factor and unattached fraction show a wide range of variations depending on the indoor aerosols conditions. Under low aerosol conditions higher unattached fraction and lower value of the equilibrium factor was observed. The E-RIPUSU electrets are convenient instrument for measuring the equilibrium factor and unattached fraction.

Chapter Eight

Development of Passive Thoron Progeny Dosimeter

8.1. Introduction

Thoron (^{220}Rn) belongs to ^{232}Th decay series. Due to its short-half-life of 55.5 seconds it is not able to travel far. Thoron can be eliminated from the monitoring system by introducing filters or other delaying techniques. The health effect of thoron had been underestimated as compared to the radon (^{222}Rn) in the past because of the difficulties in the calibration and measurement of thoron dosimeters (Tokonami, 2005). No epidemiological studies of thoron have been done. However in the recent studies in which radon and thoron released from building materials were measured indicated dose due to thoron and its decay products may be greater than the dose delivered due to radon in the indoor environment (Tuccimei and Norcia, 2006). Research work by Yamada et al. (2006) and others (Michikuni et al., 1994; Quanfu et al., 2004; Tokonami et al., 2002) have shown that thoron plays a very important role in risk evaluation due to two reasons. First, some conventional radon monitors are sensitive to thoron (Masahiro et al., 2006) so radon concentration may be affected by the presence of thoron (Tokonami, 2003; Doi et al., 1994; Shang et al., 1997; Yuan et al., 2004). Studies have shown that thoron was present to a considerable extent in the indoor environment (Doi and Kobayashi et al., 1994; Ma et al., 1997; Tokonami et al., 2002). Radiation exposure due to the inhalation of thoron progeny has been estimated to be of the order of 10 - 20% as that compared with the short-lived radon progenies (Yamasakit et al., 1995; Guo et al., 1992).

Cave dwellings and areas having high ^{232}Th contents are suitable locations for studying indoor radon and thoron and the long-term health effects of radiation emitted by these isotopes. The longer-lived progenies, ^{212}Bi ($T_{1/2} = 60.6$ min) and ^{212}Po ($T_{1/2} = 10.6$ h) are never in equilibrium with the parent nuclide (Gargioni and Arnold, 2005).

Therefore thoron progenies cannot be estimated accurately from that of the gas itself using the equilibrium factor as in the case of radon. Therefore, direct measurement of the thoron progenies is preferable (Wiegand et al., 2000).

Significant correlation was found between the deposition rates, concentration of thoron progeny and the deposition velocity for attached radon progeny (Zhou and Iida, 2000). The ratios of the indoor Potential alpha energy concentration (PAEC) (^{220}Rn) to indoor PAEC (^{222}Rn) ranged from 0.09 to 0.58, with an overall average ratio of 0.32 (Martz et al., 1990). Two sources of indoor thoron are (1) building materials and outside air and (2) soil beneath the house (Yanxia et al., 1992). According to the Schery the origin of thoron in the atmosphere is almost entirely due to the diffusion from the top few centimeters of the soil where thoron is produced (Schery, 1990; Pearson and Spangler, 1991).

8.2. Effect of Deposition of Thoron

Dose delivered by radon/thoron depends not only on the radon/thoron gas concentration but also on the prevailing conditions in the indoor environment. Thoron concentration is mainly governed by the distance from the thoron source. The level of ventilation and the plating out of radon/ thoron daughters onto surfaces decides the extent of equilibrium between them (Ramola et al., 2003). Investigation has shown (Steinhäusler et al., 1975; Yarborough, 1980) relation between radon and thoron concentrations and meteorological parameters. Deposition onto surfaces acts to reduce the airborne concentration of radon/thoron and their decay products, thereby reducing the amount available for deposition in the respiratory tract (Knutson, 1992). The importance of deposition as a removal process in the indoor air has been studied by several groups and more decay product activity is found on the surfaces than that found in the air (Maniyan et al., 1999; Porstendörfer, 1979; Pagelkopf and Porstendörfer, 2003).

8.3. Measurement Techniques of Thoron and its Progenies

The choice of the measurement techniques depends on whether measurement of thoron or its progenies would be performed on short term (hours to days) or long term basis. For short term measurements, active techniques are preferred, whilst for long-term measurements, passive techniques are suitable. George has summarized detection

systems for thoron and its progenies: pulse ionization chambers, electrets ionization chambers, scintillation detectors with zinc sulfide ZnS (Ag), alpha particle spectrometers with silicon diodes, surface barrier or diffused junction detectors, registration of nuclear tracks in solid-state materials and gamma-ray spectrometry with NaI (Tl) scintillation crystals or germanium lithium (GeLi) detector (George, 1996). Long-term measurements of thoron concentrations can be carried out by radon and thoron discriminative measuring methods (Yonehara et al., 2005). A few of these techniques are briefly described below.

8.4. Thoron Measurement

8.4.1. ^{220}Rn Concentration using Lucas Cell

Thoron concentration may be measured using the Lucas cell. One minute counting immediately after sampling followed by another counting after a delay of 5 min for a duration of 10 min. The counts in the first counting period due to radon and its progeny are calculated from the known radon concentration and then subtracted from the total counts obtained in the first counting period. The remaining counts are due to thoron and its progeny and are used to calculate the radon concentration. The overall uncertainty of this method lies between 10% and 20% (Eappen et al., 2007).

8.4.2. Radon – Thoron Discriminative Monitors

Radon – thoron discriminative monitors, was developed by Yamada and coworkers. Similarly Doi and co-workers have developed a ^{222}Rn - ^{220}Rn discriminative passive dosimeter that can estimate both radon and thoron concentrations at the same time. Two solid-state nuclear track detectors are used in this discriminative dosimeter (Masahiro et al., 1994; Misdaq, 2002). Passive detector like CR-39 was used for the measurement of equilibrium equivalent concentration radon and thoron in which air was drawn through a filter and then CR-39 were exposed to filter after a sufficient time delay so that all the radon progeny decayed out. Thus sampling and measuring time are separated by a definite interval (Tokonami et al., 2002). Determination of ^{218}Po , ^{214}Bi , ^{214}Pb and ^{212}Pb were carried out by total alpha particle counting. A minimum of 5 h delay was employed for taking the final counts for ^{212}Pb .

8.4.3. Thoron and Radon Concentrations Measurement Through Scintillation Cells

Scintillation cell has been used for the measurement of thoron and radon concentrations

(Bigu et al., 1993). This technique is based on two measurements using the difference of the half-life between radon and thoron. Tokonami et al has developed a new technique for both radon and thoron concentration with a single scintillation cell. It is based on two measurements that use the difference in half life between radon and thoron (Tokonami et al., 2002; Hámori et al., 2006).

8.4.4. *Gamma rays Measurement*

Active sampling of thoron gas can be performed by using activated charcoal canisters, followed by measurement using the ^{212}Pb γ peak with a high purity germanium (HPGe) detector (Bigu , 1986). A peak 239 keV gammas from ^{212}Pb is usually used as it is very clearly identified in every spectrum, being one of the strongest natural lines. The nucleus ^{212}Pb decays by emitting β particle with a half-life of 10.64 h to ^{212}Bi , and 43.3% of the time gives off a γ -ray of energy 238.632 keV. There is also a weaker line at 300.1 keV (3.3%), which is also detected (Ernest Ho and. Measday,2005).

8.4.5. *Delayed Coincidence Technique for the Measurement of Thoron*

Delayed-coincidence and time-analysis (DC-TA) method is based on the use of the short decay half-life of 145 ms of ^{216}Po in order to distinguish between thoron – ^{216}Po pair counts and random coincidence pulses (i.e., chance coincidence). Generally Three time-windows in the DC-TA unit, whose opening durations are 150, 300 and 450 ms, are designed to start counting delayed pulses in each window from a trigger pulse (Iimoto et al., 2005).

8.4.6. *Beta Particles Counting Technique*

Thoron progeny concentration has been measured by using beta activity by conventional GM counters (Mohamed and El-Hussein,2005; Buzinny and Los, 2005). The counts of ^{216}Po are proportional to the local thoron activity concentration ^{216}Po due to its short half-life is always in equilibrium with the parents nuclide. ^{216}Po counts by means of a solid-state detector can be used easily to obtain thoron concentration profiles (Nikezic et al., 2006; Leonard, 2005; Wiegand et al., 2000). The total counting efficiencies for the progeny of radon and thoron using beta counting are 20% – 30% (Papp and Dezsó, 2006).

Thoron progenies Measurement

8.4.7. Wire Screen Method

The simple wire screen method provides a direct estimate of the unattached fraction from the screen count, or an indirect estimate from the difference between the reference and back-up filter counts (Khan et al., 1982). This technique can be used for active measurement of the thoron progenies concentrations (Cheng and Yeh, 1980).

8.4.8. Low-pressure Berner Cascade Impactor Technique

Attached and unattached activity size distributions of thoron and radon progeny can be collected using a low-pressure Berner cascade impactor technique. A single low-pressure impactor can cover a size range from approximately 30nm to micrometers (Mohamed and El-Hussein, 2005; Keskinen et al., 1999).

8.4.9. Diffusion Samplers

Diffusion Sampler is useful for measuring the unattached fractions of radon and thoron decay products (Kotrappa et al., 1975). To separate the contributions of radon and thoron two diffusion chambers one for recording the concentrations of radon while the other for recording the concentrations of ($^{222}\text{Rn} + ^{220}\text{Rn}$), so that the difference between the signals recorded by the SSNTDs inside the two diffusion chambers would give the thoron concentration.

8.4.10. High Efficiency Membrane or Glass Fiber Filters

Thoron progeny can be collected by high efficiency membrane or glass fiber filter paper using any convenient combination of volumetric flow rate ($2\text{--}10 \text{ l}\cdot\text{min}^{-1}$) and time (up to 60 min), followed by alpha counting of the filter after a delay of suitable time (5 h) or more after the end of sampling. By that time, ^{212}Pb (ThB), a beta emitter, is in transient equilibrium with its alpha-emitting daughters, enabling its air concentration at the time of sampling (Tokonami et al., 2004; Zhuo and Iida, 2000).

8.5. Aim or Purpose of This Study: From the above introduction about the different types of measuring instruments for the radon/thoron it is obvious that a number of instruments for the measurement of radon and thoron progenies are available using both active and passive techniques. However the instrument used for the measurement of

thoron progeny using passive surface deposition technique are very few. In most cases during the measurement of radon thoron is ignored which produces an error in the radon concentration. In this study efforts have been made to develop an instrument for measurement of thoron progeny working on the principle of surface deposition. Studies have also been conducted about the surface deposition of radon/thoron progenies and air borne radon/thoron progeny concentration was also studied. It is easier to measure surface deposition and make relation for absorbed dose due to thoron in the air. Further details of development of passive thoron progeny dosimeter are given below.

8.6. Materials and Methods

8.6.1. Theory of Measurement of Radon Progeny Dosimeter using Solid State Nuclear Track Detector

A variety of solid state nuclear track detectors are available, having different efficiencies for α - particle emitted from radon, thoron and its progenies (McLaughlin et al., 1992).

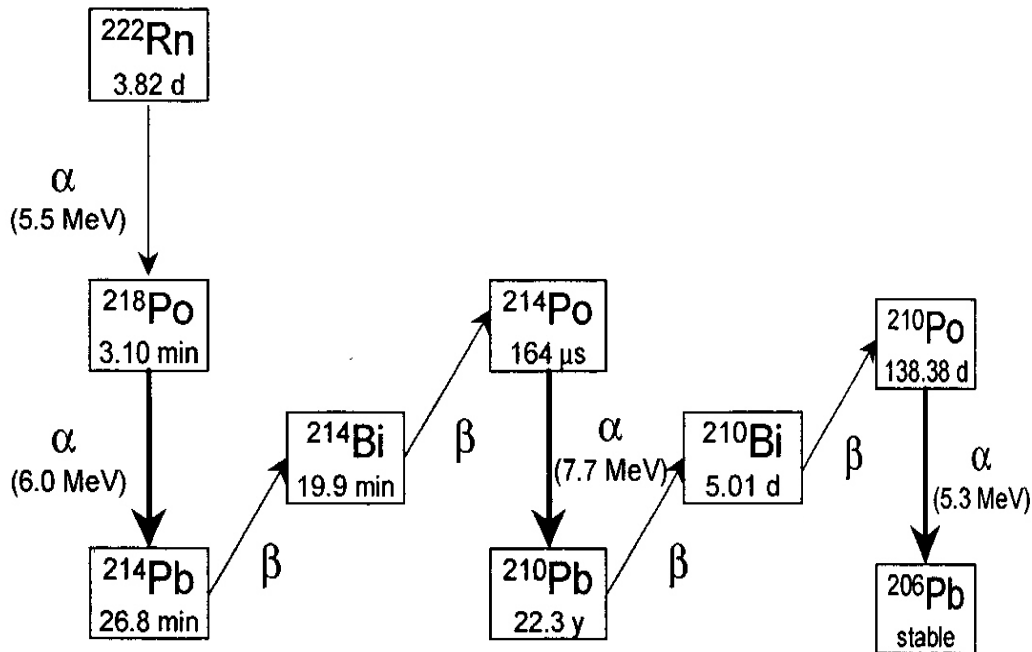


Figure 8.1: Radon decay chain

Widely used detectors in this regard are LR-115 and CR-39. LR-115 has sensitivity for a limited range of alpha energies, while CR-39 has capability to detect a wide range of α energies. Radon, thoron and their progenies are usually present in the indoor environment in the mixed form. Therefore measurement of thoron or its progenies in the mixed

environment causes difficulties. Thoron progenies have alpha energies in the range from 5.4 MeV to 8.8 MeV.

Isotope	Half Life	Types of Radiation
$^{220}_{86}\text{Rn}$ (Thoron gas)	55 s	α (6.29 MeV)
$^{216}_{84}\text{Po}$ (Polonium)	0.15 s	α (6.78 MeV)
$^{212}_{82}\text{Pb}$ (Lead)	10.64 hrs	β, γ (0.35, 0.58 MeV)
$^{212}_{83}\text{Bi}$ (Bismuth)	60.6 min	α, β, γ (5.4-6.1, 0.08-2.26 MeV)
$^{212}_{84}\text{Po}$ (Polonium)	0.34×10^{-6} s	α (8.8 MeV)
$^{208}_{85}\text{Tl}$ (Thallium)	3.05 min	β, γ (1.25-2.37 MeV)
$^{208}_{82}\text{Pb}$ (Lead)	Stable	

Figure 8.2: Thoron decay chain

This wide range of alpha energies is both help and a problem for its measurement. To measure only thoron progeny (i.e., ^{212}Po) and block the remaining radon and thoron progenies using solid state nuclear track detector, absorbing filters are placed in front of the CR-39 detector. This filter functions as an energy absorber which absorbs alpha particles energy emitted from the radon progenies to very low (zero) efficiency region, and reduces thoron energy (^{212}Po) to a range which are still detected by CR-39. Using this technique, suitable filters were identified to detect only thoron progeny (^{212}Po) and attenuate the radon progenies. CR-39 detects wide range of energies, however the efficiency of the CR-39 is not uniform for the whole energy range; and it is maximum for alpha particles having 3-6 MeV energy. So selection of such filter had double advantage in this case, first it blocked the detection of unwanted radon and thoron progenies and secondly it also reduced the energy of the desired progeny (^{212}Po) to such a range for which CR-39 had relatively higher detection efficiency. It may be mentioned here to block all the radon progenies is easier, except ^{214}Po which is a difficult task because its energy difference from the α from ^{212}Po .

8.6.2. Determination of Efficiency of Different Plastics/Filter as Energy Absorber

Filtration of radon progenies energies also attenuates the energy of the desired progeny (^{212}Po), thus a tradeoff was required between the loss of efficiency of CR-39 and the

noise created by the unwanted radon /thoron progenies for the detection of alpha particle emitted by them. To select a suitable energy filter for the detection of ^{212}Po , different types of plastics/ materials were studied for their ability to absorb some fraction of α -energy of the radon / thoron progenies. These materials were studied for their ability to absorb ^{214}Po and attenuate ^{212}Po to a desirable efficiency range.

To measure the efficiency/ability of these plastic materials ^{218}Po , ^{212}Po and ^{214}Po sources were used (these sources were constructed in the Shaffer Environmental Radiation Laboratory St. John's University USA using Uranium Jars and Thorium Oxide gas mantles). Large area semiconductor diode detectors (SDD), analyzed with a computer-based alpha spectroscopy system (APTEC), were used for these measurements. The filter material was placed between the SDD and the ^{212}Po or ^{214}Po source. The materials that were selected had different thicknesses and had a wide range of absorbing ability. The materials tested as filtering/absorbing materials are shown in table 8.1.

Before measuring the efficiency of different plastics the APTEC system was calibrated. To calibrate the APTEC (Surface barrier detector) standard sources of ^{230}Th and ^{241}Am were used. The efficiency of the detector as calculated by using ^{230}Th and ^{241}Am with no distance ($\sim 1\text{mm}$) between source and detector was 0.26. Using the flat source taking distance of 4 mm between the detector and the source the efficiency of the detector was measured as 0.19. To establish the energy calibration, ^{214}Po and ^{212}Po sources were placed under the SDD and the counts were collected for sufficient time to have a peak for the ^{214}Po and ^{212}Po . Selected plastics/materials were used to measure their efficiency for ^{218}Po , ^{214}Po and ^{212}Po . Using these materials the residual energies of α particles emitted from ^{212}Po and ^{214}Po were measured. The results of different type plastics and other materials are shown in table 8.1 which shows that efficiency of these materials ranges from 0.01 to a maximum of 0.29.

Table 8.1: Efficiency of different materials for the detection of ^{218}Po ^{214}Po and ^{212}Po .

S.No.	Filter	Gauge	^{218}Po	^{214}Po	^{212}Po
1.	Mylar	8	0.25	0.16	0.04
2.	MM	16	0.18	0.08	0.04
3.	3M2708+M	58.00	-	-	-
4.	CI75	75.00	0.19	0.22	-
5.	CI92	92.00	0.16	0.28	-
6.	CI75+2708	125.00	0.09	0.28	-
7.	3M125	145.00	0.07	0.21	-
8.	FFMM	200	0.00	0.02	0.08
9.	FFM	200	0.01	0.04	0.15
10.	FFM_07	200	-	-	0.15
11.	3M114	200.00	0.00	0.16	0.07
12.	3M146_07	285.00	-	-	0.06
13.	3MM	250.00	-	-	0.03

8.7. Technical specifications and Construction Procedure of Surface Deposition Detectors

Analyzing the data in table 8.1 suitable filtering materials for the detection of radon and thoron were selected based on the principle of surface deposition detectors. A few Surface deposition detectors were constructed using (Glass Slide Mounts device Gepe) Gepe 35 mm slide mounts. CR-39 was used as track registration chip and was held in Gepe35 mm slide mounts with an 18 mm × 24 mm opening.

Construction steps: Two sets of the progeny surface deposition detectors were manufactured. One set was used for the monitoring of radon progenies, while the other was constructed for the monitoring of the thoron progeny.

The glass side (side which is used to fix the deposition detector with a glass or any other smooth surface) could also be used for the measurement of ^{210}Po which consist of two portions, one portion consist of only Mylar layer and that “uncovered area” is more sensitive to natural contaminants in glass and the bottom is covered with a 12 mm wide strip of 3M2708 + Mylar that defines the ^{210}Po sensitive area.

The room side area (side which is exposed to the surface deposition) which is ^{214}Po sensitive is covered by 3M114 films; when developed these pits appear larger. ^{218}Po and ^{214}Po sensitive area are covered by CI-192 film. The track density will be higher in this region as the efficacy of CI-92 is high. The two regions are separated by scratched dashed line on the CR-39 chip. Metallized Mylar is used over the central opening of the Gepe using 3M 2175C double sticky mounting tape. On the inside of the holder, a 2 mm wide strip of 3M 2175C above and below the central opening was used. This is used for sticking it to the glass surface.

Room side of the thoron progeny detector (Which detects surface deposition of ^{212}Po) consists of the following parts. For the room side/side exposed to the newly deposited radon progenies, a 10 mm \times 25 mm strip of 3M 146_07 films was used to the bottom of the slide opening so that the film extends 1 mm onto edge opening. A 10 mm \times 25 mm strip of CI-192 to the top of the slide opening so that the films meet but do not overlap at the centre of the opening. Covered both films with a 26 mm \times 26 mm strip of Metallized Mylar over the central opening using the 3M 2175C tape to hold it in place. Metallized Mylar was used to remove the effects of light on the selected plastic.

The glass side of both radon and thoron progeny is same. For the construction of the thoron progeny detector room side, 10 mm \times 25mm long strip of tape FF to the bottom of the slide opening so that the tape extends 1 mm onto edge of opening. The sticky side of the tape should be away from the holder. Attached a 10 mm \times 25mm long strip of film 3M146_7 to the top of the slide opening so that the films meet but do not overlap at the centre of the opening. Covered the film with 26mm \times 26 mm strip of Metallized Mylar over the central opening using the 3M 2175C and a special Mylar coated plastic adhesive tape (FFM) to hold it in place. A light coat of antistatic fluid is sprayed to offset the electrostatic charge on the chip.

8.8. Initial Testing of the New Surface Deposition Dosimeters

To test these newly assembled/developed surface deposition radon and thoron dosimeters for its ability to register tracks in the indoor environment, a small chamber containing high concentrations of radon was constructed. The small thoron chamber having dimensions of 58 cm \times 30 cm \times 27 cm and surface to volume ratio of 18. These

surface deposition detectors were exposed in it, in order to know the track density in each region. Two different sets of surface deposition detectors were made. In one set only thick plastic material was used and in the other sets two regions were made one of 3M146_7 region and the other part was made with CI-92 materials and were exposed to thoron and its progenies in the newly constructed small sized thoron chamber. Surface deposition detector was exposed to thoron and its progenies for 7 days in this chamber. During the exposure the thoron concentration in the chamber was measured using the Rad 7 active detector (DurrIDGE Co, USA). Exposed surface deposition detectors in the test chamber were removed after the specified exposure time and its surface deposited activity of ^{212}Po was measured using the APTEC system. The results obtained are shown in table 8.2. CR-39 detectors were removed from these deposition chambers and were etched in 6M NaOH solution for 6 hours at 75C° and were counted under using an optical microscope. Experiment for studying the tracks of ^{212}Po in the thick region of the dosimeter (3M146) was repeated. The sensitivity of different regions of these surface deposition detectors are shown in the table 8.3 below for run-1.

Table 8.2: Surface deposited ^{212}Po activity in different chambers.

Experiment	Counts.s ⁻¹	Observed Surface Density	Efficiency of the detector	Actual Surface Density (Bq.mm ⁻²)
Small Chamber Run 1	2.70E-01	1.59E-04	1.81E-01	8.75E+02
Small Chamber Run 2	2.30E-01	1.35E-04	1.81E-01	7.48E+02
Medium Chamber	1.64E-01	9.62E-05	1.81E-01	5.31E+02
Exposure room	5.80E-03	3.41E-06	1.81E-01	1.88E+01

The results of the exposure in the small chamber were good as there were enough track density on the thick filter portion of the detector. As may be seen in this table, average surface deposited activity in small chamber is very high as the thoron concentrations in the chamber were high. The corresponding track densities using CR-39 detectors were high.

Table 8.3: Track density in different regions of the surface deposition detector in the small thoron chamber (Run-1).

S.No	Filter Materials	Average Tracks/FoV	Tracks.mm ⁻²	Tracks.m ⁻² .s ⁻¹
1	3M146-1	3.8	10.6	31
2	3M146-2	3.9	10.9	32
3	3M146-3	3.9	11.2	32
4	3M146-4	2.9	8.3	24
Average	3M146 Average	3.6	10.3	30
1	CI-92-1	16.2	46.0	130
2	CI-92-2	16.8	47.6	140
3	CI-92-3	14.1	40.1	120
4	CI-92-4	15.8	44.7	130
Average	CI-192 Average	15.7	44.6	140
1	3M146-1	3.5	10.0	29
2	3M146-2	3.6	10.1	29
3	3M146-3	3.4	9.7	28
4	3M146-4	3.5	10.0	29
Average	3M146 Average	3.5	9.9	31

The average activity in run 1 and run 2 (table 8.1) has the same trend as it was observed for the corresponding track density observed in the exposed CR-39 detector track density (table 8.3 and 8.5). Radon and thoron concentration during these experiments in the small chamber are shown in table 8.4 and 8.6. After analysis of the data in the primary small chamber a new medium chamber with dimensions of 130 cm × 60 cm × 63 cm having Thorium Oxide mantles inside it for the production of thoron and its progenies. A small air circulation fan was also placed inside the chamber to circulate the air in the chamber. Surface deposition detectors were exposed inside the chamber for seven days and radon and thoron concentrations were measured during that period which are shown in table 8.7.

Table 8.4: Radon and thoron concentration in the small chamber (Experiment Run-1).

Run	Date	Radon	Thoron	Run	Date	Radon	Thoron
1	19-4-2007	369±154	14689±1106	16	20-4-2007	304±231	16317±1169
2	19-4-2007	279±152	17316±1210	17	20-4-2007	392±252	17168±1214
3	19-4-2007	269±156	17797±1228	18	20-4-2007	341±250	16835±1199
4	19-4-2007	433±198	14763±1114	19	20-4-2008	226±246	17168±1199
5	19-4-2007	270±185	16206±141	20	21-4-2007	492±276	18056±1243
6	19-4-2007	400±214	16650±1184	21	21-4-2007	381±276	18611±1262
7	19-4-2007	559±242	15873±1147	22	21-4-2007	279±364	20017±1291
8	19-4-2007	370±244	16650±1195	23	22-4-2007	278±555	21756±1362
9	19-4-2007	440±251	17538±1225	24	22-4-2007	276±374	20572±1325
10	20-4-2007	500±278	15873±1154	25	22-4-2007	231±275	19425±1273
11	20-4-2007	681±290	16354±1184	26	22-4-2007	259±522	20942±1336
12	20-4-2007	440±283	17057±1210	27	22-4-2007	270±514	22163±1373
13	20-4-2007	481±215	15873±1154	28	22-4-2007	275±555	20831±1321
14	20-4-2007	411±212	16946±1203	29	22-4-2007	280±485	20128±1310
15	20-4-2007	270±211	16798±1199	30	22-4-2008	293±514	23162±1402
Average						358±299	18167±1184

After exposure these CR-39 detectors were removed and etched and its track densities were measured. The results are shown in table 8.8. As expected track density of different filtering materials was different according to their efficiencies. It is clear that 3M146 has average track density lower than the region where CI-92 is used as masking/filtering material for the CR-39. However the track density in each region was enough to be read conveniently. Measured radon and thoron concentrations show a consistent trend of high thoron concentration.

In the second experiment in medium chamber surface deposition detectors were exposed to thoron gave a similar trend as was in run-1 and 2 in the small exposure chamber. Exposing surface deposition dosimeter to high thoron concentrations for a week time produced a suitable number of tracks in CR-39 detector in the thick region (3M146).

Table 8.5: Track density in different regions of the surface deposition detector in the small thoron Chamber Run 2.

Surface Deposition detector	Filter	Average Tracks/FoV	Tracks.mm ⁻²	Tracks.m ⁻² .s ⁻¹
1	3M146_1	3.2	9.0	35
2	3M146_2	3.2	9.1	35
3	3M146_3	3.3	9.3	36
4	3M146_4	3.5	9.9	38
3M146 Average		3.3	9.3	36
1	CI-92-1	8.3	23.6	91
2	CI-92-2	16.0	45.5	175
3	CI-92-3	8.9	25.1	97
4	CI-92-4	10.2	28.9	111
CI-92 Average		10.8	30.7	120
1	3M146_1	3.7	10.5	40
2	3M146_2	4.3	12.0	47
3	3M146_3	3.9	11.1	43
3M146 Average		4.0	11.2	32

The results of the surface deposition detector in the medium exposure chamber show that different region of the detectors have different response to the surface deposition detector. Mainly there are two regions i.e. low sensitivity region of 3M146 masking material and high sensitivity region of CI-92 and 3M114. During these measurement radon and thoron concentration were measured and are shown in table 8.7.

After testing these surface deposition detectors in the small and medium chambers for the ability to register track on the CR-39, these deposition dosimeters were exposed in the exposure room which is a standard room with the dimensions 255 cm × 300 cm × 365 cm. Thorium oxide gas mantle were placed in four different locations for the production of thoron and its progenies and Natural Uranium Jars for the production of radon . These surface deposition detectors were exposed for 15 days. During this experiment thoron concentration was in the range of 3-10 pCi ℓ⁻¹ (100 – 3700 Bq.m⁻³).

Table 8.6: Radon and thoron concentration in the small chamber (Run-2).

Date	Thoron	Radon
23/4/2007	20128±1295	551±254
	20720±1332	422±248
	21571±1369	444±255
24/4/2007	20276±1295	322±174
	20683±1332	218±170
	21386±1332	366±189
25/4/2007	17538±1221	400±167
	18167±1221	407±174
	17834±1221	429±194
26/4/2007	16317±1184	292±161
	18167±1258	407±176
	18611±1258	251±175
27/4/2007	16761±1184	274±149
	18796±1258	281±163
	18500±1258	370±174
Average	19030±1268	362±188

During the exposure Rad 7 active detector was used to measure the radon and thoron concentration in the exposure room and the results obtained are shown in table 8.9. The results (table 8.10) showed that the thick region of the dosimeter has sufficient sensitivity for the determination of thoron progeny in the indoor environment if the detectors were exposed to the thoron progenies for a sufficiently long time.

Analyzing these initial results of the surface deposition detector in the small and medium chambers in the exposure room, in the next step more surface deposition detectors were assembled for the exposure in the real indoor environment in USA and Pakistan. Deposition pattern of the radon and thoron progenies depend on the ultrafine particles in the atmosphere. Therefore, a series of experiments were performed to study the airborne radon/thoron progenies under different aerosols conditions.

Table 8.7: Radon and thoron concentration in the medium sized thoron chamber.

S.No	Run ID	Date	Radon	Thoron
1.	6101	7/5/2007	68±74	3922±588
2.	6102	7/5/2007	69±79	3534±574
3.	6103	7/5/2007	99±85	3356±555
4.	6201	8/5/2007	174±103	6401±740
5.	6202	8/5/2007	138±101	6142±733
6.	6203	8/5/2007	187±118	5439±692
7.	6301	8/5/2007	107±121	4921±655
8.	6302	8/5/2007	149±138	4884±662
9.	6303	8/5/2007	159±138	4884±662
10.	6401	9/5/2007	175±128	5069±666
11.	6402	9/5/2007	80±119	4736±651
12.	6403	9/5/2007	199±131	4514±636
13.	6601	10/5/2007	146±111	6882±770
14.	6602	10/5/2007	309±143	7363±807
15.	6603	10/5/2007	139±118	7363±807
16.	6801	11/5/2007	97±99	6290±740
17.	6802	11/5/2007	79±106	7178±792
18.	6803	11/5/2007	118±114	6808±770
19.	7001	12/5/2007	29±90	4995±662
20.	7002	12/5/2007	110±104	5883±722
21.	7003	12/5/2007	139±120	5439±699
22.	7201	13/5/2007	107±97	3848±585
23.	7202	13/5/2007	209±121	4699±651
24.	7203	13/5/2007	129±109	4773±655
25.	7401	14/5/2007	156±107	5735±707
26.	7402	14/5/2007	189±123	5254±685
27.	7403	14/5/2007	129±127	5143±681
Average			137±112	5387±687

8.9. Measurement of Particle Concentration

Dose due to $^{222}\text{Rn}/^{220}\text{Rn}$ airborne progenies not only depends on Radon/ ^{220}Rn concentration but also depends on the attachment of the progenies to aerosols. Ultrafine particles contribute little to the total mass but are present in a very high number concentration. Particles of this size can almost unrestrictedly enter into the lungs and results in a greater inflammatory potential (Martell, 1983).

Table 8.8: Track density in different regions of the surface deposition detector in the medium size thoron chamber.

Surface Deposition detector	Filter	Average Tracks/FoV	Tracks.mm ⁻²	Tracks.m ⁻² .s ⁻¹
1.	3M146-1	4.3	12.3	20
2.	3M146-2	5.0	14.1	23
3.	3M146-3	4.6	12.9	21
	Average	4.6	13.1	22
1.	CI-192-1	10.1	28.7	48
2.	CI-192-2	8.9	25.3	42
3.	CI-192 -3	10.4	29.5	49
	Average	9.8	27.9	46
1.	3M146-1	5.2	14.8	24
2.	3M146-2	5.7	16.1	27
3.	3M146-3	5.2	14.8	24
	Average	5.4	15.2	25
1.	3M114-1	38.4	108.8	180
2.	3M114-2	24.6	69.8	115
3.	3M114-3	26.1	73.9	122
	Average	29.7	84.2	139
1.	CI-192-1	15.0	42.5	70
2.	CI-192-2	16.7	47.3	78
3.	CI-192 -3	15.7	44.5	74
	Average	15.8	44.8	74

In order to measure these affect in indoor environment ultrafine particles were measured on an hourly basis using the CPC P-track system. Ultrafine particle counter uses the condensation particle counting (CPC) technique (TSI MN, USA).

Table 8.9: Radon and thoron concentration in the exposure room during the exposure of the Surface Deposition Detectors in the room (15 days).

S.No	Radon	Thoron	S.No	Radon	Thoron
1.	19±135	58±148	1.	48±97	67±133
2.	0±197	48±170	2.	0±118	54±144
3.	10±158	54±158	3.	50±178	68±164
4.	0±289	47±193	4.	19±138	53±151
5.	0±158	54±158	5.	30±118	60±144
6.	30±158	60±158	6.	10±118	48±144
7.	0±77	39±125	7.	0±135	53±148
8.	20±40	54±108	8.	0±158	40±158
9.	40±79	64±128	9.	10±0	48±48
10.	39±38	63±105	10.	0±77	39±125
11.	40±40	64±108	11.	10±138	48±151
12.	10±79	48±128	12.	0±98	40±136
13.	10±193	47±167	13.	0±77	39±125
14.	40±396	64±220	14.	0±197	40±170
15.	20±197	54±170	15.	0±138	40±151
16.	0±58	39±116	16.	0±174	8±161
17.	20±316	68±202	17.	0±98	40±136
18.	0±197	54±170	18.	20±79	54±128
19.	0±295	148±477	19.	145±19	97±93
20.	10±140	48±153	20.	218±118	115±144
21.	10±98	47±135	21.	239±59	119±118
22.	39±174	63±161	22.	19±97	58±133
23.	30±59	60±118	23.	0±158	40±158
24.	69±138	76±151	24.	10±138	48±151
25.	10±77	47±125	25.	0±77	47±125
26.	10±178	48±164	26.	10±178	48±164
27.	10±178	48±164	27.	20±79	54±128
28.	10±135	47±148	28.	825±38	199±105
29.	10±178	54±164	29.	607±59	176±118
30.	20±138	54±151	30.	544±59	168±118
31.	10±97	47±133	31.	48±116	67±141
32.	40±59	64±118	32.	50±98	68±136
33.	30±98	60±136	33.	40±79	64±128
34.	19±97	53±133	34.	136±193	97±167
35.	20±59	54±118	35.	109±414	88±224
36.	20±98	54±136	36.	129±79	94±128
37.	29±116	58±141	37.	729±97	189±133
38.	20±316	54±202	38.	1110±296	232±198
39.	10±414	54±224	39.	327±97	137±128
40.	19±97	53±133	Average	80±136	67±149

Table 8.10: Track density in different regions of the surface deposition detector in the exposure room.

Filter	Average /FoV	Tracks.mm ⁻²	Tracks.m ⁻² .s ⁻¹
3M146-1	1.2	3.4	6
3M146-2	1.5	4.2	7
3M146-3	1.7	4.7	8
Average 3M146	1.5	4.1	7
3M114-1	2.1	6.1	10
3M114-2	2.2	6.3	10
3M114-3	2.1	5.9	10
Average 3M114	2.2	6.1	10
3M146-1	1.8	5.1	8
3M146-2	1.4	4.0	7
3M146-3	1.6	4.6	8
Average 3M146	1.6	4.6	8
FFM-1	5.8	16.4	27
FFM-2	2.6	7.3	12
FFM-2	4.2	12.0	20
Average FFM	4.2	11.9	20
CI-92-1	6.6	18.8	31
CI-92-2	7.3	20.7	34
CI-92-3	6.4	18.1	30
Average CI-92	6.8	19.2	32

The following different aerosol generating activities were performed in the indoor environment.

- High Efficiency Particle Air (HEPA) filter: To remove the fine and ultrafine particle form the indoor environment
- HEPA filter with ionizer: the ionizer generates negative ions and thus the attachment rate may be increased. This phenomenon reduces the particles concentration to very low level.

- Candle burning for a specified period of time
- Propane cooker: propane cooker was used for a specific period of time.
- Cigarette smoking: The Joe smoker system was used to produce smoke in the exposure room for a specified period of time

Particle concentrations show a long range of variation depending on the aerosol generating source/sink usage in the room. The particles concentrations are reduced to very low number when the indoor environment has HEPA filter working along with ionizer. In some cases the particles concentrations are reduced to such an extent that the general empirical relation defined/derived by Porstendoerfer et al., $f_p = 150 / Z (cm^3)$ was not valid and the particles concentrations reduced to less than 100 per cm^3 (Porstendörfer, 2001, 1996 & 1994; Porstendörfer and Reineking, 1999). Using the HEPA filter only the particles concentrations is in the range of 100-300 (cm^3). Thus unattached fraction of thoron /radon is high and is in the range of 60 - 90%. When aerosol generating activity is taking place in the indoor environment the particles concentration increases to very high number. Consequently the unattached fraction is reduced. The unattached fraction ranges from 0.0001- 0.2. The particle concentrations can be divided mainly into two categories. (1) low levels $\log Z \sim 2 - 3$ and (2) high levels $\log Z \sim 4 - 5$. The low levels occurs when there is no aerosol generating activity is taking place in the indoor environment or the aerosol sink like HEPA filter or HEPA filter ionizer is operating in the indoor environment. High aerosols conditions occur during the operation of a fan or some cooking or smoking activity taking place. Candle burning or cigarette smoking produces very high levels of ultrafine particles. Indoor particle concentrations increase from 10^3 to 10^5 per cm^3 , the-attached fraction of airborne radon decay products increases progressively and the deposition on the surfaces decreases. A single burning cigarette in a closed room gives rise to particle concentrations of 10^3 to 10^5 per cm^3 , because of rapid coagulation; most of the radon decay products are associated with large particles of low mobility. In the smoke-filled rooms, airborne radon progeny approach equilibrium with radon limited only by ventilation rate and particle sedimentation (detailed description of the measurements is given in the later section).

As may be seen in table 8.11 that ultrafine particle concentration is very high during the cooking and burning activities in the indoor environment and the corresponding equilibrium factor and unattached fraction have been varied accordingly. Unattached fraction calculated using filter and mesh and the empirical relation that $f_p = 150/Z(\text{cm}^{-3})$ are in good agreement. However, unattached fraction calculated using filter is relatively lower as compared to that derived by using the empirical relation. In normal conditions when no activity is taking place in the indoor environment ultrafine particles reduces to low concentration levels.

8.10. Surface deposition Rates of Radon and Thoron

In order to measure surface deposition of radon /thoron progenies in the indoor environment, smooth surfaces were exposed to a steady radon /thoron levels and different types of aerosol producing environment for several hours, during which the activities of the short-lived radon progenies /thoron progenies reached equilibrium with its parents.

A protocol was required for determining these equilibrium activities for all four short-lived progenies on a glass surface in the case of radon and ^{212}Pb , ^{212}Bi - ^{212}Po in the case of thoron. As ^{214}Pb and ^{214}Bi and ^{212}Pb are beta emitters, a model for extrapolating their activities was constructed. Since the lifetime of ^{214}Po is very short (half-life = 0.164 μs), it is always in equilibrium with the longer-lived parent ^{214}Bi (half-life = 19.7 min).

A spreadsheet was used to accept as input the raw data from the specified detectors, perform the necessary corrections and output the initial activities (equilibrium values) of ^{218}Po , ^{214}Pb , and ^{214}Bi - ^{214}Po in the case of radon progenies. After experimental consideration, the protocol developed by Dumm (Dumm, 2005) was used. This protocol contains a practical set of counting intervals that minimize uncertainty. In the case of thoron, the element of interest was ^{212}Pb which has a large half life of 10.6 hrs for which a protocol was developed to collect the count for one hour as after 10 min there were few counts.

A calibrated computerized APTEC alpha-spectroscopic multi-channel analyzer and Science Applications International Corporation (SAIC) ® Alpha Analyzers of model AP-2 were used for these measurements

Table 8.11: Ultrafine particles concentration equilibrium factor and unattached fraction of radon and thoron progenies.

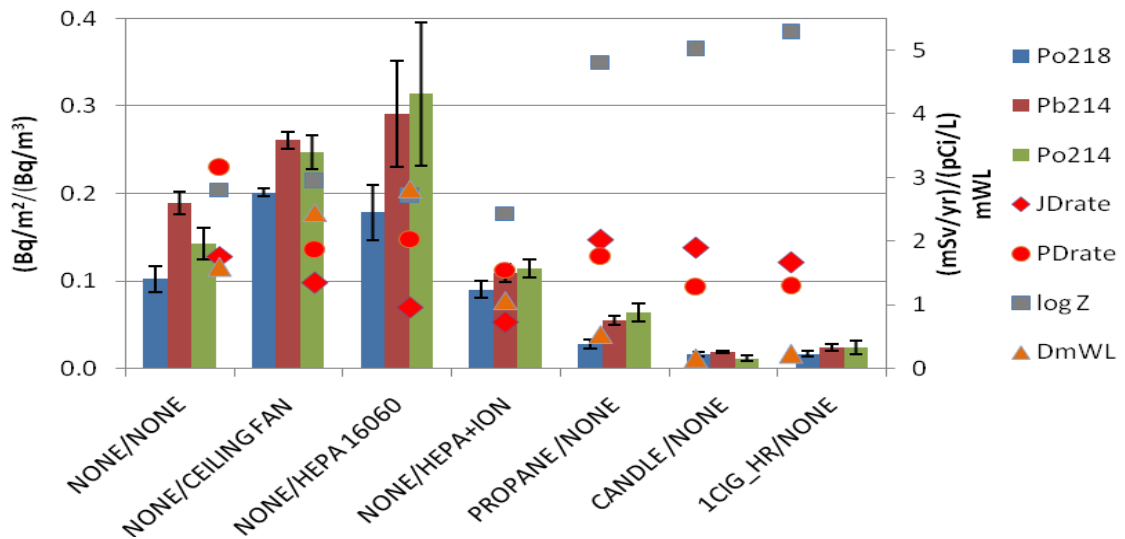
Aerosol Type	F ²²² Rn(Filter)	F ²²⁰ Rn(Filter)	F ²²² Rn Mesh	F ²²⁰ Rn Mesh	fp ²²² Rn	fp ²²² Rn	Z.cm ⁻³	Unattached by P-Track
propane cook+Candle	-0.77±0.97	0.20±0.06	0.21±0.32	0.003±0.002	-0.365	0.015	116416	0.001288
propane cook+Candle	-0.12±0.25	0.46±0.15	-0.09±-0.09	0.009±0.004	0.407	0.019	179571	0.000835
propane cook+Candle	1.84±0.67	0.11±0.04	0.26±0.23	0.002±0.002	0.125	0.015	164428	0.000912
propane cook+Candle	0.26±0.2	0.51±0.16	-0.06±-0.07	0.008±0.004	-0.272	0.015	86550	0.001733
prop ck+1Cig+Can	0.52±0.28	0.12±0.04	-0.07±-0.1	0.003±0.002	-0.163	0.024	191608	0.000783
Candle Filter	0.8±1	0.28±0.09	0.02±0.3	0.001±0.002	0.025	0.003	187933	0.001248
Candle+1Cig	1.94±0.54	0.15±0.05	-0.01±-0.13	0.002±0.002	-0.007	0.016	120233	0.000798
propane cook	0.17±0.14	0.10±0.03	-0.01±-0.05	0.001±0.001	-0.092	0.011	166275	0.000902
propane cook	0.94±0.34	0.15±0.05	0.07±0.11	0.002±0.002	0.073	0.015	104341	0.001438
propane cook+Candle	0.59±0.23	0.15±0.05	-0.01±-0.08	0.004±0.002	-0.009	0.025	110966	0.001352
propane cook	-0.26±-0.26	0.16±0.05	-0.12±-0.07	0.001±0.001	0.312	0.007	5545	0.027051
propane cook	-0.36±-0.22	0.11±0.04	-0.08±-0.07	0.001±0.001	0.185	0.010	61035	0.002458
propane cook	0.94±0.44	0.52±0.16	0±0.13	0.007±0.003	0.005	0.013	67315	0.002228
candle only	0.13±0.31	0.10±0.03	-0.03±-0.13	0.004±0.002	-0.335	0.037	88134	0.001702
propane cook	-0.43±-0.21	0.45±0.14	0.13±0.07	0.001±0.002	-0.441	0.003	188758	0.000795
propane cook+candle	-0.04±-0.17	0.11±0.03	0.03±0.07	0.003±0.002	-5.817	0.030	150950	0.000994
propane cook	0.65±0.22	0.14±0.04	0.04±0.06	0.002±0.002	0.054	0.015	158233	0.000948
propane cook	0.76±0.22	0.09±0.03	0.01±0.05	0.00044.00044	0.014	0.005	169583	0.000885
propane cook	-0.13±-0.09	0.01±0.00	-0.06±-0.03	0.00013±.0001	0.312	0.012	195733	0.000766
propane cook	0.16±0.36	0.13±0.04	0.05±0.14	0.004±0.002	0.231	0.027	143441	0.001046
propane cook	-0.83±-0.28	0.35±0.11	-0.06±-0.08	0.007±0.004	0.068	0.019	72483	0.002069
propane Lighter	0.94±0.26	0.21±0.07	0.01±0.08	0.009±0.004	0.009	0.042	101326	0.00148
propane cook	-1.41±-0.58	0.48±0.15	-0.09±-0.19	0.005±0.004	0.062	0.011	118000	0.001271
propane cook	0.88±1.56	0.07±0.02	-0.44±-0.72	0.004±0.002	-0.038	0.055	43017	0.003487
propane cook	-1.1±-0.61	0.34±0.11	-0.02±-0.22	0.01±0.004	-0.002	0.027	34106	0.004398
propane Lighter	-8.02±-2.21	0.19±0.06	-0.25±-0.67	0.008±0.005	0.030	0.041	65304	0.002297
propane Lighter	-0.03±-0.18	0.45±0.14	-0.01±-0.08	0.011±0.005	0.281	0.025	147233	0.001019
propane cook	0.81±0.6	0.22±0.07	-0.07±-0.25	0.008±0.004	-0.090	0.037	33924	0.004422
propane cook	0.04±0.26	0.15±0.05	-0.01±-0.11	0.006±0.003	-0.273	0.038	101222	0.001482
Candle	0.24±0.18	0.17±0.05	0±0.08	0.005±0.004	0.017	0.032	117425	0.001277
Candle	-0.17±-0.47	0.20±0.06	0.24±0.2	0.006±0.003	3.420	0.030	70055	0.002141
none	0.4±0.21	0.11±0.03	0.07±0.12	0.014±0.005	0.156	0.119	581	0.258176
none	0.06±0.28	0.16±0.05	-0.11±-0.15	0.015±0.006	2.114	0.084	681	0.220264
none	-0.46±-0.32	0.09±0.03	0.02±0.21	0.02±0.007	-0.048	0.180	926	0.161987
none	0.5±0.41	0.06±0.02	0.18±0.25	0.015±0.005	0.271	0.189	819	0.18315
propane cook	-0.12±-0.35	0.06±0.02	-0.48±-0.26	0.013±0.005	0.799	0.180	477	0.314465
none	0.56±0.26	0.04±0.01	0.56±0.21	0.01±0.004	0.501	0.200	1876	0.079957
Candle	-0.16±-0.73	0.10±0.03	-0.15±0.49	0.014±0.006	0.488	0.127	9900	0.015152

Summarized results for radon are shown in Figure 8.3. It is clear from this Figure that surface deposited activity depends on the aerosols conditions in the indoor air. For similar indoor radon concentrations but different aerosols conditions, the surface deposited

activities showed large variations. (see appendix A, B, C and D). Using the calibration information ^{218}Po , ^{214}Pb , and ^{214}Bi - ^{214}Po activities in case of radon and ^{212}Pb and ^{212}Bi - ^{212}Po for thoron progenies activities on the surfaces were calculated using different aerosols conditions (for further details , reader is referred to appendices A to D).

It may be seen in Figure 8.3 that under normal conditions, average normalized surface deposited ^{218}Po varies from 0.016 which is for the candle on/off conditions (Candle is on for odd hours and reading in even hours) to 0.201 when ceiling fan was operating. As may be seen in the graph when HEPA filter and HEPA+IONIZER are used as aerosol sinks, particles concentrations are reduced and the surface deposition is increased.

Figure 8.3: Normalized surface deposition rate of radon progenies under different aerosols conditions.

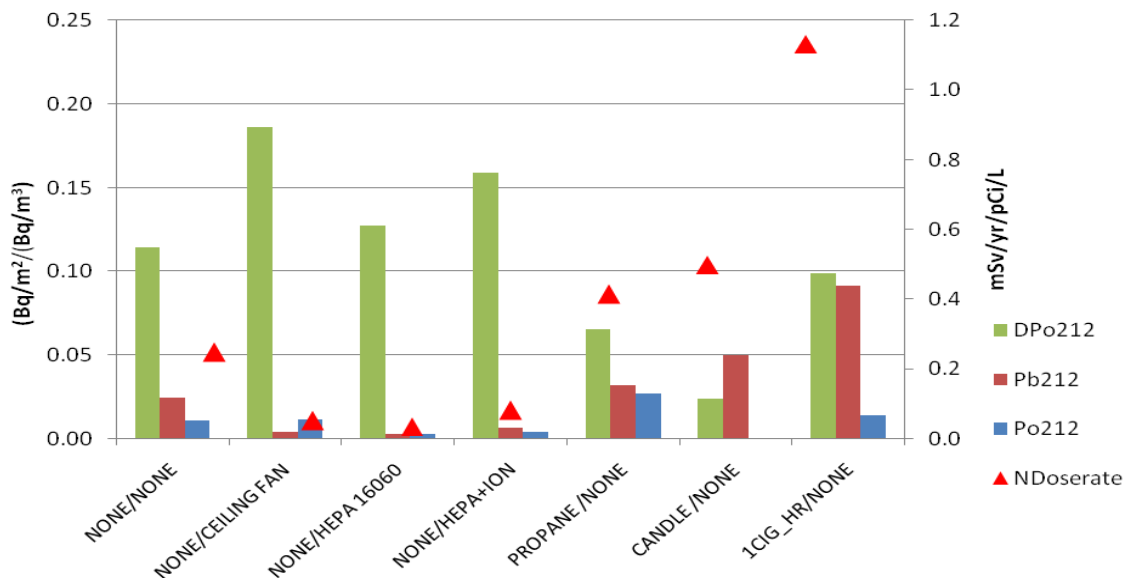


Candles, propane, cooking and cigarette smoking increases the particles concentrations and reduces surface deposition. Candle burning produces more ultrafine particles and reduces the surface deposition. A similar trend was observed for ^{214}Pb and ^{214}Po . (i.e., when aerosol generating activity was taking place surface deposition rate decreased and vice versa).

When thoron was used in the indoor environment and the experiments were repeated for different aerosol sources and sink the average. Results obtained from these experiments are shown in Figure 8.4.

In the absence of aerosol source and sinks, average normalized surface deposited ^{212}Pb - ^{212}Bi had a value of 0.179, and maximum deposition of 0.291 occurs when the ceiling fan is on, for propane cooking the normalized deposition was 0.102 and a minimum value of 0.037 occurs for candle burning. Similarly for ^{212}Po minimum deposition of 0.024 was measured for propane cooking and maximum deposition value of 0.186 was obtained for HEPA filter. Qualitatively, the behavior of radon and thoron progenies is similar. When aerosol sink was used, the particles concentration was reduced and the deposition rate increased accordingly. When aerosol generating activity was taking place, the deposition was least as more particles were available to keep the aerosol particles suspended in the ambient air.

Figure 8.4: Normalized surface deposition rate of thoron progenies under different aerosols conditions.

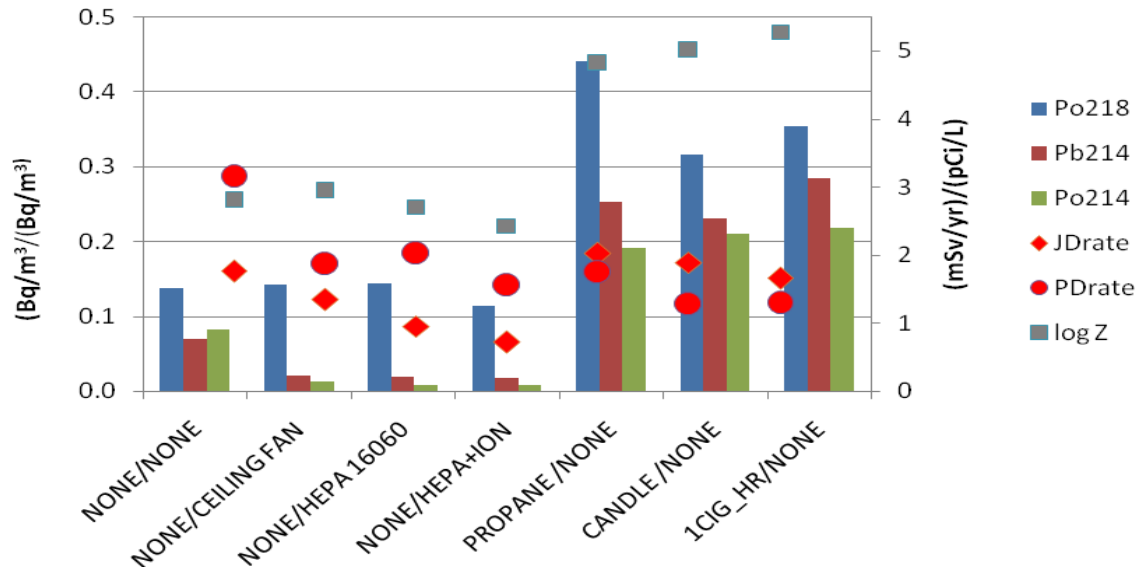


8.11. Air borne Progeny Fraction Measurement

8.11.1. Measurement of unattached fraction using Ludlum scintillation detector

To correlate the airborne radon/thoron progenies attached to the aerosols or unattached fraction of the progenies activity to the surface deposited activity, airborne progenies activity was measured simultaneously with the surface deposited activity using the active *Ludlum scintillation detector* system. For these measurements two different protocols were used due to the difference of half lives of radon and thoron progenies. For the measurement of radon progenies, the Tsivoglou method was used which is based on the one minute counting interval for 50 min for the concentration of ^{218}Po , ^{214}Pb , and ^{214}Bi - ^{214}Po after sampling of 5 min. The results obtained are shown in figure 8.5.

Figure 8.5: Normalized airborne radon progenies for different aerosols conditions.



As may be seen in the Figure 8.5 the behavior of airborne radon progeny is opposite to the surface deposited activity. Under the high aerosol conditions the airborne radon progenies concentration is lower on mesh and filter. The concentrations of radon progenies in air attached or unattached form were calculated using the data of unattached

fraction is calculated. For ^{218}Po normalized airborne radon progenies have maximum value of 0.441 for Propane On-Off/None aerosols conditions and a minimum value of 0.138 was for normal conditions was recorded and this normalized value was 0.143 when the ceiling fan was on. For airborne ^{214}Pb the maximum value of 0.284 was recorded for cigarette smoking and 0.253 occurred for the propane cooking conditions, and a minimum value of 0.010 was calculated for the None/HEPA + Ionizer was on conditions. Similarly, the airborne ^{214}Po maximum value of 0.219 was measured for cigarette smoking and a minimum value of 0.009 was measured for None/HEPA+ Ionizer on conditions. This behavior of radon progenies are just opposite to the surface deposition pattern. Thus aerosol sources increase the airborne radon progenies and decrease the deposition phenomena as the available particles for the attachment have been increased and thus attached fraction was also higher.

For the measurement of thoron progeny the counting protocol developed by KBP was used (Khan and Philips, 1986; Khan et al.,1982). In the KBP total counting time (CT) is limited to 5.5 h after the beginning of sampling. Airborne concentrations of radon and thoron daughters are measured directly from the number of counts due to the alpha disintegrations on the filter which is taken in five successive time intervals after the end of sampling (10 min sampling, 2 minutes delay). 50% cutoff of the screen was measured using the relation provided by Knutson et al.,(2001, 1996&1994; Porstendörfer and Reineking, 1999, Reineking and Porstendörfer, 1986) this data the required flow rate was calculated for the pumping through the screen and a backup filter. Screen was used to collect unattached particles and the backup filter was used to collect the aerosols attached fraction of the radioactive radon/thoron progenies particles in the indoor air. These calculations may be extended to radon and thoron daughter working levels by the use of following equations,

$$RnWL = \frac{1.03C_1 + 5.07C_2 + 3.73C_3}{1000}$$

$$RnWL = \frac{123.19C_4 + 12.67C_5}{1000}$$

$$RSWL = \frac{[(91.03S_1)^2 + (5.07S_2)^2 + (3.73S_3)^2]^{1/2}}{RnWL \times 1000}$$

$$RSTWL = \frac{[(123.19S_4)^2 + (12.67S_5)^2]^{1/2}}{TnWL \times 1000}$$

The time-weighted averages of ^{218}Po , ^{214}Pb , and ^{214}Bi - ^{214}Po ^{212}Pb and ^{212}Bi concentrations during sampling, are C_1, C_2, C_3, C_4, C_5 , and S_1, S_2, S_3, S_4, S_5 are standard deviations in concentration in measurements respectively.

During the grab sampling using filter and screen, Rad 7 was used to measure the radon and thoron concentration.

$$F = \frac{\text{Radon Progeny concentration in mWL}}{\text{Radon concentration in pCi } \ell^{-1}}$$

^{220}Rn equilibrium factor was calculated using:

$$\text{Equilibrium factor (Tn)} \quad F = \frac{\text{Thoron Progeny concentration in mWL}}{\text{Thoron concentration in pCi } \ell^{-1}}$$

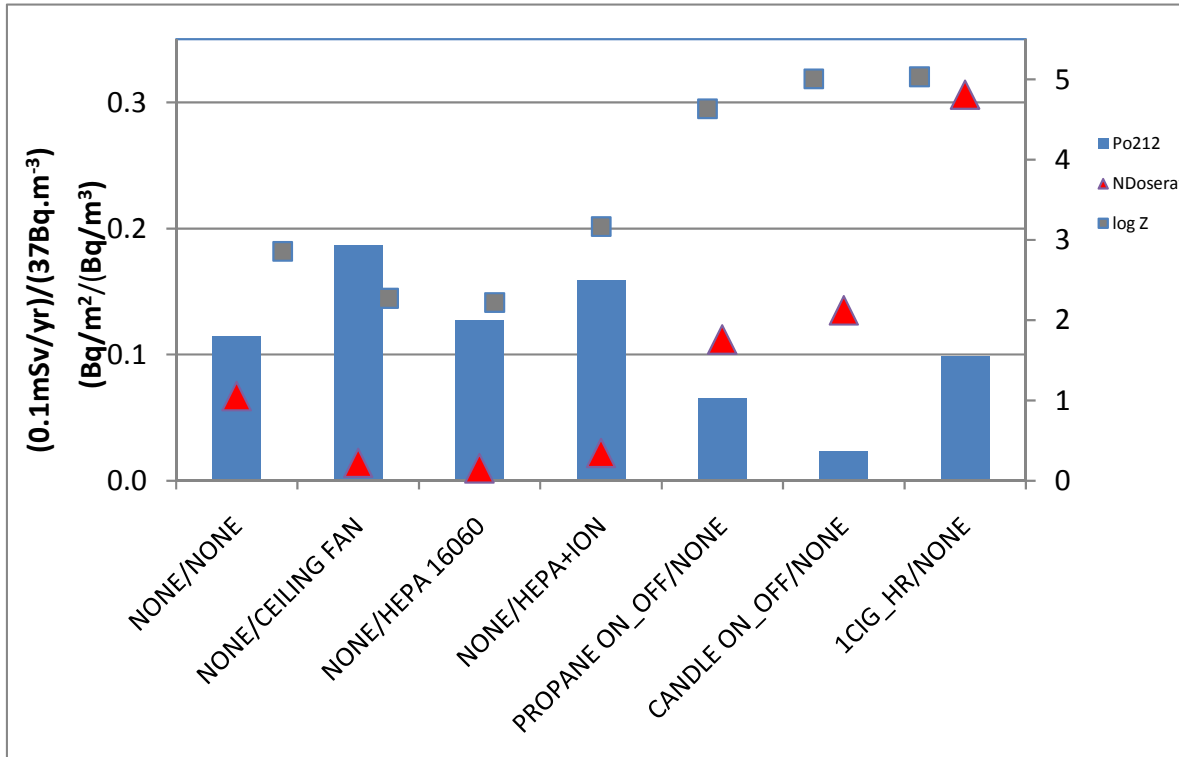
Same procedure (Protocol) was used for the measurement of filter and screen. Unattached fraction of radon and thoron was calculated using the following relation

$$f_p = \frac{(\text{Rn or Tn mWL on screen})}{((\text{Rn or Tn mWL on screen}) + (\text{Rn or Tn mWL on filter}))}$$

Thoron progeny concentration measured using the above mentioned protocol by KPB is shown in the appendix A, B,C and D. Airborne progeny concentration of thoron depends on the aerosols activity generated or present in the environment. It may be borne in mind that due to the relatively long half life of ^{212}Pb the time required to attain equilibrium between thoron progenies is relatively longer than radon. About 24 h are required in

order to measure thoron progeny before the conditions of the exposure room is changed. Summary results of the normalized thoron progenies are shown in Figure 8.6.

Figure 8.6: Airborne thoron progenies in the exposure room under different aerosols conditions.



The results show that normalized airborne ^{212}Pb has a maximum value of 0.091 when aerosol generating activity of cigarette smoking (light smoking is taking place) was taking place and a minimum average value of 0.003 was recorded when the ceiling fan was on. For the airborne normalized thoron progeny, minimum value of ~ 0.0001 was obtained for candle burning and a value of 0.003 for the conditions when HEPA+Ionizer was used as an aerosols sink and a maximum value of 0.027 was recorded for candle burning conditions.

8.11.2. Radon and Thoron Progeny Equilibrium and Unattached Fraction

As mentioned earlier, the protocols developed by Tsivoglou and Kusnetz were used for the measurement of the equilibrium factor and unattached fraction using the screen and backup filter. Tsivoglou method provides information about the concentrations of the

individual radon daughters through three alpha counts intervals. The first count is taken from second minute till fifth minute (2-5), the second from sixth till twentieth minute (6-20) and the third from twenty first till thirtieth (21-30) minutes after sampling. From the counts concentrations of the individual radon daughters (^{218}Po , ^{214}Pb , and ^{214}Bi) and the working level concentration were calculated. The total counting interval for these methods is about 50 minutes and the counting interval are (2-5), (6-20), (21-30) minutes.

Indoor $^{222}\text{Rn}/^{220}\text{Rn}$ was measured using Rad 7 for which the equilibrium attached and unattached concentrations of ^{218}Po , ^{214}Pb , ^{214}Bi - ^{214}Po , ^{212}Bi - ^{212}Po were calculated. Equilibrium factor for radon varied from 3% to 32% which were for the conditions of the ceiling fan and when HEPA 16060 filters were used as sinks for the ultrafine particles in the indoor environment. Unattached fraction varied from 2% for candle on-off to 68% when HEPA 16060 was in use and 67% for HEPA+ Ionizer air filters was used as a sink for the ultrafine particles. Unattached ratio (Uratio) was measured by multiplying the equilibrium factor and unattached fraction. The results varied from 0.5% to 2.3% which were for candle burning and normal aerosols conditions, respectively.

Equilibrium factor measured in the exposure room for the thoron under different aerosols conditions varied from 0.3% to 8.7% which were for the None / HEPA1606 and 1 Cig-hr / None aerosols conditions respectively. These results indicated that equilibrium factor depends on the aerosols sources/sinks. When ultrafine particles are reduced due to the presence of its sink, equilibrium factor is low, whilst for higher aerosols conditions it is high. Unattached fraction for thoron varied from 4.1% to 69.7% which were observed for 1 Cig-hr/None and HEPA1606 respectively. Environmental thoron levels are an order of magnitude lower than those of radon (Yu et al.,1998).

8.12. Calibration Factor for the New Thoron Surface Deposition Dosimeters

The calibration and conversion factor were calculated from the efficiency of different regions of the detector for the detection of surface deposited ^{218}Po , ^{214}Po and ^{212}Po . Calculations were performed as follows

$$S^{218}\text{Po} = \frac{\left(\frac{\text{Tracks.m}^{-2}\text{s}^{-1} \times 0.94 \times (\text{Tmm}^2 \text{ on Thin filter (CI-92)} - 1.15 \times \text{Tmm}^2 \text{ on Thick filter (3M114)}) \times \text{Efficiency of thin filter (CI-92) for } ^{214}\text{Po}}{\text{Efficiency of thick filter for (3M114)} ^{214}\text{Po}} \right)}{\text{Efficiency of thin filter for (CI-92)} ^{218}\text{Po}}$$

$$S^{214}\text{Po} = \frac{\text{Tmm}^2 \text{ on Thick filter (3M114)} \times \text{Tracks.m}^{-2}\text{s}^{-1}}{\text{Efficiency of thick filter (3M114) for } ^{214}\text{Po}}$$

$$S^{212}\text{Po} = \frac{\text{Tmm}^2 \text{ on Thick filter (3M146-7)} \times \text{Tracks.m}^{-2}\text{s}^{-1}}{\text{Efficiency of thick filter (3M146-7) for } ^{212}\text{Po}}$$

Thin filter

$$S^{212}\text{Po} = \frac{\text{Tracks.m}^{-2}\text{s}^{-1} (\text{Tmm}^2 \text{ on Thick filter (3M146-7)} - 1.15 \times \text{Tmm}^2 \text{ on Thick filter (3M114)}) \times \text{Efficiency of thick filter (3M146-7) for } ^{214}\text{Po}}{\text{Efficiency of thin filter (FFM_7) for } ^{212}\text{Po}}$$

For calculation of radon a calibration factor of 19.6 tracks.mm⁻².d⁻¹ /37 Bq.m⁻³ to determine the radon concentration and for thoron calibration factor of 33.533 tracks.mm⁻².d⁻¹ / 37 Bq.m⁻³ concentrations was used.

The results show that S²¹⁸Po varied from 0.1 ± 0.01 to 8.9 ± 3.5 which were recorded in Anbar Swabi and Islamabad area, respectively. However the uncertainty in the S²¹⁸po is high and in some case the relation gave negative values due to high uncertainty. S²¹⁴Po varied from 0.7 ± 0.2 in I-9 Islamabad to 19.1 ± 5.5 Bq.m⁻² in Narogha Mohmand agency, respectively.

S²¹²Po in the case of thoron was calculated using Thick filter and the values varied from 1.9 ± 0.8 Bq.m⁻² in I-9 Islamabad to 28.7 ± 11.5 Bq.m⁻² in Ziarat Mohmand agency, respectively. S²¹²Po measured using thin filter corrected for ²¹⁴Po gave relatively lower value because the ²¹⁴Po corrections is overestimated and therefore in the present study only Thick filter data was used for the measurements of surface deposited activity and dose calculation of the thoron progenies. However for very low concentration radon environment where thoron concentration is sought to be measured thin filter data can also be used.

8.13. Dose from Thoron Progeny

The dose conversion factor for radon is derived using two approaches, i.e., epidemiological and dosimetric approaches. However, it can not be used for thoron due to the lack of epidemiological data. Only the dosimetric approach has been used for its

dose calculations. ICRP in its latest publication addressing thoron decay products (TnDP) where assumed DCF was 0.52 based on dosimetric approach available in 1987. UNSCEAR in its 1988 report uses value of 0.42 Sv per Jhm^{-3} to all the organs considering occupancy of 100% and for 80%, occupancy the lung dose was 0.35 Sv per Jhm^{-3} . IAEA in its 1996 basic safety standards assumed a DCF equal to 0.48 Sv per Jhm^{-3} . In the 1996 Council Directive of the European Union, a DCF of 0.5 Sv per Jhm^{-3} . In ICRP 65 the DCF for TnDP is 0.3 and 0.4 Sv per Jhm^{-3} for dwellings and work places, respectively (Nuccetelli and Bochicchio,1998).

In the report of UNSCEAR 1993 the annual effective dose from thoron and its progeny was evaluated to be $75\mu\text{Sv}$, only 6% of that of radon and its progeny. The annual effective dose from thoron and its progenies was evaluated to be up to 9% of that of radon and its progenies in the report of UNSEEAR 2000. As the half-life of thoron progeny (^{212}Pb , 10.64 h) is much longer than that of radon progeny, and the alpha energy emitted from thoron progeny is high (^{212}Po , 8.8 MeV), the effective dose per unit equilibrium equivalent concentration of thoron progeny is near 4.4 times higher than that of radon progenies. It is not possible to use only the concentration of the gas in dose evaluation, since the concentration is strongly dependent on the distance from the source (UNSCEAR, 1993). Using the equilibrium equivalent concentrations, the annual effective dose may be derived as:

$$\text{Indoors: } 0.3 \text{ Bq m}^{-3} (\text{EEC}) \times 7,000 \text{ h} \times 40 \text{ nSv (Bq h m}^{-3})^{-1} = 0.084 \text{ mSv.}$$

$$\text{Outdoors: } 0.1 \text{ Bq m}^{-3} (\text{EEC}) \times 1,760 \text{ h} \times 40 \text{ nSv (Bq h m}^{-3})^{-1} = 0.007 \text{ mSv.}$$

The value of 40 nSv (Bq h m^{-3}) is for equilibrium equivalent concentrations of thoron, for evaluating exposures both indoors and outdoors (ICRP Publication50, 1987). The dose to organs other than lungs due to the transfer of ^{212}Pb from the lungs is significant due to the long half-life of ^{212}Pb . Due to the unit exposure to thoron progeny, about 20% of the dose that they receive from the same exposure to radon progeny (Comparative dosimetry, 1991; Guo et al., 2001).

Table 8.12: Indoor radon, thoron and their progenies concentration and the dose delivered by thoron progeny.

House No	Location	Rn	Tn	S ²¹⁸ Po	S ²¹⁴ Po	S ²¹² Po thick	S ²¹² Po thin	D Rate mSv.yr ⁻¹
1.	Islamabad	56	26	1.7±0.7	2.9±0.8	3.4±1.4	1.6±0.6	0.10
2.	Swabi	30	15	-0.6±-0.2	2.3±0.7	5.6±2.2	1.8±0.7	-0.19
3.	Bachai	78	155	0.8±0.3	3.5±1.0	5.6±2.2	3.4±1.4	1.63
4.	Naziabad	56	67	2.9±1.1	1.8±0.5	4.9±1.9	2.6±1.0	0.53
5.	Kaddi	93	70	4.8±1.9	1.8±0.5	7.7±3.1	4.7±1.9	0.38
6.	Rashaka	70	30	-1.4±0.6	3.3±0.9	8.7±3.5	4.1±1.6	-0.21
7.	Mathra1	59	59	2.3±0.9	2.4±0.7	4.2±1.7	2.1±0.8	0.48
8.	Mathra2	78	85	1.5±0.6	2.2±0.6	4.3±1.7	3.1±1.2	0.81
9.	Sparliwand	63	56	2.1±0.8	3.0±0.9	4.3±1.7	2.7±1.1	0.43
10.	Nilore	63	LLD	0.6±0.2	1.7±0.5	2.8±1.1	2.2±0.9	LLD
11.	I-9 Islamabad	33	19	8.9±3.5	0.7±0.2	1.9±0.8	0.5±0.2	0.12
12.	Alipur Isd	37	22	L	L	4.3±1.7	2.8±1.1	L
13.	Mamta	85	78	-5.3±-2.1	7.8±2.2	5.1±2.0	1.0±0.4	L
14.	Daudshah	89	152	-2.5±-1.0	4.5±1.3	3.8±1.5	-0.1±0.0	1.71
15.	Sardcheena	56	LLD	2.9±1.1	5.1±1.5	4.6±1.8	4.6±1.8	LLD
16.	Marghuz	52	15	1.2±0.5	2.1±0.6	2.2±0.9	0.6±0.2	-0.15
17.	Zaida	59	LLD	1.9±0.8	2.1±0.6	5.4±2.2	4.3±1.7	LLD
18.	Dhodher	48	74	1.5±0.6	2.7±0.8	3.9±1.6	1.2±0.5	0.69
19.	Kalabat	41	78	1.9±0.8	2.5±0.7	4.3±1.7	2.5±1.0	0.72
20.	Mainai	59	44	1.7±0.7	1.0±0.3	2.2±0.9	1.4±0.5	0.42
21.	Anbar	59	67	0.1±0.0	2.0±0.6	3.0±1.2	2.7±1.1	0.66
22.	Khwar	70	137	-1.4±-0.6	4.8±1.4	5.9±2.4	2.2±0.9	1.37
23.	Qala	L	L	0.4±0.2	5.6±1.6	6.4±2.6	3.4±1.4	L
24.	Ziarat	L	L	-3.7±-1.5	7.9±2.3	28.7±11.5	18.1±7.2	L
25.	Manasab	59	307	-1.3±-0.5	1.6±0.5	4.8±1.9	3.3±1.3	3.66
26.	Narogha	59	196	-11.2±-4.5	19.1±5.5	L	L	L
27.	Rupat	74	33	-0.4±-0.2	4.0±1.2	6.3±2.5	5.7±2.3	-0.01
28.	Rustum1	122	63	-1.3±-0.5	5.0±1.5	5.6±2.2	1.7±0.7	0.43
29.	Wah	48	89	-0.5±-0.2	2.3±0.7	3.2±1.3	1.8±0.7	0.94
30.	Rawalpindi	56	LLD	-1.1±-0.4	2.4±0.7	2.4±0.9	0.6±0.3	L
31.	Nawankilli	41	52	1.2±0.5	1.4±0.4	2.3±0.9	0.8±0.3	0.52
32.	Rustum2	48	44	L	L	L	L	L
33.	Birikao	52	144	0.5±0.2	2.4±0.7	3.9±1.5	1.7±0.7	1.60
34.	Gulbahar	68	LLD	2.3±0.9	4.9±1.4	2.8±1.1	0.5±0.2	LLD
35.	Habib	67	26	0.9±0.4	2.2±0.6	4.7±1.9	1.9±0.8	0.01
36.	Sufaid Dheri	63	37	-2.9±-1.2	4.3±1.2	3.4±1.4	0.3±0.1	0.25
37.	Chargul	48	148	-0.1±0.0	0.9±0.3	5.3±2.1	3.1±1.2	1.56
38.	Taja	63	67	-0.7±-0.3	3.5±1.0	3.2±1.3	0.3±0.1	0.65
39.	Khairabad	85	LLD	2.1±0.8	3.0±0.9	6.2±2.5	2.1±0.8	LLD
40.	Amjad Rustum	85	67	1.1±0.4	5.0±1.4	4.3±1.7	0.4±0.2	0.57
Min		30	15	15	1	2	0.3	0.01
Maximum		122	307	307	19	29	18	3.66
Average		62	79	79	4	5	3	0.84
ST.Dev.		18	63	63	3	4	3	0.78

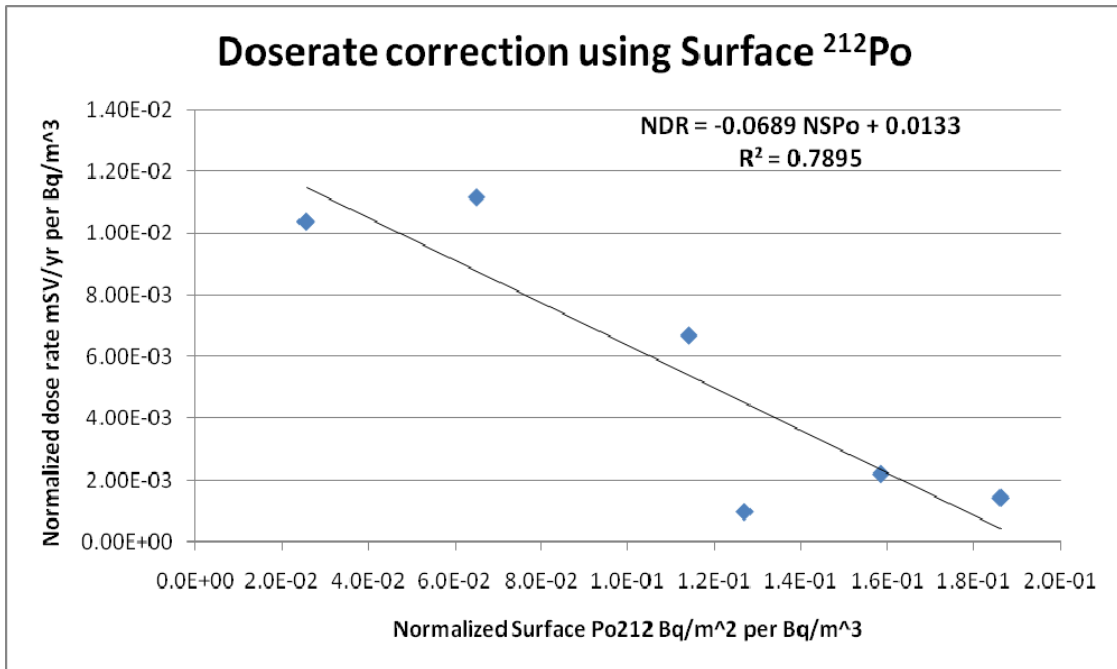
Dose conversion factor (DCF) for thoron progeny was calculated by Nikezic et al., as 4.5 mSv.WLM^{-1} , which is three times smaller than that for ^{220}Rn radon progeny (Nikezic, 2007).

The effective dose per EETC was about four times larger than the effective dose per equilibrium equivalent concentration for radon (EERC) (Ishikawa et al., 2007). Based on the measurements in the exposure room under various aerosols conditions a relation was derived to calculate the thoron progeny dose rate per year (DR).

In this relation both thoron gas concentration (TnG) and the surface deposited ^{212}Po activity density ($S^{212}\text{Po}$) from the newly surface deposition dosimeters; either thick filter alone or thin filter corrected for ^{214}Po) were used in the following relationship:

$$\text{DR (mSv/yr)} = 0.013 \times \text{TnG} - 0.069 \times S^{212}\text{Po}.$$

The results of the study conducted in different parts of Pakistan using the newly developed surface deposition dosimeter showed that thoron can not be ignored during measurement of the indoor radon concentration as in some cases its concentration is high and delivers dose to such an extent which when added to the dose delivered by radon, may exceed the limits defined by the US EPA or NRPB UK.



In the present study the dose rate varied from 0.1 to 3.66 mSv.yr⁻¹ with an average of 0.84 ± 0.78 mSv.yr⁻¹. The study showed that thoron concentration in some cases may be very high and thus should not be ignored while measuring radon concentration.

8.14. Conclusions

To conclude, a new thoron progeny dosimeter has been developed using the surface deposition principles. The study showed that using suitable filter radon and thoron progenies can be measured discriminatively in the mixed environment using passive technique. Calibration and initial laboratory test were performed which showed very good results. The results showed that this technique is reliable and inexpensive and is suitable for the large area monitoring of the thoron progenies. Aerosols sources and sinks are the main factors for determining the airborne and surface deposited activity of the radon and thoron progenies. In the low aerosols environment unattached fraction is higher resulting in low equilibrium factor. Any cooking or burning activity in the indoor environment increases the number of ultrafine particles very quickly which influences the unattached fraction and equilibrium factor of radon and thoron progenies. Ultrafine particles concentration varies very quickly with the operation of aerosol source or sink. A relation has been established for the measurement of dose of the thoron progeny. Field measurement of the of the radon and thoron progenies in different localities of Pakistan showed that thoron concentrations are high and thus while measuring indoor radon thoron concentration should also be measured.

Chapter Nine

Conclusions and Future Recommendations

This chapter presents a brief summary and main conclusions of the studies carried out during this PhD project. The present thesis is based on the experimental work carried out in the field and in the Laboratory. The first two chapters described basic introductory techniques of the solid state nuclear track detectors, materials and methods used during the experimental work and geographic geological information about the area studied. Experimental work consists of two parts. In the first part CR-39 based NRPB (HPA) dosimeters were exposed in dwellings of the selected areas of Pakistan in order to measure the seasonal and spatial variations of the indoor radon levels. Measurements of natural radioactivity in the different soil and building materials which were collected from the selected areas were performed. Experiments about the radon exhalations and the effect of moisture contents on the radon exhalation rate were also performed. In the second part of the experimental work, efforts were concentrated on the development of a passive thoron progeny dosimeter.

9.1. Conclusions

According to the review of different studies performed in Pakistan for the measurement of natural radionuclides, a wide variation was noted in the reported data. Most of these studies were conducted to measure the health hazards associated with the natural radioactivity present in the soil and other building materials. Limited data is available in Pakistan concerning the use of the natural radioactivity for the exploration of uranium and other related minerals deposits in different types of rocks and soil. In the majority of the studies related to the natural radioactivity high purity germanium detectors (HPGe) were used whereas in some cases, relatively low resolution NaI (Tl) detector has also been used using spectrum stripping technique. Fission track dating technique has also been used to measure naturally occurring uranium in rocks and water samples. In order to

measure the elemental concentration of the radionuclides in food and vegetable samples, INAA has also been reported.

The lowest reported values for ^{226}Ra , ^{232}Th and ^{40}K were as 1.45 Bq.kg^{-1} , 1.16 and 7 Bq.kg^{-1} , whilst the highest were 799 Bq.kg^{-1} , 124 Bq.kg^{-1} and 1272 Bq.kg^{-1} , respectively. Reported range of the uranium concentration in water samples is from $0.03 \pm 0.01 \mu\text{g.}\ell^{-1}$ ($0.0004 \pm 0.0001 \text{ Bq.kg}^{-1}$) to $6.67 \pm 0.14 \mu\text{g.}\ell^{-1}$ with an average value of $1.36 \pm 0.05 \mu\text{g.}\ell^{-1}$ ($0.0170 \pm 0.0006 \text{ Bq.kg}^{-1}$).

Etched track detectors for measuring radon are the dosimeters of choice, first, because they are passive and thus need no power supply and second because they measure total radon exposure, allowing averaging of the radon concentration over long time.

From the analysis of the results of the indoor radon levels variation observed in the houses surveyed of the selected area may mainly be due to the local geological formations on which these houses are built as well as ventilation system of the houses. The present work revealed that the Charsadda district and the Bajuar agency have relatively higher indoor radon levels as compared to the other studied areas. Mud houses (houses use unbaked bricks) have relatively higher indoor radon as compared to the houses which are made of the baked bricks and cement. As the cement used in Pakistan has relatively low radioactive nuclides contents, annual arithmetic mean of the present study ($72 \pm 32 \text{ Bq m}^{-3}$) lies within the published values of the indoor radon reported for different countries.

Using the ICRP recommended maximum constraint limit of 600 Bq m^{-3} (ICRP-65), EPA action level of $4 \text{ pCi. } \ell^{-1}$ (148 Bq m^{-3}) or NRPB (HPA), UK limit of 200 Bq m^{-3} (NRPB, 1990), yearly arithmetic mean values measured in the present studies of all the districts/agencies are below the recommended limits of ICRP, NRPB (HPA), UK or US EPA limits. Only in few cases the individual values of indoor radon in bedrooms or drawing rooms in the four seasons exceeded NRPB and US EPA limits.

The yearly average indoor radon values in bedrooms exceeded the EPA limit whilst no drawing room value crossed the limits. Weighted average indoor radon

concentration in one house exceeded the EPA limit, no value was higher than the NRPB (HPA) and ICRP limits. Individual values of the indoor radon showed more fluctuations showed as compared to the weighted average data. In the seasonal data, wide variation in the indoor radon levels in the different seasons was observed. Highest and lowest average indoor radon levels were observed in the winter and summer seasons, respectively.

Highest seasonal correction factor of 1.33 ± 0.3 and 1.32 ± 0.47 has been found for drawing rooms and bedrooms of the Mardan and Swabi districts in the summer season, respectively. This is ~18% higher than the overall seasonal correction factor. Seasonal correction factor is higher in spring and summer seasons and lower in winter and autumn seasons. The difference in the seasonal correction factors of bedroom and drawing rooms is not statistically significant.

Comparison of the results of yearly and seasonally exposed detectors indicated more fluctuation in the individual values of the drawing room. Yearly exposed detectors gave average values of 23%, ~19% and ~25% lower than the seasonally measured values in the Swabi, Mardan and Charsadda districts, respectively.

In the Mohmand agency the average yearly values was ~10% lower than the seasonally measured values. In the Bajuar agency, a similar trend was observed. Heat and humidity in the presence of oxygen in the air can affect the sensitivity of the etched-track detector during their use to measure radon. The magnitude of the effect depends on the detector materials, etching conditions and counting techniques. The reason of relatively low track density/ indoor radon levels from the yearly exposed detector as compared to the seasonally measured values, apart from other reason may due to the fact a layer of dust may be formed on the surface of CR-39 detector which causes reduced efficiency of CR-39 for the registration of tracks, as some of the low energy alpha may be absorbed in the dead layer of the dust above the CR-39 detectors. Seasonally measured values were comparable to that of the yearly measured values and there was ~13% difference between them.

Annual effective dose to the inhabitants of the area was with in the limits; however for radiation the ALARA principle should prevail, therefore care must be taken

while using relatively high radioactive contents materials in construction of buildings. Excess lung cancer risk was calculated using the local occupancy factor. As the occupancy factor of the area was 40% lower than that given in the ICRP or other international documents, therefore the effective dose and excess lung cancer risk was also 40% lower than that if high occupancy factor.

It is worth mentioning here that in Pakistan, ICRP recommended limits are adopted by the Pakistan Nuclear Regulatory Authority (PNRA) Pakistan. However, so far, no limits have been defined for the indoor radon concentration levels by the PNRA. At some stage PNRA has also to define indoor radon exposure limits and must take into consideration the environmental and economic conditions of Pakistan. It is suggested that the values recommended by the ICRP may be adopted in this regard.

Exhalation rate has been calculated from the soil sand and brick samples which were collected from the selected area using two different relations and the results showed that relation derived by Rehman et al. yields relatively lower exhalation rate (~6 - 13 % less) as compared to that given by Abu-Jarad et al. From dried soil samples higher average radon exhalation rate of $304 \pm 93 \text{ mBq.m}^{-2}.\text{h}^{-1}$ was found in the samples collected from the district Charsadda whereas lower value of the average radon exhalation rate of $228 \pm 60 \text{ mBq.m}^{-2}.\text{h}^{-1}$ was observed in the district Swabi. From the dried sand samples higher average radon exhalation rate of $291 \pm 13 \text{ mBq.m}^{-2}.\text{h}^{-1}$ was found in the samples collected from the district Charsadda.

Using different moisture contents levels, higher average radon exhalation rate was observed at 15% moisture content from the sample collected from the Bajuar agency with an average value of $392 \pm 50 \text{ mBq.m}^{-2}.\text{h}^{-1}$. Minimum value of $327 \pm 35 \text{ mBq.m}^{-2}.\text{h}^{-1}$ was found in the samples collected from the Mardan district. At 30% moisture content, average minimum of $377 \pm 91 \text{ mBq.m}^{-2}.\text{h}^{-1}$ was observed for the Charsadda whilst a maximum average value of $397 \pm 124 \text{ mBq.m}^{-2}.\text{h}^{-1}$ was observed from the soil samples collected from the district Swabi.

Using 45% moisture content the lower average value of $294 \pm 47 \text{ mBq.m}^{-2}.\text{h}^{-1}$ was observed in the samples from the district Charsadda whilst higher value of $340 \pm 53 \text{ mBq.m}^{-2}.\text{h}^{-1}$ was observed in samples which were collected from the Bajuar agency

respectively. Radon exhalation rate increases (as compared to the dried samples) with moisture content up to 30%. At higher value of 45% moisture content, a decreasing trend is observed. As moisture content is increased from 0% to 15%, 30% and 45%, on the average 34%, 46% and 13% increase was observed in the radon exhalation rate. It was observed that from 0% to 15% moisture content, increase in the exhalation rate was higher as compared with the increase of radon exhalation from 15-30% and 30-45% moisture content. According to the paired T-test, change in the exhalation rate as a function of the moisture content is significant at 95% confidence level. Taking dried samples as a baseline data, the change in the exhalation rate is significant for the moisture content of 15%, 30% and 45% at 95% confidence level. Between 15% and 30% moisture content, the change in exhalation rate is significant for soil and sand samples. For 30% - 5% moisture content, exhalation rate is significant in soil, sand and brick samples. The building materials studied have lower radon exhalation rate and are safe therefore for use as construction materials.

Concentration of natural radionuclides in the soil, sand, brick and cement samples collected from different localities of the selected area varied from sample to sample. A minimum value of $8 \pm 1 \text{ Bq.kg}^{-1}$ was observed for ^{226}Ra in the samples collected from the Naroga in the Mohmand and the Sabagai in the Bajuar, Agencies and maximum specific activity of $53 \pm 3 \text{ Bq.kg}^{-1}$ and $54 \pm 3 \text{ Bq.kg}^{-1}$ was found in the Swabi city and Kalambad the district Mardan, respectively. ^{232}Th activity varied from $7 \pm 1 \text{ Bq.kg}^{-1}$ in the Mohmand to $84 \pm 5 \text{ Bq.kg}^{-1}$, $86 \pm 5 \text{ Bq.kg}^{-1}$ in the Pahlawan in the district Charsadda and Kalambad Mardan, respectively. ^{40}K activity varied from $153 \pm 13 \text{ Bq.kg}^{-1}$ in the Alingar area of the Mohmand agency to a maximum value of $1018 \pm 79 \text{ Bq.kg}^{-1}$ in the Kalambad district Mardan. Radium equivalent activity showed variation from $31 \pm 2 \text{ Bq.kg}^{-1}$ to $255 \pm 17 \text{ Bq.kg}^{-1}$. In general, average maximum specific activities for ^{226}Ra , ^{232}Th and ^{40}K were observed in the samples which were collected from the district Mardan and minimum in the Mohmand agency. The areas of Narogha, Sheik Baba, Qandari of the Mohmand agency and Maskano, Sabagai, Tarakai in the Bajuar agency had little vegetation cover. The observed ^{226}Ra and ^{232}Th specific activities in the samples from Maskano, Sabagai, Tarakai, Narogha, Sheik Baba and Qandari were very low and thus safe as building materials. ^{40}K in the present study is slightly higher than the world

population weighted average value (420 Bq.kg^{-1}) as reported in the UNSCEAR 2000. Specific activities, radium equivalent activity and internal and external hazard indices of the soil samples reported in this study are within the acceptable limit and therefore the use of these soils is safe in the construction of dwellings.

Measured specific activities of ^{226}Ra , ^{232}Th and ^{40}K in the brick, sand, marble and cement samples showed a wide variation. ^{226}Ra and ^{232}Th , minimum value of $1 \pm 1 \text{ Bq.kg}^{-1}$ was observed in the marble samples of Greenish color. Maximum value of $66 \pm 4 \text{ Bq.kg}^{-1}$ was also observed in Pink-M marble samples. ^{40}K showed wide variation ranging from $25 \pm 2 \text{ Bq.kg}^{-1}$ to $1745 \pm 135 \text{ Bq.kg}^{-1}$ which were observed in the marble and sand samples, respectively. ^{226}Ra varied from $18 \pm 19 \text{ Bq.kg}^{-1}$ to $30 \pm 15 \text{ Bq.kg}^{-1}$. A relatively lesser average of ^{232}Th was 18 ± 4 in the cement samples whereas maximum activity of $41 \pm 21 \text{ Bq.kg}^{-1}$ was observed in the sand samples collected from the selected area. For ^{40}K , average minimum value of $244 \pm 29 \text{ Bq.kg}^{-1}$ was observed in the brick samples whilst average maximum value of $769 \pm 461 \text{ Bq.kg}^{-1}$ was observed in the cement samples. Averaged minimum radium equivalent value of $67 \pm 60 \text{ Bq.kg}^{-1}$ was observed in the marble samples and maximum averaged value of $129 \pm 54 \text{ Bq.kg}^{-1}$ was observed in sand samples. Average activities calculated in the present study lies within the reported values and are also lower than the world population weighted average value as reported in the UNSCEAR 2000. Specific activities, radium equivalent activity and internal and external hazard indices for all the studied samples are within the acceptable limits.

In general, soil has higher mean activity concentrations of ^{226}Ra , ^{232}Th and ^{40}K as compared to the brick, sand, marble and cement samples, which were collected from the area while marble has the least concentration of the naturally occurring radionuclides. Radium equivalent activity external and internal hazard indices are well below the acceptable hazard limit of 370 Bq kg^{-1} and 1, respectively.

Using standard radon chambers, radon concentration was measured using the short-term high sensitivity electrets in the exposure room. The results showed that electret ion chamber (EIC) were stable and the variation between the different readings of the same exposure (run) is very low.

In majority of the cases there seems a reasonably good agreement between the values of the different electrets exposed to the same environment. The exposure of five electrets for 0.33 day gave results of 36 ± 6 , 32 ± 7 pCi. ℓ^{-1} , 34 ± 7 pCi. ℓ^{-1} , 33 ± 7 pCi. ℓ^{-1} and 34 ± 6 pCi. ℓ^{-1} with an average value of 34 ± 7 pCi. ℓ^{-1} and having standard deviation of only two. Measuring radon concentrations above 148 Bq.m⁻³(i.e. 4 pCi. ℓ^{-1}) the relative difference was normally less than 20% using electrets. Low radon concentrations (below 200 Bqm⁻³). Electret-passive environmental radon monitors (E-PERM) show better performance higher indoor radon concentration.

The performance factor calculated for the alpha contamination monitors using electrets showed that long term electret can be used in the inverted form for the measurement of radon progenies. Because the voltage drop per pCi. ℓ^{-1} of radon is such that for less sensitive electrets duration of the exposure may be kept relatively longer, in order to get a suitable voltage drop.

The average performance factor calculated for the three long-term electrets varied from 0.5 to 12.51 V/d.pCi. ℓ^{-1} with an over all average of 2.68 ± 2.1 V/d.pCi. ℓ^{-1} . Only four times out of 108 runs the performance factor of the alpha contamination measurement chambers using long-term electrets failed to work as a radon progeny monitor. Long term electret showed more fluctuations in the short term reading whilst long term average had relatively less fluctuations.

In a higher radon progenies environment, the use of long-term electret as a radon progeny dosimeter would be suitable whilst for low radon concentrations, performance factor for short duration may be difficult to carry out. The performance of these low sensitivity detectors originally used for the measurement of alpha contamination may also be used as radon progeny dosimeters. In order to measure the effect of orientation of these electrets on its performance, electrets were exposed in the horizontal and vertical positions. For electrets exposed in the vertical position performance factor values varied from 0.51 to 4.8 V/d.pCi. ℓ^{-1} whilst for the other electret varied from 0.74 to 3.81 V/d.pCi. ℓ^{-1} . The average value of the performance factor in the vertical position varied from 0.62 to 4.31 V/d.pCi. ℓ^{-1} .

The performance factor of the electrets exposed in horizontal position was relatively higher as compared to those exposed in vertical positions. However, this deviation in performance factor was not significant. These short-term electrets were found most suitable for the measurement of both high and low levels of radon progeny concentration. For high radon concentration short term measurement must be performed otherwise the voltage drop may be much higher and may reach to unacceptably lower values near to zero.

Electret-radon Progeny Integrating Sampling Unit (E-RPISU) was used to measure unattached fraction and equilibrium factor of radon. Measured unattached fraction and equilibrium factor showed a wide range of variation. Maximum equilibrium factor of 87% and a minimum unattached fraction of 3% were measured in the smoky environment in the exposure room. Measurement performed under the calm conditions, equilibrium factor varied from 3% to 13% and the unattached fraction varied from 33% to 86%. When aerosol sinks were used, the equilibrium factor and unattached fraction also changed for HEPA filter as 5% and 35% and for HEPA filter + ionizer it were 4% and 32%, respectively. The results showed that the E-RIPISU electrets are convenient instrument for measuring the equilibrium factor and unattached fraction.

In order to develop a new thoron progeny dosimeters, different plastics and other materials were studied. Consequently a suitable set of materials were selected for the development of thoron dosimeter. In this study efforts have been made to develop an instrument for the measurement of thoron progeny working on the principle of surface deposition.

Using this technique, suitable filters were identified to detect only thoron progeny (^{212}Po) and attenuated the radon progenies. To block all the radon progenies is easier, except ^{214}Po which is a difficult task because its energy difference is low as compared to the alpha energy of ^{212}Po . 3M146_07 was used as thick filter for the surface deposited activity of ^{212}Po .

In the absence of the aerosol source and sink, average normalized surface deposited ^{212}Pb - ^{212}Bi has a value of 0.179 and maximum deposition of 0.291 occurred when the ceiling fan was on. Qualitatively the behavior of radon and thoron progeny is

similar. When aerosol sink was used, the particles concentration was reduced which resulted in an increase in the deposition rate.

Due to the difference of half lives of radon and thoron progenies two different protocols were used. It is confirmed that airborne radon progeny concentration is opposite to the surface deposited activity. Under the high aerosol conditions, the airborne radon progeny concentration was lower on mesh filter. Aerosol sources increases the airborne radon progeny and decreases the deposition phenomena as the available particles for the attachment have been increased and thus attached fraction was also higher. Normalized airborne ^{212}Pb had a maximum value of 0.091 when aerosol generating activity of cigarette smoking (light smoking is taking place) was taking place and a minimum average value of 0.003 was recorded when the air fan was on.

Equilibrium factor measured in the exposure room for the thoron under different aerosols conditions varied from 0.3 to 8.7 % which were for the NONE / HEPA1606 and 1 Cig-Hr / None aerosols conditions respectively.

$S^{214}\text{Po}$ varied from 0.7 ± 0.2 in I-9 Islamabad to Narogha Mohmand $19.1 \pm 5.5 \text{ Bq.m}^{-2}$.

$S^{212}\text{Po}$ in the case of thoron was calculated using thick filter and the observed values varied from 1.9 ± 0.8 in I-9 Islamabad to 28.7 ± 11.5 in Ziarat Mohmand agency. In the case of lower radon environment thoron concentration is measured, thin filter data may also be used. Based on the measurements in the exposure room under various aerosols conditions, following relation was derived to calculate the thoron progeny dose rate per year (DR).

$$\text{DR (mSv/yr)} = 0.013 \times \text{TnG} - 0.069 \times S^{212}\text{Po}.$$

TnG = Thoron gas concentration and $S^{212}\text{Po}$ surface deposited ^{212}Po activity density from the newly surface deposition thoron dosimeters. In the light of results obtained from the study conducted in different parts of Pakistan using the newly developed surface deposition it may be concluded that thoron concentration can not be ignored

9.2. Future Recommendations

- Indoor radon levels were measured in some selected areas of Pakistan and therefore it is recommended that those areas which have not been studied so far should be studied.
- Due to the unavailability of active detectors these measurements were performed using only passive detectors, therefore daily and short term variations could not be studied. Therefore, if suitable active detectors are comprehensive study should be conducted to study short term variations in the indoor radon levels.
- Using active detectors measurement of the radon attached and unattached fraction in the different indoor environment should be measured.
- Using active detectors for the measurement of radon exhalation rate field measurements should be performed in order to reduce the effect of crushing on the radon exhalation rate.
- Further experiments are needed to perform to study the Electret ion chamber for the measurement of radon and thoron progenies.
- The study of the surface deposition thoron dosimeter showed that further studies are needed to be performed to know the thoron contribution to the radiation dose.
- Intercomparison of the newly developed thoron progeny dosimeter with other thoron progenies dosimeter is recommended.

References

1. Abu-Jarad., Fremlin, F. and Bull, R. A. Study of radon emitted from building materials using plastic a-track detectors. *Phys. Med. Biol.*, 25(4), 683-694(1980).
2. Ahmed, N., Matiullah, Khatibeh, A. J. A. H., Ma'ly, A. and Kenwy, M. A. Measurement of natural radioactivity in Jordanian sand. *Radiat. Meas.*, 28,341-344 (1997).
3. Ahn, G.H. and Lee, J.K. Construction of an environmental radon monitoring system using CR-39 nuclear track detectors. *Nucl. Eng. and Tech.*, 37(4) (2005).
4. Akhtar, N. and Tufail, M. Natural radioactivity intake into wheat grown on fertilized farms in two districts of Pakistan. *Radiat. Protect. Dosim.*, 123(1), 103-112 (2007).
5. Akhtar, N., Tufail, M. and Ashraf, M. Natural environmental radioactivity and estimation of radiation exposure from saline soils. *Intern. J. Environ. Science and Tech.*, 1(4), 279-285(2004a).
6. Akhtar, N., Tufail, M., Ashraf, M. and Iqbal, M. M. Measurement of environmental radioactivity for estimation of radiation exposure from saline soil of Lahore, Pakistan. *Radiat. Meas.*, 39, 11–14 (2005).
7. Akhtar, N., Tufail, M., Chaudhry M. A. and Iqbal, M. Estimation of radiation exposure associated with the saline soil of Lahore, Pakistan. *J. of Research (Science)*, Bahauddin Zakariya University Multan, Pakistan. 15(1), 59-65(2004b).
8. Akhtar, N., Tufail, M., Choudhry, M.A., Orfi, S.D. and Waqas, M. Radiation dose from natural and manmade radionuclides in the soil of niab, Faisalabad, Pakistan. *The Nucleus*, 41 (1-4) ,27-34 (2004).
9. Akhter, P., Ashraf, N., Mohammad, D., Orfi, S.D. and Ahmad, N. Nutritional and radiological impact of dietary potassium on the Pakistani population. *Food Chem. Toxicol.*, 41(4), 531-4 (2003a).
10. Akhter, P., Iqbal, S., Orfi, S. D., Kawamura, H. and Ahmad, N. Thorium concentration in Pakistani diet. *Health Phy.*, 84(6), 784-787 (2003b).
11. Akhter, P., Rahman, K., Orfi, S.D. and Ahmad, N. Radiological impact of dietary intakes of naturally occurring radionuclides on Pakistani adults. *Food Chem. Toxicol.*, 45(2), 272-7 (2007).
12. Akram, M., Khattak, N. U., Qureshi, A. A., Iqbal, A., Tufail, M. and Qureshi, I. E. Fission track estimation of Uranium Concentrations in drinking water from Azad Kashmir, Pakistan. *Health Phy.*, 86(3), 296-302 (2004).
13. Akram, M., Khattak, N.U., Iqbal, A., Qureshi, A.A., Ullah, K. and Qureshi, I.E. Measurement of radon concentration in dwellings of Skardu city, Pakistan. *Radiat. Meas.*, 40, 695 – 698 (2005).

14. Akram, M., Khattak. N.U., Iqbal. A .A. and Qureshi, A.A. Measurement of radon concentrations in dwellings of Skardu city, Pakistan. *Radiat. Meas.*, 40,695-698 (2005).
15. Akram, M., Qureshi, R.M., Ahmad, N. and Solaija T.M. Determination of gamma-emitting radionuclides in the inter-tidal sediments off Baluchistan (Pakistan) coast, Arabian Sea. *Radiat. Protect. Dosim.*, 123(2), 268-273 (2007).
16. Akram, M., Qureshi, R.M., Ahmad, N., Solaija, T.J., Mashiatullah, A., Afzal, M., Faruq, M.U. and Zeb, L. Concentration of natural and artificial radionuclides in bottom sediments of Karachi Harbour/Manora Channel, Pakistan Coast (Arabian Sea). *J. of the Chem. Society of Pakistan*, 28(3), 306-312 (2006).
17. Akram, M., Qureshi, R.M., Ahmad, N., Solaija, T.M. Gamma-emitting radionuclides in the shallow marine sediments off the Sindh coast, Arabian Sea. *Radiat. Protect. Dosim.* 118(4), 440-447 (2006).
18. Alam, M.N., Chowdhury, M.I., Kamal, M., Ghose, S., Islam, M.N., Mustafa, M.N., Miah, M.M.H. and Ansary, M.M. The ^{226}Ra , ^{232}Th and ^{40}K activities in beach sand minerals and beach soils of Cox's Bazar, Bangladesh. *J. Environ. Radioact.*, 46, 243–250 (1999).
19. Aldenkamp, E. J., de Meijer, R. J., Put, L. W, and Stoop, P. An assessment of in situ radon exhalation measurements. and the relation between free and bound exhalation rates. *Radiat. Prot. Dosim.*, 45, 449 - 453 (1992).
20. Ali, A., Orfi, S.D. and Qureshi, A.A. Assessment of the natural radioactivity and its radiological hazards in Shewa-Shahbaz Garhi igneous complex, Peshawar Plain, NW Pakistan. *Health Phys.*, 82(1),74-9 (2002).
21. Ali, S., Tufail, M., Jamil, K., Ahmad, A. and Khan, H.A. Gamma-ray activity and dose rate of brick samples from some areas of North West Frontier Province (NWFP), Pakistan. *Sci. Total. Environ.*, 87(3), 247-52 (1996).
22. Al-Jarallah, M.I., Fazal-ur-Rehman, Musazay, M.K. and Aksoy, M.S. A correlation between radon exhalation and radium content in granite samples used as construction material in Saudi Arabia. *Radiat. Meas.*, 40, 625 – 629 (2005).
23. Amgarou, K. Long-term measurements of indoor radon and its progeny in the presence of thoron using nuclear track detectors: A Novel Approach PhD Thesis April, 2002 University of Barcelona (2002).
24. Amrani, D. and Cherouati, D. E. Radon exhalation rate in building materials using plastic track detectors. *J. Radioanal. Nucl. Chem.*, 242(2), 269-271(1999).
25. Amutha, R., Brahmanandhan, G.M., Malathi, J., Khanna, D., Selvasekarapandian, S., Sarida, R., Meenakshisundaram, V. and Gajendran, V. Study of background radiation from soil samples of Pollachi taluk, Tamilnadu, India. *International Congress Series*, 1276, 331– 332 (2005).
26. Arvela, H. Seasonal variation in radon concentration of 3000 dwellings with model comparisons. *Radiat. Prot. Dosim.*, 59(1), 33–42 (1995).

27. Aslam, M., Orfi, S. D., Khan, K. and Jabbar, A. Radiological significance of Pakistani marble used for construction of dwellings. *J. Radioanal. Nucl. Chem.*, 253(3), 483-487 (2002).
28. Bahtijari, M., Stegnar, P., Shemsidini, Z., Ajazaj, H., Halimi, Y., Vaupotič, J. and Kobal, I. Seasonal variation of indoor air radon concentration in schools in Kosovo. *Radiat. Meas.*, 42(2), 286-289 (2007).
29. Baixeras, C., Erlandsson, B., Font, L., Jonsson, G. Radon emanation from soil samples. *Radiat. Meas.*, 34, 441– 443 (2001).
30. Baysson, H., Billon, S., Laurier, D., Rogel, A. and Tirmarche, M. Seasonal correction factors for estimating radon exposure in dwellings in France. *Radiat. Prot. Dosim.*, 104(3), 245–252 (2003).
31. BEIR-VI (Committee on Health Risks of Exposure to Radon -National Research Council), Health effects of exposure to radon. National Academy Press, Washington, DC. ISBN: 0-309-52374-5, 516 (1999).
32. Bennett, B.G. Exposure to natural radiation worldwide. Proceedings of the Fourth International Conference on High Levels of Natural Radiation: Radiation Doses and Health Effects, Beijing, China. Elsevier, Tokyo, 15–23 (1997).
33. Beretka, J. and Matthew, P.J. Natural radioactivity of Australian building materials industrial wastes and by-products. *Health Phys.*, 48, 87–95 (1985).
34. Bigu, J. Radon-220 determination using activated “C” and a high purity Ge detector. *Health Phys.*, 51, 534- 538 (1986).
35. Bigu, J., Callumand, Mc, B. A., Grasty, R.L. Environmental levels of thoron, Radon and their progeny in Manitoba, Canada: Paper Presented at 26th Midyear Topical Meeting of the Health Physics Society, LLRWMO-GN-TP-93-007, 373-389 (1993).
36. Billon, S., Morin, A., Caër S., Baysson, H., Gambard, J. P., Backe, J. C., Rannou, A., Tirmarche, M. and Laurier, D. French population exposure to radon, terrestrial gamma and cosmic rays. *Radiat. Prot. Dosim.*, 113(3) 314–320 (2005).
37. Bochicchio, F. Case-control studies on residential radon and lung cancer: A concise review. *Arch. Oncol.*, 12(1), 19-24 (2004).
38. Bochicchio, F. Radon epidemiology and nuclear track detectors: Methods, results and perspectives. *Radiat. Meas.*, 40, 177 – 190 (2005).
39. Brounstein, R. and Johnson, W.H. Influence of fiber-reinforced concrete on radon concentrations. *J. of Materials in Civil Eng.*, 16 (6) 646–649 (2004).
40. Burbank, D.W. and Tahirkhele, A.R.K., Magnetostratigraphy fission track dating and stratigraphic evolution of the Peshawar intermountain basin, north Pakistan. *Geological society of America.*, 96, 539-552 (1985).
41. Butt, K. A., Amanat, A. and Qureshi, A. A. Estimation of environmental gamma background radiation levels in Pakistan. *Health Phys.*, 75(1), 63-66 (1998).

42. Buzinny M. and Los, I. Comparative measurements of radon thoron and their daughters. In: Proceedings of European Conference on Protection against Radon at Home and at Work. Praha, 2 - 6, 33 – 48 (1997).
43. Cartwright, B.G., Shirk, E.K. and Price, P.B. A nuclear track recording polymer of unique sensitivity and charge resolution. Nucl. Instrum. Methods 153, 457–460 (1978).
44. Chalupnik S. and Wysocka, M. Development of the method for measurement of radon exhalation from the ground. Proceedings of ICGG7: 62–64c Copernicus GmbH 2003 ICGG7 (2003).
45. Chaudhry, Z. S., Khan, H. M., Khan, K., Aslam, M., Jabbar, A. and Orfi, S. D. Terrestrial absorbed dose rate measurement in the Jhangar valley of Pakistan. J. Radioanal. and Nucl. Chem., 253(3), 497-499 (2002).
46. Cheng, Y. S and Yeh, H. C. Theory of a screen-type diffusion battery. Journal of Aerosol Science, 11(3), 313-320 (1980).
47. Clouvas, A. Xanthos, S. and Antonopoulos-Domis, M. Simultaneous measurements of indoor radon, radon–thoron progeny and high-resolution gamma spectrometry in Greek dwellings. Radiat. Protect. Dosim., 118(4), 482-90 (2006).
48. Cohen B. L. and Nason R.; A diffusion barrier charcoal adsorption collector for measuring Rn concentration in indoor air. Health Phys., 50- 457 (1986).
49. Colle', R., Kotrappa, P. and Hutchinson, J. M. R. Calibration of electret-based integral using NIST polyethylene-encapsulated ²²²Rn emanation (PERE) standards. J. Res. Natl. Inst. Stand. Technol., 100(6), 629 (1995).
50. Comparative dosimetry of radon in mines and homes. National Academy Press Washington, D.C ISBN: 0-309-57233-9, 256 (1991).
51. Cozmuta, I., Van der Graaf, E.R. and de Meijer, R.J. Moisture dependence of radon transport in Concrete: measurements and modeling. Health Phys., 85(4), 438-456 (2003).
52. Cozmuta, I., van der Graaf, E.R.. Methods for measuring diffusion coefficients of radon in building materials. The Science of the Total Environment 272, 323-335 (2001).
53. Daniel, K., Lubin, J. H., Zielinski, J. M., Alavanja, M., Vanessa ,S., Catalan Field, R. W. Klotz, J. B., Le'tourneau, E., Lynch, C. F., Lyon, J. L., Sandler, D. P, Schoenberg, J. B., Steck, D. J., Stolwijk, J.A., Weinberg, C. and Wilcox, H. B. A Combined Analysis of North American Case–Control Studies of Residential Radon and Lung Cancer: An Update. Radiat. Research, 158(6), 785-790 (2002).
54. Darby, S., Hill, D., Auvinen, A., Barros-Dios, J. M., Baysson, H., Bochicchio, F., Deo, H., Falk, R., Forastiere, F., Hakama, M., Heid, I., Kreienbrock, L., Kreuzer, M., Lagarde, F., Mäkeläinen, I., Muirhead, C., Oberaigner, W., Pershagen, G., Ruano-Ravina, A., Ruostenoja, E., Rosario, A.S., Tirmarche, M., Tomásek, L., Whitley, E., Wichmann H.E, Doll, R. Radon in homes and risk of lung cancer: collaborative

- analysis of individual data from 13 European case-control studies. *B M J*, 330; 330(7485), 223 (2005).
55. Denman, R. Groves-Kirkby, C.J., Phillips, P.S., Crockett, R.G.M., Woolridge, A. and Gillmore, G.K. The practical use of electrets in a public health radon remediation campaign. *J. of Environ. Radioact.*, 84(3), 375-380 (2005).
 56. Dissanayake, C. Of stones and health: Medical geology in Sri Lanka. *Global voices of science. Science*, 309, 883-85 (2005).
 57. District census Report of Charsadda January 2000. Report No. 68.
 58. District census Report of Mardan July 1999. Report No. 28.
 59. District census Report of Swabi April 2000. Report No. 83.
 60. Dixon, D.W. and Scivyer, C. Radon and remedial issues. *Structural Survey*, 17(3), 154–159 (1999).
 61. Doi, M. and Kobayashi, S. Spatial distribution of Radon and thoron concentrations in the indoor air of a traditional Japanese wooden house. *Health Phys.*, 66, 43–49 (1994).
 62. Doi, M., Fujimoto, K., Kobayashi, S. and Yonehara, H. Spatial distribution of thoron and Radon concentrations in the indoor air of a traditional Japanese wooden house. *Health Phys.*, 66, 43– 49 (1994).
 63. Doi, Masahiro; Fujimoto, Kenzo; Kobayashi, Sadayoshi; Yonehara, Hidenori. Spatial Distribution of thoron and radon concentrations in the indoor air of traditional Japanese wooden house. *Health Phys.*, 66(1), 43-49 (1994).
 64. Dua, S K., Kotrappa, P., Srivastava, R., Ebadian, M.A, Stieff, L.R. Measurement of alpha particle energy using windowless electret ion chambers. *Health Phys.*, 83(4), 549-52 (2002)
 65. Dua, S.K., Kotrappa, P., Srivastava, R., Ebadian, M. A. and Stieff, L. R. Measurement of alpha particle energy using windowless electret ion chambers. *Health Phys.*, 83(4): 549-52 (2002).
 66. Nikezi Ć, D and Yu, K. N. Uncertainty in radon measurements with CR39 detector due to unknown deposition of ^{218}Po . *Nucl. Instrum. and Methods in Phys. Research A* 450, 568-572 (2000).
 67. Dumm, J.P. Factors affecting deposition, implantation, and retention of radon progeny in glass a thesis. The Honors Program, St. John's University/College Of St. Benedict, MN, USA(Supervised By Dr. Daniel J. Steck) (2005).
 68. Durrani, S. A. and Ilić, R. Radon measurements by etched track detectors: Applications in radiation protection, earth sciences and the environment (Singapore: World Scientific Publishing Co. Pte Ltd) ISBN 9810226667 (1997).
 69. Durrani, S.A. Radon as a health hazard at home: what are the facts? *Nucl. Tracks Radiat. Meas.*, 22, 303-317 (1993).

70. Durrige Company Inc., 2000, Durrige Company Inc., Rad 7 Radon Detector. Part No. 1280, Durrige Company Inc., Bedford, MA (2000).
71. Dwivedia, K.K., Mishra, R. and Tripathy, S.P. An extensive indoor $^{22}\text{Rn}/^{220}\text{Rn}$ monitoring in north-east India. *Radiat. Meas.*, 40,621– 24 (2005).
72. Eappen, K.P. Nair, R.N. and Mayya, Y.S. Simultaneous measurement of radon and thoron using Lucas scintillation cell. *Radiat. Meas.*, doi:10.1016/j.radmeas.2007.07.007.
73. Eisenbud, M. and Gesell, T., Eds; Environmental radioactivity. 4th ed. San Diego: Academic Press. pp. 134-200 (1997).
74. El-Bahi, S. M. Assessment of radioactivity and radon exhalation rate in Egyptian cement. *Health Phys.*, 86(5), 517-522 (2004).
75. EPA Assessment of Risks from Radon in Homes. United States Environmental Protection Agency. EPA 402-R-03-003 (2003).
76. EPERM System Manual Rad Elec Inc., 5714-C, Industry Lane, Frederick, MD 21703 Part-II Section. Manual of E-PERMS Part-II II.4.Alpha Rev#0 (1994)
77. Ernest, C. Y., Ho and David, F. Measday. A simple model for describing the concentration of ^{212}Pb in the atmosphere. *J.of Environ. Radioact.*, 78(3), 289-309 (2005).
78. Espinosa, G., Golzarri, J.I., Martínez, T., Navarrete, M., Bogard, J., Martínez, G., Juárez, F. Indoor ^{220}Rn and ^{222}Rn concentration measurements inside the Teotihuacan pyramids using NTD and E-PERM methodologies. *Radiat. Meas.*, 40 646 – 649(2005).
79. E. A. MARTELL. α -Radiation dose at bronchial bifurcations of smokers from indoor exposure to radon progeny. *Proc. Nati Acad. Sci. USA*, 80, 1285-1289 (1983).
80. Faheem, M., Mujahid, S.A. and Matiullah. Assessment of radiological hazards due to the natural radioactivity in soil and building material samples collected from six districts of the Punjab province-Pakistan. *Radiat. Meas.* doi:10.1016/j.radmeas.2008.02.014 (2008).
81. Fatima, I., Zaidi, J. H., Arif, M. and Tahir, S.N. Measurement of natural radioactivity in bottled drinking water in Pakistan and consequent dose estimates. *Radiat. Protect. Dosim.*, 123 (2), 234-40 (2007).
82. Fatima, I., Zaidi, J. H., Arif, M., Daud, M., Ahmad, S. A. and Tahir, S. N. A. Measurement of natural radioactivity and dose rate assessment of terrestrial gamma radiation in the soil of southern Punjab, Pakistan. *Radiat. Protect. Dosim.*, 128(2), 206-212 (2008).
83. Ferry, C., Beneito, A., Richon, P. and Robe, M.C. An automatic device for measuring the effect of meteorological factors on radon-222 flux from soils in the long term. *Radiat. Prot. Dosim.*, 93(3),271–274 (2001).

84. Fleischer, R.L., Price, P.B. and Walker, R.M. Nuclear Tracks in Solids. University of California Press, Berkley, 1975.
85. Fournier, F., Groetz, J. E., Jacob, F., Crolet, J. M. and Lettner, H. Simulation of radon transport through building materials: influence of the water content on radon exhalation rate. *Transp. Porous Med.*, 59,197–214 (2005).
86. Fricke, V. WSRC-TR-99-00460. E-Perm Alpha Surface Monitor. Westinghouse Savannah River Company Savannah River Site Aiken, South Carolina 29808
87. Friedmann, H. “A portable radon meter”. *Radiat. Protect., Dosim.* 4:118-121 (1983).
88. Galmarini, S. ^{222}Rn concentration in the atmospheric surface layer. *Atmos. Chem. Phys.*, 6, 2865–2887 (2006).
89. Gargioni, E. and Arnold, D. Reference fields and calibration techniques for Rn-220 measuring instruments. *International Congress Series*, 1276, 85-88 (2005).
90. George A.C. State-of-the-art instruments for measuring Radon thoron and their progeny in dwellings: A review. *Health Phys.*, 70(4):451-463 (1996).
91. Gervino, G., Barca, D., Bruno, S., Bonetti, R. and Manzoni, A. Annual average and seasonal variations of indoor radon concentrations in Piedmont (Italy) using three different detection techniques. *Nuclear Instruments and Methods in Physics Research Section A: 572(1)*, 254-256 (2007).
92. Gervino, G., Bonetti, R., Cigolini, C., Marino, C., Prati, P. Pruiti, L. Environmental radon monitoring: comparing drawbacks and performances of charcoal canisters, alpha-track and E-PERM detectors. *Nuclear Instruments and Methods in Physics Research A*, 518, 452–455 (2004).
93. Gingrich, J.E. Radon as a geochemical exploration tool. 10th international geochemical exploration symposium, Finland (1983).
94. Knoll, G.F. *Radiation Detection and Measurement* Wiley; 3 edition ISBN-10: 0471073385 (2000).
95. Godoy, M., Hadler, J.C.N., Iunes, P.J., Mestanza, S.N., Oliveira, R.A., Osorio Ac, A.M., Paulo, S.R. Effects of environmental conditions on the radon daughters spatial distribution. *Radiat. Meas.*, 35, 213 – 221 (2002).
96. Grainger, P., Shalla, S. H., Preece, A. W., Goodfellow, S. A. Home radon levels and seasonal correction factors for the Isle of Man. *Phys. Med. Biol.*, 45, 2247–2252 (2000).
97. Groves-Kirkby C.J., Denman, A.R., Crockett, R.G.M., Phillips, P.S., Woolridge, A.C., Gillmore, G.K. Time-integrating radon gas measurements in domestic premises: comparison of short-, medium-and long-term exposures. *Journal of Environ. Radioact.* 86, 92-109 (2006).
98. Guo, Q, Cheng, J., Shang, B. and Sun, J. The levels of indoor thoron and its progeny in four areas in China. *Journal of Nuclear Science and Technology*, 38(9), 799–803 (2001).

99. Guo, Q., Shimot, M., Ucebet, Y. and Minatof, S. The study of thoron and Radon concentrations in dwellings in progeny Japan. *Radiat. Protect. Dosim.*, 45, 357-359 (1992).
100. Hafez, A.F., Hussein, A.S. and Rasheed, N.M. A study of radon and thoron release from Egyptian building materials using polymeric nuclear track detectors. *J. App. Radiat. and Isotopes.*, 54, 291-298 (2001).
101. Hámori, K., Váradi, M. and Csikai, J. Space charge effect on the electrostatic collection of thoron decay products. *Applied Radiation and Isotopes*, 64(7), 854-857 (2006).
102. Health Effects of Exposure to Radon. BEIR VI Committee on Health Risks of Exposure to Radon. National Research Council, ISBN: 0-309-52374-5 (1999).
103. Heath, C.W. Jr., Bond, P.D., Hoel, D.G., Meinhold, C.B. Residential Radon Exposure and Lung Cancer Risk: Commentary. *Journal of Exposure Analysis and Environmental Epidemiology* 15(3), 243 (2005).
104. Hewamanna, R., Sumithrarachchi, C. S., Mahawatte, P., Nanayakkara, H. L. and Ratnayake, H. C. Natural radioactivity and gamma dose from Sri Lankan clay bricks used in building construction. *Appl. Radiat. Isot.*, 54(2), 365-9 (2001).
105. High-Resolution Gamma-Ray Spectroscopy Equipment Needed From EG&G ORTEC
106. Hofmann, W. Overview of radon lung dosimetry. *Radiat. Prot. Dosim.*, 79(1-4), 229-236 (1998).
107. Homer, J. B. and Miles, J.C.H. The effect of heat and humidity before, during after exposure on the response of PDAC (CR-39) to alpha particles. *Nucl. Tracks*, 12(1-6), 133-136 (1986).
108. Hosoda, M., Shimo, M., Sugino, M., Furukawa, M. and Fukushi, M. Relation between the radon and thoron exhalation rates and the environmental gamma-ray dose rate and the natural radionuclide concentrations. *Japanese Journal of Health Physics* 41(1), 18-26, 20060300 (ISSN 03676110) (2006).
109. IARC (International Agency for Research on Cancer. Radon and man-made mineral fibres. monographs on the evaluation of carcinogenic risks to humans. IARC, Lyon 43,(1988).
110. ICRP (International Commission on Radiological Protection). Lung cancer risk from indoor exposures to radon daughters. ICRP Publication 50. *Ann. ICRP* 17 (1), 1-60 (1987).
111. ICRP (International Commission on Radiological Protection). Protection against radon-222 at home and at work. ICRP Publication 65. *Ann. ICRP* 23 (2), 1-45 (1993).
112. ICRP publication 60. Recommendations of the international commission on radiological protection, Elsevier Publishing Limited ISBN-10: 0080411444 (1990).

113. Iimoto, T., Nagai, T., Sugiura, N. and Kosako, T. Emanating power of ^{220}Rn from a powdery radiation source. International Congress Series, 1276, 303-304 (2005).
114. International Commission on Radiological Protection. Lung cancer risk from indoor exposures to Radon daughters. ICRP Publication 50. Annals of the ICRP 17(1). Pergamon Press, Oxford, (1987).
115. International Commission on radiological protection. Protection against radon-222 at home and at work, ICRP Publication 65. Annals of the ICRP 23, (1993).
116. Iqbal, A., Baig, M. S., Akram, M., Qureshi, R. K., Rahim, S. and Quershi, A. A., Measurement of radon concentration using SSNTD in dwellings of Rawalakot area, Azad Jammu and Kashmir, sub-Himalayas, Pakistan Euro. J of Scientific Res., 17(3) 392-398 (2007c).
117. Iqbal, A., Baig, M. S., Akram, M., Bashir, A. and Quershi, A, A, Measurements of radon concentration in dwellings of Muzaffarabad city, Azad Kashmir, northwest Himalayas Pakistan. Euro. J of Scientific Res., 17 (3) 373-378 (2007b).
118. Iqbal, A., Baig, M. S., Akram, M., Qureshi, R. K. and Quershi, A. A. Measurement of radon concentration using SSNDT in dwellings of Jhelum valley, Azad Jammu and Kashmir, sub-Himalayas, northeast Pakistan. Euro. J of Scientific Res., 17 (3) 366-372 (2007a).
119. Iqbal, M., Tufail, M. and Mirza, S.M. Measurement of natural radioactivity in marble found in Pakistan using a NaI(Tl) gamma-ray spectrometer. J. Environ. Radioact., 51(2),255-265 (2000).
120. Ishikawa, T., Tokonami, S. and Nemeth, C. Calculation of dose conversion factors for thoron decay products. J. Radiol. Prot. 27, 447–456(2007).
121. Planinic, J., Faj, D., Vukovic, B., Faj, Z., Radolic, V. and Suveljak, B. Radon exposure and lung cancer. J. Radioanal. and Nucl. Chem., 256(2), 349–352 (2003).
122. Jabbar, T., Subhani, M. S., Khan, K., Rashid, A., Orfi, S. D. and Khan, A. Y. Natural and fallout radionuclide concentrations in the environment of Islamabad. J. Radioanal. and Nucl. Chem., 258 (1), 143-149 (2003).
123. James, A. C., Birchall, A. and Akaban, G. Comparative Dosimetry of BEIR VI Revisited. Radiat. Prot. Dosim., 108(1), 3-26 (2004).
124. James, A. C., Strona, J. C., Cliff, K. D. and Strandén, E.. The Significance of equilibrium and attachment in radon daughter dosimetry. Radiat. Protect. Dosim., 24(114), 451 - 455 (1988).
125. Jamil, K., Ali, S., Iqbal, M., Qureshi A. A. and Khan, H. A. Measurements of radionuclides in coal samples from two provinces of Pakistan and computation of external γ ray dose rate in coal mines. J. Environ. Radioact. 41(2), 207-216 (1998).
126. Jang, M., Kang, C.S., Moon, J. H. Estimation of Rn release from the phosphogypsum board used in housing panels. . J. Environ. Radioact., 80,156-160(2005).

127. Wiegand, J., Feige, S., Quingling, X., Schreiber, U., Wieditz, K., Wittmann, C. and Xiarong, L. Radon and thoron in cave dwellings (Yan'an, China). *Health Phys.*, 78(4), 438-44 (2000).
128. Jing, C. A review of radon doses. *Radiat. Protect. Manag.*, (22) 4, 27-31(2005).
129. Keskinen, J., Marjama, M., Annele Virtanen k., Makelat, T. and Hillamot R. Electrical calibration method for cascade Impactor. *J. Aerosol Sci.*, 30(1),111-116 (1999).
130. Kainan Sun, Marek Majdan, Daniel W. Field, and R. William Field. Field comparison of commercially available short-term radon detectors. *Health Phys.*, 91(3):221–226 (2006).
131. Karpińska, M., Mnich, Z., Kapała, J., Antonowicz, K., and Przystalski, M. Time changeability in radon concentration in one-family dwelling houses in the northeastern region of Poland. *Radiat. Protect. Dosim.*, 113, 300-307 (2005).
132. Kasper, K. Passive alpha electret ion chambers. *Health Phys.*, 76(5):475-476 (1999).
133. Khalil Amgarou. Long-Term Measurements of Indoor Radon and its Progeny in the Presence of Thoron Using Nuclear Track Detectors: A Novel Approach. PhD Thesis University of Barcelona (April, 2002).
134. Khan, S. A., Ali, S., Tufail, M. and Qureshi, A. A. Radon concentration levels in Fatima Jinnah women university Pakistan. *Radioprotection*, 40(1) 11-27 (2005).
135. Khan, A. and Philips, C.R. A simple two –count method for routine Monitoring og Rn-222 and Rn-220 progeny working level in U Mines. *Health Phys.*, 50(3), 381-388 (1986).
136. Khan, A., Busigin, A. and Philips, C.R. An Optimization scheme for measurement of the concentration of the decay products of radon and thoron. *Health Phys.*, 42(6), 809-826 (1982).
137. Khan, A., Phillips, C.R. and Duport, P. Analysis of errors in the measurement of unattached fractions of radon and thoron progeny in a Canadian uranium mine using wire screen methods. *Health Phys.*, 42(6),801-808 (1982).
138. Khan, E.U., Tufail, M., Ahmad, N., Malik, Q.N., Amjad, M. and Zulqarnain, S.M.Q. Natural radioactivity from the building materials used in Dera Ismail Khan Pakistan. *Turkish. J. Nucl. Sci.*, 22, 37–47(1995).
139. Khan, K. and Khan, H.M. Natural gamma-emitting radionuclides in Pakistani Portland cement. *Appl. Radiat. Isot.*, 54(5), 861-5 (2001).
140. Khan, K., Akhter, P. and Orfi, S. D. Estimation of radiation doses associated with natural radioactivity in sand samples of the north western areas of Pakistan using Monte Carlo simulation. *J. Radioanal. and Nucl. Chem.*, 265(3), 371-375 (2005).
141. Khan, K., Aslam, M., Orfi, S.D. and Khan, H.M. Radiological significance of building bricks in Pakistan. *Radiat. Protect. Dosim.*, 95 (3): 263–266 (2001).

142. Khan, K., Aslam, M., Orfi, S.D. and Khan, H.M. Norm and associated radiation hazards in bricks fabricated in various localities of the North-West Frontier Province (Pakistan). *J. Environ. Radioact.*, 58(1),59-66 (2002).
143. Khan, K., Akhter, P. and Orfi, S. D. Estimation of radiation doses associated with natural radioactivity in sand samples of the north western areas of Pakistan using Monte Carlo simulation. *J. of Radioanal. and Nucl.Chem.*, 265(3), 371-375 (2005).
144. Khan, K., Akhter, P., Orfi, S.D., Malik, G.M. and Tufail, M. Natural radioactivity levels in river, stream and drinking water of the northwestern areas of Pakistan. *J. Radioanal. Nucl. Chem.*, 256(2), 289-292 (2003).
145. Khan, K., Khan, H. M , Tufail, M., Khatibeh A. J. A. H. and Ahmad, N. Radiometric Analysis of Hazara Phosphate Rock and Fertilizers in Pakistan. *J. Environ. Radioact.*, 38(1), 77-84 (1998).
146. Khan, R.M. Khan, M.K., G.N., 1998. Geology of Koi Barmol and adjoining areas, district Mardan NWFP, Pakistan (BS Thesis University of Peshawar, Pakistan).
147. Killip, I. R. Radon hazard and risk in Sussex, England and the factors affecting radon levels in dwellings in chalk terrain. *Radiat. Protect. Dosim.*, 113, 99–107 (2004).
148. Kim, C., Lee, S.C., Lee, D.M, Chang, B.U., Rho, B.H. and Kang, H.D. Nationwide survey of radon levels in korea. *Health Phys.*, 84(3),354 –360 (2003).
149. Kitto, M. E. Interrelationship of indoor radon concentrations, soil gas flux, and meteorological parameters. *J. Radioanal. Nucl. Chem.*, 264(2), 381-385 (2005).
150. Klement Jr. A.W. Hand-book of environmental radiation, CRC Press, 1982,15– 21 (1982).
151. Knutson, E.O., Hubbards, L. M. and Balker, B. M. Determination of the surface to volume ratio in homes from measurements of radon and its progeny introduction. *Radiat. Protect. Dosim.*, 42(2), 121-126 (1992).
152. Kotrappa, P. and Stieff, L.R. Recent advances in electret ion chamber technology for radiation measurements. *Radiat. Prot. Dosim.*, 47,461–464 (1993).
153. Kotrappa, P. et al Development of Electret Technology to Measure Indoor Radon daughter concentration. UNC/GJ-TMC-5, UC-511, Project: UNC 88024 (1989).
154. Kotrappa, P., Bhanti, D. P. and Dhandayutham, R. Diffusion sampler useful for measuring diffusion coefficients and unattached fraction of Radon and thoron decay products. *Health Phys.* 29(1), 155-162 (1975).
155. Kotrappa, P., Dempsey, J. C., Hickey, J. R. and Stieff, L. R. An electret passive environmental ²²²Rn monitor based on ionization measurement. *Health Phys.*, 54(1), 47-56 (1988).
156. Kotrappa, P., Rampsey, J. C., Ramsey, R. W., Stieff, L. R. Practical E-PERM TM (Electret Passive Environmental Radon Monitor) system for indoor ²²²Rn measurement. *Health Phys.* 58 (4), 461-467 (1990).

157. Kotrappa, P. and Stieff, L. R. Elevation Correction Factors for E-Perm Radon Monitors. *Health Physics.*, 62(1), 82-86 (1992).
158. Kumar, R., Sengupta, D. and Prasad, R. Natural radioactivity and radon exhalation studies of rock samples from Surda Copper deposits in Singhbhum shear zone. *Radiat. Meas.*, 36, 551 – 553 (2003).
159. Lavi, N., Alfassi, Z.B. Development of Marinelli beaker standards containing thorium oxide and application for measurements of radioactive environmental samples *Radiat. Meas.*, 39, 15 – 19 (2005).
160. Lee, S.C., Kim, C.K., Lee D.M. and Kang. H. D. Natural radionuclides contents and radon exhalation rates in building materials used in south Korea *Radiat. Prot. Dosim.*, 94(3), 269–274 (2001).
161. Lee, T.K.C, Yu, K.N. Effects of air conditioning, dehumidification and natural ventilation on indoor concentrations of ^{222}Rn and ^{220}Rn . *J. of Environ. Radioact.*, 47, 189-199,(2000).
162. Leonard, B. Radioisotope deposition on interior building surfaces: Air flow and surface roughness influences. *Nuclear Technology, Nucl. Technol.*, 152(3), 339-353 (2005).
163. Levin, I., Born, M., Cuntz, M., Langendörfer, U., Mantsch, S., Naegler, T., Schmidt, M., Varlagin, A., Verclas, S. and Wagenbach, D. Observations of atmospheric variability and soil exhalation rate of radon-222 at a Russian forest site Technical approach and deployment for boundary layer studies. *TELLUS*, ISSN 0280–6509 (2002).
164. Li, Y., Schery, S. D., Turk, B. Soil as a Source of Indoor ^{220}Rn . *Health Phys.*, 62(5):453-457 (1992).
165. Lide D. L. Chemical Rubber Company (CRC). *Handbook of Chemistry and Physics*, The CRC Press, 82th Edition (2001).
166. Lubin, J.H., Boice Jr., J.D., Edling, C. , Hornung, R.W., Howe, G.R., Kunz, E., Kusiak, R.A., Morrison, H.I., Radford, E.P., Samet, J.M., Tirmarche, M., Woodward, A., Xiang, Y.S., Pierce. D.A., 1994. *Radon and Lung Cancer Risk: A Joint Analysis of 11 underground miners studies*. Vol. NIH Publication No. 94-3644. Washington, DC: US Department of Health and Human Services (1994).
167. Lubin, J.H., Boice, J.D., Edling, C., Hornung, R.W., Howe, G.R., Kunz, E., Kusiak, R.A., Morrison, H.I., Radford, E.P., Samet, J.M., Tirmarche, M., Woodward, A., Yao, S.X. and Pierce, D.A. Lung cancer in radon-exposed miners and estimation of risk from indoor exposure. *J. of the National Cancer Institute*, 87(11), 817-827 (1995).
168. Lucas, H. F. Improved low level alpha scintillation counter for radon. *Rev. Scient. Instrum.* 28: 680 (1957).
169. M. A. Misdaq, F. Ait Nouh, W. Bourzik the influence of the soil and plant natures and pollution. *J. Radioanal. Nucl. Chem.*, 247(2), 357-361 (2001).

170. Ma, J., Yonehara, H., Aoyama, T., Doi, M., Kobayashi, S. and Sakaunoe, M. Influence of air flow on the behavior of thoron and its progeny in a traditional Japanese house. *Health Phys.*, 72, 86–91 (1997).
171. Maged, A.F. and Ashraf, F.A. Radon exhalation rate of some building materials used in Egypt. *Environ. Geoch. and Health.*, (27), 485–489 (2005).
172. Mahat, R. H., Bradley, D. A., Amin, Y. M., Wong, C. Y. and Su, L. D. The effect of humidity on the accuracy of measurement of an electret radon dosimeter. *Radiat. Phys. and Chem.*, 61(3-6), 489-490 (2001).
173. Mahmud, K. R. Radionuclide content of local and imported cements used in Egypt. *J. Radiol. Prot.*, 27, 69-77 (2007).
174. Majborn, B. Seasonal variations of radon concentrations in single-family houses with different sub-structures. *Radiat. Prot. Dosim.*, 45(1–4), 443–447 (1992).
175. Maniyan, C. G., Haridasan, P. P., Paul, A. C. and Rudran, K. Influence of plate out of thoron progeny on formation of tracks in SSNTD films (LR-115-II) *Radiat. Protect. Dosim.*, 82, 263-269 (1999).
176. Martell E. A. Biophysics a-Radiation dose at bronchial bifurcations of smokers from indoor exposure to Radon progeny *Proc. Nati. Acad. Sci. USA.* 80, 1285-1289 (1983).
177. Martin, N.R., Siddique, S.F.A. and King, B.H. Geological reconnaissances of the region between lower swat and Indus river of Pakistan. *Geo. Bull. Punjab Univ.* 2, 1-13 (1962).
178. Martinez, T., Lartigue, J., Navarrete, M., Cabrera, L., Gonzalez, P., Ramirez, A. and Elizarraras, V. Long term equilibrium factor and indoor radon measurements. *J. Radioanal. Nucl. Chem.*, 236(1-2), 231-238 (1998).
179. Martz, D. E., Falco, R.J., Langner, G. and Harold, Jr. Time-averaged exposures to ^{220}Rn and ^{222}Rn progeny in Colorado homes. *Health Phys.*, 58(6), 705-713 (1990).
180. Matiullah, Ahad, A., Rehman, S. and Mirza, M. L. Indoor radon levels and lung cancer risk estimates in seven cities of the Bahawalpur division, Pakistan. *Radiat. Protect. Dosim.*, 107(4) 269–276 (2003).
181. Matiullah, Ahad, A., Rehman, S.U., Rehman, S.U. and Faheem, M. Measurement of radioactivity in the soil of Bahawalpur division Pakistan. *Radiat. Protect. Dosim.*, 112, 443–447 (2004).
182. Matiullah, Ahad, A., Rehman. S. and Mirza, M. L. Indoor radon levels and lung cancer risk estimates in seven cities of the Bahawalpur division, Pakistan. *Radiat. Protect. Dosim.*, 107 (4), 269–276 (2003).
183. Matiullah, Bashir, A., Kudo, K. and Yang, X.. Radon measurements in some houses of Tsukuba science city - Japan. *Nucl. Tracks and Radiat. Meas.*, 22, 395–398 (1993a).

184. McLaughlin, J.P., Miles, J.C.H., Olast, M., Rannou, A., Tommasino, L., Torri, G.C. and Wasiolek, P. French/Irish/Italian field intercomparison of passive alpha track radon detectors. *Radiat. Protect. Dosim.*, 45,53-55 (1992).
185. Meinhold, B. Dosimetric and epidemiological approaches to assessing radon doses. *Health Phys.*, 87(6), 647–655 (2004).
186. Merdanoglu, B. and Altinsoy, N. Radioactivity concentrations and dose assessment for soil samples from Kestanol granite area, Turkey. *Radiat. Prot. Dosim.*, 121, 399–405 (2006).
187. Michael, J. S., Health criteria for radon indoors. *Environ. Manag. and Health*, 6(2), 34-36 (1995).
188. Michikuni, S. Jun, S., Tadashi, T., Keizo, Y. and Tsuneo, Y. Development of in-situ type radon/thoron exhalation rate measuring system, 10 (19941230), 19-26. Gifu College of Medical Technology ISSN:09120513 (1994).
189. Misdaq, M. A. Use of three new SSNTD methods for evaluating thorium contents in different building materials and measuring thoron and its progeny concentrations inside dwellings. *Applied Radiation and Isotopes*, 57(2), 285-289 (2002).
190. Misdaq, M. A., Ezzahery, H., Lamine, J. Influence of the building material and ventilation rate on the concentration of radon, Thoron and their progenies in dwelling rooms using SSNTD and Monte Carlo simulation. *J. of Radioanal. and Nucl. Chem.*, 252(1) 67– 74 (2002).
191. Mishra, R., Tripathy, S. P., Khathing, D. T. and Dwivedi, K. K. An extensive indoor $^{222}\text{Rn}/^{220}\text{Rn}$ monitoring in Shillong, India. *Radiat. Protect. Dosim.*, 112(3), 429–433 (2004).
192. Mohamed, A and El-Hussein, A. Comparison of outdoor activity size distributions of ^{220}Rn and ^{222}Rn progeny. *Appl. Radiat. Isot.*, 62 (6), 955-9 (2005).
193. Mohamed, A. and El-Hussein, A. Comparison of outdoor activity size distributions of ^{220}Rn and ^{222}Rn progeny. *Applied Radiation and Isotopes*, 62, 955–959 (2005).
194. Mujahid, S.A. Hussain, S. Dogar, A.H., Karim, S. Determination of porosity of different materials by radon diffusion. *Radiat. Meas.*, 40, 106 – 109 (2005).
195. Najeeb, R., Hussain, E. and Masood, U. Determination of radiological doses of radon and natural radionuclides in the open environment of the Lahore and Kasur districts, Pakistan. *International journal of scientific research* 14, 11-17 (2005).
196. National Research Council (US). Committee on the Health Risks of Exposure to Radon (BEIR VI). Health Effects of Exposure to Radon. Committee on the Biological Effects of Ionizing Radiations, Board of Radiation Effects Research, Committee on Life Sciences, National Research Council. Washington, DC: National Academy Press (1999).
197. National Research Council. Committee on the Biological Effects of Ionizing Radiations. Health risks of radon and other internally deposited alpha-emitters: BEIR IV; Washington, D.C. National Academy Press (1988).

198. Natural Ionizing Radiation and Health Proceedings from a symposium held at the Norwegian Academy of Science and Letters, Oslo 6-7 June 2001 Edited by B. Bølviken, Geological Survey of Norway, Sondheim, Norway (2001).
199. NEA/OECD (Nuclear Energy Agency /Organisation for Economic Co-operation and Development)(1983), "Dosimetry aspects of exposure to radon and thoron decay products", Expert Group Report, OECD, Paris.
200. Neman, R., Hadler, J.C., N, Iunes, P.J., Paulob, S.R., Guedes, S., Curvo, E.A.C. Inter-comparison of three techniques for radon activity measurements. *Radiat. Meas.*, 40, 295 – 298 (2005).
201. Nero, A. V. Radon and its decay products in indoor air. New York: John Wiley; 1-47 (1988).
202. Neznal, M. and Neznal, M. International intercomparison measurement of soil-gas radon concentration, of radon exhalation rate from building materials and of radon exhalation rate from the ground Czech republic. Radon, v.o.s. corp., Novákových 6, 180 00 Praha 8, Czech Republic (2002).
203. Nikezic, D. and K.N. Yu. Computer program TRACK_TEST for calculating parameters and plotting profiles for etch pits in nuclear track materials *Computer Physics Communications* 174, 160–165 (2006).
204. Nikezic, D. and Stevanović, N. Room model with three modal distributions of attached ^{220}Rn progeny and dose conversion factor. *Radiat. Protect. Dosim.*, 123(1),95-102 (2007).
205. Nikezic, D. and Yu, K. N. Are radon gas measurements adequate for epidemiological studies and case control studies of radon-induced lung cancer? *Radiat. Prot. Dosim.*, 113(2), 233–235 (2005).
206. Nikezic, D., Markovic, P., Uzarov, D.B. Calculating the calibration coefficient for radon measurements with the bare LR115-II track detector. *Health Phys.*, 62 239 (1992).
207. Nishikawa, T., Okabe, S. and Aoki, M.. Seasonal variation of radon daughters concentrations in the atmosphere and in precipitation at the Japanese coast of the sea of Japan. *Radiat. Protect. Dosim.*, 24(114), 93-95 (1988).
208. NRPB 1990. Board Statement on limitation of human exposure to Radon in Homes. Documents of the NRPB, 1(1) HMSO, ISBN 0-89591-322-X (1990).
209. NRPB. Exposure to radon daughters in Dwellings NRPB ,Chilton, NRPB (1987).
210. Nuccetelli, C. and Bochicchio, F. The Thoron issue: monitoring activities, measuring techniques and dose conversion. *Radiat. Protect. Dosim.* 78, 59-64 (1998).
211. OECD. Exposure to radiation from natural radioactivity in building materials. Report by a group of experts of the OECD Nuclear Energy Agency Paris France (1979).
212. Oufni, L. Determination of the radon diffusion coefficient and radon exhalation rate in Moroccan quaternary samples using the SSNTD technique *J. Radioanal. Nucl. Chem.*, 256(3), 581–586 (2003).

213. Pagelkopf, P. and Porstendörfer, J. Neutralisation rate and the fraction of the positive Po-218 clusters in air. *Atmos. Environ.*, 37, 1057–1064 (2003).
214. Papp, G., Marx, G., Szalai, S. and Tóth, E. Year by year changes of indoor radon levels. *J. of Radioanal. and Nucl. Chem.*, 250(3), 541–545 (2001).
215. Papp, Z. and Dezső, Z. Measuring radon progeny and thoron progeny in air by absolute beta counting subsequent to grab sampling. *Radiat. Meas.*, 41(5), 617–626 (2006).
216. Paschoa, A.S. More than forty years of studies of natural radioactivity in Brazil. *Technology*, 7, 193–212 (2000).
217. Paulus, L. R., Walker, D. W. and Thompson, K. C. A field test of electret ion chambers for environmental remediation verification. *Health Phys.*, 85(3), 371–376 (2003).
218. Pearson, M.D. and Spangler, R.R. Calibration of α -track monitors for measurement of thoron(^{220}Rn). *Health Phys.*, 60(5), 697–701 (1991).
219. Pilkte, L and Butkus, D. Influence of gamma radiation of indoor radon decay products on absorbed dose rate. *JRNL of Environmental Engineering and Landscape Management* ISSN 1648-6897, 8(2), 65-72 (2005).
220. Pilkyte, L., Butkus, D. and Morkunas, G. Assessment of external dose indoors in Lithuania. *Radiat. Prot. Dosim.*, 121(2), 140–147 (2006).
221. Pinel, J., Fearn, T., Darby, S.C. and Miles, J.H.C. 1995. Seasonal correction factors for indoor radon in the UK exposure in dwellings in France. *Radiat. Prot. Dosim.*, 58(2), 127–132 (1995).
222. Porstendörfer, J. Radon: measurement related to dose. *Environment international* 232, 1 1563–583 (1996).
223. Porstendörfer, J. and Mercer, T. T. Influence of electric charge and humidity upon the diffusion coefficient of Radon decay products. *Health Phys.*, 37, 191–199 (1979).
224. Porstendörfer, J. and Reineking, A. Radon: characteristics in air and dose conversion factors, *Health Physics*, 76(3), 300–305 (1999).
225. Porstendörfer, J. Physical parameters and dose factors of the radon and thoron decay products. *Radiat. Prot. Dosim.*, 94, 365–373 (2001).
226. Porstendörfer, J. Properties and behaviour of radon and thoron and their decay products in the air. *J. of Aerosol Science*. 25(2), 219–263 (1994).
227. Prichard, H. M., Venso, E. A., and Dodson, C. L. Liquid scintillation analysis of ^{222}Rn in water by alpha/beta discrimination. *Radioact. and Radio chem.* 3(10), 28–36 (1991).
228. Progeny Group Limited at <http://www.progenygrp.com/>
229. Qazi, J.I. and Jafri, R.H. Uptake and concentration of uranium in animals and plants from a natural radioactive terrestrial ecosystem in Pakistan Punjab University. *Punjab Univ. J. Zool.*, 11, 51–56 (1996).

230. Ramola, R. C., Negi, M. S. and Choubey, V. M. Measurement of equilibrium factor "F" between radon and its progeny and thoron and its progeny in the indoor atmosphere using nuclear track detectors. *Indoor Built Environ.*, 0,1–5(2003).
231. Rehman, F., Al-Jarallah, M.I., Musazay, M.S., Abu-Jarad, F. Application of the can technique and radon gas analyzer for radon exhalation measurements. *Appl. Radiat. and Isotopes*, 59, 353–358 (2003).
232. Rehman, S., Matiullah, Rehman, S. and Rahman, S. Studying ^{222}Rn exhalation rate from soil and sand samples using CR-39 detector. *Radiat. Meas.*, 41(6), 708-713 (2006).
233. Reineking, A. and Porstendörfer, J. High-volume screen diffusion batteries and α -spectroscopy for measurement of the radon daughter activity size distributions in the environment. *Journal of Aerosol Science*, 17(5), 873-879 (1986).
234. Righi, S. and Bruzzi, L. Natural radioactivity and radon exhalation in building materials used in Italian dwellings. *J. of Environ. Radioact.*, 88(2) , 158-170 (2006).
235. Roelofs, L.M. and Scholten, L.C. The effect of aging, humidity, and fly-ash additive on the radon exhalation from concrete. *Health Phys.* 67(3), 266-271(1994).
236. Rowland, R. E. <http://www.rerowland.com/K40.html>
237. S. J. Denagbe Radon-222 concentration in subsoils and its exhalation rate from a soil sample. *Radiat. Meas.*, 32(1), 27-34 (2000).
238. Samer, M., Abdallah, Rima, R., Rida, H, Nuwayhid, Y., Chatila, M. and Gabriel K. Radon measurements in well and spring water in Lebanon. *Radiat.Meas.*, 42(2), 298-303 (2007).
239. Sasaki, T., Gunji, Y. and Okuda, T. Mathematical modeling of radon emanation *Journal of Nucl. Science and Tech.*, 41(2),142–151 (2004).
240. Schery, S.D. Thoron in the Environment. *J. Air Waste Manag. Assoc.*, 40,493-497 (1990).
241. Schwarz, G.F., Rybach, L., Baerlocher, C.K. and Klingele, E.E. "Development and calibration of an airborne radiometric measuring system" In: "Application of uranium exploration data and techniques in environmental studies", IAEA-TECDOC-827, Vienna 25-34 (1995a).
242. Segovia, N., Tamez, E., Peña, P., Gaso, I., Mireles, F., Davila I. and Quirino, L. Atmospheric radon: Origin and transfer. *Radiat. Protect. Dosim.*,56(1-4),157-160 (1994).
243. Shamshad, K.M. The meteorology of Pakistan: The climate and weathers of Pakistan. Royal book company, sadder, Karachi, Pp-313, ISBN, 9694070821 (1988).
244. Shang, B., Wang, Z., Iida, T., Ikebe, Y., and Yamada, K. Influence of ^{220}Rn on ^{222}Rn measurement in Chinese cave dwellings. In *Radon and thoron in the human environment*, eds. A. Katase, and M. Shimo, pp. 379–384. Singapore: World Scientific (1997).

245. Sharma, N. and Virk, H.S. Exhalation rate study of radon and thoron in some building materials. *Radiat. Meas.*, 34, 467–469 (2001).
246. Shweikani, and Hushari, R.M. The correlations between Radon in soil gas and its exhalation and concentration in air in the southern part of Syria. *Radiat. Meas.*, 40, 699 – 703 (2005).
247. Sima, O. Monte Carlo simulation of radon SSNT detectors. *Radiat. Meas.*, 34, 181–186 (2001).
248. Singh, S., Kumar, M. and Mahajan, R.K. The study of indoor radon in dwellings of Bathinda district, Punjab, India and its correlation with uranium and radon exhalation rate in soil. *Radiat. Meas.*, 39, 535 – 542 (2005).
249. Singh, S., Rani, A. and Mahajan, R.K. ^{226}Ra , ^{232}Th and ^{40}K analysis in soil samples from some areas of Punjab and Himachal Pradesh, India using gamma ray spectrometry. *Radiat. Meas.*, 39, 431–439 (2005).
250. Siraj, A.A., Zaryani, M.A. and Afridi, A.A. Geology of the Michani area Mohmand agency (FATA), NWFP. B.S Thesis University of Peshawar, Pakistan (unpublished data) (2000).
251. Sohrabi, M. The state-of-the-art on worldwide studies in some environments with elevated naturally occurring radioactive materials (NORM). *Appl. Radiat. Isot.* 49, 169–188 (1998).
252. Somogyi, G. and Szalay, S. Track diameter kinetics in dielectric track detectors. *Nucl. Inst. Meth.*, 109, 211-232, (1973)
253. Sroor, A., El-Bahi, S.M., Ahmed, F. and Abdel-Haleem, A.S. Natural radioactivity and radon exhalation rate of soil in southern Egypt. *J. App. Radiat. and Isotopes.*, 55, 873–879 (2001).
254. Steck, D, Field, R.W. Dosimetric challenges for residential radon epidemiology. *J. of Toxicol. and Environ. Health, Part A*, 69, 655-664 (2006).
255. Steinhäusler, F. Epidemiological evidence of radon-induced health risks. In *Radon and its decay products in indoor air*, eds. W. W. Nazaroff, and A. V. Nero, pp. New York: Wiley and Sons (1998).
256. Steinhäusler, F. Long-term measurements of ^{222}Rn , ^{220}Rn , ^{214}Pb and ^{212}Pb concentrations in the air of private and public buildings and their dependence on meteorological parameters. *Health Phys.*, 29,705–713 (1975).
257. Strandén, E., Ulbakt, K., Ehdwall, H. and Jonassentt, N. Measurements of radon exhalation from the ground: a usable tool for classification of the radon risk of building ground? *Radiat. Prot. Dosim.*, 12 (1), 33-38 (1985).
258. Summery initial environmental examination (SIEE). Asian development bank's (ADB's) environment policy online available at www.adb.org/Documents/Environment/PAK/tribal-areas-rural. PDF (2005).
259. Sun, K., Guo, Q. and Zhuo, W. Feasibility for mapping radon exhalation rate from soil in China. *J. Nucl. Science and Tech.*, 41(1), 86–90 (2004).

260. Sun, Q., Tokonami, S., Hou, C., Zhang, S., Akiba, S., Zhuo, W., Furukawa, M., Ishikawa, T., Yonehara, H. and Yamada, Y. Epidemiological Potentials of Radon - and Thoron-Prone Area in China. *Japan Health Physics Society*, 39(3), 257-26), ISSN:03676110 (2004)
261. Sunta, C.M., 1993. A review of the studies of high background radiation areas of the S-W coast of India. in proceedings of the international conference on high levels of natural radiation areas, 1990, Ramsar, Iran. IAEA Publication Series, IAEA, Vienna, 71–86 (1990).
262. Tahir, S. N. A., Jamil, K., Zaidi, J. H, Arif, M., Ahmed, N. and Syed A. A. measurements of activity concentrations of naturally occurring radionuclides in soil samples from Punjab province of Pakistan and assessment of radiological hazards *Radiat. Prot. Dosim.*, 113(4), 421–427 (2005).
263. Tahir, S. N. A., Jamil, K., Zaidi, J. H., Arif, M., Ahmed, N. and Ahmad, S. A. Measurements of activity concentrations of naturally occurring radionuclides in soil samples from Punjab province of Pakistan and assessment of radiological hazards *Radiat. Protect. Dosim.*, 113, 421–427(2005).
264. Theakston, F. (editor) *Air quality guidelines for Europe* ISBN 92 890 1358 3 1987
265. Tokonami, S. Summary of dosimetry (Radon and Thoron) studies. *Int. Congress Series* 1276, 151–154 (2005).
266. Tokonami, S. Zhuo, W., Ryo, H., Yonehara, H., Yamada, Y. and Shimo, M. Instrument performance of a radon measuring system with the alpha-track detection technique. *Radiat. Prot. Dosim.*, 103,69-72 (2003).
267. Tokonami, S., Sun, Q., Akiba, S., Zhuo, W., Furukawa, M., Ishikawa, T., Hou, C., Zhang, S., Narazaki, Y., Ohji, B., Yonehara, H. and Yamada, Y. Radon and thoron exposures for cave residents in Shanxi and Shaanxi provinces. *Radiation Research*, 162, 390–396 (2004).
268. Tokonami, S., Sun, Q., Yonehara, H. and Yamada, Y. A Simple Measurement Technique of the Equilibrium Equivalent Thoron Concentration with a CR-39 Detector. 37(1), 59-63 (20020000). *Japan Health Physics Society* ISSN:03676110 (2002).
269. Tokonami, S., Sun, Q., Yonehara, H., Yamada, Y. A Simple measurement technique of the equilibrium equivalent thoron concentration with a CR-39 detector. *Japan Health Physics Society*, 37(1). 59-6, (2002).
270. Tokonami, S., Yang, M., Yonehara, H. and Yamada, Y. Simple discriminative measurement technique for Radon and thoron concentrations with a single scintillation cell. *Rev. Sci. Instrum.*, 73(1), 69-72 (2002).
271. Tokonami, S., Yonehara, H., Zhuo, W., Sun, Q., Sanada, T. and Yamada, Y. Understanding of high Radon concentrations observed in a well- ventilated Japanese wooden house. In: *Proceedings of the ninth International Conference on Indoor Air Quality and Climate*, Monterey, USA, 30 June–5 July. 1, 665–669 (2002).

272. Tommasino, L. Passive sampling and monitoring of radon and other gases. *Radiat. Prot. Dosim.*, 78(1), 55–58 (1998).
273. Trevisi, R., Bruno, M., Orlando, C., Ocone, R., Paoletti, C., Amici, M., Altieri, A. and Antonelli, B. Radiometric characterization of more representative natural building materials in the province of Rome. *Radiat. Protect. Dosim.*, 113, 168–172 (2005).
274. TSI Incorporated 500 Cardigan Road, Shoreview, MN 55126 U.S.A
275. Tuccimei, M. Moroni and Norcia, D. Simultaneous determination of ^{222}Rn and ^{220}Rn exhalation rates from building materials used in Central Italy with accumulation chambers and continuous solid state alpha detector: influence of particle size, humidity and precursors concentration. *Appl. Radiat. Isot.*, 64, 254–263(2006).
276. Tufail, M, Matiullah, Ahmad, N., Guo, S. L., Khan, E. U. and Bashir, A. Estimation of internal and external equivalent dose rates for dwellers of Dera Ismail Khan, Pakistan. *Nucl. Tracks. Radiat. Meas.*, 22(1-4) 479-482 (1993).
277. Tufail, M., Ahmad, N., Almakky, S., Zafar, M. S. and Khan H. A. Natural radioactivity in the ceramics used in dwellings as construction material. *The Science of The Total Environ.*, 127(3), 243-253 (1992a).
278. Tufail, M., Ahmad, N., Khan H.A. and Zafar, M.S. Gamma Activity in the bricks used for the construction of dwellings in Rawalpindi and Islamabad areas of Pakistan. *Radiat. Protect. Dosim.*, 37,197-200 (1991).
279. Tufail, M., Akhtar, N. and Waqas, M. Measurement of terrestrial radiation for assessment of gamma dose from cultivated and barren saline soils of Faisalabad in Pakistan. *Radiat. Meas.*, 41(4), 443-451 (2006b).
280. Tufail, M., Akhtar, N. and Waqas, M. Radioactive rock phosphate: the feed stock of phosphate fertilizers used in Pakistan. *Health Phy.*, 90(4), 361-370 (2006a).
281. Tufail, M., Akhtar, N., Javied, S. and Hamid, T. Natural radioactivity hazards of building bricks fabricated from saline soil of two districts of Pakistan. *J. Radiol. Protect.*, 27, 481-492 (2007).
282. Tufail, M., Iqbal, M. and Mirza, S. M. Radiation doses due to the natural radioactivity in Pakistan marble. *Radioprotection*, 35 (3), 299-310 (2000).
283. Tufail, M., Khan, H.A. and Zafar, M.S. Gamma activity in the bricks used for the construction of dwellings in Rawalpindi and Islamabad areas of Pakistan. *Radiat. Protect. Dosim.*, 37,197–200 (1991).
284. Tufail, M., Khan, M. A., Ahmad, N., Khan, H, A, and Zafar, M. S. Measurements of Radon Concentration in Some Cities of Pakistan. *Radiat.Protect. Dosim.*, 40 39-44 (1992).
285. Tufail, M., Matiullah, Ahmad, N., Guo, S. L., Khan, E. U. and Bashir, A. Estimation of internal and external equivalent dose rates for dwellers of Dera Ismail Khan, Pakistan. *Nucl. Tracks. Radiat. Meas.*, 22(1-4), 479-482 (1993).

286. Tufail, M., Matiullah, Aziz, S., Ansari, F., Qureshi, A. A. and Khan, H, A. Preliminary radon concentration-survey in some houses of Islamabad. Nucl. Tracks. Radiat. Meas., 15(1-4) 659-662 (1988b)
287. Tufail, M., Rashid, T., Mahmood, A.B. and Ahmad, N. Radiation doses in Pakistani houses. Sci Total, Environ., 142(3),171-7 (1994).
288. Tufail, M, Ahmad, N., Mirza, S. M., Mirza N. M , Sohail S. M.and Zafar, M. S. Natural radioactivity in cements manufactured by various factories in Pakistan. Int. J. Radiat. Appl. Instum., E, Nucl. Geophys.,6(4), 553-559 (1992b).
289. Tzortzis, M. and Tsertos, H. Determination of thorium, uranium and potassium elemental concentrations in surface soils in Cyprus. J. of Environ. Radioact., 77, 325–338 (2004).
290. Tzortzis, M., Tsertos, H., Christodes, S. and Christodoulides, G. Gamma-ray measurements of naturally occurring radioactive samples from Cyprus characteristic geological rocks. Radiat. Meas., 37, 221 – 229 (2003).
291. United Nations Scientific Committee on the Effect of Atomic Radiation. Sources, effects and risks of ionizing radiation (NY: UNSCEAR) (1988).
292. United Nations Scientific Committee on the Effects of Atomic Radiation. Report to the general assembly. Annex B: exposures from natural radiation sources. (NY: UNSCEAR), ISBN-10: 9211422388 (2000).
293. United Nations. Sources and Effects of Ionizing Radiation. United Nations Scientific Committee on the Effects of Atomic Radiation, 1993 Report to the General Assembly, with scientific annexes. United Nations sales publication E.94.IX.2. United Nations, New York (1993).
294. Usman, S, Spitz, H and Lee, S. Analysis of electret ion chamber radon detector response to ^{222}Rn and interference from background gamma radiation. Health Phys., 76 (1), 44-9 (1999).
295. Van Dijk, W. and de Jong, P. Determining the ^{222}Rn exhalation rate of building materials using liquid scintillation counting. Health Phys., 61(4), 501-509 (1991).
296. Vargas, A. and Ortega, X. Influence of Environmental Changes on Integrating Radon Detectors: Results of an Intercomparison Exercise. The Science of the Total Environment., 272, 97-103 (2001).
297. Vaupotič, J. and Kobal, I. Radon doses based on alpha spectrometry. Acta Chim. Slov., 51, 159-168 (2004).
298. Veiga, R., Sanches, N., Anjos, R.M., Macario, K., Bastos, J., Iguatemy, M., Aguiar, J.G. Santos, A.M.A., Mosquera, B., Carvalho, C., Baptista Filho, M. and Umisedo, N.K. Measurement of natural radioactivity in Brazilian beach sands. Radiat. Meas., 41,189–196 (2006).
299. Waheed, S., Siddique, N., Rahman, A., Zaidi, J. H. and Ahmad, S. INAA for dietary assessment of essential and other trace elements in fourteen fruits harvested and consumed in Pakistan. J.of Radioanalyt. and Nucl.Chem., 260(3), 523-531 (2004).

300. Wang, Z., Lubin, J. H., Wang, L., Zhang, S., Boice, J., Cui, H., Zhang, S., Conrath, S., Xia, Y., and Kleinerman, R. A. Residential Radon and lung cancer risk in a high-exposure area of Gansu province, China. *Am. J. Epidemiol.*, 155, 554–564 (2002).
301. Wei, L. and Sugahara, T. An introductory overview of the epidemiological study on the population at the high background radiation areas in Yangjiang, China. *J. Radiat. Res.* 41 (Suppl.), 1–7 (2000).
302. Wiegand, J., Feige, S., Quingling, X., Schreiber, U., Wieditz, K., Wittmann, C. and Xiarong, L. Radon and thoron in cave dwellings (Yan'an, China). *Health Phys.*, 78(4),438-44 (2000).
303. Winkler, R., Ruckerbauer, F. Trautmannsheimer, M., Tschiersch, J., Karg, E. Diurnal and seasonal variation of the equilibrium state between short-lived radon decay products and radon gas in ground-level air. *Radiat. Environ. Biophys.*, 40,115–123 (2001).
304. Wrixon, A. D., Green, B. M. R., Lomas, P. R.,; Miles, J. C. H., Cliff, K.D., Francis, E. A. Driscoll, C. M. H., James, A.C. and O' Riordan, M. C. Natural radiation exposure in UK Dwellings. NRPB R-190, HMSO, London (1988).
305. Xinwei, L. Natural radioactivity in some building materials of Xi'an, China. *Radiat. Meas.*, 40, 94 – 97 (2005).
306. Xinwei, L. Radioactive analysis of cement and its products collected from Shaanxi, China. *Health Phys.*, 88(1), 84-6 (2005).
307. Yahong, M., Yigang, L., Guang, Z. and Xiaolei and H. The studies on radiological limits of color-glazed tiles used in home decoration. *Health Phys.*, 82(4):510-512 (2002).
308. Yamada, Y., Sun, Q., Tokonami, S., Akiba, S., Zhuo, W. Hou, C. Zhang, S., Ishikawa, T., Furukawa, M., Fukutsu, K. and Yonehara, H. Radon–thoron discriminative measurements in Gansu province, china, and their implication for dose estimates. *J. of Toxicology and Environ. Health, Part A*, 69:723–734 (2006).
309. Yamasakit, T., Guot, Q. and Iida, T. Distributions of thoron progeny concentrations in dwellings. *Radiat. Protect. Dosim.*, 59,135-140 (1995).
310. Yarborough, K. A. Radon - and thoron-produced radiation in National Park Service caves. In: Gesell, T. F., Lowder, W. M., eds. *Natural radiation environment III*. Washington: United States Department of Energy; CONF-780422, 2, 1371–1395 (1980).
311. Yonehara, H., Tokonami, S., Zhuo, W., Ishikawa, T., Fukutsu, K. and Yamada, Y. Thoron in the living environments of Japan. *International Congress Series*, 1276, 58-61 (2005).
312. Yuan, Y., Morishima, H., Shen, T., Koga, T., Wei, L. and Sugahara T. Measurement of ^{222}Rn , ^{220}Rn and their decay products in the Environmental air of the high background radiation area of Yangjiang China., 41 , 25-30 (2000).

313. Younis, M., Subhani, M. S., Khan, K. and Orfi, S. D. Radioactivity mapping of north western areas of Pakistan. *J. Radioanal. and Nucl. Chem.*, 266(2), 325-332 (2005).
314. Yu, K. N., Young, E. C. M., Chan, T. F., Lo, T. and Balendran, R. V. The variation of radon exhalation rates from concrete surfaces of different ages. *Building and Environ.*, 31(3), 255-257 (1996).
315. Yu, K., Guan, N.Z. J., Young, E. C. M. and Stokes, M. J.. Active Measurements of Indoor Concentrations of Radon and Thoron Gas using Charcoal Canisters. *Appl. Radiat. Isot.*, 49(12), 1691-1694 (1998).
316. Yu, K.N., Nikezi'c, D., Ng, F.M.F., Leung, J.K.C., Long term measurements of radon progeny concentration with solid state nuclear track detectors (2005). *Radiat. Meas.*, 40(2-6) 560-568 (2005).
317. Zaidi, J. H., Arif, M., Ahmad, S., Fatima, I. and Qureshi, I. H. Determination of natural radioactivity in building materials used in the Rawalpindi/Islamabad area by γ -ray spectrometry and instrumental neutron activation analysis. *App. Radiat. and Isot.*, 51(5), 559-564 (1999).
318. Zaidi, J.H., Arif, M. and Fatima, I. Determination of natural radioactivity in building materials used in the Karachi area by γ -ray spectrometry and INAA. *Radiochimica, Acta*, 92 (12), 945-949 (2004).
319. Zhuo, W. and Iida, T. Estimation of thoron progeny concentrations in dwellings with their deposition rate measurements. *Jpn. J. Health Phys.*, 35, 365–370 (2000).
320. Zikovsky, L. and Kennedy, G. Radioactivity of building materials available in Canada. *Health Phys.*, 63, 449–452 (1992).

APPENDICES

Appendix A: Surface deposited radon progenies in Bq.m⁻² measured using active detector and smooth glass surfaces.

Experiment Run ID	Aptec	Surface Activity (Bq.m ⁻²)	SA1	SA3
71607A	²¹⁸ Po	243±61	129±23	236±34
Run 1	²¹⁴ Pb	1366±84	309±39	224±44
	²¹⁴ Bi- ²¹⁴ Po	1487±58	307±27	447±31
	²¹⁸ Po	218±41	196±29	558±45
Run 2	²¹⁴ Pb	440±50	472±47	452±47
	²¹⁴ Bi- ²¹⁴ Po	519±34	454±33	433±32
	²¹⁸ Po	294±43	207±28	344±38
Run 3	²¹⁴ Pb	407±50	243±42	360±44
	²¹⁴ Bi- ²¹⁴ Po	531±34	391±29	406±30
	²¹⁸ Po	260±38	224±27	287±34
Run 4	²¹⁴ Pb	394±41	424±35	391±40
	²¹⁴ Bi- ²¹⁴ Po	324±28	181±23	290±27
	²¹⁸ Po	375±47	244±30	422±42
Run 5	²¹⁴ Pb	558±53	294±42	411±47
	²¹⁴ Bi- ²¹⁴ Po	577±37	371±29	462±33
	²¹⁸ Po	143±30	203±26	108±25
71707A	²¹⁸ Po	143±30	203±26	108±25
Run 1	²¹⁴ Pb	167±33	133±30	116±33
	²¹⁴ Bi- ²¹⁴ Po	245±23	202±21	256±23
	²¹⁸ Po	92±27	46±16	109±23
Run 2	²¹⁴ Pb	321±34	167±30	174±29
	²¹⁴ Bi- ²¹⁴ Po	211±23	182±20	175±20
	²¹⁸ Po	76±28	84±19	163±26
Run 3	²¹⁴ Pb	135±35	67±28	160±29
	²¹⁴ Bi- ²¹⁴ Po	292±25	184±20	171±20
	²¹⁸ Po	277±34	68±17	188±28
Run 4	²¹⁴ Pb	314±30	207±26	147±28
	²¹⁴ Bi- ²¹⁴ Po	128±20	106±17	153±19
	²¹⁸ Po	153±30	106±20	201±28
Run 5	²¹⁴ Pb	159±34	182±30	230±30
	²¹⁴ Bi- ²¹⁴ Po	253±24	189±21	163±20
	²¹⁸ Po	329±38	152±23	170±24
Run 6	²¹⁴ Pb	177±36	150±32	195±28
	²¹⁴ Bi- ²¹⁴ Po	275±25	221±22	150±19
	²¹⁸ Po	289±37	131±22	266±29
Run 7	²¹⁴ Pb	424±39	187±30	253±30
	²¹⁴ Bi- ²¹⁴ Po	271±26	178±20	159±20
	²¹⁸ Po	245±35	103±21	148±27
71807A	²¹⁸ Po	245±35	103±21	148±27
Run 1	²¹⁴ Pb	394±38	281±33	423±35
	²¹⁴ Bi- ²¹⁴ Po	250±25	202±22	194±23
	²¹⁸ Po	168±32	104±20	150±26
Run 2	²¹⁴ Pb	472±38	161±31	315±34

	^{214}Bi - ^{214}Po	230±25	214±22	204±23
Run 3	^{218}Po	122±26	140±23	153±26
	^{214}Pb	375±30	45±30	133±31
	^{214}Bi - ^{214}Po	113±19	235±22	222±22
71907A	^{218}Po	55±16	32±13	63±17
Run 1	^{214}Pb	98±18	55±20	62±21
	^{214}Bi - ^{214}Po	49±12	93±14	99±15
Run 2	^{218}Po	61±20	8±10	45±17
	^{214}Pb	109±23	64±21	41±23
	^{214}Bi - ^{214}Po	108±16	97±15	129±16
Run 3	^{218}Po	39±26	56±15	61±18
	^{214}Pb	294±36	5±20	62±22
	^{214}Bi - ^{214}Po	257±25	107±15	109±15
Run 4	^{218}Po	75±19	21±11	33±16
	^{214}Pb	186±21	9620±20	73±22
	^{214}Bi - ^{214}Po	53±13	80±14	113±16
71907B	^{218}Po	295±49	351±36	628±49
Run 1	^{214}Pb	689±61	491±53	674±54
	^{214}Bi - ^{214}Po	791±42	605±37	564±37
Run 2	^{218}Po	645±59	265±32	557±47
	^{214}Pb	891±65	492±49	614±53
	^{214}Bi - ^{214}Po	846±45	491±34	535±36
Run 3	^{218}Po	521±52	525±42	617±47
	^{214}Pb	711±57	529±53	597±49
	^{214}Bi - ^{214}Po	623±39	565±36	436±33
Run 4	^{218}Po	609±59	500±43	629±51
	^{214}Pb	861±66	638±61	850±61
	^{214}Bi - ^{214}Po	878±45	801±42	719±42
Run 5	^{218}Po	712±59	418±38	711±53
	^{214}Pb	1012±63	740±53	537±57
	^{214}Bi - ^{214}Po	701±42	496±35	694±40
72107A & B	^{218}Po	5±7	41±12	30±11
Run 1	^{214}Pb	51±10	18±8	23±8
	^{214}Bi - ^{214}Po	11±6	11±5	11±5
Run 2	^{218}Po	47±12	4±6	
	^{214}Pb	43±9	30±10	
	^{214}Bi - ^{214}Po	5±5	14±6	
Run 3	^{218}Po	47±15	40±12	-15±5
	^{214}Pb	23±15	34±11	36±13
	^{214}Bi - ^{214}Po	49±10	197±7	34±9
Run 4	^{218}Po	110±20	1±7	49±14
	^{214}Pb	46±16	39±14	65±15
	^{214}Bi - ^{214}Po	51±11	44±10	38±10
72307A	^{218}Po	61±20	5±6	15±9
	^{214}Pb	67±23	44±9	22±10
	^{214}Bi - ^{214}Po	115±16	7±5	21±7
Run 2	^{218}Po	8±7	3±6	14±9
	^{214}Pb	61±9	20±12	30±11

	^{214}Bi - ^{214}Po	2±5	32±8	25±8
Run 3	^{218}Po	103±21	37±12	87±19
	^{214}Pb	10±18	59±15	64±22
	^{214}Bi - ^{214}Po	78±13	40±10	109±15
72407A	^{218}Po	27±20	11±9	13±13
	^{214}Pb	31±27	84±18	96±20
	^{214}Bi - ^{214}Po	183±19	62±12	79±14
Run 2	^{218}Po	34±11	16±8	23±11
	^{214}Pb	48±9	34±10	47±15
	^{214}Bi - ^{214}Po	4±5	14±6	42±10
Run 3	^{218}Po	3±8	29±10	28±11
	^{214}Pb	48±11	33±8	38±11
	^{214}Bi - ^{214}Po	22±15	3±4	18±7
Run4	^{218}Po	37±18	16±8	86±18
	^{214}Pb	81±13	45±10	37±16
	^{214}Bi - ^{214}Po	18±7	12±6	53±11
Run 5	^{218}Po	42±15	62±14	69±15
	^{214}Pb	23±16	-5±13	49±10
	^{214}Bi - ^{214}Po	63±11	46±9	6±6
81607 ONE/NONE	^{218}Po	192±39		267±34
Run 1	^{214}Pb	584±49		314±41
	^{214}Bi - ^{214}Po	453±33		340±28
Run 2	^{218}Po	314±41	27±19	303±34
	^{214}Pb	247±44	229±45	186±34
	^{214}Bi - ^{214}Po	425±30	484±32	251±24
Run 3	^{218}Po	221±38	18127±	212±31
	^{214}Pb	365±44	145±41	363±39
	^{214}Bi - ^{214}Po	404±30	419±30	281±26
Run 4	^{218}Po	369±45	104±23	355±39
	^{214}Pb	567±50	421±45	233±44
	^{214}Bi - ^{214}Po	474±34	417±31	439±31
Run 5	^{218}Po	306±45	113±24	222±34
	^{214}Pb	721±54	200±45	560±46
	^{214}Bi - ^{214}Po	555±37	483±32	386±31
Run 6	^{218}Po	327±41	91±23	449±41
	^{214}Pb	308±44	351±45	401±42
	^{214}Bi - ^{214}Po	414±30	430±31	332±28
Run7	^{218}Po	253±45	106±22	371±39
	^{214}Pb	471±56	290±38	264±44
	^{214}Bi - ^{214}Po	683±39	289±26	418±30
Run8	^{218}Po	445±50	88±21	164±31
	^{214}Pb	554±54	232±40	350±43
	^{214}Bi - ^{214}Po	605±37	357±28	390±30
Run 9	^{218}Po	211±43	161±26	381±38
	^{214}Pb	554±55	264±40	428±40
	^{214}Bi - ^{214}Po	634±38	351±28	272±26
Run10	^{218}Po	178±44	239±31	460±44

	^{214}Pb	521±57	210±48	381±52
	$^{214}\text{Bi-}^{214}\text{Po}$	701±39	563±34	603±36
Run 11	^{218}Po		107±23	262±36
	^{214}Pb		503±44	462±48
	$^{214}\text{Bi-}^{214}\text{Po}$		371±30	469±33
81707A Candle	^{218}Po	101±27	14±12	46±20
Run 1	^{214}Pb	34±30	37±25	12±31
	$^{214}\text{Bi-}^{214}\text{Po}$	236±22	159±18	255±22
Run 2	^{218}Po	5±11	2±7	4±11
	^{214}Pb	38±16	34±13	6±17
	$^{214}\text{Bi-}^{214}\text{Po}$	54±11	35±9	75±12
Run 3	^{218}Po	34±11	4±6	38±13
	^{214}Pb	34±8	4±9	-6±12
	$^{214}\text{Bi-}^{214}\text{Po}$	7±5	19±6	41±9
Run 4	^{218}Po	27±12	37±12	8±10
	^{214}Pb	0±11	35±14	59±15
	$^{214}\text{Bi-}^{214}\text{Po}$	33±8	45±10	45±10
Run 5	^{218}Po	29±11	4±6	17±9
	^{214}Pb	-3±10	7±10	-2±7
	$^{214}\text{Bi-}^{214}\text{Po}$	27±7	24±7	15±5
Run 6	^{218}Po	23±9	-8±2	17±9
	^{214}Pb	49±7	8±8	3±8
	$^{214}\text{Bi-}^{214}\text{Po}$	-3±4	13±5	14±5
Run 7	^{218}Po	56±14	15±9	17±9
	^{214}Pb	31±11	-8±11	1±8
	$^{214}\text{Bi-}^{214}\text{Po}$	20±7	37±8	15±5
Run 1 FAN	^{218}Po	521±57	88±24	259±37
	^{214}Pb	1034±67	291±50	378±50
	$^{214}\text{Bi-}^{214}\text{Po}$	875±46	602±36	560±35
Run 2	^{218}Po	315±42	290±33	396±42
	^{214}Pb	527±47	590±50	400±50
	$^{214}\text{Bi-}^{214}\text{Po}$	408±32	473±34	530±34
Run 3	^{218}Po	625±57	275±33	567±48
	^{214}Pb	725±61	382±50	328±54
	$^{214}\text{Bi-}^{214}\text{Po}$	741±41	537±34	668±38
Run 4	^{218}Po	441±52	117±27	542±48
	^{214}Pb	891±60	562±55	830±58
	$^{214}\text{Bi-}^{214}\text{Po}$	672±41	626±38	637±39
Run 5	^{218}Po	302±49	331±36	427±41
	^{214}Pb	760±61	878±58	413±46
	$^{214}\text{Bi-}^{214}\text{Po}$	758±42	618±39	436±32
Run 6	^{218}Po	812±65	216±33	530±47
	^{214}Pb	936±69	741±63	572±55
	$^{214}\text{Bi-}^{214}\text{Po}$	964±47	822±43	613±38
Run 7	^{218}Po	344±49	220±32	780±55
	^{214}Pb	554±57	557±57	656±60
	$^{214}\text{Bi-}^{214}\text{Po}$	707±40	693±39	722±41
Run 8	^{218}Po	563±56	274±33	525±46

	^{214}Pb	1226±64	555±51	548±51
	$^{214}\text{Bi-}^{214}\text{Po}$	677±42	511±35	512±35
Run 9	^{218}Po	708±51	243±31	600±49
	^{214}Pb	467±51	496±48	530±54
	$^{214}\text{Bi-}^{214}\text{Po}$	530±35	464±33	600±37
Run 10	^{218}Po	524±46	189±30	371±42
	^{214}Pb	732±55	376±54	545±55
	$^{214}\text{Bi-}^{214}\text{Po}$	549±37	669±38	625±38
Run 1	^{218}Po	76±22		1±14
PROPANE				
	^{214}Pb	276±28		106±25
	$^{214}\text{Bi-}^{214}\text{Po}$	111±18		137±17
Run 2	^{218}Po	86±18	45±14	
	^{214}Pb	108±16	35±19	
	$^{214}\text{Bi-}^{214}\text{Po}$	33±10	91±14	
Run 3	^{218}Po	93±24	46±14	
	^{214}Pb	113±28	61±19	
	$^{214}\text{Bi-}^{214}\text{Po}$	168±19	76±13	
Run 4	^{218}Po	96±23	16±12	36±15
	^{214}Pb	146±25	138±25	60±21
	$^{214}\text{Bi-}^{214}\text{Po}$	114±17	120±17	105±15
Run 5	^{218}Po	74±22	79±17	28±16
	^{214}Pb	132±26	10±21	90±25
	$^{214}\text{Bi-}^{214}\text{Po}$	144±18	122±16	135±17
Run 6	^{218}Po	100±25	102±19	57±18
	^{214}Pb	150±29	117±24	133±24
	$^{214}\text{Bi-}^{214}\text{Po}$	181±20	112±16	117±17
Run 7	^{218}Po		32±13	53±18
	^{214}Pb		154±22	103±26
	$^{214}\text{Bi-}^{214}\text{Po}$		80±15	143±18
Run 8	^{218}Po	203±30	52±17	96±24
	^{214}Pb	183±30	152±33	167±33
	$^{214}\text{Bi-}^{214}\text{Po}$	181±21	253±23	242±a

Appendix B: Surface deposited radon and thoron progenies in Bq.m⁻² measured using active detectors and smooth glass surfaces.

	Propane cook				Cigarette smoke			
	APTEC	AP-1	AP-2	AP-3	APTEC	AP-1	AP-2	AP-3
²¹⁸ Po	31	32	29	85	26	96	39	25
²¹⁴ Po	6	1	10	14	9	14	9	19
²¹² Po	29	37	31	52	32	112	26	32
²¹² Po Act	32.5	44.6	41.4	58.7	35.9	139.4	34.5	34.8
²¹⁸ Po	32	45	35	40	52	26	22	33
²¹⁴ Po	16	1	6	18	20	3	3	6
²¹² Po	28	31	22	35	77	27	23	20
²¹² Po Act	31.4	37.0	29.1	38.4	86.3	31.8	30.8	21.9
²¹⁸ Po	21	34	42	44	23	27	33	60
²¹⁴ Po	5	2	8	8	9	3	4	10
²¹² Po	27	26	30	59	34	26	33	48
²¹² Po Act	30.3	30.6	40.1	67.5	38.1	30.5	44.7	54.4
²¹⁸ Po	36	30	41	46	31	26	22	30
²¹⁴ Po	14	1	2	13	5	1	3	6
²¹² Po	64	54	8	46	20	21	14	20
²¹² Po Act	71.7	66.3	9.9	51.8	22.4	24.3	18.2	21.9
²¹⁸ Po	50	43	42	24	37	34	45	45
²¹⁴ Po	12	1	8	2	7	3	4	5
²¹² Po	39	38	30	18	22	25	24	11
²¹² Po Act	43.7	45.9	40.1	19.9	24.7	29.2	32.1	11.5
²¹⁸ Po	20	53	36	28	17	25	39	77
²¹⁴ Po	16	3	6	9	3	2	3	23
²¹² Po	27	43	32	35	22	13	58	83
²¹² Po Act	30.3	52.1	43.1	39.2	24.7	14.0	79.6	94.3
²¹⁸ Po	15	46	36	32	25	32	60	37
²¹⁴ Po	8	3	6	11	11	3	3	7
²¹² Po	13	27	32	33	19	25	28	33
²¹² Po Act	14.6	31.8	43.1	36.7	21.3	29.2	37.8	37.1
²¹⁸ Po	64	60	54	40	20	23	28	37
²¹⁴ Po	18	2	16	13	7	16	10	9
²¹² Po	43	35	36	37	22	13	14	24
²¹² Po Act	48.2	42.0	47.9	41.2	24.7	13.3	17.7	26.3
²¹⁸ Po	32	26	38	37	35	37	34	37
²¹⁴ Po	13	3	7	12	12	8	11	16
²¹² Po	40	31	34	48	14	16	13	16
²¹² Po Act	44.8	36.9	45.8	54.2	15.7	17.5	16.2	16.3
²¹⁸ Po	50	45	56	36	20	24	51	46
²¹⁴ Po	18	3	7	8	6	1	6	6
²¹² Po	56	26	35	52	33	13	25	40
²¹² Po Act	62.7	30.5	47.2	59.3	37.0	14.1	33.3	45.4
²¹⁸ Po	24	33	27	35	16	22	31	37
²¹⁴ Po	7	1	3	9	2	1	3	7
²¹² Po	27	13	21	41	17	25	24	33
²¹² Po Act	30.3	14.1	28.0	46.3	19.0	29.3	32.2	37.1
²¹⁸ Po	27	30	30	27	32	28	36	31
²¹⁴ Po	12	2	4	8	7	1	6	11
²¹² Po	37	37	4	41	16	24	31	31
²¹² Po Act	41.5	44.6	4.2	46.4	17.9	28.1	41.7	34.4
²¹⁸ Po	37	48	48	47	16	26	37	37
²¹⁴ Po	9	9	7	7	0	1	3	3
²¹² Po	28	28	41	40	10	13	33	9
²¹² Po Act	31.4	32.7	55.6	45.3	11.2	14.1	44.8	9.3
²¹⁸ Po	22	42	32	34	26	47	29	38
²¹⁴ Po	11	4	4	9	2	12	1	1
²¹² Po	33	45	24	46	20	23	3	18
²¹² Po Act	37.0	54.6	32.1	52.2	22.4	26.2	3.0	20.0
²¹⁸ Po	31	48	39	35	13	41	26	22
²¹⁴ Po	3	1	9	5	3	1	2	8
²¹² Po	22	18	22	32	7	26	19	26
²¹² Po Act	24.7	20.4	28.9	36.1	7.8	30.6	25.3	28.8
²¹⁸ Po	29	33	30	28	32	33	37	20
²¹⁴ Po	6	4	7	10	3	2	7	5
²¹² Po	22	35	29	27	9	17	18	16
²¹² Po Act	24.7	41.9	38.8	29.8	10.1	19.1	23.5	17.3
²¹⁸ Po	26	31	32	136	24	29	41	24

²¹⁴ Po	13	3	3	12	7	4	2	13
²¹² Po	34	28	27	37	21	6	18	10
²¹² Po Act	38.1	33.1	36.4	41.3	23.5	5.0	23.9	9.6
	39.7	40.7	38.1	47.4	26	29.1	31.7	30.6

(Appendix B: Continued)

Progenies	Candle On/Off				Fan Experiment				HEPA			
	APTEC	AP-1	AP-2	AP-3	APTEC	AP-1	AP-2	AP-3	APTEC	AP-1	AP-2	AP-3
²¹⁸ Po	34	33	45	47	35	53	34	59	47	68	38	47
²¹⁴ Po	4	4	7	3	3	12	13	18	15	12	22	14
²¹² Po	14	15	21	24	38	59	36	39	36	61	60	69
²¹² Po Act	15.7	16.5	27.7	26.9	42.6	72	48.1	43.1	40.3	74.6	80.8	78.7
²¹⁸ Po	17	17	24	41	22	45	73	46	67	32	46	76
²¹⁴ Po	4	2	7	8	8	8	11	15	23	9	17	22
²¹² Po	14	10	16	33	25	60	29	43	54	35	61	77
²¹² Po Act	15.7	10.2	20.7	37	28	73.5	38.5	48.1	60.5	41.6	82.7	87.3
²¹⁸ Po	31	29	26	30	59	77	61	22	18	17	38	60
²¹⁴ Po	5	1	1	8	19	10	17	15	8	7	4	15
²¹² Po	18	21	19	23	67	50	39	28	29	18	55	65
²¹² Po Act	20.2	24.3	25.4	25.3	75.1	60.7	52	30.5	32.5	20.1	75.4	73.9
²¹⁸ Po	24	22	24	35	31	35	42	33	32	64	50	59
²¹⁴ Po	19	2	6	1	8	3	11	25	16	11	18	23
²¹² Po	29	11	12	15	17	26	39	51	36	60	60	71
²¹² Po Act	32.5	11.5	15.2	16.5	19	30.5	52.5	56.5	40.3	73.4	81.2	80.2
²¹⁸ Po	16	31	23	26	41	54	44	34	78	46	41	60
²¹⁴ Po	3	5	5	4	20	5	12	7	18	13	16	23
²¹² Po	21	12	19	24	40	72	18	20	66	59	57	80
²¹² Po Act	23.5	12.6	25	26.8	44.8	89	23.1	21.8	74	72	77.2	90.7
²¹⁸ Po	38	38	34	27	41	56	54	33	59	69	40	26
²¹⁴ Po	4	6	5	2	20	13	23	14	26	8	10	6
²¹² Po	20	19	8	14	60	47	30	56	67	68	19	39
²¹² Po Act	22.4	21.4	9.7	15.3	67.2	56.7	38.9	63.4	75.1	83.7	24.6	44.2
²¹⁸ Po	14	41	43	32	39	58	35	73	52	23	59	46
²¹⁴ Po	6	2	5	10	13	6	14	18	13	6	13	25
²¹² Po	13	9	16	19	35	29	20	55	38	20	51	58
²¹² Po Act	14.6	8.9	20.9	20.4	39.2	34.2	25.7	61.9	42.6	22.7	69	64.8
²¹⁸ Po	7	56	19	20	75	68	30	63	47	32	45	49
²¹⁴ Po	6	1	6	2	22	14	15	9	7	4	17	8
²¹² Po	14	14	12	13	81	44	32	40	55	30	50	35
²¹² Po Act	15.7	15.3	15.2	14.1	90.8	52.8	42.4	45.1	61.6	35.5	67.3	39.3
²¹⁸ Po	19	27	53	12	39	73	28	42	47	54	48	49
²¹⁴ Po	3	3	10	10	9	14	13	11	5	9	21	22
²¹² Po	9	7	14	12	43	61	45	26	69	51	61	68
²¹² Po Act	10.1	6.3	17.7	12.2	48.2	74.5	60.7	28.5	77.3	62	82.3	76.8
²¹⁸ Po	10	15	18	27	48	53	37	41	62	33	41	45
²¹⁴ Po	5	1	1	5	11	10	14	15	24	9	19	22
²¹² Po	12	9	12	14	36	61	28	39	51	43	47	77
²¹² Po Act	13.4	9	15.6	15	40.3	74.7	36.9	43.4	57.1	51.8	63	87.3

²¹⁸ Po	15	34	32	38	39	83	59	55	36	53	63	82
²¹⁴ Po	3	3	7	3	6	12	21	15	15	11	19	16
²¹² Po	5	10	8	13	48	99	43	60	38	51	48	66
²¹² Po Act	5.6	10.1	9.5	14	53.8	123	57.2	68	42.6	61.9	64.4	75
²¹⁸ Po	9	38	44	45	45	80	36	34	74	35	75	66
²¹⁴ Po	4	3	6	4	25	9	13	19	18	11	18	20
²¹² Po	9	13	6	5	69	86	48	35	73	46	52	64
²¹² Po Act	10.1	14	6.8	4.5	77.3	106.6	64.9	38.3	81.8	55.5	70	72.3
²¹⁸ Po	11	15	15	26	48	81	46	29	42	55	46	45
²¹⁴ Po	0	2	16	3	15	13	15	10	14	11	7	6
²¹² Po	6	5	15	11	46	63	48	44	26	49	35	33
²¹² Po Act	6.7	3.8	18.5	11.6	51.5	77.1	64.7	49.7	29.1	59.4	47.2	37.2
²¹⁸ Po	22	47	16	38	38	51	43	42	57	83	46	34
²¹⁴ Po	4	1	5	2	14	9	12	21	13	30	13	22
²¹² Po	5	9	4	7	51	55	44	66	59	84	28	54
²¹² Po Act	5.6	9	4.1	7	57.1	67.1	59.4	74.5	66.1	102.9	36.9	60.3
²¹⁸ Po	15	42	25	31	80	46	61	41	27	39	36	44
²¹⁴ Po	2	1	3	5	38	8	21	11	17	5	11	20
²¹² Po	10	7	7	8	107	33	49	35	45	24	30	54
²¹² Po Act	11.2	6.4	8.5	7.9	119.9	39.2	65.6	39.1	50.4	27.9	39.9	60.5
²¹⁸ Po	23	35	38	14	57	43	32	54	73	44	82	81
²¹⁴ Po	1	2	9	3	13	12	9	17	19	10	28	24
²¹² Po	7	6	11	7	59	55	47	30	51	43	55	62
²¹² Po Act	7.8	5.1	13.5	7	66.1	66.9	63.8	32.6	57.1	51.8	73.4	69.5
²¹⁸ Po					27	49	33	38	44	53	39	61
²¹⁴ Po					13	9	6	23	13	8	16	24
²¹² Po					27	45	60	40	51	49	40	57
²¹² Po Act					30.3	54.4	82.2	43.8	57.1	59.5	53.4	63.7
	14.4	11.5	15.8	16.3	56	67.8	51.5	46.4	52.5	53.1	60.5	64.5

(Appendix B: Continued)

	None				HEPA+ION				Candle (Repeat)			
	APTEC	AP-1	AP-2	AP-3	APTEC	AP-1	AP-2	AP-3	APTEC	AP-1	AP-2	AP-3
²¹⁸ Po	49	39		42	58	57	68	48	40	17	39	39
²¹⁴ Po	31	16		15	25	9	6	14	9	1	8	23
²¹² Po	51	34		32	71	52	41	69	19	4	17	46
²¹² Po Act	57.1	40.0		35.2	79.6	63.3	55.7	78.7	21.3	2.6	22.0	50.9
²¹⁸ Po	34	45	33	24	55	48	40	42	23	30	29	28
²¹⁴ Po	12	12	12	12	24	7	10	12	8	2	5	14
²¹² Po	42	38	30	43	63	51	52	32	24	10	13	47
²¹² Po Act	47.1	45.3	39.8	48.4	70.6	62.1	70.7	35.5	26.9	10.2	16.7	52.9
²¹⁸ Po	48	30	31	48	90	52	45	37	14	24	2	26
²¹⁴ Po	21	27	9	20	29	6	8	17	0	3	25	9
²¹⁸ Po	42	65	32	28	71	71	32	52	2	27	11	27
²¹⁴ Po	47.1	78.9	42.9	30.0	79.6	87.6	42.9	58.5	22.0	31.8	12.2	29.9
²¹² Po	33	32	35	44	36	46	60	32	32	21	30	32
²¹² Po Act	8	4	13	14	17	4	14	24	10	0	5	2
²¹⁸ Po	20	18	22	49	66	54	48	29	24	8	21	6
²¹⁴ Po	22.4	20.3	28.6	55.2	74.0	66.1	64.8	30.8	26.9	7.8	27.8	5.9
²¹² Po	46	30	41	24	59	68	29	44	28	31	22	26
²¹² Po Act	21	10	18	9	31	8	7	22	3	11	3	2
²¹⁸ Po	49	33	18	18	81	71	20	42	18	23	20	27
²¹⁴ Po	54.9	39.0	22.6	19.3	90.8	87.5	26.3	46.3	20.2	26.3	26.6	30.5
²¹⁸ Po	31	43	72	34	54	71	54	36	10	26	44	27
²¹⁴ Po	14	14	20	4	18	7	4	7	5	2	3	7
²¹² Po	49	25	36	41	52	60	52	42	10	21	9	10
²¹² Po Act	54.9	28.7	47.5	46.7	58.3	73.6	71.2	47.6	11.2	24.2	11.3	10.1
²¹⁸ Po	43	50	30	36	49	57	53	36	20	41	45	20
²¹⁴ Po	18	19	12	14	11	3	11	14	2	4	3	6
²¹² Po	50	45	40	47	46	44	27	44	10	14	21	15
²¹² Po Act	56.0	53.8	53.8	52.9	51.5	53.4	35.7	49.3	11.2	15.2	28.0	16.1
²¹⁸ Po	30	4	38	59	39	56	29	27	23	28	16	25
²¹⁴ Po	9	18	13	17	27	6	5	8	3	0	9	6
²¹⁸ Po	46	35	41	85	52	43	18	30	18	3	11	3
²¹⁴ Po	51.5	41.2	55.1	97.2	58.3	52.0	23.7	33.5	20.2	1.4	13.5	2.0
²¹² Po	33	36	37	70	86	69	45	45	29	19	16	23
²¹² Po Act	14	2	17	19	37	14	4	14	5	2	0	4
²¹⁸ Po	23	46	42	71	67	89	35	46	19	11	18	13
²¹⁴ Po	25.8	56.0	56.1	80.6	75.1	110.1	47.5	51.7	21.3	11.5	24.1	13.9
²¹² Po	52	32	51	46	67	40	35	41	5	33	27	25
²¹² Po Act	16	13	16	24	25	7	6	10	0	1	2	7
²¹⁸ Po	36	40	49	82	55	38	41	29	12	9	14	9
²¹⁴ Po	40.3	47.8	66.0	93.0	61.6	45.6	55.7	32.1	13.4	9.0	18.3	8.9
²¹⁸ Po	44	44	50	32	45	56	56	69	18	35	45	15
²¹⁴ Po	17	16	20	15	16	4	7	19	4	2	6	5
²¹² Po	46	47	63	43	51	53	37	50	10	9	10	10
²¹² Po Act	51.5	56.5	85.2	48.1	57.1	64.8	50.0	55.9	11.2	8.9	12.4	10.3
²¹⁸ Po	65	46	50	32	42	39	35	50	21	22	18	17
²¹⁴ Po	17	8	20	15	16	10	8	21	5	4	4	5
²¹² Po	51	22	63	43	42	23	39	49	13	11	12	10
²¹² Po Act	57.1	25.2	85.2	48.1	47.1	26.3	52.7	54.6	14.6	11.4	15.4	10.3
²¹⁸ Po	41	45	32	39	33	51	35	73	13	8	28	22
²¹⁴ Po	13	11	12	17	16	7	6	16	4	3	4	7
²¹⁸ Po	41	43	42	48	49	49	29	65	9	9	17	13
²¹⁴ Po	45.9	51.7	56.6	53.8	54.9	59.6	38.9	73.8	10.1	8.9	22.3	13.6
²¹² Po	47	30	51	51	40	37	55	51	20	22	16	17
²¹² Po Act	7	7	6	18	38	10	7	22	3	2	6	0
²¹⁸ Po	39	39	31	47	56	38	49	84	7	6	10	9
²¹⁴ Po	43.7	46.8	41.7	52.5	62.7	45.4	66.7	95.5	7.8	5.1	12.4	9.6
²¹² Po					63	67	51	50	19	29	21	19
²¹² Po Act					22	5	4	33	8	1	2	7
²¹⁸ Po					79	42	32	76	14	8	9	10
²¹⁴ Po					88.5	50.8	43.3	85.1	15.7	7.7	11.3	10.1
²¹⁸ Po									15	32	38	32
²¹⁴ Po									8	2	1	2
²¹² Po									8	11	9	9
²¹² Po Act									9.0	11.5	11.4	9.4
	46.8	45.1	48.6	54.3	67.3	63.2	49.7	55.3	16.4	12.1	17.9	17.8

Appendix C: Airborne attached and unattached radon progenies in Bq.m⁻³

²¹⁸ Po	²¹⁴ Pb	²¹⁴ Po	²¹⁸ Po	²¹⁴ Pb	²¹⁴ Po	Total
-5±34	7±11	13±11	208±58	21±15	12±17	203
77±39	37±12	-13±13	354±62	24±14	-13±17	431
1±42	12±13	23±14	115±47	-1±11	18±13	116
40±35	36±12	-5±12	83±42	5±11	16±12	123
-12±43	30±14	23±15	227±50	9±11	-1±13	215
-30±36	-2±11	31±12	263±53	12±12	-5±14	234
72±44	46±14	-2±15	167±45	23±12	-5±13	239
-21±33	1±10	16±11	197±53	28±14	0±15	176
-37±34	-3±10	25±11	249±51	-5±10	-1±13	212
77±106	142±33	154±36	271±65	21±17	20±19	348
67±105	164±34	142±36	235±68	11±17	41±20	302
-29±84	49±25	126±28	198±55	23±14	9±16	169
695±163	348±49	254±53	98±47	9±12	20±14	793
278±159	324±49	333±53	50±40	7±11	18±12	328
658±177	500±55	299±59	-40±42	16±14	39±15	618
1250±248	913±77	646±83	125±53	26±15	20±16	1375
-22±59	29±18	56±20	317±64	27±16	4±18	295
27±59	28±18	43±19	361±63	33±15	-11±17	388
50±57	49±18	24±19	380±65	-5±13	6±17	430
183±55	33±15	-2±16	80±58	1±15	44±18	263
23±56	27±17	40±18	479±72	56±18	-27±20	502
415±163	325±50	333±54	-8±24	-2±7	13±8	407
958±231	752±72	606±77	16±31	2±9	13±10	974
685±220	576±67	639±73	-1±33	21±11	11±12	684
838±255	933±80	814±86	75±39	13±11	7±12	912
204±156	383±50	310±53	48±32	9±9	4±10	252
959±222	814±70	483±74	-20±27	12±9	11±10	939
666±205	646±64	464±69	19±31	20±10	6±11	685
633±175	407±54	337±58	34±26	19±9	-4±9	666
563±152	261±45	249±49	52±28	5±7	1±8	615
968±237	780±74	655±79	62±31	16±9	-2±10	1029
345±183	406±57	466±61	43±29	32±10	-8±10	388
847±201	568±62	428±67	66±33	21±10	-3±10	913
178±102	122±31	105±34	337±70	18±17	20±20	516
150±108	160±34	120±36	265±82	30±22	71±25	416
217±108	154±34	107±36	605±80	68±20	-30±22	822
141±120	186±38	164±41	685±91	65±23	-7±25	826
-44±102	84±32	174±34	554±85	108±23	-22±25	510
72±73	75±23	51±25	617±87	44±21	3±24	689
204±106	137±33	109±35	482±81	78±22	-3±24	686
76±75	50±23	69±25	341±67	23±16	8±19	417
92±71	49±21	55±23	261±67	28±17	25±20	354
212±113	179±36	120±38	563±82	68±21	-15±23	775
475±121	303±39	34±41	454±82	46±21	21±24	929
615±201	509±62	417±67	-1±46	22±14	36±16	614
846±234	553±71	634±77	-5±27	9±9	11±9	841
282±186	386±58	442±63	85±35	31±11	-9±11	367
1382±260	898±81	602±86	21±42	17±13	24±14	1403
1126±285	920±88	921±95	101±36	17±10	-5±10	1227
934±250	785±78	661±84	-10±34	9±10	21±11	924
1150±268	984±84	702±90	77±37	35±12	-7±12	1227
54±61	39±19	28±20	232±50	19±12	-10±13	286
22±73	33±22	69±24	225±52	20±13	-2±15	247

96±69	66±22	27±23	203±51	11±12	3±14	299
18±52	25±16	23±17	236±57	2±13	16±16	254
-24±44	10±14	24±15	261±57	7±13	6±15	237
83±69	17±19	51±22	317±60	21±14	-6±16	400
448±107	198±33	16±35	25±42	18±13	22±14	473
329±154	226±47	274±51	34±44	20±13	25±15	363
395±161	327±50	254±54	203±63	60±18	11±20	599
426±180	444±57	325±61	196±59	52±17	7±18	622
908±159	448±50	67±52	317±62	69±17	-24±18	1225
1204±270	923±84	720±90	149±62	65±19	17±20	1353
411±185	409±58	379±62	131±57	7±15	37±17	542

Appendix D: Airborne attached and unattached radon and thoron progenies in Bq.m⁻³

²¹⁸ Po	²¹⁴ Pb	²¹⁴ Po	²¹² Pb	²¹² Bi	²¹⁸ Po	²¹⁴ Pb	²¹⁴ Po	²¹² Pb	²¹² Bi
33±25	-6±9	-15±7	6±1	20±8	6±9	0±3	-1±2	0.5±0.2	2±2
-60±25	-6±11	12±9	13±1	17±11	12±8	7±3	3±2	1.4±	-6±3
3±18	3±7	9±6	6±1	-3±7	17±11	-5±3	-6±3	0.7±0.3	6±3
-4±16	10±8	7±6	6±1	-3±7	12±7	0±2	-2±2	0.5±0.2	0±2
-27±19	0±9	5±7	8±1	8±8	9±8	-5±3	-8±2	0.3±0.2	7±3
-24±17	5±8	11±7	7±1	0±8	7±8	3±3	3±2	1.2±0.3	-4±3
-6±15	14±7	16±6	6±1	-11±6	15±9	8±3	4±3	1.8±0.3	-7±3
13±9	0±2	-3±1	0±0	1±1	3±8	2±3	1±2	0.7±0.2	0±2
3±10	-4±2	-2±2	0±0	5±2	-10±5	2±3	6±2	1.30.3±	-3±3
-11±5	-4±2	-1±2	0±0	5±2	-4±4	-3±2	-2±2	0.5±0.2	4±2
-4±8	-2±2	-2±2	0±0	4±2	18±10	-3±3	-6±2	0.3±0.2	5±2
-26±	0±2	7±2	1±0	-1±2	30±12	5±3	3±3	1.7±0.3	-6±3
-8±	-4±3	-5±2	0±0	6±3	-13±8	4±3	8±3	1.3±0.3	-3±3
58±39	29±16	22±13	28±2	-7±16	4±8	-2±2	-1±2	0.6±0.2	2±2
70±42	24±18	19±15	34±2	-2±17	-7±1	0±3	0±2	1±0.3	1±3
1±30	4±14	-1±11	19±1	16±13	-6±5	4±3	5±2	1.1±0.3	-3±3
73±38	43±16	33±13	28±2	-25±15	-4±4	1±2	1±1	0.4±0.2	0±2
73±47	33±21	11±17	45±2	8±20	-4±4	-2±2	-2±2	0.2±0.2	3±2
18±16	-6±4	-1±4	2±0	5±4	-4±5	0±2	-1±2	0.5±0.2	2±2
-3±9	-4±4	-4±3	1±0	6±4	10±7	4±2	1±2	0.9±0.2	-3±2
-11±9	9±4	15±3	3±0	-11±4	-2±6	-1±2	0±2	0.2±0.1	1±2
-11±11	4±4	7±3	2±0	-2±3	-15±2	-3±2	1±2	0.1±0.1	3±2
-15±6	1±3	2±3	1±0	2±3	15±11	-3±2	-2±2	0.4±0.2	2±2
-41±26	-17±13	-4±10	15±1	28±12	-2±4	-3±3	-3±2	0.4±0.2	4±2
-9±32	-17±15	-10±12	22±1	33±15	-3±5	4±3	5±2	1.6±0.3	-4±3
36±28	8±12	-2±10	16±1	6±12	8±7	-3±2	-4±2	0.3±0.2	4±2
51±31	25±12	9±10	16±1	-6±12	2±7	-1±2	-4±2	0.1±0.2	4±2
-33±24	11±13	8±10	17±1	7±12	-14±3	-2±3	-1±2	0.7±0.2	4±3
6±42	0±19	6±16	37±2	28±18	3±7	2±3	0±3	1.3±0.3	0±3
9±8	4±2	3±2	1±0	-4±2	-12±1	-4±2	-2±1	-0.2±0.1	5±1
-5±	-3±2	-5±2	0±0	5±2	10±8	-3±2	-2±2	0.2±0.2	2±2
-1±4	-2±2	0±2	0±0	1±2	-2±5	10±2	8±2	1.3±0.3	-8±2
-4±4	-1±3	-3±2	1±0	3±3	1±	6±2	1±2	0.9±0.2	-3±2
-6±5	-3±3	-2±2	0±0	4±3	5±6	2±2	1±2	0.8±0.2	-2±2
-7±4	-3±2	-5±1	0±0	5±2	7±9	2±2	3±2	0.8±0.2	-3±2
25±34	19±14	14±11	19±1	1±13	7±8	4±2	3±2	0.9±0.2	-3±2
-19±45	29±20	19±16	41±2	19±19	0±4	5±2	5±2	0.9±0.2	-5±2
122±67	92±17	79±15	25±1	-17±15	-1±7	4±	4±2	1±0.3	-3±2
7±34	24±15	13±12	24±1	2±15	-4±	4±2	2±2	0.8±0.2	-2±2
-35±44	19±20	18±16	39±2	23±19	2±3	1±2	-1±1	0.2±0.1	0±1
19±26	-6±11	-3±9	12±1	14±11	-7±2	5±3	4±2	1.2±0.3	-3±3
18±30	0±14	-11±11	19±1	21±14	0±6	-3±2	-3±2	0.2±0.2	4±2
-28±29	-5±13	2±11	18±1	20±	12±7	4±2	1±2	0.8±0.2	-3±2
-5±39	2±18	-12±15	312±	37±17	-5±5	2±3	1±2	0.8±0.3	0±3
11±26	15±12	5±15	14±1	2±11	7±9	-3±4	-3±3	1.4±0.3	3±4
22±33	14±14	14±12	21±1	1±14	4±6	-3±2	-4±2	0.3±0.2	4±2
15±32	25±15	11±13	27±1	-2±15	6±6	1±2	0±2	0.6±0.2	0±2
52±28	-14±11	-16±9	12±1	23±11	10±8	5±3	2±2	1.1±0.3	-4±3